

THE DESIGN AND SYNTHESIS OF CONSTRAINED
AVPI PEPTIDOMIMETICS.

A DISSERTATION SUBMITTED TO THE FACULTY OF THE
GRADUATE SCHOOL OF THE UNIVERSITY OF MINNESOTA BY

CORY KENDING

IN PARTIAL FULFILLMENT OF THE REQUIREMENTS FOR THE
DEGREE OF THE DOCTOR OF PHILOSOPHY

RODNEY LYLE JOHNSON, ADVISOR

DECEMBER 2008

Acknowledgements

I would first and foremost like to thank my advisor Prof. Rodney Johnson who has shown me more patience and understanding than I could have hoped for during my graduate career.

I would also like to thank the current and past members of the Johnson lab who have shared that space with me; Swapna Bhagwanth, Bhooma Raghavan, Ashish Vartak, Ravi Somu and Abigail Fischer. Our discussions of life and chemistry have made the graduate school experience one that I have treasured.

I would also like to thank my committee who take time from their busy schedules to guide me through my orals and my final defense. Thank you Dr. Fecik, Dr. Wagner and Dr. Noland.

I would also like to thank my beautiful daughter, Kaija Rose-Kending, who has been my light and inspiration during the darkest moments of these last five years and will always be.

Abstract

Recent studies have demonstrated that breast cancer cell lines are sensitive to the XIAP (X-linked inhibitor of apoptotic proteins) antagonist Smac (second mitochondrial activator of caspases). Specifically the terminal tetrapeptide, AVPI, inhibits XIAP and thus sensitizes the breast cancer cells to various apoptotic therapeutics. These peptides are poor drug candidates due to their size, hydrophilicity and potential for peptidase cleavage. To address these issues we systematically synthesized peptide mimics that are constrained at various torsion angles along the peptide backbone.

The compounds were tested *in vivo* and *in vitro* utilizing the laboratories of the Mayo Medical School. One compound, HCl•NH₂-(*R*)- α Me- γ -Lactam-L-Val-L-Pro-L-Ile-OMe (**3.1**), increased the apoptotic signals above the assay background. Retro-modeling analysis utilizing the Schödinger flexible docking program suite did not provide an easy explanation for why this might be the case. The *in silico* models suggest that compound **3.1** interacts with only the primary pocket of the AVPI binding site and does not interact, like the native peptide, with both pockets in the active site.

The *R* stereochemistry of the bicyclic compounds is predicted by our models to have a binding efficacy above that of the native peptide presumably due to the interaction with both pockets of the binding site as well as *d*-orbital interactions of the thiazole ring system with the neighboring tryptophan. The *S* stereochemistry was also initially proposed as a negative control for the biological assays, however, the instability of the molecule provided several daunting challenges to an already challenging and low yielding synthesis and the negative controls were abandoned when it was clear that the synthesis was futile.

Our research shows limited evidence that our AVPI peptidomimetics are a potential scaffold to base other drug-like molecules upon. Future biological data from the bicyclic compounds will hopefully prove our hypothesis and molecular modeling studies correct.

Table of Contents

Acknowledgements	i
Abstract	ii
Table of Contents	iv
List of Figures	ix
List of Schemes	xi
List of Tables	xii
Abbreviations	xiii
Chapter 1. The Role of AVPI in Apoptosis Regulation	1
1.1. Clinical Observations	1
1.2. Apoptosis Background	1
1.3. Regulation of Apoptosis	6
1.4. Therapeutic XIAP Inhibitors	9
1.5. Summary	13
1.6. References	13
Chapter 2. The Stereoselective Synthesis of ϕ_1 Constrained AVPI	
Peptidomimetics	23
2.1. Design and Scope	23
2.2. Sequential Synthetic Strategy	24
2.3. Dipeptide Segment Coupling Strategy	28
2.4. Non-Sequential Alternative Method	31
2.5. Synthesis of the Final Compounds	33
2.6. Biological Activity	35
2.7. Retro-Modeling Analysis	36
2.8. Experimentals	44
N-Boc-L-Pro-L-Ile-OMe (2.11)	45
N-Boc-L-Val-L-Pro-L-Ile-OMe (2.12)	46
N-Boc- α Me-D-Pro-L-Val-OMe (2.15)	48
α -Me-D-Pro-OH (2.7)	50
N-Boc- α -Me-D-Pro-OH (2.8)	52
N-Boc-Val-Pro-OMe (2.19)	53
N-Boc- α -Me-D-Pro-L-Val-L-Pro-OMe (2.20)	54
N-Boc- α -Me-D-Pro-L-Val-L-Pro-L-Ile-OMe (2.13)	56
α -Me-D-Pro-Val-Pro-Ile-OMe • HCl (2.2)	58
α -Me-D-Pro-Val-Pro-Ile-OH • HCl (2.1)	59

	α -Me-D-Pro-Val-Pro-Ile-NHMe • HCl (2.3)	61
2.9.	References	64
Chapter 3.	The Stereoselective Synthesis of ψ_1 Constrained AVPI mimics	67
3.1.	Design and Scope	67
3.2.	Synthetic Strategy	68
3.3.	Stereoselective Alkylation of L-Alanine	69
3.4.	Biological Testing	76
3.5.	Retro – Modeling Analysis of the ψ_1 Constrained Peptidomimetics	78
3.6.	Experimentals	80
	(<i>S,S</i>)-4-Methyl-5-oxo-2-phenyl-oxazolidine-3-carboxylic Acid Benzyl Ester (3.4)	80
	4-Allyl-4-methyl-5-oxo-2-phenyl-oxazolidine-3-carboxylic Acid Benzyl Ester (3.5)	81
	2-Benzyloxycarbonylamino-2-methyl-pent-4-enoic Acid Methyl Ester (3.6)	83
	2-Benzyloxycarbonylamino-2-methyl-4-oxo-butyric Acid Methyl Ester (3.7)	84
	N-[2(<i>R</i>)-Benzyloxycarbonylamino-2-methoxycarbonyl-4-butyl]-L-Val-L-Pro-L-Ile-OMe (<i>intermediate only</i>) (3.9)	85
	Cbz-[(<i>R</i>)-3-amino-3-methylpyrrolidin-2-one]-L-Val-Pro-Ile-OMe (3.10)	87
	Boc-Ile-NHMe (3.14)	88
	Boc-L-Pro-Ile-NHMe (3.15)	89
	Boc-L-Val-L-Pro-L-Ile-NHMe (3.16)	91
	Cbz-NH-(<i>R</i>)- α Me- γ -Lactam-L-Val-L-Pro-L-Ile-NHMe (3.11)	93
	HCl•NH ₂ -(<i>R</i>)- α Me- γ -Lactam-L-Val-L-Pro-L-Ile-OMe (3.1)	94
	HCl•NH ₂ -(<i>R</i>)- α Me- γ -Lactam-L-Val-L-Pro-L-Ile-NHMe (3.2)	95
3.7.	References	97
Chapter 4.	The Stereoselective Synthesis of ψ_2 , ϕ_3 Constrained AVPI Mimics	99
4.1.	Design and Scope	99
4.2.	Synthetic Strategy: Sequential	101
4.3.	Synthetic Strategy: Convergent	109
4.4.	Sequential Strategy Revisited: Zirconium Trans-Amidation	115
4.5.	Modeling Analysis	122
4.6.	Experimentals	129
	(<i>S,S</i>)-(+)-Pseudoephedrine Glycinamide (4.6)	129
	Pseudoephedrine D-Allyl Glycinamide(4.7)	130
	Boc- α -Allyl-D-Gly-OH (4.10)	132
	(<i>R</i>)-2-(tert-Butoxycarbonylamino)hex-5-enoic acid (4.16)	134
	HCl•NH ₂ -D-Cys-OMe	136
	HCl•NH ₂ -L-Hcy-OMe	137

(3 <i>S</i> , 6 <i>R</i> , 7 <i>aR</i>)-6- <i>tert</i> -Butoxycarbonylamino-5-oxo-hexahydro-pyrrolo[2,1- <i>b</i>]thiazole-3-carboxylic Acid Methyl Ester (4.12)	138
(3 <i>S</i> , 6 <i>R</i> , 7 <i>aS</i>)-6- <i>tert</i> -utoxycarbonylamino-5-oxo-hexahydro-pyrrolo[2,1- <i>b</i>]thiazole-3-carboxylic Acid Methyl Ester (4.13)	138
(4 <i>S</i> , 7 <i>R</i> , 8 <i>aR</i>)-7- <i>tert</i> -Butoxycarbonylamino-6-oxo-hexahydro-pyrrolo[2,1- <i>b</i>][1,3]thiazine-4-carboxylic acid methyl ester. (4.14)	142
(4 <i>S</i> , 7 <i>R</i> , 8 <i>aS</i>)-7- <i>tert</i> -Butoxycarbonylamino-6-oxo-hexahydro-pyrrolo[2,1- <i>b</i>][1,3]thiazine-4-carboxylic acid methyl ester. (4.15)	142
(3 <i>S</i> ,6 <i>R</i> ,8 <i>aS</i>)-methyl-6- <i>tert</i> -Butoxycarbonylamino-5-oxo-hexahydro-thiazolo[3,2- <i>a</i>]pyridine-3-carboxylic acid methyl ester (4.18)	145
(3 <i>S</i> ,6 <i>R</i> ,8 <i>aR</i>)-methyl-6- <i>tert</i> -Butoxycarbonylamino-5-oxo-hexahydro-thiazolo[3,2- <i>a</i>]pyridine-3-carboxylic acid methyl ester (4.19)	145
2- <i>tert</i> -Butoxycarbonylamino-pent-4-enoic Acid Benzyl Ester (4.27)	147
2- <i>tert</i> -Butoxycarbonylamino-hex-5-enoic Acid Benzyl Ester	148
(<i>R</i>)-Benzyl 2-((<i>S</i>)-2-(<i>tert</i> -Butoxycarbonylamino)-propanamido)pent-4-enoate (4.28)	149
Boc- α -Allyl-Gly-OMe (4.20)	151
Boc-L-Ala-(<i>R</i>)- α -allyl-Gly-OMe (4.21)	152
Boc-NH-Hcy-Hcy-NHBn (4.23)	154
(4 <i>S</i> ,7 <i>R</i> ,8 <i>aR</i>)-7-(2- <i>tert</i> butoxycarbonylamino-propanoyl)-6-oxohexahydro-2 <i>H</i> -pyrrolo[2,1- <i>b</i>][1,3]thiazine-4- <i>N</i> -benzyl-carboxamide (4.26)	155
(4 <i>S</i> , 7 <i>R</i> , 8 <i>aR</i>)-7- <i>tert</i> -Butoxycarbonylamino-6-oxo-hexahydro-pyrrolo[2,1- <i>b</i>][1,3]thiazine-4- <i>N</i> -benzyl-carboxamide (4.30)	158
(4 <i>S</i> ,7 <i>R</i> ,8 <i>aR</i>)-7-(2- <i>tert</i> butoxycarbonylamino-propanoyl)-6-oxohexahydro-2 <i>H</i> -pyrrolo[2,1- <i>b</i>][1,3]thiazine-4-benzyl-carboxamide (4.26)	160
(4 <i>S</i> , 7 <i>R</i> , 8 <i>aR</i>)-7- <i>tert</i> -Butoxycarbonylamino-6-oxo-hexahydro-pyrrolo[2,1- <i>b</i>][1,3]thiazine-4- <i>N</i> -benzyl-carboxamide (4.30)	162
(4 <i>S</i> , 7 <i>R</i> , 8 <i>aR</i>)-7- <i>tert</i> -Butoxycarbonylamino-6-oxo-hexahydro-pyrrolo[2,1- <i>b</i>][1,3]thiazine-4- <i>N</i> -benzyl-carboxamide (4.31)	165
Methyl(4 <i>S</i> ,7 <i>R</i> ,8 <i>aR</i>)-7-(2- <i>tert</i> -Butoxycarbonylamino-propanoyl)-6-oxohexahydro-2 <i>H</i> -pyrrolo[2,1- <i>b</i>][1,3]thiazine-4-carboxylate (4.32)	166
Methyl(4 <i>S</i> ,7 <i>R</i> ,8 <i>aS</i>)-7-(2- <i>tert</i> -Butoxycarbonylamino-	

propanoyl)-6-oxohexahydro-2 <i>H</i> -pyrrolo[2,1- <i>b</i>][1,3]thiazine-4-carboxylate (4.33)	168
Methyl(3 <i>S</i> ,6 <i>R</i> ,7 <i>aR</i>)-6-(2- <i>tert</i> -Butoxycarbonylamino-propanoyl)-5-oxohexahydropyrrolo[2,1- <i>b</i>]thiazole-3-carboxylate (4.38)	170
Methyl(3 <i>S</i> ,6 <i>R</i> ,7 <i>aS</i>)-6-(2- <i>tert</i> -Butoxycarbonylamino-propanoyl)-5-oxohexahydropyrrolo[2,1- <i>b</i>]thiazole-3-carboxylate (4.39)	172
(4 <i>S</i> ,7 <i>R</i> ,8 <i>aR</i>)-7-(2- <i>tert</i> -Butoxycarbonylamino-propanoyl)amino-6-oxohexahydro-2 <i>H</i> -pyrrolo[2,1- <i>b</i>][1,3]thiazine-4- <i>N</i> -benzyl-carboxamide (4.35)	174
(4 <i>S</i> ,7 <i>R</i> ,8 <i>aS</i>)-7-(2- <i>tert</i> -Butoxycarbonylamino-propanoyl)amino-6-oxohexahydro-2 <i>H</i> -pyrrolo[2,1- <i>b</i>][1,3]thiazine-4- <i>N</i> -benzyl-carboxamide (4.34)	176
[(3 <i>S</i> ,6 <i>R</i> ,7 <i>aR</i>)-6-(<i>tert</i> -Butoxycarbonylamino-propanoyl)amino-5-oxohexahydropyrrolo[2,1- <i>b</i>]thiazole-3- <i>N</i> -benzyl-carboxamide] (4.40)	178
[(3 <i>S</i> ,6 <i>R</i> ,7 <i>aS</i>)-6-(<i>tert</i> -Butoxycarbonylamino-propanoyl)amino-5-oxohexahydropyrrolo[2,1- <i>b</i>]thiazole-3- <i>N</i> -benzyl-carboxamide] (4.41)	180
TFA•(4 <i>S</i> ,7 <i>R</i> ,8 <i>aR</i>)-7-(2-amino-propanoyl)amino-6-oxohexahydro-2 <i>H</i> -pyrrolo[2,1- <i>b</i>][1,3]thiazine-4- <i>N</i> -benzyl-carboxamide (4.37)	182
TFA•[(3 <i>S</i> ,6 <i>R</i> ,7 <i>aS</i>)-6-(amino-propanoyl)amino-5-oxohexahydropyrrolo[2,1- <i>b</i>]thiazole-3- <i>N</i> -benzyl-carboxamide] (4.43)	183
4.7 References	185
Chapter 5. The Stereoselective Synthesis of ϕ_1 , ϕ_3 , ψ_3 , and ϕ_3 , ψ_3 Constrained AVPI Mimics	189
5.1. Design and Scope	189
5.2. Synthetic Strategy	190
5.3. Biological Testing	195
5.4. Retrosynthetic Modeling Analysis of the Constrained Peptidomimetics	197
5.5. Experimentals	202
α -Allyl-L-Pro-OH (5.4)	202
Boc- α -Allyl-L-Pro-OH (5.5)	204
N-Boc- α -Allyl-L-Pro-OMe (5.6)	205
(<i>R</i>)- <i>N</i> -(<i>tert</i> -Butoxycarbonyl)-2-(formylmethyl)proline Methyl Ester (5.7)	206
(<i>R</i>)- <i>tert</i> -Butoxycarbonyl-7-Benzyl-6-oxo-1,7-diazaspiro[4.4]nonane (5.8)	207
N-Boc- 2-[2-(Benzhydryl-amino)-ethyl]-Pro-OMe(5.9)	209
5-(<i>R</i>)-1- <i>tert</i> -Butoxycarbonyl-7-benzhydryl-6-oxo-1,7-diazaspiro[4.4]nonane-1-carboxylic Acid <i>tert</i> -Butyl	

Ester (5.12)	210
5-(<i>R</i>)-1-(2-(<i>S</i>)-(tert-Butoxycarbonyl)amino-3-methylbutanoyl)-7-benzyl-6-oxo-1,7-diazaspiro[4.4]nonane (5.18)	212
5-(<i>R</i>)-1-(2-(<i>S</i>)-(tert-Butoxycarbonyl)amino-3-methylbutanoyl)-7-benzhydryl-6-oxo-1,7-diazaspiro[4.4]nonane (5.19)	214
Boc-L-Ala-L-Val-(<i>R</i>)-7-benzyl-6-oxo-1,7-diazaspiro[4.4]nonane (5.20)	216
Boc-L-Ala-L-Val- (<i>R</i>)-7-benzhydryl-6-oxo-1,7-diazaspiro[4.4]nonane (5.21)	218
Boc- α -Me-D-Pro-L-Val- (<i>R</i>)-7-benzyl-6-oxo-1,7-diazaspiro[4.4]nonane (5.22)	220
Boc- α -Me-D-Pro-L-Val-(<i>R</i>)-7-benzhydryl-6-oxo-1,7-diazaspiro[4.4]nonane (5.23)	222
L-Ala-L-Val-(<i>R</i>)-7-benzyl-6-oxo-1,7-diazaspiro[4.4]nonane•HCl (5.26)	224
α -Me-D-Pro-L-Val- (<i>R</i>)-7-benzyl-6-oxo-1,7-diazaspiro[4.4]nonane•HCl (5.24)	225
NH ₂ -L-Ala-L-Val- (<i>R</i>)-7-benzhydryl-6-oxo-1,7-diazaspiro[4.4]nonane•HCl (5.27)	226
α -Me-D-Pro-L-Val-(<i>R</i>)-7-benzhydryl-6-oxo-1,7-diazaspiro[4.4]nonane•HCl (5.25)	227
5.6. References	229
Comprehensive Bibliography	232

List of Figures

Figure 1.1.	Mechanism of Caspase Activation	3
Figure 1.2.	Apoptosis Overview	5
Figure 1.3.	Interaction of AVPI with XIAP-BIR3 Binding Domain	8
Figure 1.4.	Previously Synthesized AVPI Peptidomimetics	10
Figure 1.5.	SAR Analysis of Allowed and Disallowed Modifications to the AVPI Backbone	12
Figure 2.1.	Effects of Peptidomimetics 2.1 , 2.2 , and 2.3 on Drug-induced Apoptosis	34
Figure 2.3.	GScore v. K_i Correlations of the Wang Compounds	40
Figure 2.4.	GScore v. K_i Correlations of the Wang Compounds	41
Figure 2.5.	φ_1 Constrained AVPI Mimic Methyl Ester Derivative 2.2 in the XIAP BIR3 Active Site	42
Figure 2.6.	φ_1 constrained AVPI Mimic Carboxylic Acid Derivative (2.1) in the XIAP BIR3 Active Site	43
Figure 2.7.	φ_1 constrained AVPI Mimic Methyl Amide Derivative (2.3) in the XIAP BIR3 Active Site	44
Figure 3.1.	Retrosynthetic Analysis of ψ_1 Constrained AVPI Mimic	69
Figure 3.2.	Concentration Depend Binding Assay of AVPI Peptidomimetics	77
Figure 3.3.	Retro-Modeling Analysis of ψ_1 Constrained AVPI Methyl Ester Derivative (3.1)	78
Figure 3.4.	Retro-Modeling Analysis of ψ_1 Constrained AVPI Methyl Amide Derivative (3.2)	79
Figure 4.1.	Overview of Sequential Synthetic Strategy	101
Figure 4.2.	Base Catalyzed Epimerization of Bicyclic Thiazabicycloalkanes	108
Figure 4.3.	Overview of Convergent Synthetic Strategy	110
Figure 4.4.	Acid Catalyzed Iminium Equilibrium	118
Figure 4.5.	TFA•NH ₂ -Ala-[(3 <i>S</i> ,6 <i>R</i> ,7 <i>aR</i>)-6-amino-N-benzyl-5-oxohexahydropyrrolo[2,1- <i>b</i>]thiazole-3-carboxamide] (4.42)	122
Figure 4.6.	TFA•NH ₂ -Ala-[(3 <i>S</i> ,6 <i>R</i> ,7 <i>aS</i>)-6-amino-N-benzyl-5-oxohexahydropyrrolo[2,1- <i>b</i>]thiazole-3-carboxamide] 4.43	124
Figure 4.7.	TFA•NH ₂ -Ala-[(4 <i>R</i> ,7 <i>R</i> ,8 <i>aS</i>)-7-amino-N-benzyl-6-oxohexahydro-2 <i>H</i> -pyrrolo[2,1- <i>b</i>][1,3]thiazine-4-carboxamide] 4.37	125
Figure 4.8.	TFA•NH ₂ -Ala-[(4 <i>R</i> ,7 <i>R</i> ,8 <i>aR</i>)-7-amino-N-benzyl-6-oxohexahydro-2 <i>H</i> -pyrrolo[2,1- <i>b</i>][1,3]thiazine-4-carboxamide] 4.36	126
Figure 4.9.	TFA•NH ₂ -Ala-[(3 <i>R</i> ,6 <i>R</i> ,8 <i>aR</i>)-6-amino-N-benzyl-5-oxohexahydro-2 <i>H</i> -thiazolo[3,2- <i>a</i>]pyridine-3-carboxamide	127
Figure 4.10.	TFA•NH ₂ -Ala-[(3 <i>R</i> ,6 <i>R</i> ,8 <i>aS</i>)-6-amino-N-benzyl-5-oxohexahydro-2 <i>H</i> -thiazolo[3,2- <i>a</i>]pyridine-3-carboxamide	128
Figure 4.11	NOE Structure Confirmation of (3 <i>S</i> , 6 <i>R</i> , 7 <i>aR</i>)-6-tert-Butoxycarbonylamino-5-oxo-hexahydro-pyrrolo[2,1- <i>b</i>]thiazole-3-carboxylic Acid Methyl Ester and (3 <i>S</i> , 6 <i>R</i> , 7 <i>aS</i>)-6-tert-Butoxycarbonylamino-5-oxo-hexahydro-pyrrolo[2,1- <i>b</i>]thiazole-3-carboxylic Acid Methyl Ester.	128

Figure 4.12	NOE Structure Confirmation of (4 <i>S</i> , 7 <i>R</i> , 8 <i>aR</i>)-7-tert-Butoxycarbonylamino-6-oxo-hexahydro-pyrrolo[2,1- <i>b</i>][1,3]thiazine-4-carboxylic Acid Methyl Ester (4.14) and (4 <i>S</i> , 7 <i>R</i> , 8 <i>aS</i>)-7-tert-Butoxycarbonylamino-6-oxo-hexahydro-pyrrolo[2,1- <i>b</i>][1,3]thiazine-4-carboxylic Acid Methyl Ester (4.15).	128
Figure 5.1.	Concentration Depend Binding Assay of AVPI Peptidomimetics	196
Figure 5.2.	Retrosynthetic Modeling of NH ₂ -Ala -Val-[7-Benzyl-6-oxo-1,7-diaza-spiro[4.4]nonane] (5.26)	198
Figure 5.3.	Retrosynthetic Modeling of NH ₂ -Ala-Val-7-Benzhydryl-6-oxo-1,7-diaza-spiro[4.4]nonane (5.27)	199
Figure 5.4.	Retrosynthetic Modeling of NH ₂ - α -Me-D-Pro-Val-[7-Benzyl-6-oxo-1,7-diaza-spiro[4.4]nonane](5.24)	200
Figure 5.5.	Retrosynthetic Modeling of NH ₂ - α -Me-D-Pro-Val-[1-(7-benzhydryl-6-oxo-1,7-diaza-spiro[4.4]nonane)] (5.25)	201

List of Schemes

Scheme 2.1.	Synthesis of α -Me-D-Proline	25
Scheme 2.2.	Linear Synthesis of AVPI Peptide Backbone	27
Scheme 2.3.	Dipeptide Segment Coupling Strategy	29
Scheme 2.4.	Mechanism of Valine Epimerization via Azlactone Formation	30
Scheme 2.5.	Non-Sequential Peptide Coupling Strategy	32
Scheme 2.6	Final Derivatization of the AVPI ϕ_1 Peptidomimetics	33
Scheme 3.1.	ZnCl ₂ Mediated Synthesis of Dialkyl Alanine	70
Scheme 3.2.	Confirmation of Enantiomeric Purity of Alkylated Alanine	71
Scheme 3.3.	Reductive Amination of Alpha-Aldehyde	71
Scheme 3.4.	Thermal Cyclization / Lactamization of the Methyl Ester	72
Scheme 3.5.	Optimization of Methyl Ester Transformation to Methyl Amide	73
Scheme 3.6.	Hydrolysis and Coupling Methyl Amide Strategy	74
Scheme 3.7.	Methyl Amide Coupling to Boc-Isoleucine	75
Scheme 3.8.	Thermal Cyclization / Lactamization of the Methyl Ester	76
Scheme 4.1.	Pseudoephedrine as a Chiral Auxiliary in Asymmetric Alkylation of Glycine	103
Scheme 4.2.	Modified Meyers Asymmetric Synthesis	104
Scheme 4.3.	Condensation and Cyclization to the 5,5 Bicyclic Lactams	105
Scheme 4.4.	Condensation and Cyclization to the 5,6 Bicyclic Lactams	106
Scheme 4.5.	Condensation and Cyclization to the 6,5 Bicyclic Lactams	107
Scheme 4.6.	Synthesis of Subunit AB	111
Scheme 4.7.	Synthesis of Subunit CD	112
Scheme 4.8.	Complete Condensation of 5,6 Bicyclic Lactam (4.26)	113
Scheme 4.9.	Condensation and Cyclization of Subunit A and B	114
Scheme 4.10.	Synthesis of 5,6 Bicycles: Condensation of A + CD	115
Scheme 4.11.	Zirconium Mediated Trans-Amidation	116
Scheme 4.12.	Synthesis of the 5,6 Tetrapeptides via Standard Sequential Coupling Chemistry	117
Scheme 4.13.	Synthesis of the 5,5 Tetrapeptides via Standard Sequential Coupling Chemistry	119
Scheme 5.1.	Synthesis of D-Allyl Proline	191
Scheme 5.2.	Reductive Amination of Benzyl and Dibenzyl Methyl Amine	192
Scheme 5.3.	Synthesis of Benzyl and Dibenzyl 4.4 Spirocycles	193
Scheme 5.4.	Synthesis of α -Me-D-Proline	193
Scheme 5.5.	Coupling and Deprotection of Benzyl Derivatives	194
Scheme 5.6.	Coupling and Deprotection of Dibenzyl Derivatives	195

List of Tables

Table 2.1.	Reactions Conditions and Yields in the Synthesis of Compounds 2.13	28
Table 2.2.	Structures of Smac Peptidomimetics and Their Binding Affinities to XIAP BIR3 Protein as Compared to GScore Values	38
Table 4.1.	Reaction Conditions and Yield in the Synthesis of 4.35 and 4.41	121

Abbreviations

Bn	benzyl
BnBr	benzyl bromide
BnOH	benzyl alcohol
Boc ₂ O	di- <i>tert</i> -butoxy dicarbonate
<i>n</i> -BuLi	<i>n</i> -butyllithium
<i>t</i> -Bu-CHO	pivalaldehyde
Cbz	benzyloxycarbonyl
CbzCl	benzyloxychloroformate
CDCl ₃	deuterated chloroform
TFA	trifluoroacetic acid
CH ₂ Cl ₂	dichloromethane
CH ₃ CN	acetomitrile
CH ₂ N ₂	diazomethane
COSY	correlation spectroscopy
DBU	diazobicyclo[5.4.0]undec-7-ene
DCC	1,3-dicyclohexylcarbodiimide
DEA	diethylamine
DMF	dimethylformamide
DMSO-D ₆	deuterated dimethyl sulfoxide
EDC	1-[3-(dimethylamino)propyl]-3-ethylcarbodiimide
eq	equivalents
EtOH	ethanol
Et ₃ N	triethylamine
ESI	electron spray ionization
HATU	O-(7-azabenzotriazol-1-yl)-N,N,N',N'-tetramethyluronium hexafluorophosphate
H ₂ O	water
HCl	hydrochloric acid
H ₂ SO ₄	sulfuric acid
HMBC	heteronuclear multiple bond correlation
HMQC	heteronuclear multiple quantum coherence
gHMQC	gradient heteronuclear multiple quantum coherence
HOAt	1-hydroxy-7-azabenzotriazole
HOBt	1-hydroxybenzotriazole
HPLC	high pressure liquid chromatography
HRMS	high resolution mass spectrometry
IBCF	isobutylchloroformate
K ₂ CO ₃	potassium carbonate
LDA	lithium diisopropylamide
LiCl	lithium chloride
LiOH	lithium hydroxide
Lit.	literature reference
MeI	methyl iodide
MeOD	deuterated methanol

MeOH	methanol
mp	melting point
MsCl	methane sulfonyl chloride
Mukaiyama's Reagent	2-chloro-1-pyridinium iodide
NaIO ₄	sodium periodate
NaH	sodium hydride
NaHCO ₃	sodium bicarbonate
NaOH	sodium hydroxide
NMM	<i>N</i> -methyl-morpholine
NMR	nuclear magnetic resonance
NOE	nuclear overhauser effect
OsO ₄	osmium tetroxide
Pd/C	palladium on carbon
Psi	pounds per square inch
RCM	ring closing metathesis
Ref.	reference
R _f	retention factor
rt	room temperature
SAR	structure activity relationship
SiO ₂	silica gel
THF	tetrahydrofuran
TLC	thin layer chromatography
t _R	retention time
<i>p</i> -TsOH	para-toluenesulfonic acid

Chapter 1. The Role of AVPI in Apoptosis Regulation

1.1. Clinical Observations

In cancer, the accumulation of neoplastic cells can occur through either enhanced proliferation or through diminished cell turn-over or a combination of both processes. Ideally, a therapeutic agent designed to halt tumor formation should only target neoplastic cells while sparing normal cells and toxic damage to the organism. This ideal drug is far from being developed despite intense efforts. Instead, the field of chemotherapy has been confronted with problems of toxicity, lack of specificity, rapid drug metabolism and multiple modes of drug resistance. Drug resistance, in particular, will continue to be a problem in the future given the adaptability of tumor cell lines and the preference for chemotherapeutics in cancer treatment regimes.^{1,2}

Drug resistance within cancer cells evolved first from the preference of early researchers to target cells which had enhanced proliferation. These therapies, quite predictably, interfered with normally rapidly dividing cells within the body.³⁻⁶ The cellular response this interference elicited from the tumor cells allowed a small percentage of cells to overcome the toxic effects of the drug and effectively selects for cells that are resistant to the drug.

1.2. Apoptosis Background

One such method of multi-drug resistance, and possibly the most studied mechanism, is apoptosis. Apoptosis was initially discovered after several clinical

observations were made. The first observation was that some neoplasms, such as chronic lymphocytic leukemia and other lymphomas accumulate despite the presence of very few rapidly dividing cells.^{7,8} Secondly, clinicians observed that Bcl-2, a polypeptide, occurred consistently in follicular lymphomas.⁷ When Bcl-2 was over-expressed, it was found that it inhibited cell death.^{9, 10} These were the first pieces of evidence which suggested that an oncogene could act by inhibiting cell turnover instead of enhancing proliferation. Inhibition of apoptosis is now generally accepted as a means of drug resistance and cancer cell proliferation.

Morphologically apoptosis results in intranuclear DNA degradation, decreased DNA repair, disruption of the cell-cycle progression, inhibition of protein synthesis, cleavage of major structural proteins in the cytoplasm and nucleus, and the disruption of signal transduction required for cellular homeostasis.^{11,12} These events, in particular, the cleavage of major structural proteins are responsible for apoptosis induced cell death and are the result of the activity of a family of intracellular cysteine proteases.¹²

This family of proteases shares several traits, the first of which is the ability to cleave peptide bonds on the carboxyl side of aspartic acid.^{12,13} The second shared trait is that family members are all $\alpha_2\beta_2$ tetramers of two 17-35 kDa subunits, p20 domain, and two 10-12 kDa subunits, the p10 domains.¹²⁻¹⁴ Most caspases are activated through proteolytic cleavage of the zymogen between the p20 and p10 domains probably by an already active caspase in an autocatalytic fashion (**Figure 1.1.a**).¹⁵⁻¹⁷

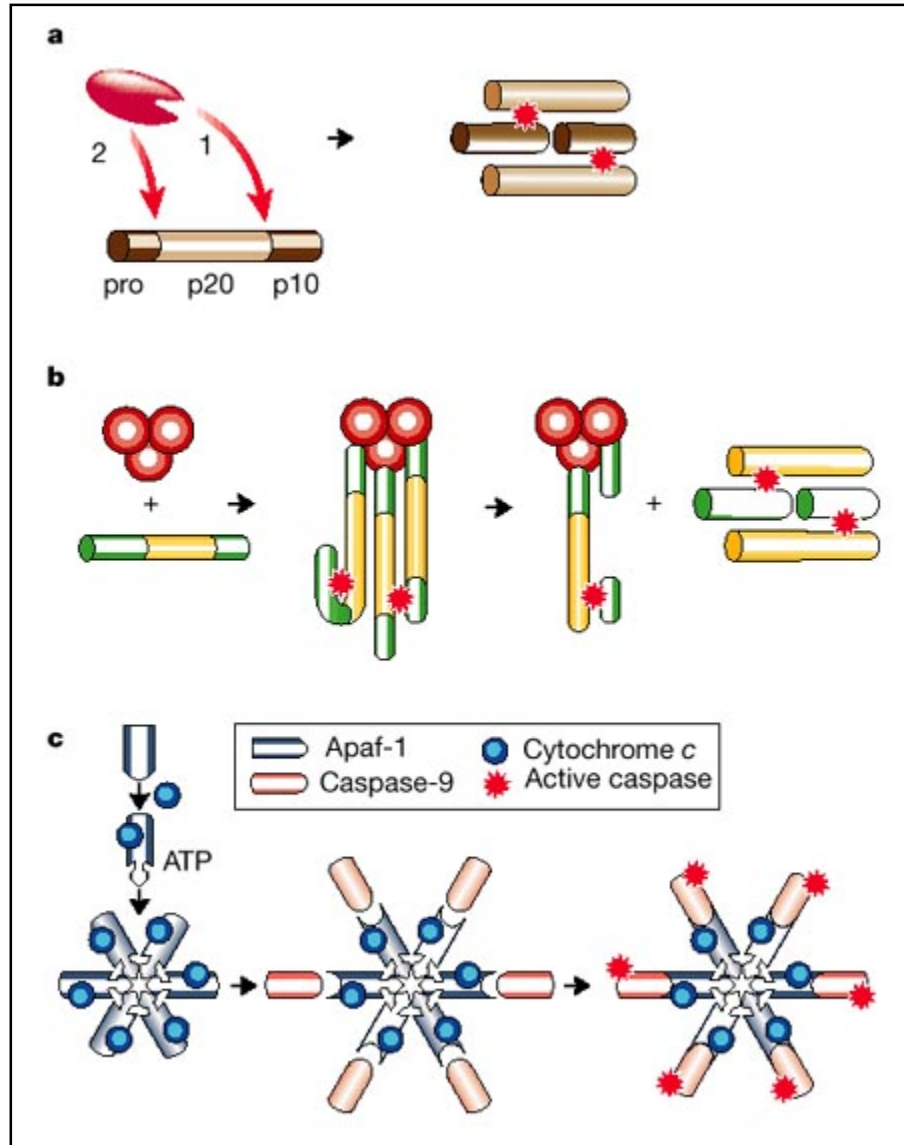


Figure 1.1. Mechanism of Caspase Activation ¹⁷

This autocatalytic ‘caspase cascade’ approach explains the amplification of the death pathway, but it doesn’t explain how the first caspase is initially activated. One model for the initial activation is the induced proximity model which most evidence suggests is the initial activating signal for procaspase-8.¹⁸⁻²⁰ This model suggests that when procaspase-8 is brought into proximity with itself, through cell membrane

signaling, the local concentration of the zymogen increases (**Figure 1.1.b**). Some researchers suggest that the low intrinsic caspase activity is enough to cleave a procaspase-8 to caspase-8 given a high enough local concentration of the zymogen.²⁰

The second mechanism to explain the initiation of the caspase cascade and by far the most complex, is that used by caspase-9. The key factor for procaspase-9 activation is the association with its cofactor, Apaf-1.²¹⁻²⁴ The Apaf-1/caspase-9 complex is thought to be the 'active' form of caspase-9.²¹ Association with Apaf-1 in a large complex changes the conformation of procaspase-9 to its active form without cleavage. The active caspase-9/Apaf-1 forms a complex holoenzyme with cytochrome c known as the apoptosome which is the key regulatory protein of the extrinsic pathway (**Figure 1.1.c**).^{25,26}

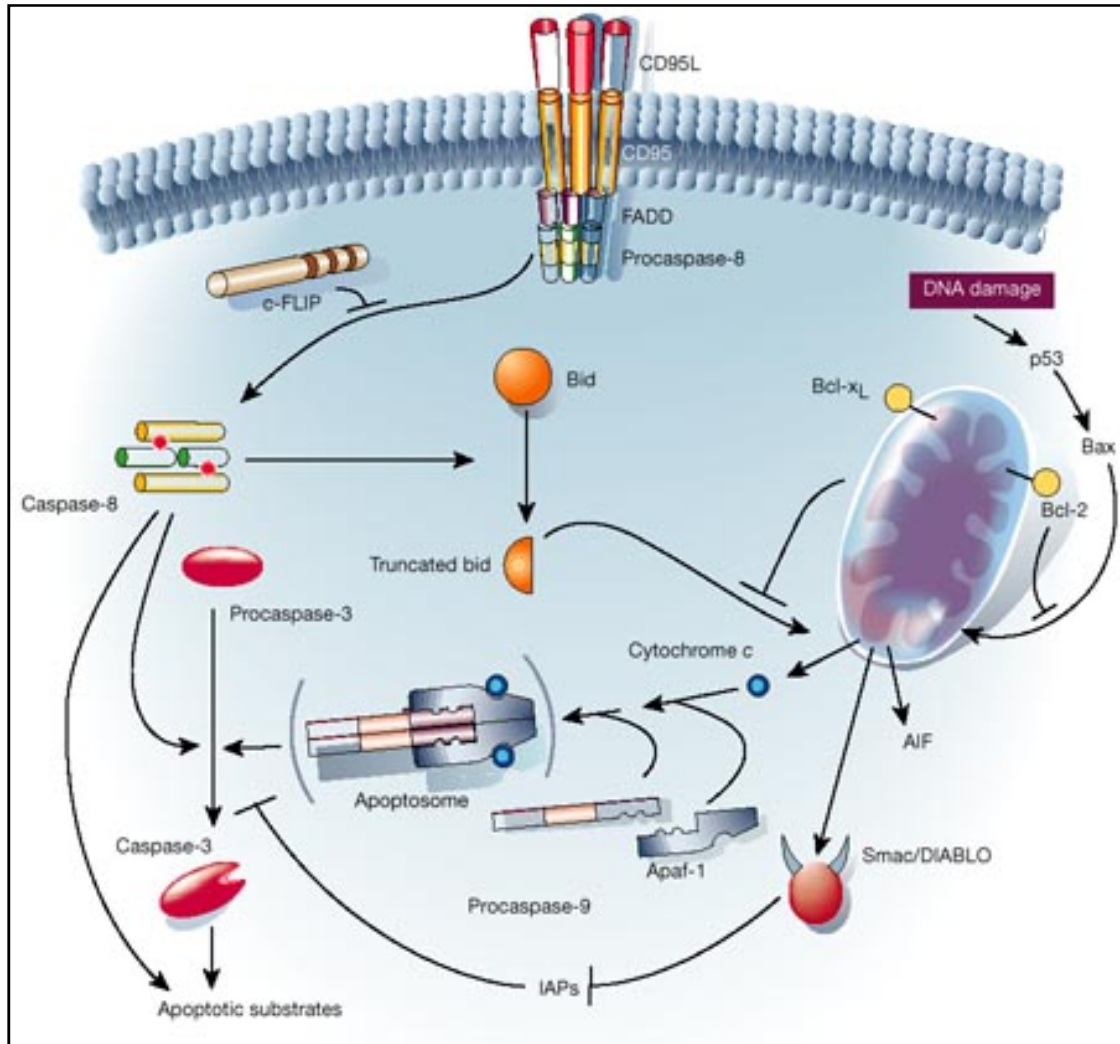


Figure 1.2. Apoptosis Overview ¹⁷

The mitochondrial pathway is one of the two major pathways for the upstream signaling necessary to promote caspase activation (**Figure 1.2**). The other pathway named the death receptor pathway is caused by receptor mediated signaling at the cell membrane by CD95 and TNF1 receptor. The binding of the ligand to the TNF1 receptor induces the formation of a multi-subunit death signaling complex which is composed in part by FADD (Fas-associated death domain protein).²⁷ Formation of the complex attracts and thus increases the concentration of procaspase-8 molecules, through its FADD

monomer. Procaspase-8 is then activated to caspase-8 through the proximity induced model by its increased local concentration.^{28,29} This caspase-8 activation can also be regulated by c-FLIP, a caspase homologue.³⁰⁻³² The mitochondrial pathway is initiated in response to cellular damage from ionizing radiation among other extracellular signals. Pools of pro-apoptotic proteins, BH3 only proteins, such as Bax, Bad, Bim and Bid are redirected by these signals to the mitochondria. At the surface of the mitochondria these pro-apoptotic signals are met by anti-apoptotic proteins and battle for control of the mitochondria takes place.^{33,34} If the cellular damage is severe enough the pro-apoptotic signaling proteins will win control of mitochondria and hence regulation of cytochrome c. The pro-apoptotic signaling allows the passive release of cyt. c which associates with Apaf-1 and then procaspase-9 to form a complex called the apoptosome.^{12,35,36}

The apoptosome and caspase-8 converge in the cascade with the activation of procaspase-3 to caspase 3.³⁷ Caspase-3 and caspase-7, the ‘effector’ caspases, in turn cleave and activate a myriad of substrates which cause DNA degradation, disruption of integral components of the cytoskeleton and the well known morphological changes associated with apoptosis.³⁷⁻³⁹

1.3. Regulation of Apoptosis

Evolutionarily speaking, one would expect a family of proteins that can cause the death of any cell within the body to be very tightly regulated. This is in fact the case with apoptosis and particularly so with caspases. The death receptor pathway is regulated at many levels, first at the expression of various membrane receptors for the “death signal inducing complex”.⁴⁰ Second, some cells employ “decoy” receptors upon the cell surface

that bind the death ligands with greater affinity than the actual death receptors and do not transduce the signal for formation of the FADD receptor complex. As already mentioned, the third means of regulation is mediated by procaspase-8 which is regulated by c-FLIP.³⁰⁻³² The mitochondrial pathway is also tightly regulated. Anti-apoptotic Bcl-2 members inhibit cytochrome c release from the mitochondria as well as many other means of regulation that is beyond the scope of this dissertation.^{41,42}

The indirect regulators of both the intrinsic and extrinsic pathways are just part of the regulatory machinery surrounding caspase activation. Direct regulation of the effector caspases is facilitated in part by IAPs (inhibitors of apoptotic proteins). These highly conserved proteins (cIAP1, cIAP2, XIAP and survivin) share baculovirus inhibitor repeat (BIR) domains and ring finger domains.^{43,44} XIAP (X-linked inhibitor of apoptotic proteins), is the most potent inhibitor of the IAP family.^{45,46} XIAP contains three BIR domains, the third of which is specific for caspase-9.⁴⁷ The linker region between BIR1 and BIR2 of XIAP inhibits caspases-3 and 7, but does not interact with caspase-9.⁴⁸⁻⁵⁰ Caspase-9's role as the initiator caspase within the apoptosome complex makes this interaction with XIAP very critical to the apoptotic cascade.

Crystallographic analysis of the XIAP / caspase-9 dimer illustrated that XIAP binds to the BIR3 domain of caspase-9 and traps the initiator caspase in its inactive form. Protein-protein interactions of this type are normally characterized by large areas of interactions defined by roughly 20Å of surface area (**Figure 1.3**).^{50,51} The protein-protein interaction of XIAP and caspase-9 is surprisingly facilitated by a small, well defined groove at the XIAP – BIR3 interface. This small pocket is accessed by the four N-terminal residues of caspase-9, ATPF,^{50,51} and represents a very attractive target for

enterprising chemists who are willing to design competitive small molecules. A correctly designed compound would be selective for neoplastic cells and would competitively inhibit the activity of XIAP thus allowing the apoptotic cascade to proceed which would reduce or eliminate apoptosis induced drug resistance within tumor cells.

Nature already provided chemists with the necessary template with which to build upon in the form of Smac / Diablo (second mitochondrial activator of caspase / direct IAP binding protein with low PI). When Smac is released from the mitochondria during the extrinsic induction it directly interacts with the same well-defined BIR3 binding groove on XIAP as caspase-9. Its binding is facilitated by four N-terminal residues, in this case, AVPI, which binds in a manner similar to ATPF of caspase-9.⁵²⁻⁵⁵

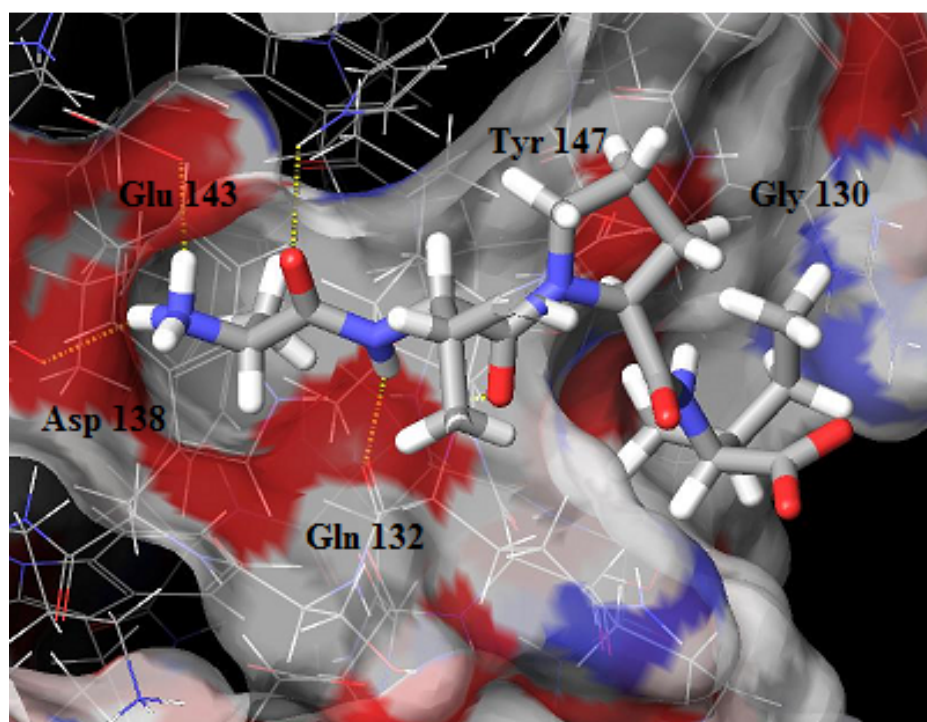


Figure 1.3. Interaction of AVPI with XIAP-BIR3 Binding Domain

1.4. Therapeutic XIAP Inhibitors

Preliminary studies into the efficacy of Smac therapeutics have demonstrated that peptides as short as four amino acids can effectively bind to the XIAP-BIR3 domain with the same affinity as the native protein (**Figure 1.3**).⁵³⁻⁵⁵ Much more importantly, however, binding also eliminated XIAP inhibition of caspase-9. Biological assays utilizing cell permeable fusion protein constructs of XIAP showed significant decrease in the resistance of neoplastic cells to therapeutic agents both *in vitro* and *in vivo*.⁵⁶⁻⁵⁹ Also of great significance is the fact that Smac peptides have shown excellent selectivity for only those cells that are cancerous.^{60,61} *In vivo* and *in vitro* studies of cell permeable Smac mimics have almost no toxicity for normal cells. This selectivity is tentatively thought to be from the upregulation of XIAP within cancer cells as opposed to normal cells and is supported by evidence from several groups. First, mice lacking XIAP develop normally, suggesting that XIAP is not essential in normal cells.⁶⁰ Second, ongoing clinical trials examining the ability of anti-sense oligonucleotides to target Bcl-2 (B cell lymphoma 2), another apoptotic inhibitor, have failed to demonstrate a major increase in normal tissue toxicity.⁶¹

The promising preliminary data from the highly selective peptide fragments was very encouraging, however, several major hurdles needed to be crossed in order to have a viable therapeutic agent. The first of which is that peptides do not make good drugs. In general peptide therapeutics are limited by poor *in vivo* stability and poor bioavailability due in part to the action of peptidases and the hydrophobicity of the peptides. Several groups have addressed these issues and developed peptide based small molecule inhibitors of XIAP which have improved upon the binding affinity and pharmacological properties of the AVPI tetrapeptide.

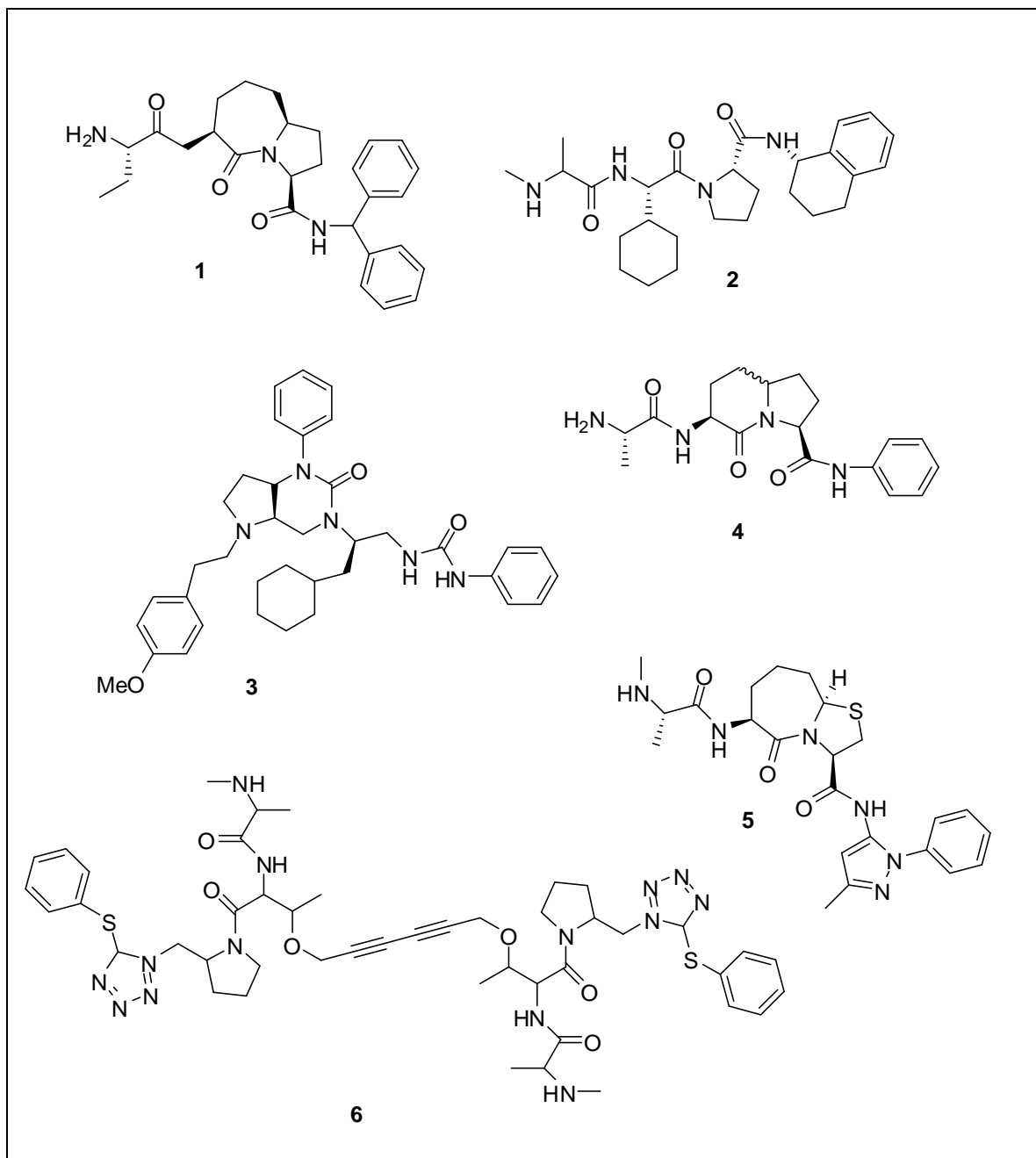


Figure 1.4. Previously Synthesized AVPI Peptidomimetics

Five compounds (**1**, **2**, **4**, **5**, **6**) were designed and synthesized based upon crystallographic data of the XIAP-BIR3 domain.^{50,58, 59,62,63} Not surprisingly these compounds inhibited the interaction of Smac and caspase-9 at the BIR3 domain. Compound **1** was synthesized by the Sun group.⁵⁰ HMQC-NMR analysis suggests a

binding affinity of 25 nM to the Smac binding site which sensitized tumor cells to apoptosis. The second compound, **2**, induces apoptosis directly in some cells lines and inhibits the growth of human breast cancer xenographs in mice.⁵⁹ NMR derived structure analysis and binding assays demonstrated a 16 nM affinity for the Smac binding site. Compound **3** was derived from screening a large library of compounds for the activation of caspase-3 in the presence of XIAP.⁵⁸ The researchers determined a 20 nM affinity for the BIR2 domain while not interfering with the Smac binding site. This caspase-3 dependent compound inhibited tumor growth in two mouse models. The Wang series of compounds (**4**) showed 0.29 μM K_i in an FP-based assay for the BIR3 domain as well as inducing apoptosis within human prostate PC-3 cancer cells.⁵⁰ Genentech also developed a series of compounds based upon the AVPW tetrapeptide interactions. Their compounds showed a 0.27 μM affinity for the XIAP-BIR3 interface and a structural preference for the (*R*) stereochemistry at the bridgehead position.⁵⁰ Compound **6**, was developed as a bivalent binding agent to the Smac site which has an affinity of 120 nM. They found that it sensitizes cells to apoptosis and is caspase-3 dependent.⁵⁰

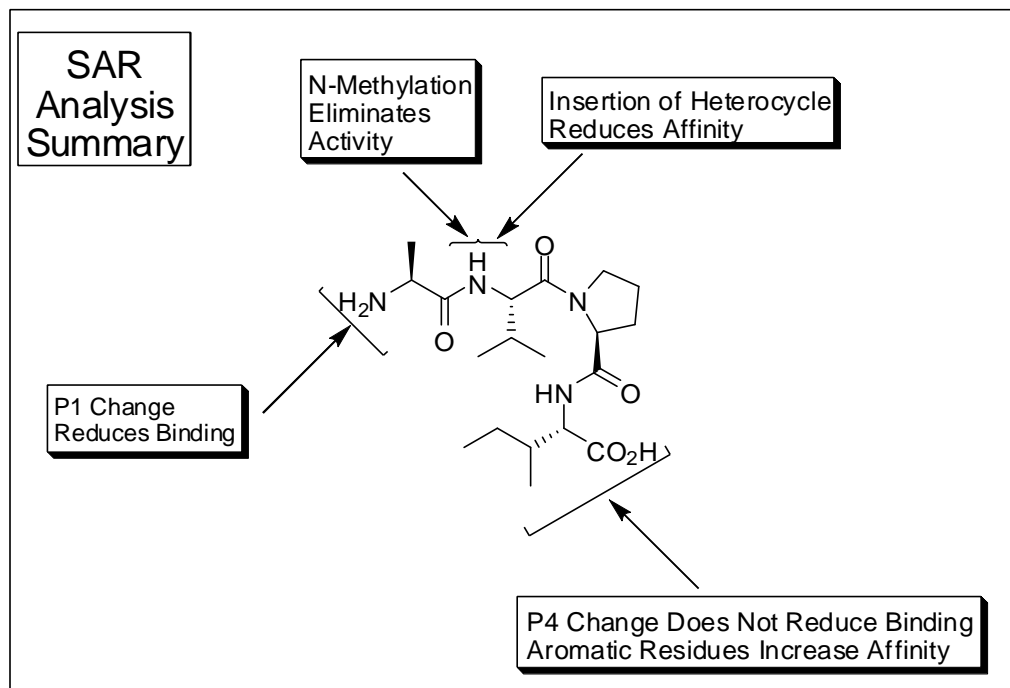


Figure 1.5. SAR Analysis of Allowed and Disallowed Modifications to the AVPI Backbone

Based upon the data from these compounds and the extrapolated SAR data we summarized the allowable changes to AVPI (**Figure 1.5**).⁶⁴ It was found that modification of Ala at the P1 position dramatically reduces binding affinity, whereas Ile at the P4 position did not have such a deleterious effect.⁶⁴ Aromatic residues such as Phe or Trp increased the binding affinity when placed at the P4 position.⁶⁴ Insertion of a heterocycle at the first peptide bond caused a modest reduction in binding activity but not as much as replacement of the Ala side chain. N-Methylation of the first peptide bond also dramatically reduced the binding affinity of the peptidomimetic.⁶⁴

1.5. Summary

In short, the current research being pursued in the area of XIAP inhibition provides ample data for the design and synthesis of an improved inhibitor of XIAP. This can be achieved through the systematic constraint of the amino acid backbone to elucidate the bioactive conformation and provide enhanced *in vivo* stability. The research undertaken in this thesis was explored with this goal in mind.

1.6. References

1. Kaufmann, S. H.; Vaux, D. L. Alterations in the apoptotic machinery and their potential role in anticancer drug resistance. *Oncogene* **2003**, *22*, 7414 – 7430.
2. Greenless, R. T.; Hill-Harmon, M. B.; Murray, T.; Thun, M. Cancer Statistics, 2001. *CA-A Cancer J. Clin.* **2001**, *51*, 15 – 36.
3. Theodoropoulos, P. A.; Polioudake, H.; Kostake, O.; Derdas, S. P.; Georogoulis, V.; Dargemont, C.; Georgatos, S. D. Taxol affects nuclear lamina and pore complex organization and inhibits import of karyophilic proteins into the cell nucleus. *Cancer Res.* **1999**, *59*, 4625 – 4633.
4. Blajewski, A. L.; Kaufmann, S. H. A multistep model for paclitaxel-induced apoptosis in human breast cancer cell lines. *Exp. Cell. Res.* **2001**, *270*, 277 – 288.

5. Hashimoto, H.; Chatterjee, S.; Berger, N. A. Mutagenic activity of topoisomerase I inhibitors. *Clin. Cancer Res.* **1995**, *1*, 369 – 376.
6. Ryan, A. J.; Squires, S.; Strutt, H. L.; Johnson, R. T. Camptothecin cytotoxicity in mammalian cells is associated with the induction of persistent double strand breaks in replicating DNA. *Nucleic Acid Res.* **1991**, *19*, 3295 – 3300.
7. Vaux, D. L.; Cory, S.; Adams, J. M. Bcl-2 Gene promotes haemopoietic cell survival and cooperates with c-myc to immortalize pre-B cells. *Nature* **1998**, *355*, 400 – 442.
8. Kaufmann, S. H.; Gores, G. J. Apoptosis in cancer cause and cure. *Bioessays* **2000**, *22*, 1007 – 1017.
9. Liu, X.; Zou H.; Slaughter, C.; Wang, X. DFF, a heterodimeric protein that functions downstream of caspase-3 to trigger DNA fragmentation during apoptosis. *Cell* **1997**, *89*, 175 – 184.
10. Enari, M.; Sakahira, H.; Yokohama, H.; Okawa, K.; Iwamatsu, A.; Nagata, S. A caspase-activated DNase that degrades DNA during apoptosis, and its inhibitor ICAD. *Nature* **1998**, *391*, 43 – 50.
11. Porter, A. G.; Ng. P.; Janicke, R. U. Death substrates come alive. *Bioessays* **1997**, *19*, 501 – 507.
12. Earnshaw, W. C.; Martins, L. M.; Kaufmann, S. H. Mammalian caspases: structure, activation, substrates and functions during apoptosis. *Ann. Rev. Biochem.* **1999**, *68*, 383 – 424.

13. Nicholson, D. W. Caspase structure, preteolytic substrates, and function during apoptotic cell death. *Cell Death Diff.* **1999**, *6*, 1028 – 1042.
14. Slee, E. A.; Adrain, C.; Martin, S. J. Serial killers: ordering caspase activation events in apoptosis. *Cell Death Diff.* **1999**, *6*, 1067-1074.
15. Kottke, T. J.; Blajeski, A. L.; Meng, X.; Svingen, P. A.; Ruchaud, S.; Mesner Jr, P. W.; Boerner, S. A.; Samejima, K.; Henriquez, N. V.; Chilcote, T. J.; Lord, J.; Salmon, M.; Earnshaw, W. C.; Kaufmann, S. H. Lack of correlation between caspase activation and caspase activity assays in paclitaxel-treated MCF-7 breast cancer cells. *J. Biol. Chem.* **2002**, *277*, 804 – 815.
16. Slee, E. A.; Harte, M. T.; Kluck, R. M.; Wolf, B. B.; Casiano, C. A.; Newmeyer, D. D.; Wang H-G.; Reed, J. C.; Nicholson, D. W.; Alnemri, E. S.; Green D. R.; Martin, S. J. Ordering the cytochrome c-initiated cascade: hierarchical activation of caspases-2, -3, -6, -7, -8, and -10 in a caspase-9-dependent manner. *J. Cell. Biol.* **1999**, *144*, 281 – 292.
17. Hengartner, M. O. The biochemistry of apoptosis *Nature* **2000**, *407*, 770 – 776.
18. Muzio, M.; Stockwell, B. R.; Stennicke, H. R.; Salvesen, G. S.; Dixit, V. M. An induced proximity model for caspase-8 activation. *J. Biol. Chem.* **1998**, *273*, 2926 – 2930.

19. Yang, X.; Chang, H. Y.; Baltimore, D. Essential role of CED-4 oligomerization in CED-3 activation and apoptosis. *Science* **1998**, *281*, 1355 – 1357.
20. Salvesen, G. S.; Dixit, V. M. Caspase activation: the induced proximity model. *Proc. Natl. Acad. Sci. USA*, **1999**, *96*, 10964 – 10967.
21. Rodriguez, J.; Lazebrink, Y. Caspase-9 and APAF-1 form an active holoenzyme. *Genes Dev.* **1999**, *13*, 3179 – 3184.
22. Zou, H.; Henzel, W. J.; Lie, X.; Lutschg, A.; Wang, X. Apaf-1, a human protein homologous to *C. elegans* CED-4, participates in cytochrome c-dependent activation of caspase-3. *Cell* **1997**, *90*, 405 – 413.
23. Li, P. Cytochrome c and dATPF-dependent formation of Apaf-1/caspase-9 complex initiates an apoptotic protease cascade. *Cell* **1997**, *91*, 479 – 489.
24. Stennicke, H. R. Caspase-9 can be activated without proteolytic processing. *J. Biol. Chem.* **1999**, *274*, 8359 – 8362.
25. Beere, H. M. Heat shock protein 70 inhibits apoptosis by preventing recruitment of procaspase-9 to the Apaf- apoptosome. *Nature Cell Biol.* **2000**, *2*, 469 – 475.
26. Cain, K.; Brown, D. G.; Langlais, C.; Cohen, G. M. Caspase activation involves the formation of the apoptosome, a large (approximately 700 kDa) caspase-activation complex. *J. Biol. Chem.* **1999**, *274*, 22686 – 22692.

27. Schulze-Osthoff, K.; Ferrari, D.; Los, M.; Wesselborg, S.; Peter, M. E. Apoptosis signaling by death receptors. *Eur. J. Biochem.* **1998**, *254*, 439 – 459.
28. Peter, M. E.; Krammer, P. H. Mechanisms of CD95 (APO-1/Fas)-mediated apoptosis. *Curr. Opin. Immunol.* **1998**, *10*, 545-551.
29. Ashkenazi, A.; Dixit, V. M. Apoptosis control by death and decoy receptors. *Curr. Opin. Cell Biol.* **1999**, *11*, 255 – 260.
30. Irmeler, M. Inhibition of death receptor signals by cellular FLIP. *Nature* **1997**, *388*, 190 – 195.
31. Thome, M.; Schneider, P.; Hofmann, K.; Fickenscher, H.; Meinl, E.; Neipel, F.; Mattmann, C.; Burns, K.; Bodmer, J. L.; Schroter, M.; Scaffidi, C.; Krammer, P. H.; Peter, M. E.; Tschopp J. Viral FLICE-inhibitory proteins (FLIPs) prevent apoptosis induced by death receptors. *Nature* **1997**, *386*, 517 – 521.
32. Medema, J. P.; de Jong, J.; van Hall, T.; Melief, C. J.; Offringa, R. Immune escape of tumors *in vivo* by expression of cellular FLICE-inhibitory protein. *J. Exp. Med.* **1999**, *190*, 1033 – 1038.
33. Adams, J. M.; Cory, S. The Bcl-2 protein family: arbiters of cell survival. *Science* **1998**, *281*, 1322 – 1326.
34. Huang, D. C. S.; Strasser, A. BH3-only proteins-essential initiators of apoptotic cell death. *Cell* **2000**, *103*, 839 – 842.

- 35.** Budihardjo, I.; Oliver, H.; Lutter, M.; Luo, X.; Wang, X. Biochemical pathways of caspase activation during apoptosis. *Ann. Rev. Cell Dev. Biol.* **1999**, *15*, 269 – 290.
- 36.** Rodriguez, J.; Lazebnik, Y. Caspase-9 and APAF-1 form an active holoenzyme. *Genes Dev.* **1999**, *13*, 3179 – 3184.
- 37.** Liu, X.; Zou, H.; Slaughter, C.; Wang, X. DFF, a heterodimeric protein that functions downstream of caspase-3 to trigger DNA fragmentation during apoptosis. *Cell* **1997**, *89*, 175 – 184.
- 38.** Enari, M. A caspase-activated DNase that degrades DNA during apoptosis, and its inhibitor ICAD. *Nature* **1998**, *391*, 43-50.
- 39.** Sakahira, H.; Enari, M.; Nagata, S. Cleavage of CAD inhibitor in CAD activation and DNA degradation during apoptosis. *Nature* **1998**, *391*, 96 – 99.
- 40.** Ashkenazi, A.; Dixit, V. M. Apoptosis control by death and decoy receptors. *Curr. Opin. Cell. Biol.* **1999**, *11*, 255 – 260.
- 41.** Reed, J. C.; Bcl-2 family proteins. *Oncogene* **1998**, *17*, 3225 – 3236.
- 42.** Gross, A.; McDonnell, J. M.; Korsmeyer, S. J. BCL-2 family members and the mitochondria in apoptosis. *Genes Dev.* **1999**, *13*, 1899 – 1911.
- 43.** Crook, N. E.; Clem, R. J.; Miller, L. K. An apoptosis-inhibiting baculovirus gene with a zinc finger-like motif. *J. Virol.* **1993**, *67*, 2168 – 2174.

44. Huang, H. K.; Joazeiro, C. A. P.; Bonfoco, E.; Kamada, S.; Levenson, J. D.; Hunter, T. The inhibitor of apoptosis, cIAP2, functions as a ubiquitin-protein ligase and promotes *in vitro* monoubiquitination of caspases 3 and 7. *J. Biol. Chem.* **2000**, *275*, 26661 – 26664.
45. Suzuki, Y., Nakabayashi, Y.; Takahashi, R. Ubiquitin-protein ligase activity of X-linked inhibitor of apoptosis protein promotes proteasomal degradation of caspase-3 and enhances its anti-apoptotic effect in Fas-induced cell death. *Proc. Natl. Acad. Sci. USA* **2001**, *98*, 8662 – 8667.
46. Yang, Y.; Fang, S.; Jensen, J. P.; Weissman, A. M.; Ashwell, J. D. Ubiquitin protein ligase activity of IAPs and their degradation in proteasomes in response to apoptotic stimuli. *Science* **2000**, *288*, 874 – 877.
47. Srinvasula, S. M.; Hegde, R.; Saleh, A.; Datta, P.; Shiozaki, E.; Chai, J.; Lee, R. A.; Robbins, P. D.; Fernandes-Alnemri, T.; Shi, Y.; Alnemri, E. S. A conserved XIAP-interaction motif in caspase-9 and Smac/DIABLO regulates caspase activity and apoptosis. *Nature* **2001**, *410*, 112 – 116.
48. Wu, G.; Chai, J.; Suber, T. L.; Wu, J. W.; Du, C.; Wang, X.; Shi, Y. *Nature* **2000**, *408*, 1008 – 1012.
49. Lie, Z.; Sun, c.; Olejniczak, E. T.; Meadows, R.; Betz, S. F.; Oost, T.; Herrmann, J.; Wu, J. C.; Fesik, S. W. Structural basis for binding of Smac/DIABLO to the XIAP BIR3 domain. *Nature* **2000**, *408*, 1004 – 1008.

50. Sun, H.; Nikolovska-Coleska, Z.; Chen, J.; Yang, C.; Tomita, Y.; Pan, H.; Yoskioka, Y.; Krajewski, K.; Roller, P. P.; Wang, S. Structure – based design, synthesis and biochemical testing of novel and potent Smac peptido-mimetics. *Biorg. Med. Chem. Lett.* **2005**, *15*, 793 – 797.
51. Wu, G.; Chai, J.; Suber, T. L.; Wu, J.; Du, C.; Wang, X.; Shi, Y. Structural basis of IAP recognition by Smac / DIABLO. *Nature* **2000**, *408*, 1008-1012.
52. Salvesen, G. S.; Duckett, C. S. IAP proteins: blocking the road to death's door. *Nat. Rev. Mol. Cell Bio.* **2002**, *3*, 401 – 410.
53. Srinivasula, S. M. *sickle* a novel *Drosophila* death gene in the *reaper-hid-grim* region, encodes an IAP-inhibitory protein. *Curr. Biol.* **2002**, *12*, 125 – 130.
54. Christich, A. The damage-responsive *Drosophila* gene *sickle* encodes a novel IAP binding protein similar to but distinct from *reaper*, *grim*, and *hid*. *Curr. Biol.* **2000**, *12*, 137 – 140.
55. Wright, C. W.; Clem, R. J. Sequence requirements for hid binding and apoptosis regulation in the anti-apoptotic baculovirus protein Op-IAP: hid binds Op-IAP in a manner similar to Smac binding of XIAP. *J. Biol. Chem.* **2001**, *277*, 2454 – 2462.
56. Glover, C. J.; Hite, K.; Delosh, R.; Scudiero, D. A.; Fivash, M. J.; Smith, L. R.; Fisher, R. J.; Wu, J. W.; Shi, Y.; Kipp, R. A.; McLendon, G. L.; Sausville, E. A.; Shoemaker, R. H. A high throughput screen for identification of molecular mimics of

Smac/Diablo utilizing a fluorescence polarization assay. *Anal. Biochem.* **2003**, *320*, 157 – 169.

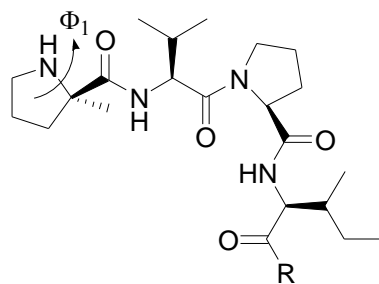
- 57.** Wu, T. Y.; Wagner, K. W.; Bursulaya, B.; Schultz, P. G.; Deveraux, Q. L.
Development and characterization of nonpeptidic small molecule inhibitors of the XIAP/caspase-3 interaction. *Chem. Bio*, **2003**, *10*, 759 – 767.
- 58.** Schimmer, A.D.; Welsh, K.; Pinilla, C.; Wang, Z.; Krajewska, M.; Bonneau, M. J.; Pedersen, I. M.; Kitada, S.; Scott, F. L.; Bailly-Maitre, B.; Glinsky, G.; Scudiero, D.; Sausville, E.; Salvesen, G.; Nefzi, A.; Ostresh, J. M.; Houghten, R. A.; Reed, J. C.
Small-molecule antagonists of apoptosis suppressor XIAP exhibit broad antitumor activity. *Cancer Cell*, **2004**, *5*, 25 – 35.
- 59.** Oost, T. K.; Sun, C.; Armstrong, R. C.; Al-Assaad, A. S.; Betz, S. F.; Deckwerth, T. L.; Ding, H.; Elmore, S. W.; Meadows, R. P.; Olejniczak, E. T.; Oleksijew, A.; Oltersdorf, T.; Rosenberg, S. H.; Shoemaker, A. R.; Tomaselli, K. J.; Zou, H.; Fesik, S. W.
Discovery of potent antagonists of the antiapoptotic protein XIAP for the treatment of cancer. *J. Med. Chem.* **2004**, *47*, 4417 – 4426.
- 60.** Banerjee, D.; Genasense (Genta Inc). *Curr. Opin. Inves. Drugs.* **2001**, *2*, 574-580.
- 61.** Tolcher, A. W. Regulators of apoptosis as anticancer targets. *Hematology/Oncology Clinics of N. Amer.* **2002**, *16*, 1255 – 1267.
- 62.** Zobel, K.; Wang, L.; Varfolomeev, E.; Franklin, M. C.; Elliott, L. O.; Wallweber, J. J. A.; Okawa, D. C.; Flygare, J.A.; Vucic, D.; Fairbrother, W. J.; Deshayes, K. Design,

synthesis, and biological activity of a potent Smac mimetic that sensitizes cancer cells to apoptosis by antagonizing IAPs. *ACS Chem. Biol* **2006**, *1*, 525 – 533.

63. Li, L.; Thomas, R. M.; Suzuki, H.; Debrabander, J. K.; Wang, X.; Harran, P. G. A small molecule Smac mimic potentiates TRAIL- and TNFalpha-mediated cell death. *Science* **2004**, *305*, 1471 – 1474.

64. Park, C.; Sun, C.; Olejniczak, E. T.; Wilson, A. E.; Meadows, R. P.; Betz, S. F.; Elmore, S. W.; Fesik, S. W. Non-peptidic small molecule inhibitors of XIAP. *Bioorg. Med. Chem. Lett.* **2005**, *15*, 771 – 775.

Chapter 2. The Stereoselective Synthesis of ϕ_1 Constrained AVPI Peptidomimetics



- 2.1: R = OH
 2.2: R = OMe
 2.3: R = NHMe

2.1. Design and Scope

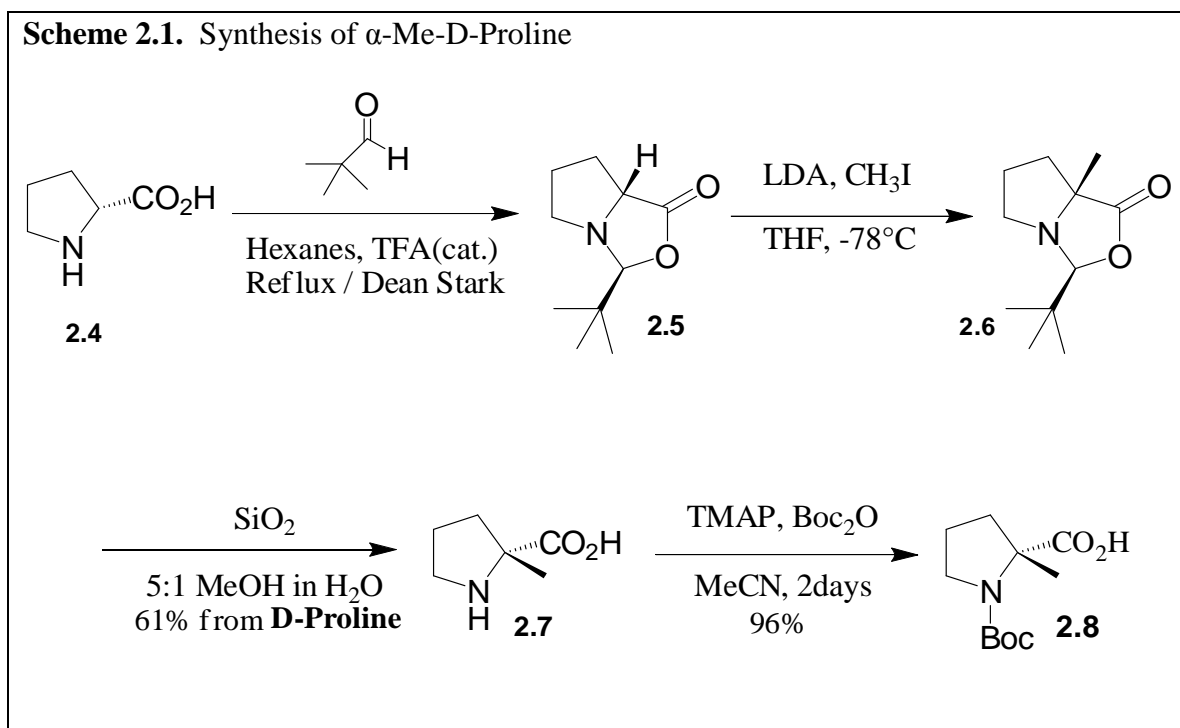
As discussed above, studies within the Kauffman group and others have demonstrated that the Smac N-terminal tetrapeptide, AVPI, can penetrate the cell membrane¹ and improve the chemotherapeutic potential of various drug therapies.² This peptide would not, however, be a viable therapeutic agent due to its susceptibility to degradation by peptidases and its limited cell permeability. In order to retain the low nM activity of the native protein as well as to improve the pharmacological properties of the tetrapeptide our research group constrained the ϕ_1 torsion angle at the P1 position.

SAR analysis, previously described in **Chapter 1**, provided evidence for the critical nature of the P1 Ala of the AVPI and AYPW native peptides. The P1 N-terminal amino group of these peptides forms hydrogen bonds to Glu142 and Asp138 and positions the alanine side chain which is absolutely critical in retaining biological activity.^{4,5} While designing this series of peptidomimetics we constrained the ϕ_1 torsion angle of the P1 residue to mimic the biological orientation of the native peptide. Initial modeling by the Pang group, utilizing its proprietary EUDOC docking program,³ suggested that a propylene constraint between the alpha carbon and C-terminal nitrogen would establish the necessary torsion angle to position the alanine side chain in the same

topological space as the native side chain. We also modified the C-terminus of the peptidomimetics to the methyl ester and the methyl amide to study the effect of these modifications upon cell permeability. These modifications will decrease the degrees of freedom of the peptide mimics, hopefully constraining the compound to a greater degree to its bioactive conformation. Constraints should also increase the bioavailability of the tetrapeptides as well as increasing their *in vivo* stability.

2.2. Sequential Synthetic Strategy

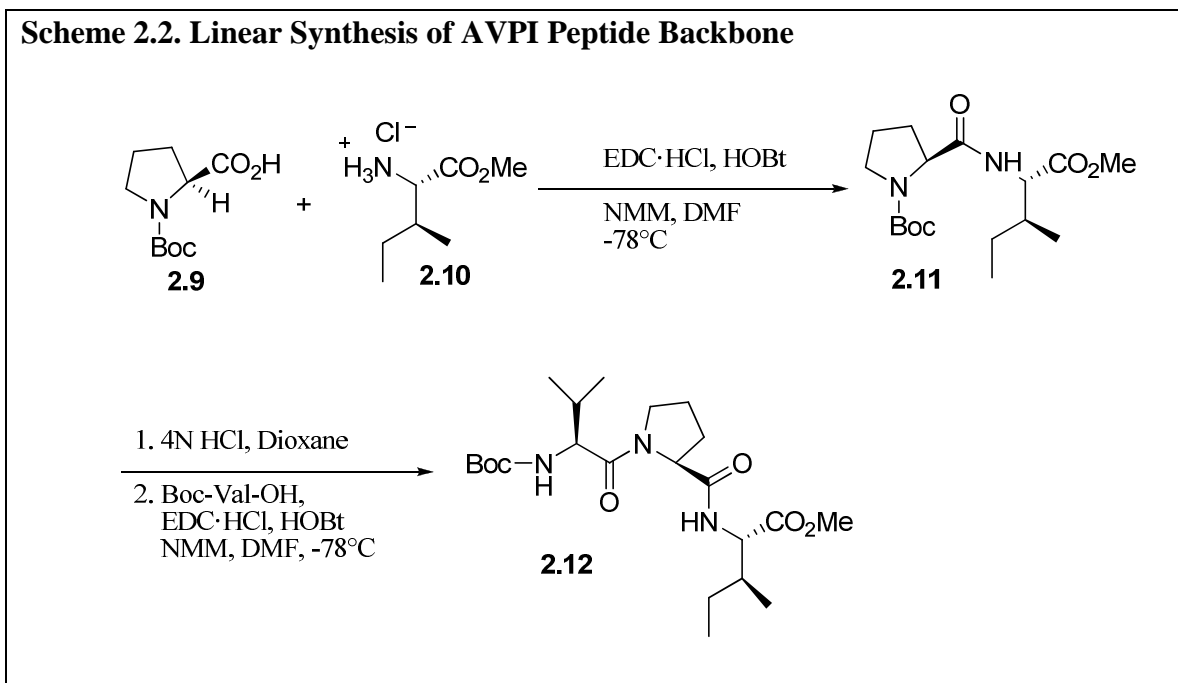
The initial strategy that I pursued was a simple sequential strategy of peptide backbone building blocks coupled together using solution phase chemistry. The first synthetic challenge was the stereoselective alkylation of D-proline. Seebach's method of self-reproduction of chirality,⁶ which has been used extensively within our lab and modified to its current optimized form by Dr. Ashish Vartak, was selected as the preferred means of alkylation.



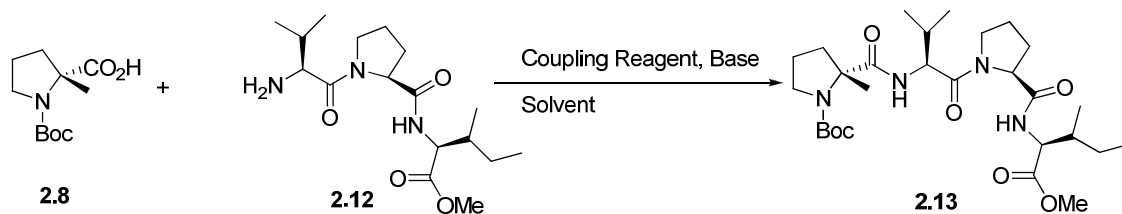
Dr. Vartak modified the Seebach methodology by using hexanes instead of pentanes within the procedure, which decreased the reaction time from 4 days to 1 day. This reduction in time was due mainly to the ability of hexanes to azeotrope a higher percentage of water than pentanes. The lessened reaction time decreased the amount of coloration (due to side products) of the reaction mixture as well as reducing the equivalents of pivalaldehyde needed from 5 to 3. Once proline was condensed with pivalaldehyde to form the oxazolidinone **2.5**, the enolate was formed using LDA as a base and alkylated with iodomethane. The alkylated oxazolidinone, **2.6**, was taken forward immediately to the hydrolysis breakdown reaction which consisted of stirring compound **2.6** with silica gel in 5:1 MeOH / H₂O for 2 days. Workup gives the light yellow product **2.7**. The crude material can then be triturated with ether and crystallized from isopropyl alcohol and ether to give white needles of α -Me-D-proline in 61% yield from the initial amino acid **2.4**. Boc-protection conditions for this hindered amino acid

were worked out in our laboratory by Dr. Ehab Khalil⁷ who discovered that the use of the phase-transfer catalyst tetramethyl ammonium hydroxide · 5 H₂O (TMAP) and an organic solvent (MeCN) was sufficient to provide the desired product **2.8** in 97% yield.

While this building block was being synthesized, the peptide backbone was coupled together with standard solution phase chemistry. The appropriately protected amino acids were dissolved in anhydrous DMF and cooled to -78 °C. To this stirred solution EDC·HCl (1-[3-(dimethylamino)propyl]-3-ethylcarbodiimide hydrochloride), HOBt (hydroxybenzotriazole) and NMM (N-methyl morpholine) were added. The reaction mixture was allowed to warm overnight to room temperature and then stirred for an additional 1-3 days at room temperature (**Scheme 2.2**). These coupling reactions proceeded in 88% for the dipeptide **2.11** coupling and 82% for the synthesis of tripeptide **2.12**.



Attaching the final building block in a sequential manner proved problematic. The combined hindered nature of the alkylated proline along with the steric bulk of the tripeptide reduced the yield of this reaction to a very poor 15% (**Table 2.1**). In attempts to optimize the reaction conditions, we left out HOBT, since there was no potential for racemization, and used EDC·HCl alone. This afforded a slightly improved, but not very useful yield of 26%. Further coupling conditions including Mukaiyama's reagent⁸ and HOAt did not afford any isolatable product.

Table 2.1. Reactions Conditions and Yields in the Synthesis of Compounds 2.13

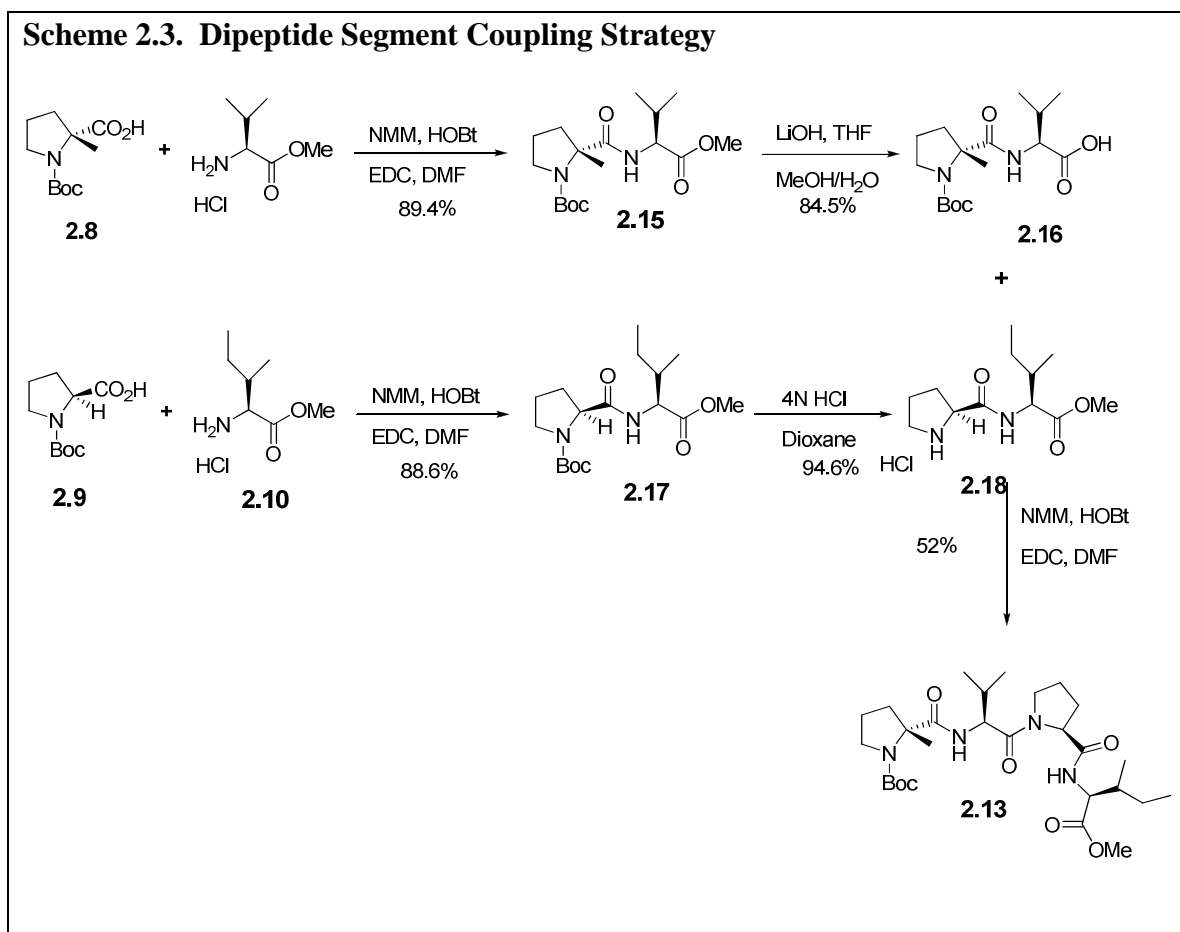
Reaction	Coupling Reagent	Base	Solvent	Yield	(+/-) ^a
1	HOBt, EDC·HCl	TEA	DCM/DMF	15%	-
2	EDC·HCl	TEA	DCM/DMF	26%	-
3	EDC·HCl, HOAt	TEA	DCM/DMF	N.R. ^b	
4	Mukaiyama Reagent	TEA	DCM	N.R.	

^a(+/-) refers to the presence or absence of diastereoisomers. ^b N.R. = No Reaction

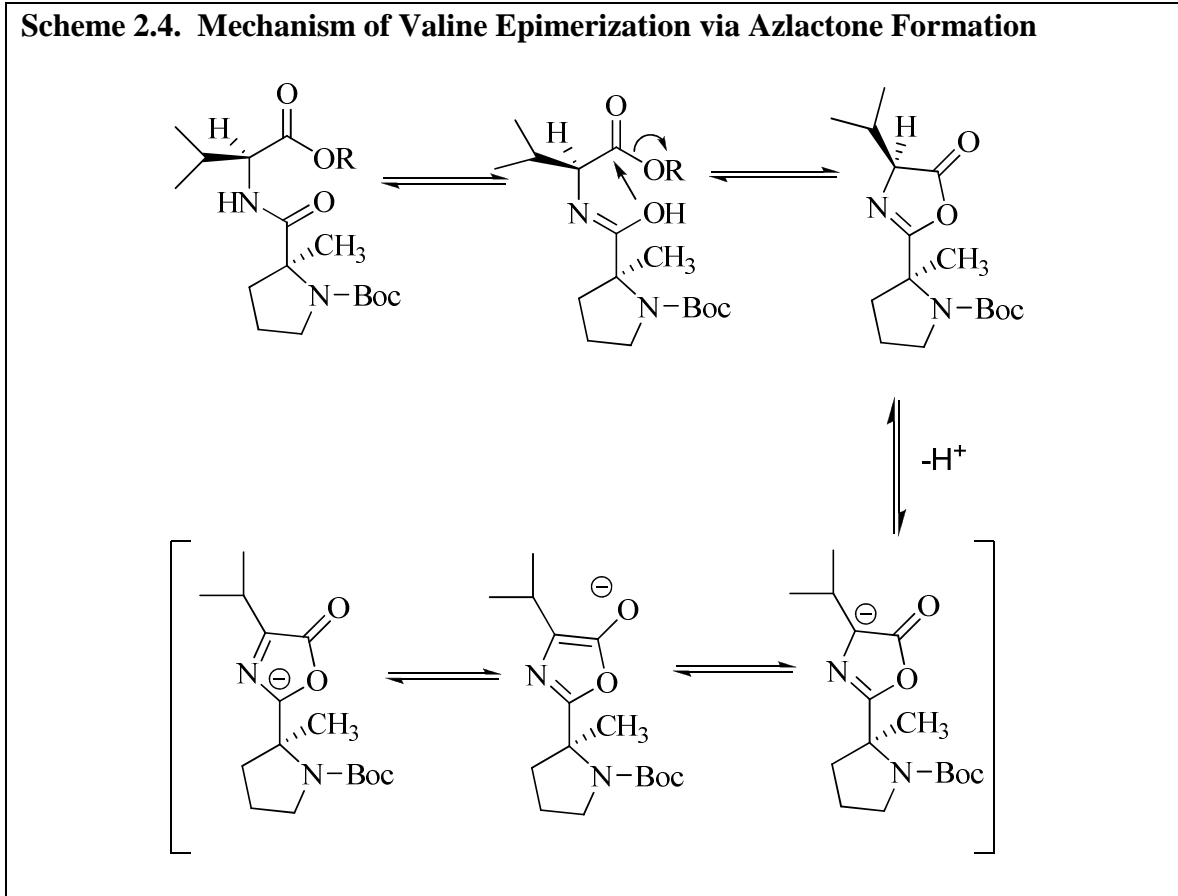
2.3. Dipeptide Segment Coupling Strategy

While the coupling conditions in **Table 2.1** were being assessed, two parallel strategies for the peptide backbone formation were being tried to solve this coupling problem. The first strategy was the coupling of Boc- α -Me-D-Pro-Val-OH and HCl·H₂N-Pro-Ile-OMe. This strategy minimizes the steric bulk that was encountered coupling to the highly hindered alkylated proline **2.8**. The same solution phase chemistry conditions that were used above in **Scheme 2.2** were used in the synthesis of Boc- α -Me-D-Pro-Val-OH. This reaction proceeded in a useful 56% yield, while the other segment, HCl·H₂N-Pro-Ile-OMe, was obtained in a 91% yield as illustrated in **Scheme 2.3**. Ester hydrolysis and Boc deprotection followed by the final coupling reaction between the two dipeptide

segments yielded the tetrapeptide in an efficient 72% yield after purification by flash chromatography.



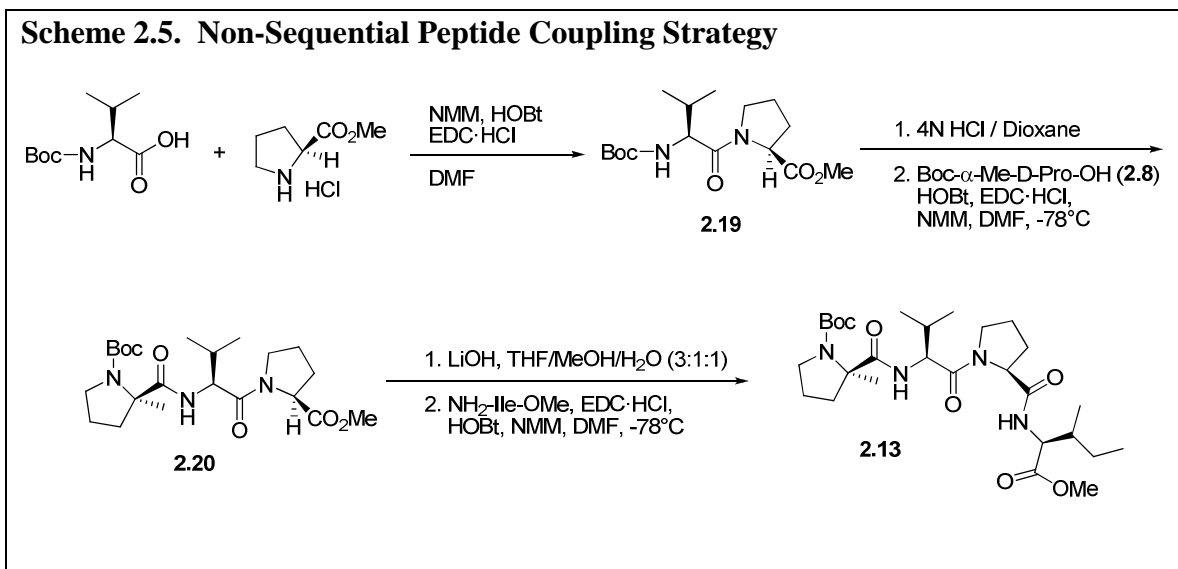
However, upon further analysis two compounds were isolated upon column chromatography; each corresponding to a diastereomer due to epimerization of the alpha center of valine. The major component possessed the necessary L-Val stereochemistry, while the epimerized product accounted for between 26% and 44% of the total yield. A thorough literature search discovered that racemization in C-terminal couplings is known to occur through the formation of an azlactone derivative⁹ (**Scheme 2.4**).



These azlactones tend to racemize based upon the ease with which the acidic proton can be abstracted from the alpha center of the amino acid, in our case valine. The acidity of this proton is due, for the most part, to the resonance stabilization of the resulting carbanion.⁹ Thus, resulting in racemization at the alpha position of valine under very mildly basic conditions.

2.4. Non-Sequential Alternative Method

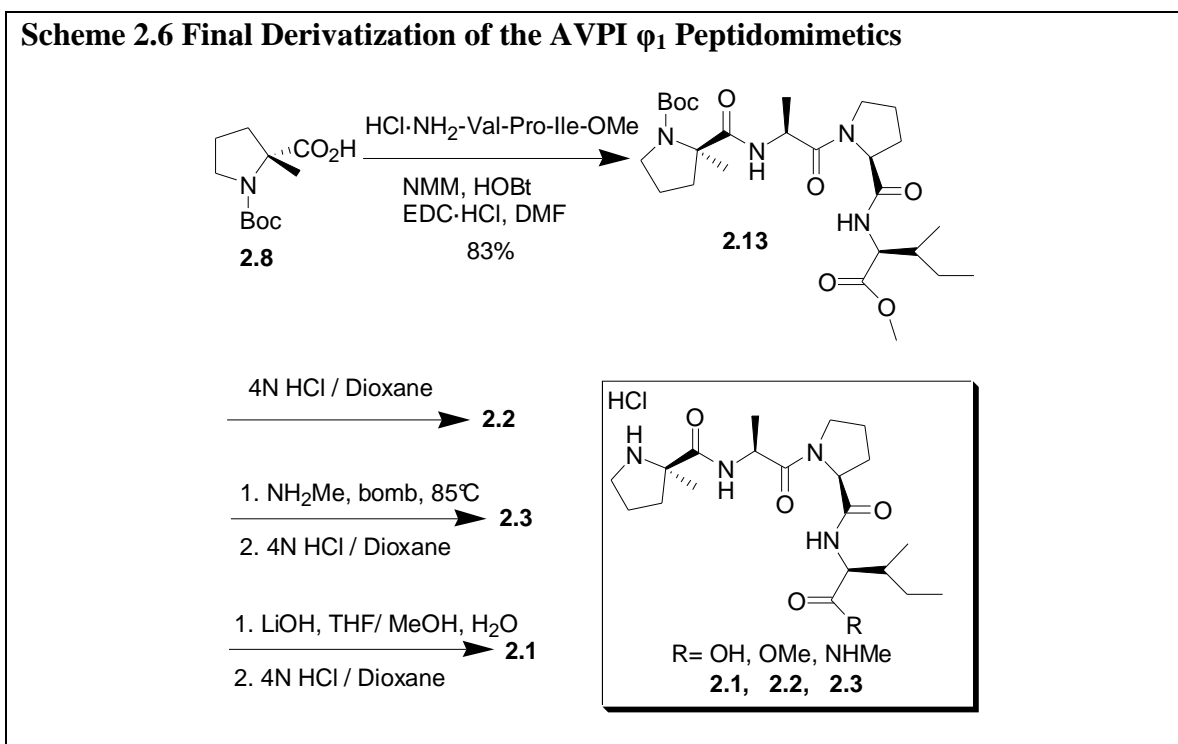
The second alternative method for synthesizing the peptide backbone was attempted with the intention of avoiding all mechanisms of racemization while also reducing the bulk of the peptide coupled to the α -Me-proline. This strategy was explored in parallel with the other two coupling strategies; the dipeptide segment coupling strategy (**Scheme 2.3**) and the sequential coupling strategy (**Scheme 2.2**). In order to minimize any chance for racemization compound **2.19** was synthesized first as illustrated in **Scheme 2.5**. This dipeptide was then coupled to the hindered α -Me-proline (**2.8**), which has no racemizable alpha proton, to yield the tripeptide **2.20**. Finally, the methyl ester of this tripeptide was hydrolyzed using LiOH in a 3:1:1 solution of THF:MeOH:H₂O. The free acid of **2.20** was then coupled to isoleucine methyl ester (**2.14**) to yield the key intermediate **2.13** without formation of diastereomers. Solution-phase coupling conditions once again proceeded rapidly with yields between 62% and 88% in the building of the peptide backbone. In the synthesis a side product was isolated in several reactions accounting for an average of 15% of the isolated yield but in one isolated instance it was 44% of the total isolated yield. Upon analysis of the isolated side product, it was found that two unknown peaks at 2.87 and 3.00 ppm were present in the ¹H NMR spectrum.



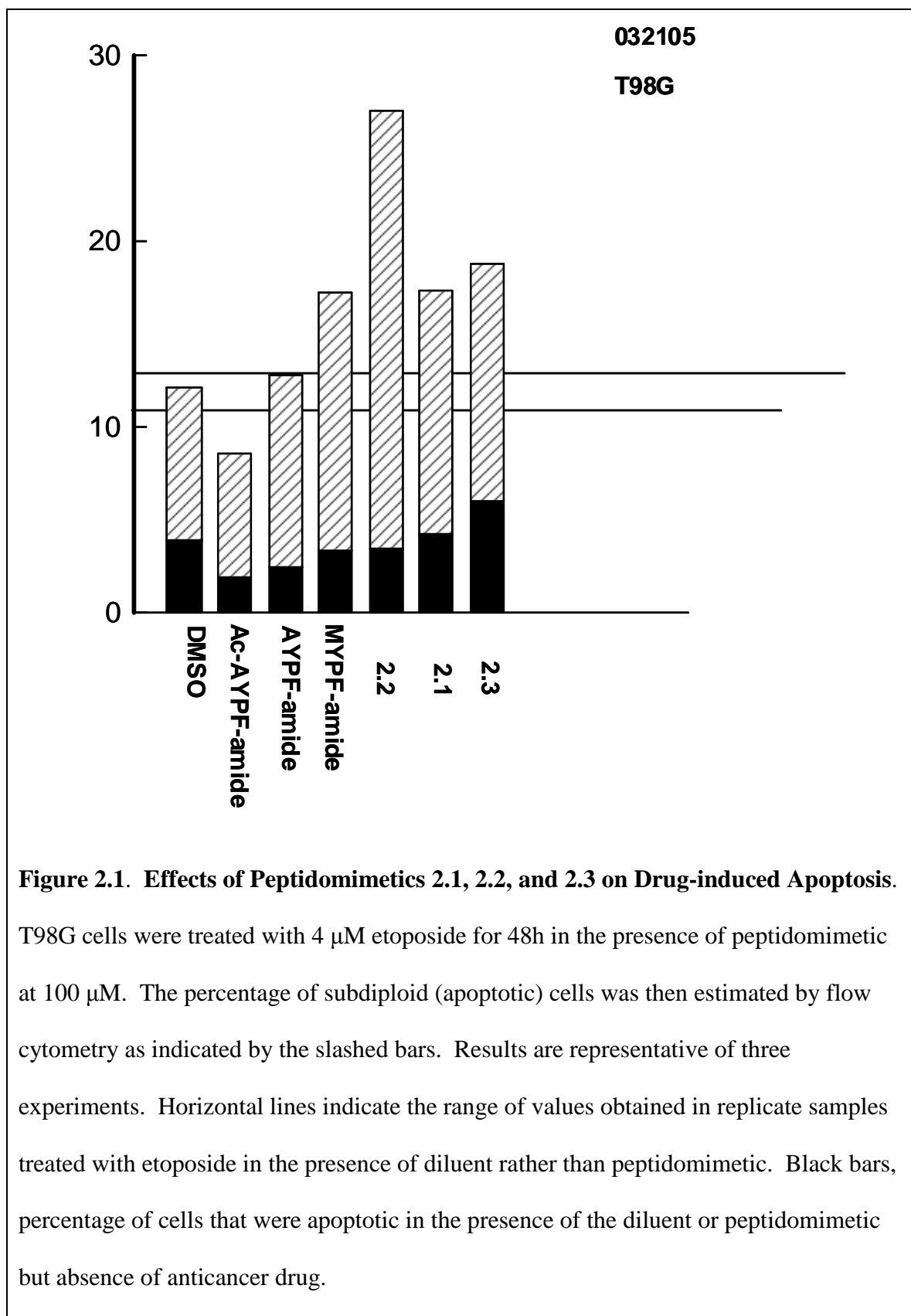
After thorough searching for a possible explanation for such a byproduct it was found that N,N-dimethylformamide is known to decompose to carbon monoxide gas and dimethyl amine near its boiling point of 153°C. Furthermore, DMF decomposes more rapidly in the presence of basic or acidic materials so that a significant portion of DMF may be degraded even at room temperature.⁹ The NMR analysis of the N-t-Boc-L-Val-L-Pro-OMe coupling reaction byproduct showed a spectrum that corresponded to the literature reported spectrum for N-t-Boc-L-Val-N(CH₃)₂.¹⁰ We hypothesized that DMF left upon the alumina column of the departmental solvent system degrades if left unused for any significant length of time. These degradation products are gaseous at room temperature, however, dimethyl amine (b.p. 6.9 °C) would be trapped within the collection vial and upon cooling during the coupling reaction (-78 °C) would become liquid and a potential reactant. Exchanging the solvent system dried DMF for DMF that was stored in the presence of 5Å molecular sieves eliminated this problem.

2.5. Synthesis of the Final Compounds

After exploring the various strategies (**Scheme 2.2, 2.3** and **2.5**) to finish the tetrapeptide scaffolding it was found that an increase in the molarity of the reaction mixture from 0.1M to 1.0 – 1.5M and the use of anhydrous, dimethyl amine free DMF allowed us to obtain an 83% yield for the coupling of the final segment to the hindered proline (**Scheme 2.6**).



The methyl ester at the P4 position was derivatized to the methyl amide by heating within a bomb at 85 °C in the presence of gaseous methyl amine. Hydrolysis of the ester by the use of LiOH in THF:MeOH:H₂O (3:1:1) afforded the free carboxylic acid. Deprotection of the three compounds with 4N HCl in dioxane provided the final compounds which were submitted to Dr. Scott Kaufmann of the Mayo Medical Clinic for biological testing.



2.6. Biological Activity

The initial screen used by the Kauffman group was established with the goal of selecting compounds that enhanced chemotherapy-induced apoptosis since this is the critical property necessary for a clinically useful therapeutic agent.

T98G human glioblastoma cells were cultured in RPMI 1640 medium containing 10% fetal calf serum. The cells were then exposed to a well known apoptosis inducing cancer therapeutic, etoposide (4 μ M), for 48 hours in the presence or absence of the peptidomimetics and control peptides (100 μ M). After the 48 hour incubation period, both adherent and non-adherent cells were combined, sedimented, and lysed in buffer. The samples were then analyzed by flow microfluorimetry on a FACScan flow cytometer. The data were analyzed for the amount of particles exhibiting apoptotic properties with less than 2n DNA fluorescence. This experimental indicator of apoptosis inducement is based upon the well documented evidence of DNA fragmentation in apoptotic cells.

A positive result from our compounds would show an increase in the amount of subdiploid / apoptotic cells as defined by the < 2n DNA fluorescence.

Dr. Kaufman found that the methyl ester (**2.2**, **Figure 2.1**) when administered at 100 μ M concentration caused at least a doubling of the number of apoptotic cells without inducing toxicity on its own (black bars). In contrast **2.1**, the carboxylic acid derivative, and **2.3**, the methyl amide derivative, failed to significantly alter the amount of drug induced apoptosis in the T98G cells.

2.7. Retro-Modeling Analysis

The modest biological activity of compounds **2.1**, **2.2** and **2.3** prompted further study of the possible orientation of these compounds within the active site of the XIAP BIR-3 domain. Previous research by the Shi group at Princeton University elucidated the crystal structure of Smac/DIABLO complexed with the BIR3 domain of XIAP to 2.0 Å resolution.⁴ The XIAP – BIR3 domain consists of six α -helices, a three stranded β -sheet and a zinc atom chelated by three cysteine residues. The terminal tetrapeptide of Smac binds to a surface groove, 892 Å total surface area, on BIR3 formed by the β -strand and the α 3 helix. Val2 and Pro3 form a short anti-parallel β -strand. The native AVPI forms a total of eight inter-molecular hydrogen bonds with the BIR3 domain. Ala1 of the tetrapeptide forms 5 of the eight hydrogen bonds with Glu142 and Asp138 as well as with Glu132, thus, demonstrating the critical nature of the Ala1 in the tight binding of the peptide to the surface groove.

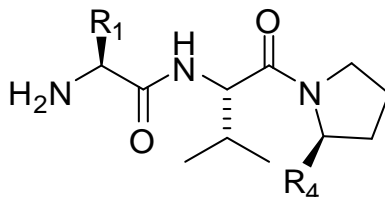
This crystal structure data was used to develop an *in silico* model of the active site of XIAP using the Schrödinger software suite.¹¹ The docking program used by Schrödinger, Glide, is optimally designed to begin from a co-crystallized protein-ligand complex. Minimal preparation of the PDB structure is necessary, however, checking the accuracy of multiple bonds, cofactors, protonation states, additional structural waters and hydrogens was performed. Once the protein is prepared, we used the Glide flexible docking function to model our ligands into the prepared protein active site. This function uses an internal conformation generator which assumes that all rotatable bonds are variables to be optimized. The flexible docking option also defines the ligand center as the midpoint between the two most widely separated atoms within the core region, as

opposed to rigid docking which uses the two most widely separated atoms in the whole molecule. This allows for a more flexible docking option which minimizes the amount of negative conformations that are generated because the molecule won't 'fit' into the active site. Once the compounds are docked they are scored using GScore that incorporates a modified CScore scoring functions, which separates and weights values differently.

In order to ascertain whether the *in silico* model of the active site was correct we performed two test experiments to confirm its validity. The first confidence experiment was to superimpose the conformation of the *in silico* docked AVPI onto the crystal structure conformation of the docked tetrapeptide with XIAP. Our model showed a 0.32 rms deviation from the crystal structure docked conformation which is within the accepted measure of confidence of 0.5 rms.

Secondly, we wanted to build confidence in our model and the scoring function by establishing a correlation between actual biological results and the GScore of the compounds used within those assays. One way to establish an actual correlation between the theoretical GScore and *in vivo* or *in vitro* results is to model an independent set of compounds and compare the GScore prediction to actual experimental values.

Table 2.2. Structures of Smac Peptidomimetics and Their Binding Affinities to XIAP BIR3 Protein as Compared to GScore Values.



Compound	R ₁	R ₄	K _i ± SD (μM) ^a	GScore
1	CH ₃	CONHCH ₂ Ph	0.29 ± 0.07	-9.58
2	CH ₃	CONHCH ₂ CH(CH ₃) ₂	13.40 ± 1.6	-8.34
3	CH ₃	CONHCH ₂ CH(CH ₂ CH ₃) ₂	2.45 ± 0.7	-8.69
4	CH ₃	CONHCH ₂ CH(CH ₂) ₂	4.41 ± 1.5	-8.63
5	CH ₃	CONHCH ₂ (C ₆ H ₁₀)	1.27 ± 0.2	-8.90
6	CH ₃	CONHCH ₂ (C ₄ H ₄ O)	0.22 ± 0.07	-9.37
7	CH ₃	CONHCH ₂ (C ₄ H ₄ S)	0.18 ± 0.07	-9.23
8	CH ₃	CONH(C ₆ H ₅)	4.9 ± 2.1	-8.76
9	CH ₃	CONHCH ₂ CH ₂ (C ₆ H ₅)	0.15 ± 0.09	-9.44
10	CH ₃	CONHCH(C ₆ H ₅) ₂	0.028 ± 0.020	-8.69
11	C ₂ H ₅	CONHCH(C ₆ H ₅) ₂	0.024 ± 0.020	-8.86
12	CH ₃	CH ₂ CH ₂ CH ₂ (C ₆ H ₅)	1.2 ± 0.4	-9.07
13	C ₂ H ₅	CONHCH ₂ (C ₆ H ₅)	0.081 ± 0.06	-9.72
14	<i>i</i> -C ₃ H ₇	CONHCH ₂ (C ₆ H ₅)	4.15 ± 1.2	-7.72
15	<i>n</i> -C ₃ H ₇	CONHCH ₂ (C ₆ H ₅)	54 ± 7	-8.38

^a K_i are calculated from dose dependent binding assays are carried out using serial dilutions of the test compounds as well as the probe. Polarization values were plotted and a least squares regression analysis was used to determine the IC₅₀ values and K_i values were determined from those calculations

We performed this validity analysis with a set of compounds from the Wang group of the University of Michigan.^{12,13} Dr. Wang and colleagues developed and established an assay which uses a fluorescently labeled AVPI peptide probe. Dose dependent binding assays are carried out using serial dilutions of the test compounds as well as the probe. Polarization values were plotted and a least squares regression analysis was used to determine the IC₅₀ values and K_i values were determined from those calculations (**Table 2.2**).

We docked the Wang group's compounds into our prepared protein and compared the GScore results to the calculated K_i. The tabulated results were plotted as GScore vs. K_i and analyzed through regression analysis. Utilizing all of Dr. Wang's compounds we showed a very loose R² correlation of 0.3565 (**Figure 2.3**). However, knowing that the Glide program has had trouble with graphing large dibenzyl compounds in our previous studies, we excluded this data from the study as well as the outlying 13.4 μM compound **2** of **Table 2.2**. When these data were plotted as K_i versus GScore values the regression analysis provided an R² coefficient of 0.6598 (**Figure 2.4**). Keeping these exceptions in mind this linear analysis should provide a loose correlation between the GScore values and the affinity assay as performed by the Wang group with the exception of large dibenzyl compounds which will be analyzed individually.

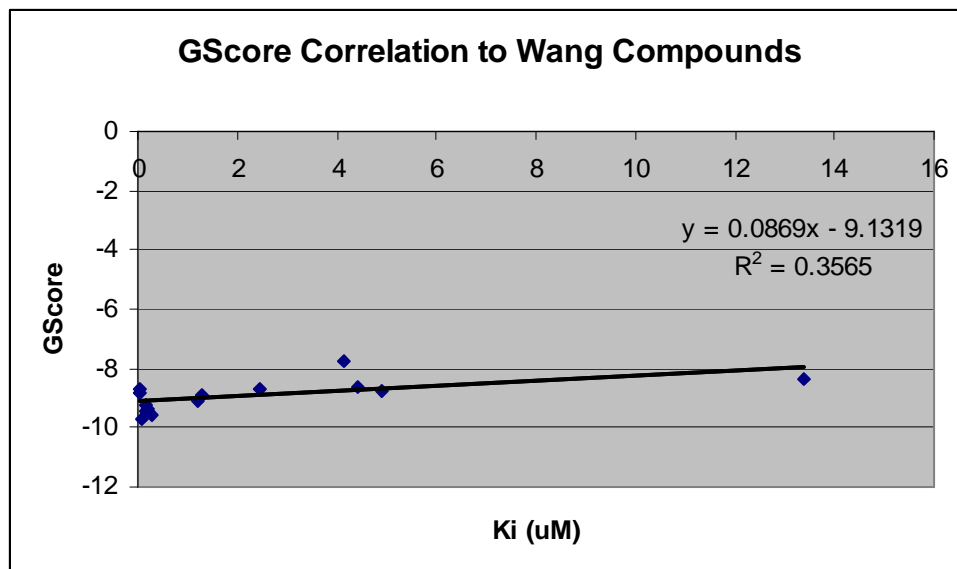


Figure 2.3. GScore versus K_i Correlations of the Wang Compounds

Taken as a whole, these data provided us with a reasonable measure of confidence in the preparation of the XIAP BIR3 active site as well as confidence in drawing a loose correlation to biological results from our *in silico* model. With the active site in hand we attempted to garner as much information as possible from the biological data by elucidating a rough approximation of the mode of binding of our compounds to the XIAP BIR3 interface.

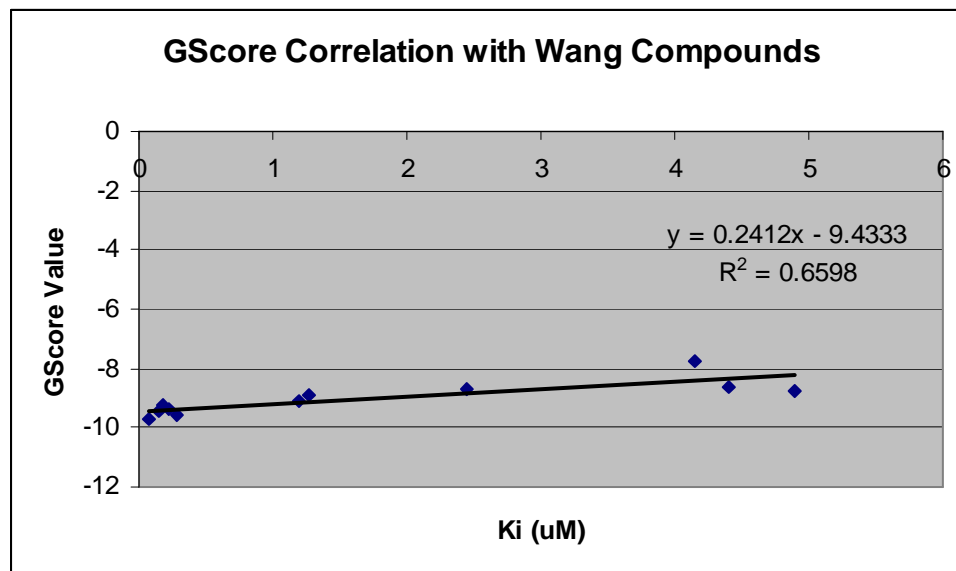


Figure 2.4. GScore versus K_i Correlations of the Wang Compounds

The methyl ester **2.2** was modeled first (**Figure 2.5**) and docked into the active site using a flexible docking option of the Glide software with 1000 iterations of possible conformations being selected for all modeling attempts. The gross morphology of the docking of the methyl ester is the same as that for AVPI. The constraints at the P1 position places the side chain into the same hydrophobic pocket as well as having the same hydrogen bonding at P1 to Glu142. The molecule is, however, missing the second H-bond to Asp138 that AVPI displays. The P2 nitrogen of valine forms a hydrogen bond with Gln132, which is similar to AVPI and Gly130, which is not. Taken together the Glide program assigned a GScore value of -6.60 as compared to the -8.01 value it assigned to the native ligand, AVPI. The GScore value should correlate to an activity within the Wang assay of greater than a 100 μM K_i which is roughly consistent with the biological results that were determined.

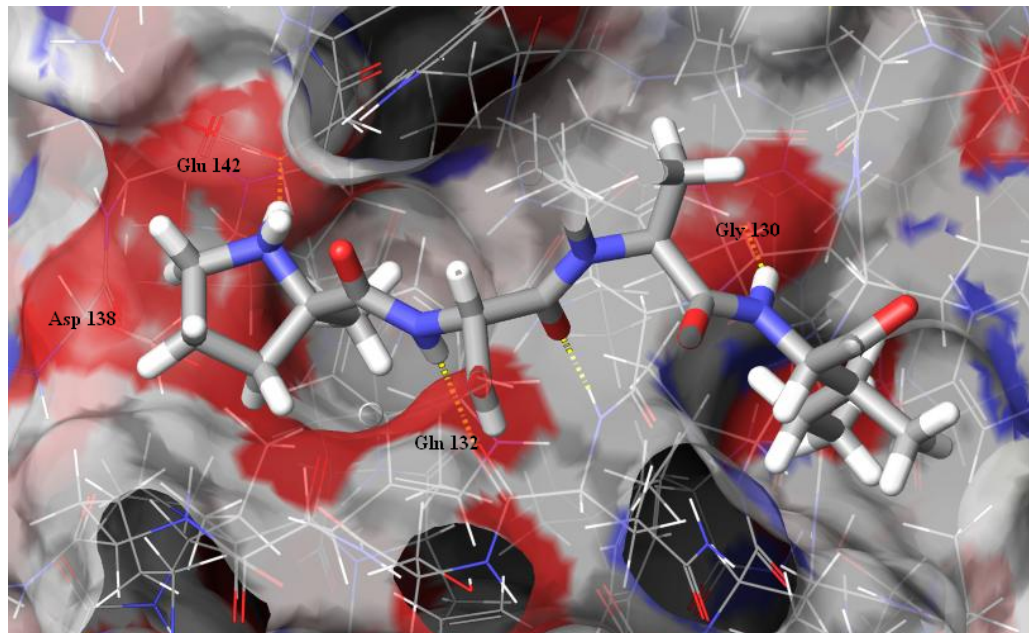


Figure 2.5. ϕ_1 Constrained AVPI Mimic Methyl Ester Derivative 2.2 in the XIAP BIR3 Active Site.

The carboxylic acid and methyl amide ϕ_1 constrained mimics were also modeled using the same parameters as the methyl ester derivative (**Figure 2.5 and 2.6**). This yielded a surprising result where the AVPI molecules switched orientation of the backbone within the active site. The P4 Ile residue now positions itself in the spatial orientation that the P1 Ala resides in the native AVPI ligand.

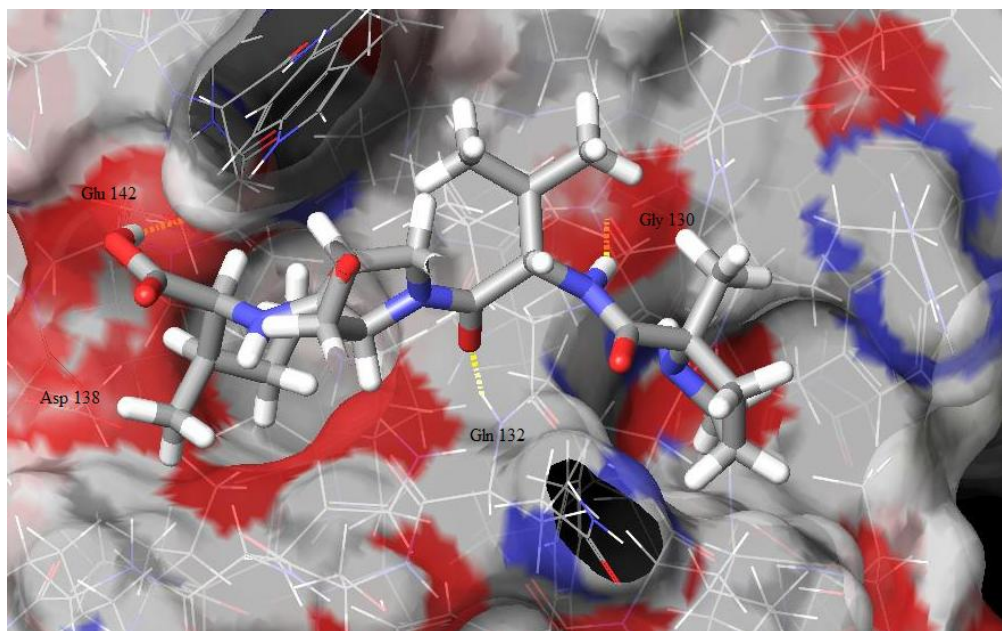


Figure 2.6. ϕ_1 Constrained AVPI Mimic Carboxylic Acid Derivative (2.1) in the XIAP BIR3 Active Site.

This preference seems to be due to the hydrogen bonding capabilities of the carboxylic acid and the methyl amide to Glu142. Hydrogen bonding to Glu132 and Gly130 still occur just like the AVPI backbone chain with the constrained P1 position fitting into the secondary pocket. The GScore of -6.04 is consistent with the decreased activity that these compounds showed versus the methyl ester derivative.

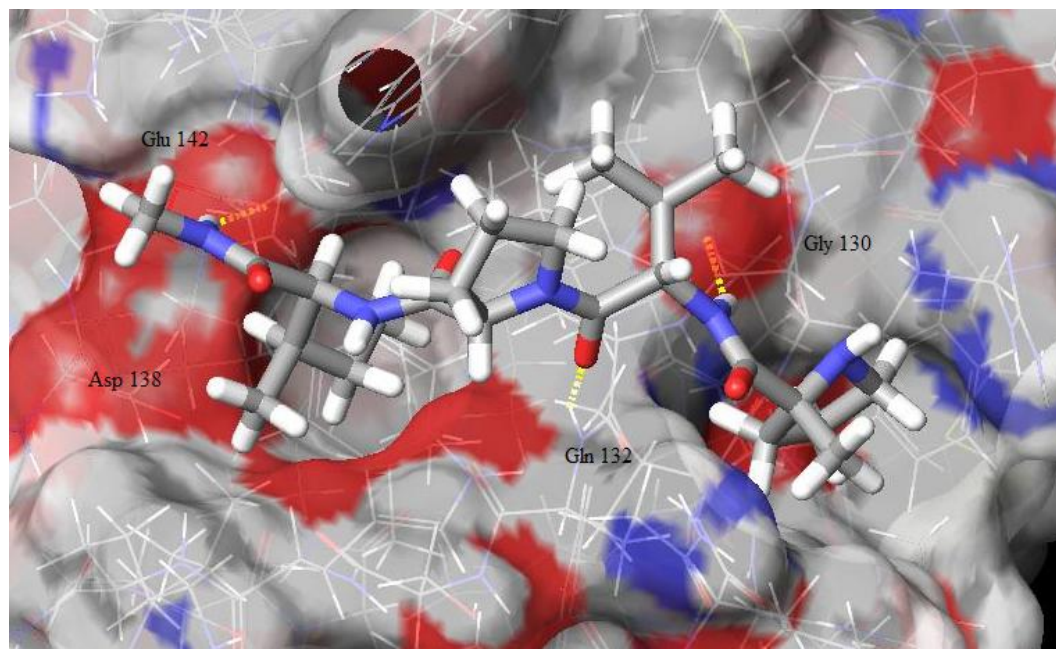
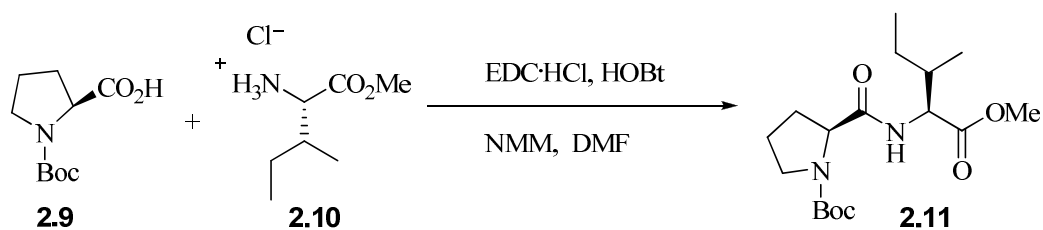


Figure 2.7. ϕ_1 Constrained AVPI Mimic Methyl Amide Derivative (2.3) in the XIAP BIR3 Active Site.

2.8. Experimentals

N-Boc-L-Pro-L-Ile-OMe (2.11)



Boc-L-proline (**2.9**, 3.0 g, 13.9 mmol) and isoleucine-OMe • HCl (**2.10**, 3.0 g, 16.7 mmol) were dissolved in DMF which had been dried over 5 Å molecular sieves.

While this solution was stirred, HOBt (2.3 g, 16.7 mmol) was added and the solution was cooled to $-78\text{ }^{\circ}\text{C}$. EDC \cdot HCl (3.2 g, 16.7 mmol) and NMM (3.8 mL, 34.8 mmol) were added consecutively to the cooled solution, which then was allowed to warm slowly to room temperature, whereupon it was stirred for 3 days. On the third day the reaction mixture was concentrated *in vacuo* to give an orange residue to which a small portion of xylenes was added to remove the traces of DMF. The orange residue was then partitioned between H_2O (100 mL) and EtOAc (100 mL). The organic layer was washed consecutively with 0.5 M HCl (100 mL), 1 M NaHCO_3 (100 mL) and brine (100 mL), dried with MgSO_4 and concentrated under reduced pressure to yield 2.92 g of crude product (**2.11**). The crude Boc-L-Pro-L-Ile-OMe (**2.11**) was purified by silica gel chromatography using 15 cm of silica gel within a 5 cm diameter column. Product was eluted with 1:1 ethyl acetate in hexanes to yield 3.85 g (85.6 %) of a clear oil.

TLC $R_f = 0.38$ (EtOAc/Hexanes, 1:2)

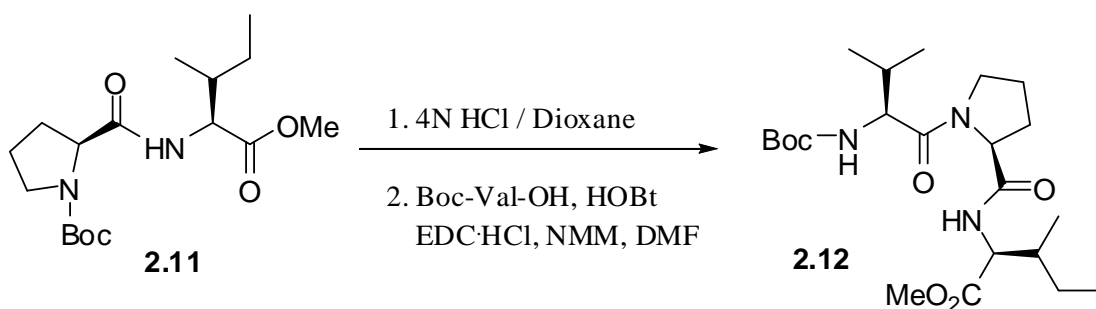
$[\alpha]_D -71.8$ (*c* 0.5, CHCl_3)

^1H NMR (300 MHz, CDCl_3 , COSY, TOCSY) δ 7.55 (br s, 0.5 H, Ile-NH), 6.55 (br s, 0.5 H, Ile-NH), 4.48 (br m, 1H, Pro α -CH), 4.29 (br m, 1H, Ile α -CH), 3.71 (s, 3H, CO_2CH_3), 3.40 (br m, 2H, δ - CH_2), 2.38 (br m, 0.5H, β - CH_2) 2.10 (br m, 0.5 H, β - CH_2), 1.84 – 1.98 (br m, 4H, Pro β - CH_2 , Pro γ - CH_2 , Ile β -CH), 1.42(s, 9H, Boc-C(CH_3) $_3$), 1.38-1.43 (m, 1H, Ile γ - CH_2), 1.11-1.20 (m, 1H, Ile γ - CH_2), 0.89 (dd, $J = 7.5$ Hz., 6H, Ile- CH_3)

^{13}C NMR (75 MHz, CDCl_3 , DEPT) δ 170.8 (Pro-CONH, Ile- CO_2CH_3), 154.5 (Boc-COC(CH_3) $_3$), 79.2 (Boc-COC(CH_3) $_3$), 59.9 (Pro α -CH), 58.5 (Ile α -CH), 55.5 (Ile-COCH $_3$), 50.9 (Pro δ - CH_2), 36.6 (Ile β -CH), 27.2 (Boc-C(CH_3) $_3$), 26.5 (Pro β - CH_2), 23.9, 22.7 (Ile γ - CH_2 , Pro γ - CH_2), 14.5 (Ile-CHCH $_3$), 10.5 (Ile- CH_2CH_3)

ESI HRMS m/z calcd for $C_{17}H_{31}N_2O_5$ (MH)⁺, 343.2243; found, 343.2233.

N-Boc-L-Val-L-Pro-L-Ile-OMe (2.12)



N-Boc-L-Pro-L-Ile-OMe (**2.11**, 2.42 g, 8.7 mmol) was dissolved in 10 mL of 4N HCl in dioxane and the solution was stirred under nitrogen for 4-24 hours, while it was monitored by TLC. Upon completion, the reaction was concentrated under reduced pressure. The residue was dissolved in CH_2Cl_2 and then allowed to dry under vacuum for 24 – 48 hours. This was done three times. The white solid was then used in the subsequent coupling reaction without further purification.

Boc-L-valine (1.71 g, 7.9 mmol) and L-proline-L-isoleucine-OMe • HCl (8.7 mmol) were dissolved in DMF which had been dried over 5 Å molecular sieves. While this solution was stirred, HOBt (1.3 g, 9.5 mmol) was added and the solution was cooled to -78 °C. EDC • HCl (1.83 g, 9.5 mmol) and NMM (2.2 mL, 19.8 mmol) were added consecutively to the cooled solution, which then was allowed to warm slowly to room temperature, whereupon it was stirred for 3 days. On the third day the reaction mixture was concentrated *in vacuo* to give an orange residue to which a small portion of xylenes was added and then removed under reduced pressure to eliminate the remaining traces of

DMF. The orange residue was then partitioned between H₂O (100 mL) and EtOAc (100 mL). The organic layer was washed consecutively with 0.5 M HCl (100 mL), 1M NaCO₃ (100 mL) and brine (100 mL), dried with MgSO₄ and concentrated under reduced pressure to yield 3.5 g of crude product (**2.12**). The crude Boc-L-Val-L-Pro-L-Ile-OMe was purified by silica gel chromatography using 15 cm of silica gel within a 5 cm diameter column. Elution with 2% MeOH in ethyl acetate yielded 2.9 g (83.3 %) of pure product (**2.12**) as a clear, colorless oil.

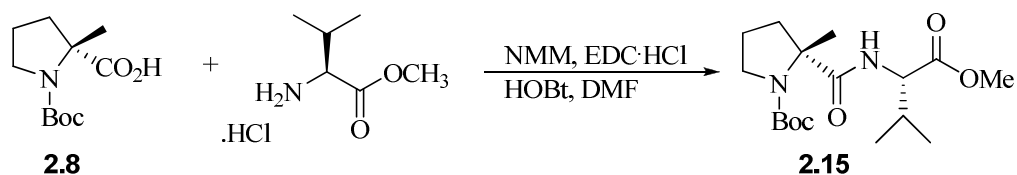
TLC $R_f = 0.64$ (2% MeOH in EtOAc)

$[\alpha]_D -68.1$ (c 2.4, CHCl₃)

¹H NMR (300 MHz, CDCl₃, COSY, TOCSY) δ 7.25 (d, $J = 12$ Hz, 1H, Val-NH), 5.26 (d, $J = 4.8$ Hz, 1H, Ile-NH), 4.59 (dd, $J = 12.3$ Hz, 15 Hz, 1H, L-Pro α -CH), 4.46 (dd, $J = 12$ Hz, 15.6 Hz, 1H, Val α -CH), 4.27 (dd, $J = 9.6$ Hz, 11.4 Hz, 1H, Ile α -CH), 3.67-3.75 (m, 1H, Pro δ -CH), 3.70 (s, 3H, CO₂CH₃), 3.51-3.59 (m, 1H, Pro δ -CH), 2.30-2.37 (m, 1H, Val β -CH) 1.79-2.18 (m, 5H, Pro β -CH₂, Pro γ -CH₂, Ile β -CH), 1.41 (s, 9H, Boc-C(CH₃)₃), 1.38-1.41 (m, 1H, Ile γ -CH₂) 0.97 (d, 3H, Val γ -CH₃), 0.85 - 0.92 (m, 9H, Val γ -CH₃, Ile-CH₂CH₃, Ile-CHCH₃).

¹³C NMR (75 MHz, CDCl₃, HMQC) δ 172.2 (Pro-CONH, Ile-COCH₃), 171.2 (Val-CONH), 155.9 (Boc-CO), 79.6 (Boc-C(CH₃)₃), 60.1 (Pro α -CH), 57.1 (Ile α -CH), 56.9 (Val α -CH), 52.2 (Ile-COCH₃), 47.9 (Pro δ -CH₂), 38.0 (Ile β -CH(CH₃)CH₂CH₃), 31.7 (Val β -CH(CH₃)₂), 28.6 (Boc-C(CH₃)₃), 27.8 (Pro β -CH₂), 25.3 and 25.5 (Ile γ -CH₂ and Pro γ -CH₂), 19.8 (Val γ -CH(CH₃)₂), 17.8 (Val γ -CH(CH₃)₂), 15.7 (Ile-CH(CH₃)CH₂CH₃), 11.9 (Ile-CH(CH₃)CH₂CH₃)

HRMS (FAB) m/z calcd for C₂₂H₃₉NaN₃O₆ (MNa)⁺, 464.2758; found, 464.2737.

N-Boc- α -Me-D-Pro-L-Val-OMe (2.15)

Boc- α -Me-D-proline (**2.8**, 1.0 g, 4.4 mmol) and valine-OMe \cdot HCl (1.5 g, 8.7 mmol) were dissolved in DMF which had been dried over 5 Å molecular sieves. While this solution was stirred, HOBT (1.2 g, 8.7 mmol) was added and the solution was cooled to -78 °C. EDC \cdot HCl (1.7 g, 8.7 mmol) and NMM (1.8 mL, 17.9 mmol) were added consecutively to the cooled solution, which then was allowed to warm slowly to room temperature, whereupon it was stirred for 3 days. On the third day, the reaction mixture was concentrated *in vacuo* to give an orange residue to which a small portion of xylenes was added to remove the traces of DMF. The orange residue was then partitioned between H₂O (100 mL) and EtOAc (100 mL). The organic layer was washed consecutively with 0.5 M HCl (100 mL), 1 M NaHCO₃ (100 mL) and brine (100 mL), dried with MgSO₄ and concentrated under reduced pressure to yield 1.67 g of crude product (**2.15**). The crude Boc-L-Pro-L-Ile-OMe (**2.15**) was purified by silica gel chromatography using 15 cm of silica gel within a 5 cm diameter column which was eluted with 1:1 ethyl acetate in hexanes to yield 1.32 g (88.6 %) of a clear oil.

TLC R_f = 0.56 (EtOAc/Hexanes, 1:3)

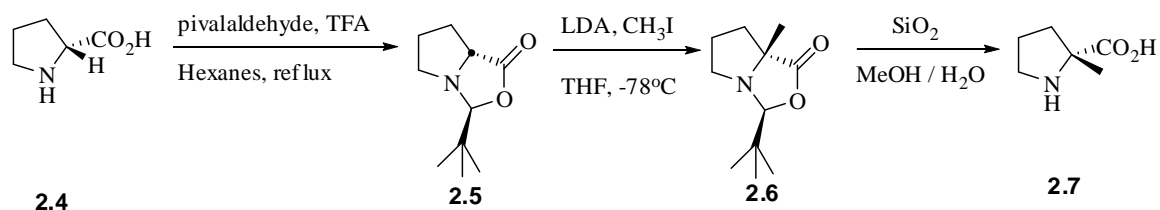
$[\alpha]_D$ 97.2 (*c* 1.9, CHCl₃)

¹H NMR (CDCl₃, 300 MHz) δ 7.45 (br s, 0.5 H, Val-NH), 6.42 (br s, 0.5H, Val-NH), 4.49 (dd, J = 4.8 Hz, 8.7 Hz, 1H, Val α -CH), 3.71 (s, 3H, Val-CO₂CH₃), 3.71-3.30 (br m,

2H, Pro γ -CH₂), 2.42-2.63 (br m, 1H, Pro β -CH), 2.18 (dq, $J = 4.8$ Hz, 6.9 Hz, 1H, Val β -CH(CH₃)₂), 1.66-1.88 (br m, 3H, Pro β -CH, Pro γ -CH₂), 1.62 (s, 3H, Pro α -CCH₃), 1.46 (s., 9H, Boc-C(CH₃)₃), 0.96 (d, $J = 6.9$ Hz, 3H, Val δ -CH₃), 0.89 (d, $J = 6.9$ Hz, 3H, Val δ -CH₃).

¹³C NMR (CDCl₃, 75MHz) δ 174.5 (Val-CONH), 172.5 (Pro-CONH), 154.6 (Boc-COC(CH₃), 80.0 (Boc-COC(CH₃), 67.0 (Pro α -C), 57.2 (Val α -CH), 52.0 (CO₂CH₃), 48.6 (Pro δ -CH₂), 41.7 (Pro α -CCH₃), 39.1 (Pro β -CH₂), 31.1 (Pro γ -CH₂), 28.4 (Boc-C(CH₃)₃), 22.4 (Val β -CH₃), 19.1 (Val γ -CH₃), 17.8 (Val γ -CH₃)

HRMS (FAB) m/z calcd for C₁₇H₃₁N₂O₅ (MH)⁺, 343.2233; found, 343.2303.

α -Me-D-Pro-OH (2.7)

D-Proline (**2.4**, 3 g, 26 mmols) was flame dried under vacuum for 10-15 minutes and then pulverized into a fine powder. To this powder was added 1 drop of TFA mixed in hexanes. The hexanes were evaporated under a light stream of N₂. To the resulting white powder was added 50 mL of hexanes and pivalaldehyde (8.5 mL, 78 mmols). The reaction was then heated overnight using a Dean Stark trap for water capture. In the morning, the reaction was carefully concentrated *in vacuo* to a yellow oil. The resultant oxazolidinone **2.5** was then carried on to the alkylation reaction without any further purification.

Freshly distilled THF (40 mL) was added to the round bottom flask containing the oxazolidinone **2.5**. The solution was then cooled to -78 °C before a 1 M solution of LDA (29 mL) was cannulated into the reaction with vigorous stirring. After 10 minutes of stirring iodomethane (1.8 mL, 29 mmol) was added via syringe to the solution. The reaction temperature was then allowed to rise to room temperature over 2-3 hours. The reaction was concentrated under reduced pressure with minimal heat and partitioned between Et₂O and water. The pH of the water layer was checked to confirm basicity and then washed 2 more times with Et₂O. The organic layers were concentrated under

reduced pressure after being dried over MgSO_4 . The alkylated oxazolidinone was taken forward to the next step without further purification.

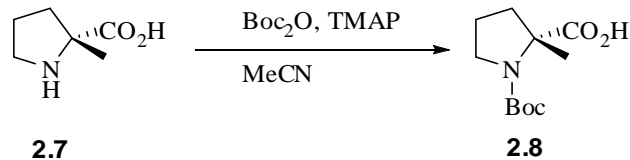
The alkylated oxazolidinone (**2.6**) was hydrolyzed by dissolving it in a 5:1 MeOH / H_2O with a total volume of 104 mL. Silica gel (5 g) was added to that solution and the resulting suspension was stirred at room temperature for 48-72 hours. The reaction mixture was filtered on a fritted Buchner funnel and the filtrate was evaporated *in vacuo* to give a yellowish solid. This solid was then boiled in ethyl acetate until a white solid resulted and the ethyl acetate turned yellow. The resulting white solid was then crystallized from methanol and isopropyl alcohol to yield 1.62 g of clear crystals (48.6%).

TLC $R_f = 0.16$ (Propanol/ NH_4OH , 4:1)

$[\alpha]_D 70.3$ (c 1.0, MeOH)

^1H NMR (300 MHz, CD_3OD)^{14, 15} δ 4.94 (d, 1H, NH), 3.32-3.47 (m, 1H, $\delta\text{-CH}_2$), 3.25-3.31 (m, 1H, $\delta\text{-CH}_2$), 2.38-2.45 (dd, 1H, $\beta\text{-CH}_2$), 1.80-2.10 (m, 3H, $\beta\text{-CH}_2$, $\gamma\text{-CH}_2$), 1.59 (s, 3H, $\alpha\text{-CH}_3$).

^{13}C NMR (75 MHz, CDCl_3) δ 175.5 (CO_2H), 70.5 ($\alpha\text{-C}$), 45.2 ($\delta\text{-CH}_2$), 35.9 ($\alpha\text{-C}(\text{CH}_3)$), 23.4 ($\beta\text{-CH}_2$), 21.1 ($\gamma\text{-CH}_2$).

N-Boc- α -Me-D-Pro-OH (2.8)

Alpha-methyl proline (**2.7**, 1 g, 7.73 mmol) and tetramethylammonium pentahydrate (1.54 g, 8.50 mmol) were added to MeCN (50 mL) which had been freshly distilled from CaH₂. The mixture was stirred at room temperature until a solution formed. Boc₂O (3.37 g, 15.46 mmol) was added to the stirred solution and stirring of the reaction mixture was allowed to continue for 1 day. On the second day, another equivalent of Boc₂O (0.84 g, 3.87 mmol) was added and the solution was stirred for another day after which MeCN was removed *in vacuo*. The residue was then partitioned between H₂O and Et₂O. The aqueous layer was washed with an additional portion of ether and then acidified with solid citric acid to pH 3-4. The aqueous fraction was then extracted 3 times with ethyl acetate. The combined organic fractions were washed with H₂O and brine, dried with MgSO₄, and then concentrated *in vacuo* to give N-Boc- α -Me-D-proline (**2.8**) as a white solid. The white solid was crystallized from boiling ethyl acetate to yield 1.6 g of product (90.4%).

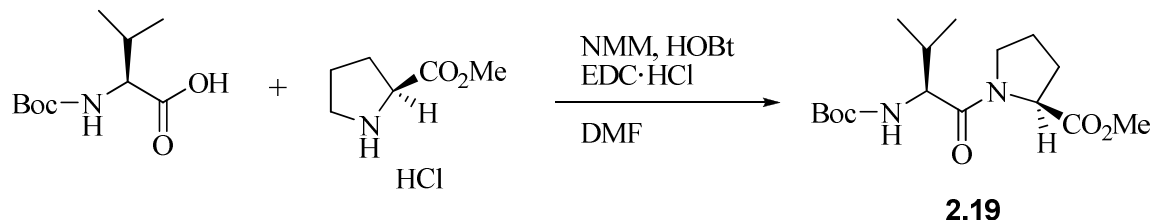
TLC R_f = 0.65 (2% MeOH in EtOAc)

[α]_D 38.5 (*c* 1.0, CHCl₃)

¹H NMR (CDCl₃, COSY, *rotamers present 1 : 1.75*)⁷ δ 11.51 (br s, 1H, CO₂H), 3.37-3.63 (m, 2H, δ -CH₂), 2.33-2.38 (m, 0.5 H, β -CH₂), 2.19 - 2.30 (m, 0.5 H, β -CH₂), 1.83 - 1.97 (m, 3H, β -CH, γ -CH₂), 1.56 (s, 3H, α -C(CH₃)), 1.48 (s, 3H, α -C(CH₃)) 1.42 (s, 9H, Boc C(CH₃)₃), 1.39 (s, 9H, Boc C(CH₃)₃).

^{13}C NMR (75Hz, CDCl_3 , rotamers present) δ 181.1 and 178.2 ($\alpha\text{-CO}_2\text{H}$), 153.8 (Boc $\text{NCO}_2\text{C}(\text{CH}_3)_3$), 81.2 and 80.7 (Boc CCH_3), 66.3 and 65.0 ($\alpha\text{-C}$), 48.8 and 48.1 ($\delta\text{-CH}_2$), 40.7 ($\alpha\text{-CCH}_3$), 39.1 ($\beta\text{-CH}_2$), 28.8 and 28.7 (Boc- $\text{C}(\text{CH}_3)_3$), 23.3 and 23.2 ($\gamma\text{-CH}_2$).

N-Boc-Val-Pro-OMe (2.19)



Boc-L-valine (9.21 mmol) and proline-OMe \cdot HCl (1.8 g, 11.1 mmol) were dissolved in DMF, which had been dried over 5 Å molecular sieves. While this solution was stirred, HOBT (1.52 g, 11.1 mmol) was added and the solution was cooled to -78°C . EDC \cdot HCl (2.14 g, 11.1 mmol) and NMM (2.43 mL, 22.2 mmol) were added consecutively to the cooled solution, which then was allowed to warm slowly to room temperature whereupon it was stirred for 3 days. On the third day, the reaction mixture was concentrated *in vacuo* to give an orange residue to which a small portion of xylenes was added to assist in the removal of traces of DMF. The orange residue was then partitioned between H_2O (100 mL) and EtOAc (100 mL). The organic layer was washed consecutively with 0.5 M HCl (100 mL), 1 M NaHCO_3 (100 mL) and brine (100 mL), dried with MgSO_4 and concentrated under reduced pressure to yield 2.92 g of crude product. The crude Boc-L-Val-L-Pro-OMe (2.19) was purified by silica gel chromatography using 15 cm of silica gel within a 5 cm diameter column. The column was eluted with 1:1 ethyl acetate / hexanes to yield 2.75 g (91%) of pure product (2.19).

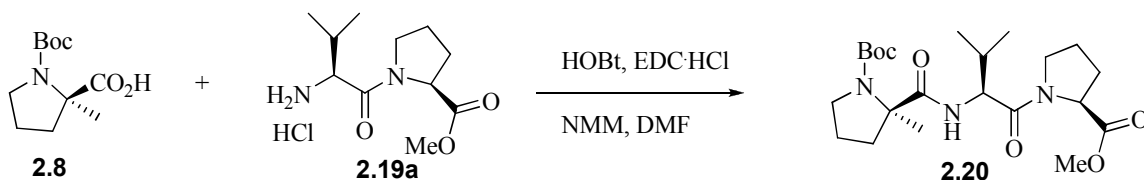
TLC $R_f = 0.44$ (EtOAc / Hexanes, 1:1)

$[\alpha]_D -73.8$ (c 1.11, CHCl_3)

^1H NMR (300 MHz, CDCl_3 , COSY, TOCSY)¹⁷ δ 5.35 (d, 1H, Val-NH), 4.46-4.50 (m, 1H, Pro α -CH), 4.25 (dd, 1H, Val α -CH), 3.67 (s, 3H, Pro-CO₂CH₃) 3.62-3.80 (m, 2H, Pro δ -CH₂), 2.15-2.24 (m, 1H, Pro β -CH₂) 1.90-2.07 (m, 4H, Pro β -CH₂, Pro γ -CH₂, Val β -CH), 1.39 (s, 9H, Boc-C(CH₃)₃), 1.00 (d, 3H, Val γ -CH₃), 0.90 (d, 3H, Val γ -CH₃).

^{13}C NMR, DEPT (75 MHz, CDCl_3 , DEPT) δ 172.3 and 170.9 (Pro-CO₂CH₃, Val-CONH), 155.8 (Boc-CO), 79.2 (Boc-CCH₃), 58.9 (Pro α -C), 56.9 (Val α -C), 52.1 (Pro-CO₂CH₃), 47.2 (Pro δ -CH₂), 31.4 (Val β -CH), 29.2 (Pro β -CH₂), 28.5 (Boc-C(CH₃)₃), 25.2 (Pro γ -CH₂), 19.4 (Val γ -CH₃), 17.6 (Val γ -CH₃).

N-Boc- α -Me-D-Pro-L-Val-L-Pro-OMe (2.20)



Boc- α -Me-D-proline \cdot HCl (**2.8**, 3.36 mmol) and L-valine-L-proline-OMe \cdot HCl (**2.19a**, 1.33 g, 5.04 mmol) were dissolved in DMF which had been dried over 5 Å molecular sieves. While this solution was stirred HOBt (0.55 g, 4.03 mmol) was added and the solution was cooled to -78 °C. EDC \cdot HCl (0.79 g, 4.03 mmol) and NMM (1.00 mL, 9.07 mmol) were added consecutively to the cooled solution, which then was allowed to warm slowly to room temperature whereupon it was stirred for 3 days. On the

third day, the reaction mixture was concentrated *in vacuo* to give an orange residue to which a small portion of xylenes was added to assist in the removal of the traces of DMF. The orange residue was then partitioned between H₂O (100 mL) and EtOAc (100 mL). The organic layer was washed consecutively with 0.5 M HCl (100 mL), 1 M NaHCO₃ (100 mL) and brine (100 mL), dried with MgSO₄ and concentrated under reduced pressure to yield 1.48 g of crude product. The crude Boc- α -Me-D-Pro-L-Val-L-Pro-OMe (**2.20**) was purified by silica gel chromatography using 15 cm of silica gel within a 5 cm diameter column which was eluted with 2% MeOH in ethyl acetate to yield 0.96 g (67 %) of pure product.

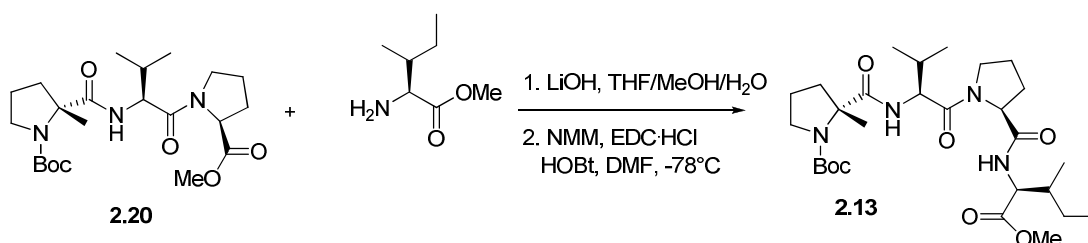
TLC R_f = 0.41 (2% MeOH in EtOAc)

[α]_D 10.0 (*c* 0.58, CHCl₃)

¹H NMR (300 MHz, CDCl₃) δ 4.45 (dd, *J* = 9.3 Hz, 8.7 Hz, 1H, L-Pro α -CH), 4.33-4.37 (m, 1H, Val α -CH), 3.66-3.71 (m, 1H, Pro δ -CH), 3.58 (s, 3H, CO₂CH₃), 3.33-3.55 (m, 3H, L-Pro δ -CH₂, D-Pro- δ -CH₂), 1.67-2.15 (m, 9H, D-Pro β -CH₂, L-Pro β -CH₂, D-Pro γ -CH₂, L-Pro γ -CH₂, Val β -CH), 1.46 (s, 3H, D-Pro α -CCH₃), 1.31 (s, 9H, Boc-C(CH₃)₃), 0.93 (d, *J* = 6.9 Hz, 3H, Val γ -CH₃), 0.81 (d, *J* = 6.3 Hz, 3H, Val γ -CH₃)

¹³C NMR (75 MHz, CDCl₃) δ 174.2 (Pro-CO), 172.4 (Pro-CO), 170.7 (Val-CO), 153.7 (Boc-COC(CH₃)₃), 80.5 and 80.0 (Boc-C(CH₃)₃), 66.8 and 66.3 (D-Pro α -C), 59.0 (L-Pro α -C), 55.8 (Val α -CH), 52.4 (CO₂CH₃), 48.6 (D-Pro δ -CH₂), 47.4 (L-Pro δ -CH₂), 42.0 (D-Pro β -CH₂), 40.3 (L-Pro β -CH₂), 31.4 (D-Pro γ -CH₂), 29.3 (L-Pro γ -CH₂), 28.7 (Boc-C(CH₃)₃), 25.3 (D-Pro-CCH₃), 23.0 and 22.0 (Val γ -CH₃), 19.7 (Val β -CH₂), 17.9 and 17.4 (Val- γ -CH₃).

ESI HRMS *m/z* calcd for C₂₂H₃₈N₃O₆ (MH)⁺, 440.2761; found, 440.2777.

N-Boc- α -Me-D-Pro-L-Val-L-Pro-L-Ile-OMe (2.13)

Boc- α -Me-D-Pro-L-Val-L-Pro-OMe (**2.20**, 0.5 g, 1.22 mmol) and LiOH (3.66 mmol) was dissolved in a 20 mL mixture of THF/MeOH/H₂O (3:1:1) and stirred for 24 hours while it was monitored by TLC. Upon completion the reaction was concentrated under reduced pressure. The white solid was then used in the subsequent coupling reaction without further purification.

L-Ile-OMe • HCl (2.44 mmol) and Boc- α -Me-D-Pro-L-Val-OH (0.43 g, 1.04 mmol) were dissolved in DMF which had been dried over 5 Å molecular sieves. While this solution was stirred, HOBt (0.25 g, 1.83 mmol) was added and the solution was cooled to -78 °C. EDC • HCl (0.35 g, 1.83 mmol) and NMM (0.47 mL, 4.27 mmol) were added consecutively to the cooled solution, which then was allowed to warm slowly to room temperature whereupon it was stirred for 3 days. On the third day, the reaction mixture was concentrated *in vacuo* to give an orange residue to which a small portion of xylenes was added to aid in the removal of trace amounts of DMF. The orange residue was then partitioned between H₂O (100 mL) and EtOAc (100 mL). The organic layer was washed consecutively with 0.5 M HCl (100 mL), 1M NaHCO₃ (100 mL) and brine (100 mL), dried with MgSO₄ and concentrated under reduced pressure to yield 0.6 g of crude product. The crude Boc- α -Me-D-Pro-L-Val-L-Pro-L-Ile-OMe was purified by silica gel chromatography using 15 cm of silica gel within a 3 cm diameter column. The

column was eluted with 2% MeOH in ethyl acetate to yield 0.42 g. (79.2 %) of pure product.

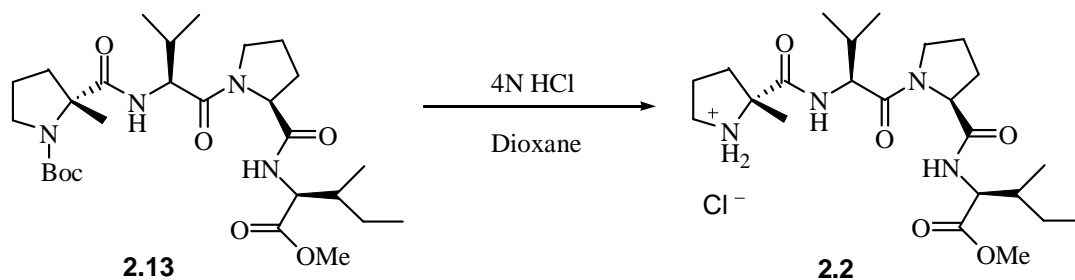
TLC R_f = 0.35 (2% MeOH in EtOAc)

$[\alpha]_D - 296.3$ (c 0.27, MeOH)

^1H NMR (300 MHz, CDCl_3 , COSY) δ 7.20 (br s, 1H, Val - NH), 6.91 (br s, 1H, Ile - NH), 6.55 (br s, 0.5H, Ile - NH), 4.48-4.55 (m, 2H, Val α -CH, Pro α -CH), 4.88 (dd, J = 5.1 Hz, 8.1 Hz, 1H, Ile α -CH), 3.65-3.74 (m, 1H, Pro δ -CH₂), 3.65 (s, 3H, CO₂CH₃), 3.40-3.65 (m, 3H, Pro δ -CH₂, Pro δ -CH₂), 1.75-2.28 (m, 9H, Pro β -CH₂, Pro γ -CH₂, Val β -CH₂), 1.54 (Pro CH₃), 1.40 (s, 10H, Boc C(CH₃)₃, Ile γ -CH₂), 1.06-1.16 (m, 1H, Ile γ -CH₂), 0.95 (d, J = 6.6 Hz, 3H, Val CH₃), 0.88 (d, J = 6.9 Hz, 3H, Val CH₃), 0.80-0.85 (m, 6H, Ile (CH₃)₂).

^{13}C NMR, DEPT (CDCl_3 , 75 MHz, *rotamers present*) δ 174.8 (Pro-CO), 172.1 (Ile-CO), 170.9 (Val-CO), 154.1 (Boc-CO), 80.0 and 80.7 (Boc-C(CH₃)₃), 66.9 (Pro α -C), 60.0 (Pro α -C), 57.0 (Ile α -C), 55.9 (Val α -C), 52.2 (CO₂CH₃), 48.7 (Pro δ -C), 47.9 (Pro δ -C), 40.1 and 42.1 (Pro β -C), 37.9 (Pro β -C), 31.6 (Ile β -C), 28.7 (Boc-C(CH₃)₃), 27.5 (Pro γ -C), 25.5 (Pro γ -C), 25.4 (Val β -C), 21.3 and 22.9 (Pro CCH₃), 19.9 (Val γ -C), 17.7 (Val γ -C), 18.1 (Ile γ -C), 15.7 (Ile CH₃), 11.9 (Ile CH₃).

ESI HRMS m/z calcd for C₂₂H₄₈NaN₄O₇ (MNa)⁺, 575.3421; found, 575.3398.

α -Me-D-Pro-Val-Pro-Ile-OMe • HCl (2.2)

The tetrapeptide, Boc- α -Me-D-Pro-Val-Pro-Ile-OMe (**2.13**, 100 mg), was dissolved in 2.5 mL of 4N HCl in dioxane and the solution was stirred at room temperature for 16 hours. The reaction was monitored by TLC until completion and then the reaction mixture was evaporated under reduced pressure to yield 83 mg (94%) of **2.2** as a white solid.

TLC R_f = 0.42 (20% MeOH in EtOAc)

$[\alpha]_D -88.0$ (c 1.1, MeOH)

¹H NMR (COSY, D₂O, 300 MHz) δ 4.26-4.32 (2H, m, Ile α -CH, Pro α -CH), 4.10-4.12 (1H, m, Val α -CH), 3.65-3.75 (1H, m, Pro δ -CH₂), 3.57 (3H, s, Ile-CO₂CH₃), 3.50-3.57 (1H, m, Pro δ -CH₂), 3.21-3.25 (2H, m, D-Pro δ -CH₂), 2.24-2.31 (1H, m, Pro β -CH₂), 1.68-2.15 (9H, m, D-Pro γ -CH₂, Pro γ -CH₂, Pro β -CH₂, D-Pro β -CH₂, Ile β -CH((CH₂CH₃)CH₃), 1.52 (3H, s, D-Pro α -CCH₃), 1.24-1.30 (1H, m, Ile γ -CH(CH₂CH₃)CH₃), 1.10-1.13 (1H, m, Ile γ -CH(CH₂CH₃)), 0.83 (3H, d, Val γ -CH(CH₃)₂), 0.78 (3H, d, Val γ -CH(CH₃)₂), 0.69 - 0.76 (6H, m, Ile-CH(CH₃)CH₂CH₃).

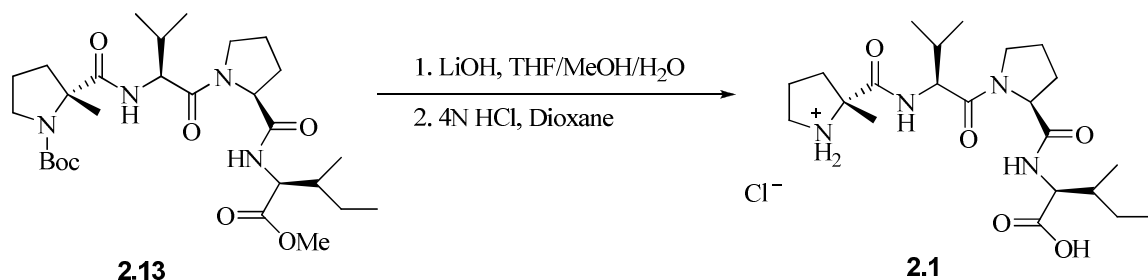
¹³C NMR, DEPT (D₂O, 75 MHz) δ 174.1 (Pro-CONH), 174.0 (D-Pro-CONH), 172.3 (Ile-COCH₃), 171.7 (Val-CONH), 70.0 (D-Pro α -C), 60.5 (Pro α -CH), 58.1 (Ile α -CH), 57.9 (Val α -CH), 52.8 (Ile-COCH₃), 48.7 (Pro δ -CH₂), 45.4 (D-Pro δ -CH₂), 36.5 (Ile β -

CH(CH₃)CH₂CH₃), 36.1 (D-Pro β-CH₂), 30.2 (Val-β CH(CH₃)₂), 29.6 (Pro β-CH₂), 25.1 and 25.0 (Ile γ-CH₂ and Pro γ-CH₂), 23.4 (D-Pro γ-CH₂), 21.4 (D-Pro-C(CH₃)₂), 18.4 (Val γ-CH(CH₃)₂), 18.0 (Val γ-CH(CH₃)₂), 15.2 (Ile-CH(CH₃)CH₂CH₃), 10.8 (Ile-CH(CH₃)CH₂CH₃)

ESI HRMS *m/z* calcd for C₂₃H₄₁N₄O₅ (MH)⁺, 453.3099; found, 453.3091.

HPLC: *t_R* (2% H₂O in 98% CH₃CN) 8.88 minutes; *t_R* (2% MeOH in 98% CH₃CN) 7.91 minutes. Sample dissolved in CHCl₃ and MeOH.

α-Me-D-Pro-Val-Pro-Ile-OH • HCl (2.1)



The tetrapeptide Boc-α-Me-D-Pro-Val-Pro-Ile-OMe (**2.13**, 110 mg) was dissolved in THF/MeOH/H₂O (3:1:1, 0.3 M total concentration). To the solution was added 14.4 mg of LiOH. The solution was then allowed to stir for 16 hours. Upon completion, the solvent was evaporated under reduced pressure to give a white solid. The solid was then resuspended in a 1:1 mixture of H₂O and EtOAc whereupon the two layers were separated. The aqueous layer was then acidified to pH 3 with 0.5 M HCl and extracted with EtOAc, dried with MgSO₄ and concentrated under reduced pressure.

The tetrapeptide was then dissolved in 2.5 mL of 4N HCl dioxane and the reaction was stirred at room temperature for 16 hours. The reaction was monitored by TLC until completion and then evaporated under reduced pressure to yield 73 mg of **2.1** as a white solid in a 84.5% yield.

TLC $R_f = 0.15$ (2-Propanol / NH_4OH , 4:1)

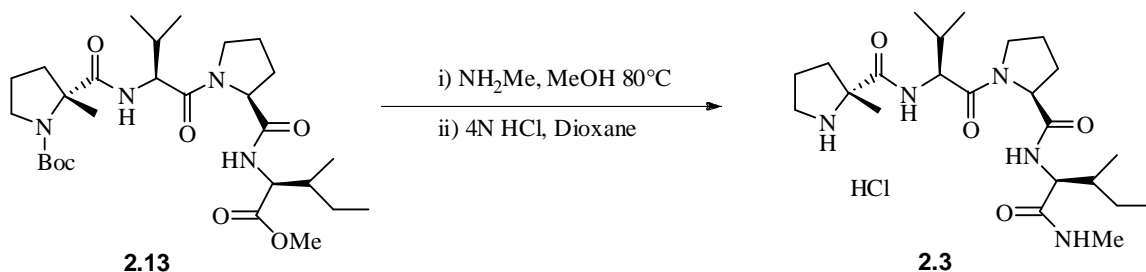
$[\alpha]_D -37.7$ (c 1.4, MeOH)

^1H NMR (COSY, TOCSY, D_2O + 1 drop of CD_3OD , 300 MHz) δ 4.22-4.27 (m, 2H, Pro $\alpha\text{-CH}$, Val $\alpha\text{-CH}$, 4.01 (d, 1H, Ile $\alpha\text{-CH}$), 3.62-3.71 (m, 1H, Pro $\delta\text{-CH}_2$), 3.41-3.51 (m, 1H, L-Pro $\delta\text{-CH}_2$), 3.19 (dd, 2H, D-Pro $\delta\text{-CH}_2$) 2.15-2.28 (m, 1H, D-Pro $\beta\text{-CH}_2$), 1.65-2.15 (m, 9H, D-Pro $\gamma\text{-CH}_2$, Pro- $\gamma\text{-CH}_2$, Pro $\beta\text{-CH}_2$, D-Pro $\beta\text{-CH}_2$, Ile $\beta\text{-CH}$, 1.47 (s, 3H, D-Pro $\alpha\text{-CH}_3$), 1.18-1.31 (m, 1H, Ile $\text{CH}(\text{CH}_2\text{CH}_3)\text{CH}_3$), 0.95-1.10 (m, 1H, Ile $\text{CH}(\text{CH}_2\text{CH}_3)\text{CH}_3$), 0.79 (d, 3H, Val $\text{CH}(\text{CH}_3)_2$), 0.73 (d, 3H, Val $\text{CH}(\text{CH}_3)_2$), 0.65-0.70 (m, 6H, Ile $\text{CH}(\text{CH}_3)\text{CH}_2\text{CH}_3$).

^{13}C NMR (DEPT, HMQC, D_2O + 1 drop of CD_3OD , 75 MHz) δ 175.5 (Pro CONH), 173.9 (D-Pro CONH), 172.2 (Ile COOH), 171.6 (Val CONH), 69.9 (D-Pro $\alpha\text{-C}(\text{CH}_3)$), 60.6 (Pro $\alpha\text{-CH}(\text{CONH})$), 58.1 (Ile $\alpha\text{-C}$), 58.0 (Val $\alpha\text{-C}$), 48.7 (Pro $\delta\text{-CH}_2$), 45.4 (D-Pro $\delta\text{-CH}_2$), 36.4 (Ile $\beta\text{-CH}$), 36.0 (D-Pro $\beta\text{-CH}_2$), 30.2 (Val $\beta\text{-CH}$), 29.5 (Pro $\beta\text{-CH}_2$), 25.0 (2 distinct peaks, Ile $\gamma\text{-CH}_2$, and Pro $\gamma\text{-CH}_2$), 23.4 (D-Pro $\gamma\text{-CH}_2$), 21.4 (D-Pro $\text{C}(\text{CH}_3)$), 18.4 (Val $\text{CH}(\text{CH}_3)_2$), 18.0 (Val $\gamma\text{-CH}(\text{CH}_3)_2$), 15.3 (Ile $\text{CH}(\text{CH}_3)\text{CH}_2\text{CH}_3$), 10.9 (Ile $\text{CH}(\text{CH}_3)\text{CH}_2\text{CH}_3$).

ESI HRMS m/z calcd for $\text{C}_{22}\text{H}_{39}\text{N}_4\text{O}_5$ (MH)⁺, 439.2942; found, 439.2917.

HPLC: t_R (2% H_2O in 98% CH_3CN) 6.15 minutes; t_R (2% MeOH in 98% CH_3CN) 7.29 minutes. Sample dissolved in CHCl_3 and MeOH

α -Me-D-Pro-Val-Pro-Ile-NHMe • HCl (2.3)

The tetrapeptide, Boc- α -Me-D-Pro-Val-Pro-Ile-OMe (**2.13**, 110mg) was dissolved in MeOH (11 mL) and anhydrous monomethyl amine gas bubbled through the solution at -78°C for 5 minutes. The solution was allowed to warm to room temperature and then was placed within a bomb and heated to 80°C overnight. The reaction was then evaporated under reduced pressure resulting in a light yellow oil that was purified by silica gel chromatography (9 cm of silica, 3 cm. diameter column, 2% MeOH / EtOAc) to yield 85 mg of **2.3** as a clear oil in a 78% yield.

TLC $R_f = 0.43$ (2% MeOH in EtOAc)

$[\alpha]_D -36.2$ (c 1.5, MeOH)

$^1\text{H NMR}$ (CDCl_3 , 300 MHz) δ 4.45-4.52 (m, 2H, Pro α -CH, Ile α -CH), 4.09-4.14 (m, 1H, Val α -CH), 3.82-3.95 (m, 1H, Pro δ -CH₂), 3.61-3.67 (m, 2H, D-Pro δ -CH₂, Pro δ -CH₂), 3.47-3.48 (m, 1H, D Pro δ -CH₂), 2.72 (s, 3H, NHCH₃), 1.77-2.19 (m, 10H, D-Pro β -CH₂, D-Pro γ -CH₂, Pro γ -CH₂, Pro β -CH₂, D-Pro β -CH₂, Ile β -CH), 1.56-1.63 (m, 1H, Ile CH(CH₂CH₃)CH₃), 1.56 (s, 3H, D-Pro α -CH₃), 1.46 (s, 9H, C(CH₃)₃), 1.16-1.29 (m, 1H, Ile CH(CH₂CH₃)CH₃), 1.02 (d, 3H, Val CH(CH₃)₂), 0.97 (d, 3H, Val CH(CH₃)₂), 0.88-0.94 (m, 6H, Ile CH(CH₂CH₃)CH₃).

Boc- α -Me-D-Pro-Val-Pro-Ile-NHMe (80 mg) was then dissolved in 4N HCl in dioxane (2.5 mL) and the solution was stirred for 16 hours at room temperature. The reaction was monitored by TLC and upon completion the solution was evaporated under reduced pressure to yield a light yellow solid (85%).

TLC R_f = 0.12 (10% MeOH in EtOAc)

$[\alpha]_D -86.5$ (c 2.1, MeOH)

^1H NMR (COSY, TOCSY, D_2O , 300 MHz) δ 4.24-4.32 (m, 2H, Ile α -CH, Pro α -CH), 3.84-3.88 (m, 1H, Val α -CH), 3.70-3.76 (m, 1H, Pro δ -CH₂), 3.49-3.58 (m, 1H, Pro δ -CH₂), 3.21-3.26 (m, 2H, D-Pro δ -CH₂), 2.56 (s, 3H, NHCH₃), 2.25-2.31 (m, 1H, Pro β -CH₂), 1.61-2.16 (m, 9H, Pro γ -CH₂, D-Pro γ -CH₂, Pro β -CH₂, Pro β -CH₂, Ile β -CH, Val β -CH), 1.52 (s, 3H, D-Pro α -C(CH₃)), 1.31-1.37 (m, 1H, Ile γ -CH₂), 1.02-1.09 (m, 1H, Ile γ -CH₂), 0.84 (d, 3H, Val CH(CH₃)₂), 0.79 (d, 3H, Val CH(CH₃)₂), 0.70-0.74 (m, 6H, Ile CH(CH₃)CH₂CH₃).

^{13}C NMR (DEPT, HMQC, D_2O , 75 MHz) δ 174.0 (Pro CONH), 173.9 (Pro CONH), 172.3 (Ile CONHMe), 171.7 (Val CONH), 70.0 (D-Pro α -C), 60.6 (Pro α -CH), 58.9 (Ile α -CH), 58.1 (Val α -CH), 48.7 (Pro δ -CH₂), 45.4 (D-Pro δ -CH₂), 36.2 (Ile β -CH), 36.1 (D-Pro β -CH₂), 30.2 (Val β -CH), 29.6 (Pro β -CH₂), 25.9 (Ile-CONHCH₃), 25.0 (2 distinct peaks, Ile γ -CH₂ and Pro γ -CH₂), 23.4 (D-Pro γ -CH₂), 21.5 (D-Pro-C(CH₃)), 18.5 (Val CH(CH₃)₂), 18.1 (Val CH(CH₃)₂), 15.0 (Ile CH(CH₃)CH₂CH₃), 10.4 (Ile CH(CH₃)CH₂CH₃)

ESI HRMS m/z calcd for C₂₃H₄₂N₅O₃ (MH)⁺, 452.3259; found, 452.3248.

HPLC: t_R (2% H₂O in 98% CH₃CN) 8.23 minutes; t_R (2% MeOH in 98% CH₃CN) 12.43 minutes. Sample dissolved in CHCl₃ and MeOH

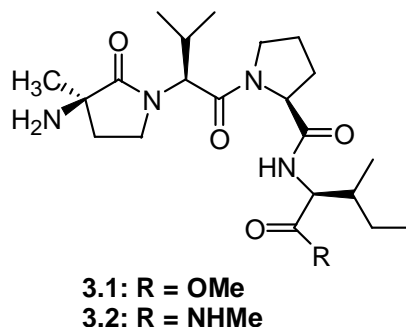
2.9. References

1. Yang, L.; Mashima, T.; Sato, S.; Mochizuki, M.; Sakamoto, H.; Yamori, T.; Oh-Hara, T.; Tsuru, T. Predominant suppression of apoptosome by inhibitor of apoptosis protein in non-small lung cancer H460 cells: therapeutic effect of a novel polyarginine-conjugated Smac peptide. *Cancer Res.* **2003**, *63*, 831 – 837.
2. Meng, X.; Lee, S.; Kaufmann, S. H. Apoptosis in the treatment of cancer: a promise kept? *Cur. Op. Cell Biol.* **2006**, *18*, 668 – 676.
3. Pang, Y. P.; Perola, E.; Xu, K.; and Prenderast, F. G. EUDOC: A computer program for identification of drug interaction sites in macromolecules and drug leads from chemical databases. *J. Comp. Chem.* **2001**, *22*, 1750 – 1771.
4. Wu, G.; Chai, J.; Suber, T. L.; Wu, J. W.; Du, C.; Wang, X.; Shi, Y. Structural basis of IAP recognition by Smac / DIABLO. *Nature* **2000**, *408*, 1008-1012.
5. Liu, Z.; Sun, C.; Olejniczak, E. T.; Meadows, R. P.; Betz, S. F.; Oost, T.; Herrmann, J.; Wu, J. C.; Fesik, S. W. Structural basis for binding of Smac/DIABLO to the XIAP BIR3 domain. *Nature* **2000**, *408*, 1004 – 1008.

6. Seebach, D.; Does, M.; Naef, R.; Schwizer, B. Alkylation of amino acids without loss of the optical activity: Preparation of *R* – substituted proline derivatives. A case of self-reproduction of chirality. *J. Am. Chem. Soc.* **1983**, *105*, 5390 – 5398.
7. Khalil, E. M.; Subasinghe, N. L.; Johnson, R. L. An efficient and high yield method for the N-tert-butoxycarbonyl protection of sterically hindered amino acids. *Tetrahedron Lett.* **1996**, *37*, 3441-3444.
8. Huang, H.; Iwasawa, N.; and Mukaiyama, T.A. A Convenient Method for the Construction of Beta-Lactam Compounds from Beta-Amino Acids. *Chem. Lett.* **1984**, 1465-1466.
9. Perrin, D. D.; Armarego, L.F. Purification of Laboratory Chemicals, 3rd Edition. Pergamon Press. pgs. 157-158.
10. Richmond, M.L.; Seto, C.T. Modular ligands derived from amino acids for the enantioselective addition of organozinc reagents to aldehydes. *J. Org. Chem.* **2003**, *68*, 7505-7508.
11. Friener, R. A.; Bank, J. L.; Murphy, R. B.; Halgren, T. A.; Kiere, J. J.; Mainz, D. T.; Repasky, M. P.; Knoll, E. H.; Shelly, M.; Perry, J. K.; Shaw, D. E.; Francis, P.; Shenkin, P. S. Glide: a new approach for rapid, accurate docking and scoring. 1. Method and assessment of docking accuracy. *J. Med. Chem.* **2004**, *47*, 1739 – 1749.

12. Nikolovska-Coleska, Z.; Wang, R.; Fang, X.; Pan, H.; Tomita, Y.; Li, P.; Roller, P. P.; Krajewski, K.; Saito, N. G.; Stuckey, J. A.; Wang, S. Development and optimization of a binding assay for the XIAP- BIR3 domain assay fluorescence polarization. *Anal. Biochem.* **2004**, *332*, 261- 273.
13. Sun, H.; Nikolovska-Coleska, Z.; Chen, J.; Yang, C.; Tomita, Y.; Pan, H.; Yoskioka, Y.; Krajewski, K.; Roller, P. P.; Wang, S. Structure – based design, synthesis and biochemical testing of novel and potent Smac peptido-mimetics. *Bioorg. Med. Chem. Lett.* **2005**, *15*, 793 – 797.
14. Shatzmiller, S.; Dolitzky, B.; Bahar, E. Preparation and use of chloromethyl (-)-menthyl ether in the synthesis of optically pure α -branched α -amino nitriles. *Liebigs Ann. Chem.* **1991**, *4*, 375-379.
15. Seebach, D.; Dziadulewicz, E.; Behrendt, L.; Cantoreggi, S.; Fitzi, R. Synthesis of Nonproteinogenic (*R*)- or (*S*)-Amino Acids Analogues of Phenylalanine, Isotopically Labelled and Cyclic Amino Acids from tert-Butyl 2-(tert-Butyl)-3-methyl-4-oxo-1-imidazolidinecarboxylate (Boc-BMI). *Liebigs Ann. Chem.* **1989**, *12*, 1215-1232.
16. Long, J.; Yuan, Yi.; Shi, Y. Asymmetric Simmons-Smith cyclopropanation of unfunctionalized olefins. *J. Am. Chem. Soc.* **2003**, *125*, 13632-13633.

Chapter 3. The Stereoselective Synthesis of ψ_1 Constrained AVPI mimics



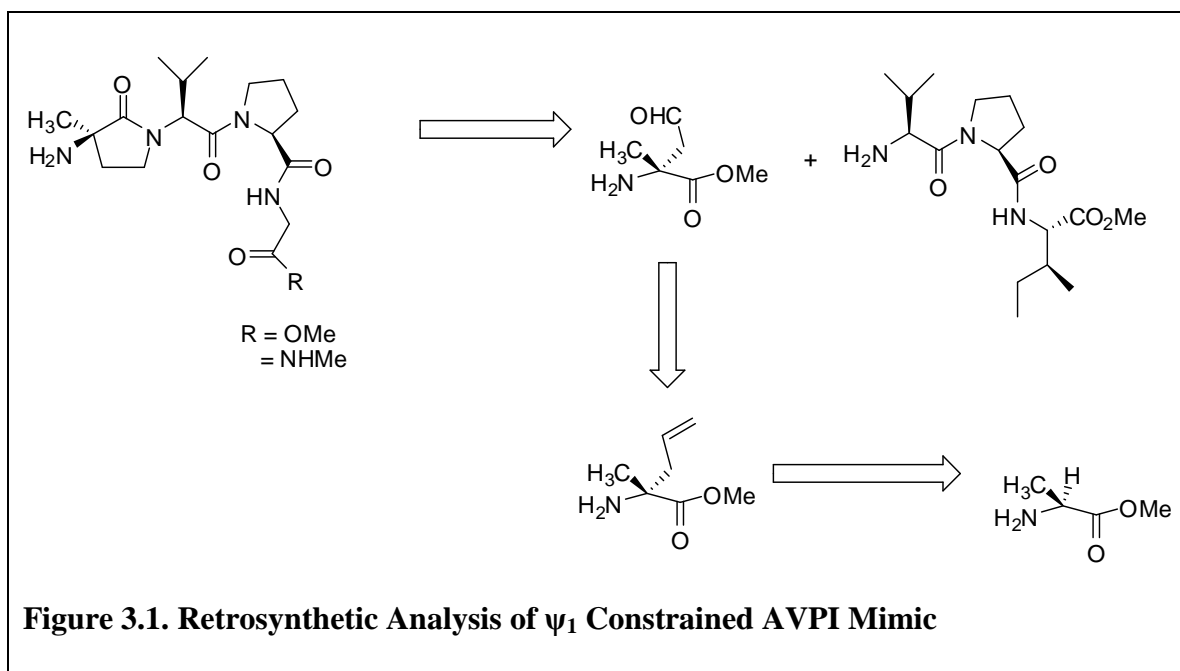
3.1. Design and Scope

SAR analysis, previously described in **Chapter 1**^{1,2}, provided evidence for the critical nature of the P1 Ala of the AVPI and AYPW native peptides. Positioning of the alanine side chain places the 3 critical hydrogens bonds of the amino group in the correct biological space within the active site. While designing the next series of peptidomimetics, we constrained the ψ_1 torsion angle of the P1 residue to mimic the biological orientation of the native peptide. Initial modeling by the Pang group suggested that an ethylene bridge between the alpha position of alanine and the nitrogen of the P2 valine would establish the necessary torsion angle to position alanine side chain correctly within the AVPI binding site. The Pang group predicts, through its proprietary EUDOC docking program, that the ψ_1 torsion angle of the constrained peptide will be approximately 146° .³ This torsion angle is similar to the AYPI peptide ψ_1 value of 159° . Theoretically, this should place the amino and methyl group of our constrained mimic within the same space as the AYPI peptide. We also synthesized peptidomimetics wherein the C-terminus existed as methyl ester and the methyl amide moieties as they were the most effective in the previous series of mimics and they provide additional opportunities for hydrogen bonding interactions. The free acid was excluded based upon

its lack of activity in previous assays and due to the conversion of the methyl ester to the amino acid via esterases *in vivo*. These modifications, like the ϕ_1 mimics, will decrease the degrees of freedom of the peptide mimics, hopefully constraining the compound to a greater degree to its bioactive conformation. Constraints should also increase the bioavailability of the tetrapeptides as well as their *in vivo* stability.

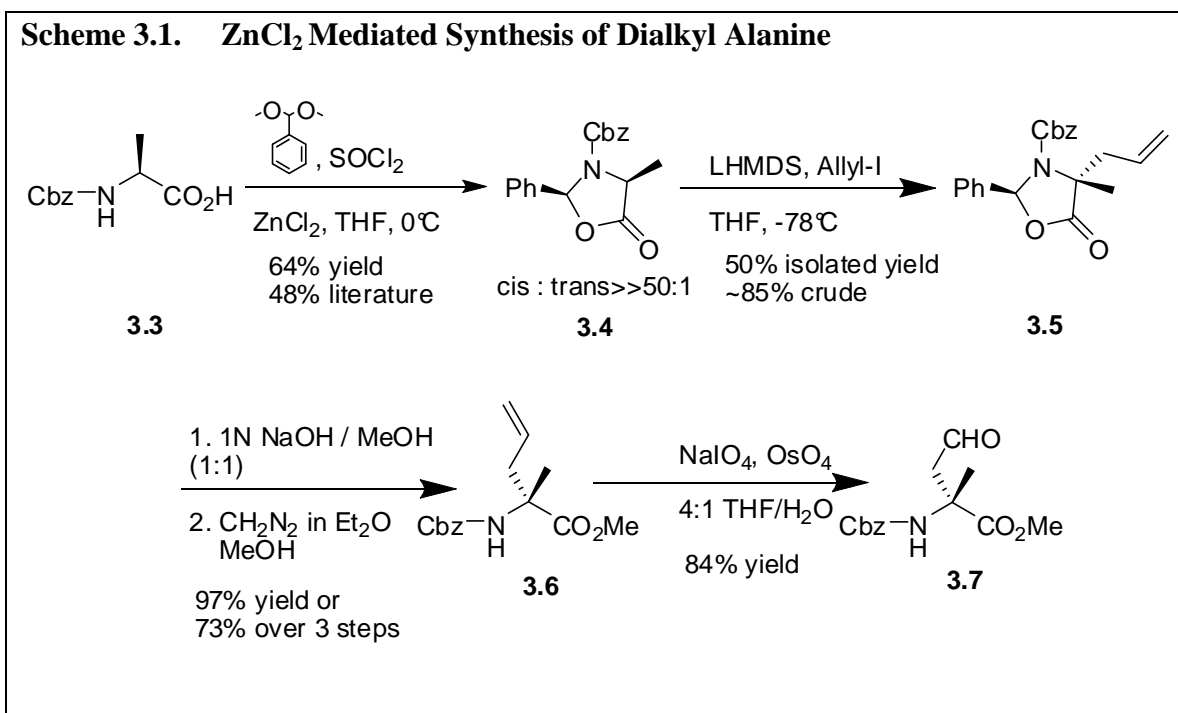
3.4 Synthetic Strategy

The ethylene bridge between the P1 alpha position and the nitrogen of P2 is easily achieved through the synthesis of a γ -lactam derivative of alanine. Several strategies have been used over the years for the synthesis of γ -lactams. Prominent among them are the Freidinger lactam synthesis which utilizes a sulfonium salt to affect an intramolecular cyclization to lactams of various sizes.⁴ Reductive amination with subsequent amination has also been used to great effect.⁵ The intramolecular Mitsunobu reaction has also been incorporated in lactam synthetic schemes.^{6,7} Dr. Bhooma Raghavan in our laboratory employed a modified version of Palomo's method⁸ of lactam synthesis that avoided the necessary α,α' alkylation of the desired amino acid. In the case of the ψ_1 constrained peptidomimetic, we chose to apply the well known reductive amination and cyclization chemistry as this had been used recently and the reactions were well known. The retrosynthetic analysis is shown in **Figure 3.1**. First, cost effective Boc-alanine was stereoselectively alkylated to the allyl alanine derivative. Subsequent derivatization to the aldehyde was achieved through standard oxidative cleavage from the alkene. Final formation of the final compounds can be envisioned to proceed through a reductive amination and cyclization to the γ -lactam constrained compound.

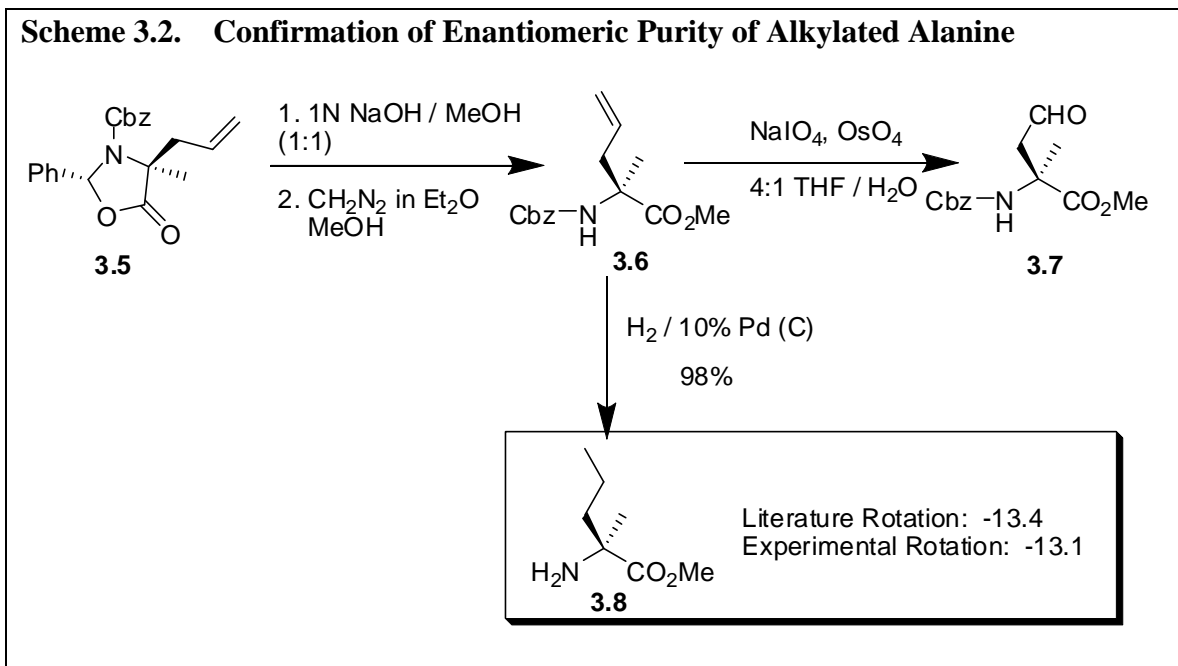


3.3. Stereoselective Alkylation of L-Alanine

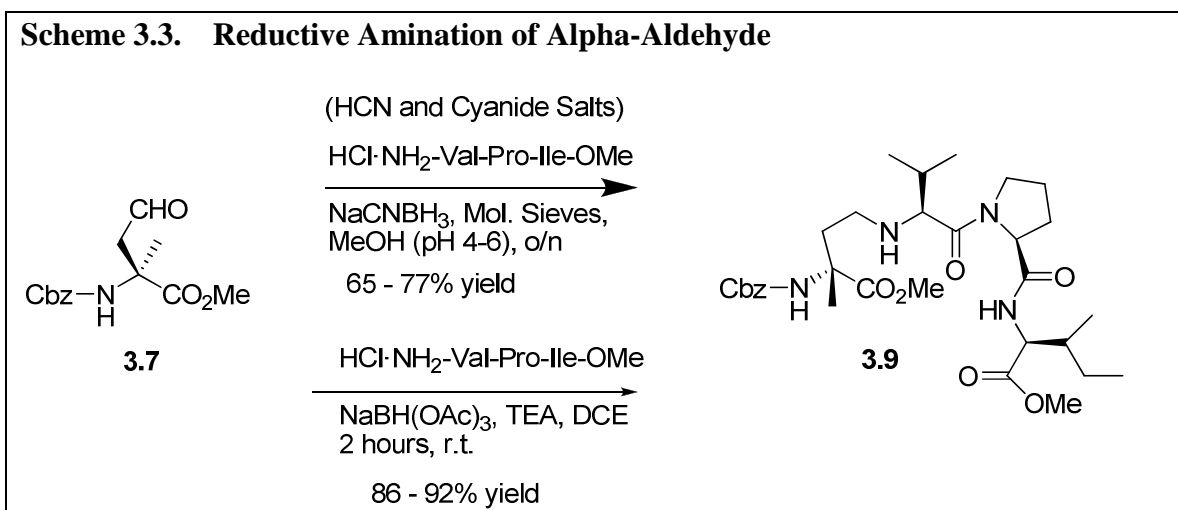
The key synthetic challenge of the ψ_1 constrained mimics was the stereoselective alkylation of L-alanine as shown in **Scheme 3.1**. The recent method of Kapadia *et. al.*⁹ allowed for a large scale synthesis of the γ -lactam utilizing inexpensive starting materials. Cbz protected L-alanine **3.3** was transformed to an oxazolidinone **3.4** with ZnCl_2 , as the Lewis acid, and thionyl chloride. This reaction proceeds through the transformation of the dimethyl acetal of benzaldehyde to a chloro ether. The oxazolidinone is formed through subsequent ester formation and stereoselective cyclization. This reaction is not completely stereoselective in and of itself, but the researchers found that an extensive aqueous workup destroyed the unstable *trans* isomer of the oxazolidinone thereby giving a greater than 50:1 selectivity of the *cis* over the *trans* isomer. Crystallization of the material within ethanol and water afforded pure *cis* product **3.4**.



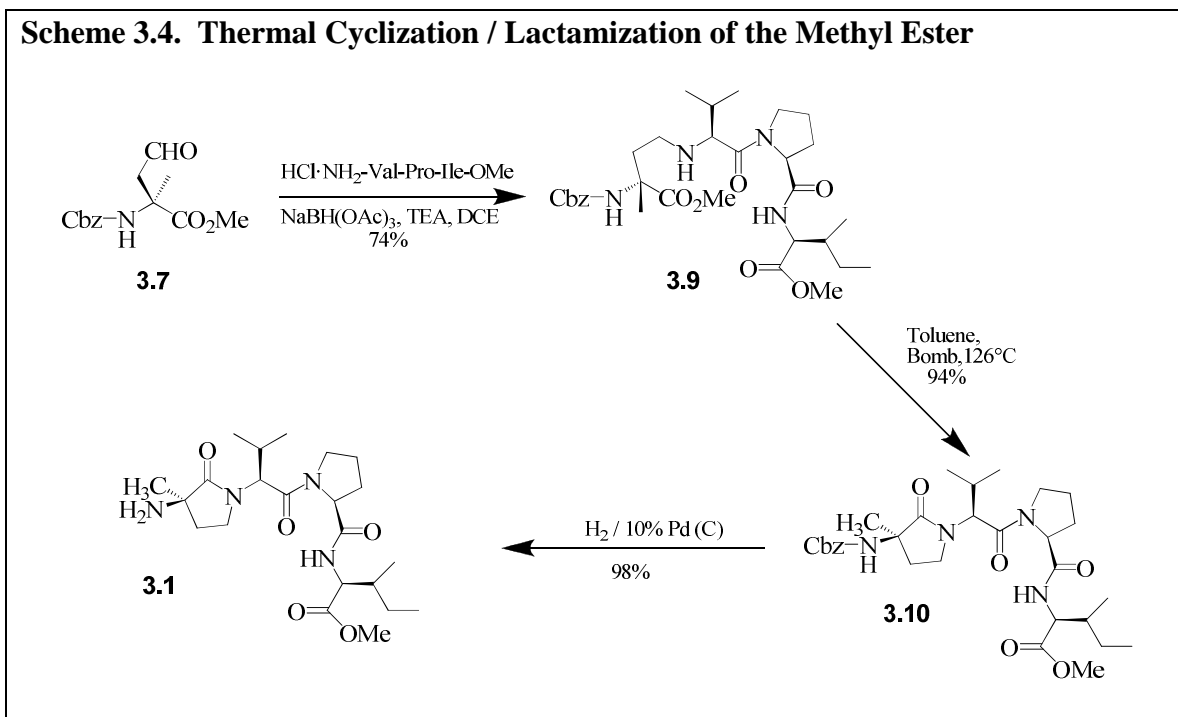
The alpha proton of the *cis* oxazolidinone **3.4** was abstracted with LHMDS in the presence of three equivalents of allyl iodide in THF at -78°C . The temperature of this reaction was carefully monitored so that it did not at any time rise above -70°C even during the quench of the reaction. The alkylated oxazolidinone **3.5** was then hydrolyzed to the free acid and esterified using diazomethane to yield compound **3.6**. Formation of the aldehyde **3.7** was effected by the standard oxidative cleavage of the alkene using sodium periodate and osmium tetroxide to produce the alpha-aldehyde **3.7**.



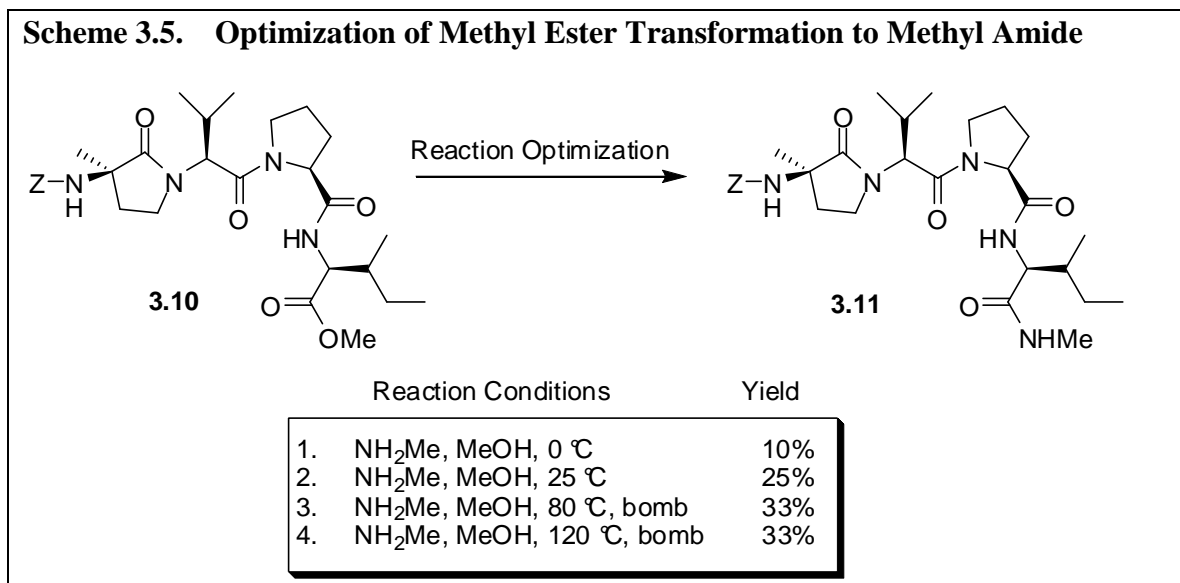
The alkylated product was then confirmed, as shown in **Scheme 3.2**, to be a single enantiomer by the Cbz deprotection to the free amine **3.8**. The optical rotation of this product was taken three times and averaged to give a value of -13.1° , which was then compared to the known literature value of -13.4° .⁹



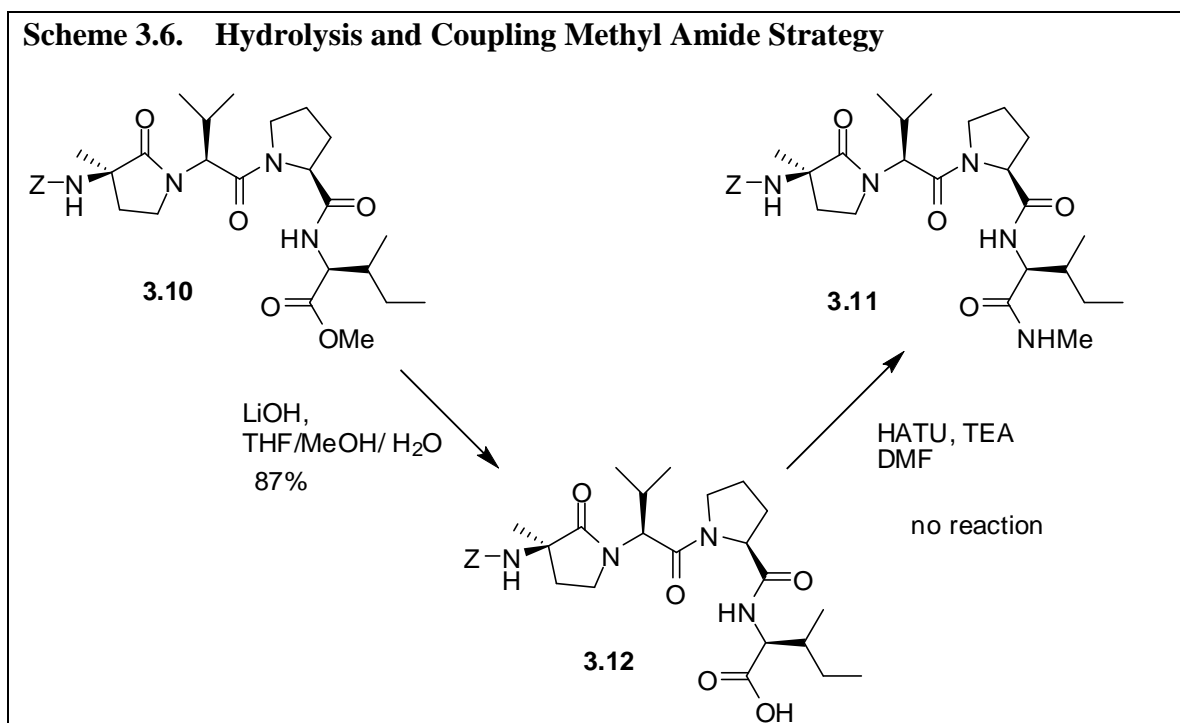
In the course of the experiments, the first method tried for reductive amination was the use of sodium cyanoborohydride which generates in the reaction dangerous HCN and cyanide salts (**Scheme 3.3**). We found that sodium triacetoxyborohydride which does not generate such dangerous side products, had a quicker reaction time and better yield than the traditional cyanoborohydride.



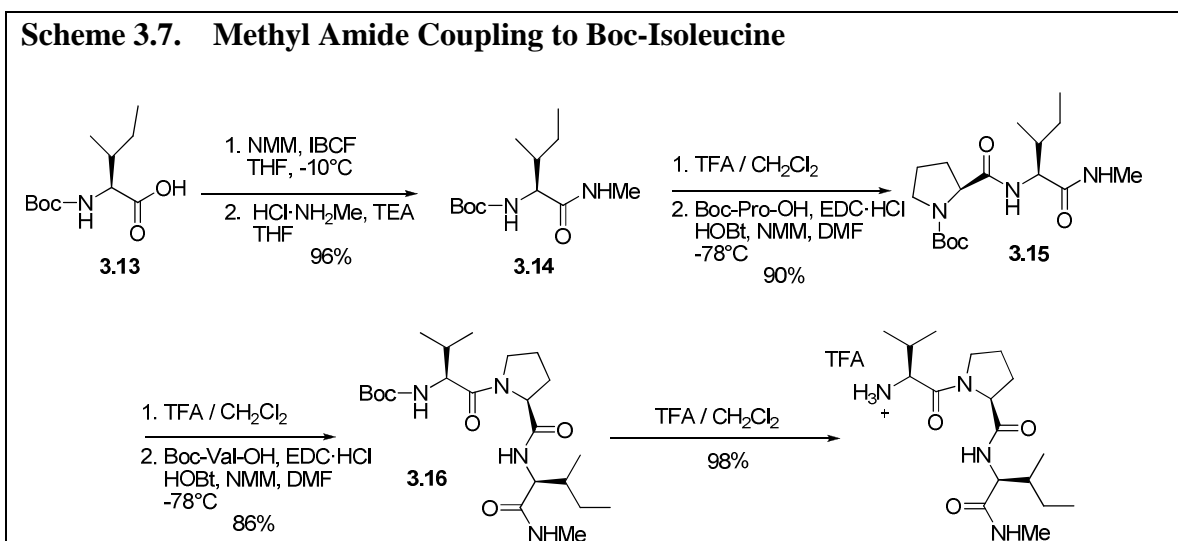
Once the enantiomer was confirmed, aldehyde **3.7** was combined through reductive amination (**Scheme 3.4**) with the hydrochloride salt of Val-Pro-Ile-OMe to yield compound **3.9**. The open form of the γ -lactam was then thermally cyclized by heating a toluene solution of **3.9** to 126°C within a sealed container to yield the protected final product **3.10**.



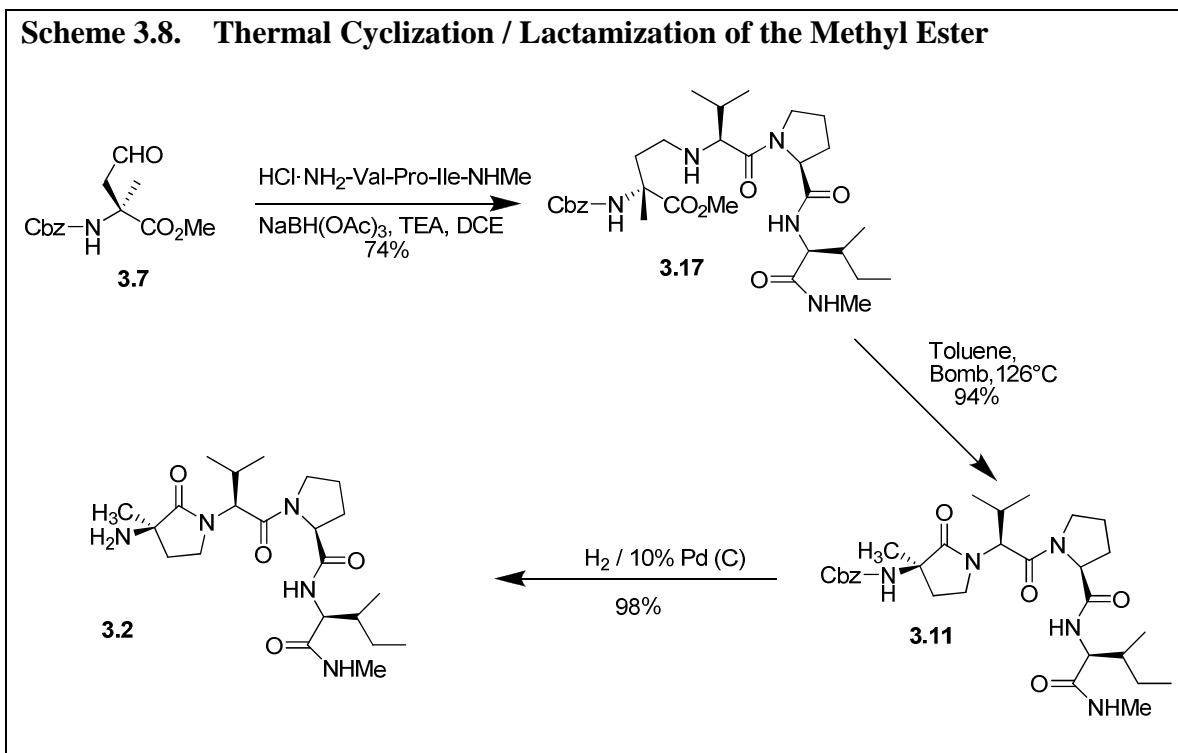
The final transformation of the methyl ester to the methyl amide proved to be problematic. Anhydrous methyl amine gas was used at various temperatures to remove the methoxy group and to replace it with methyl amine. Thermal methyl amination of the methyl ester was not effective as illustrated in **Scheme 3.5**. When it became evident that the thermal cyclization strategy may not work, we hydrolyzed the methyl ester of the final intermediate using LiOH in a solution of THF/MeOH/H₂O (3:1:1) to yield the free acid **3.12**. The attempted coupling of NH₂Me·HCl to the free acid utilizing HATU did not provide any degree of the desired product (**Scheme 3.6**).



Finally, a second fallback strategy, **Scheme 3.7**, was employed which utilized the coupling of methylamine hydrochloride salt to Boc-isoleucine. This step was accomplished using recrystallized $\text{NH}_2\text{Me}\cdot\text{HCl}$, which was first treated with NMM to yield the free amine. To a stirred solution of Boc-isoleucine, isobutyl chloroformate and triethylamine at $-78\text{ }^\circ\text{C}$ the free methylamine at the same temperature was cannulated into the reaction flask. The resultant Boc-Ile-NHMe (**3.14**) was built into tripeptide **3.17** utilizing standard solution phase coupling chemistry previously described in **Chapter 2** (**Scheme 3.7**).



Val-Pro-Ile-NHMe was subsequently exposed to reductive amination conditions with $\text{NaBH}(\text{OAc})_3$ to yield the open tetrapeptide **3.17**. This compound (**3.17**) was then thermally cyclized in toluene at 126°C to the protected final compound **3.11**. Deprotection of the Cbz protecting group with standard $\text{H}_2 / 10\% \text{ Pd}$ on carbon provided the final methyl amine derivative **3.2** of the ψ_1 constrained AVPI mimic (**Scheme 3.8**).



3.4. Biological Testing

For these compounds Dr. Kaufmann's group at the Mayo clinic investigated a new assay method. Unlike the biological assay described in **Chapter 2**, this assay is a direct binding assay utilizing a competitively binding fluorescent protein. The fluorescent protein was generated by expressing a DS-red-BIR3-GST fusion protein in *E. coli* bacteria and then purified with glutathione agarose. DS-red is the fluorescence generating segment of our fusion protein which is coupled to the caspase 9 binding domain, BIR3. This segment was then fused to the GST selection sequence which allowed this fusion protein to be purified on glutathione agarose before use in the binding assay. The completed fusion protein was over expressed with *E. coli* bacteria and subsequently purified and used in the biological assay as the competitive binding agent and 100% binding negative control.

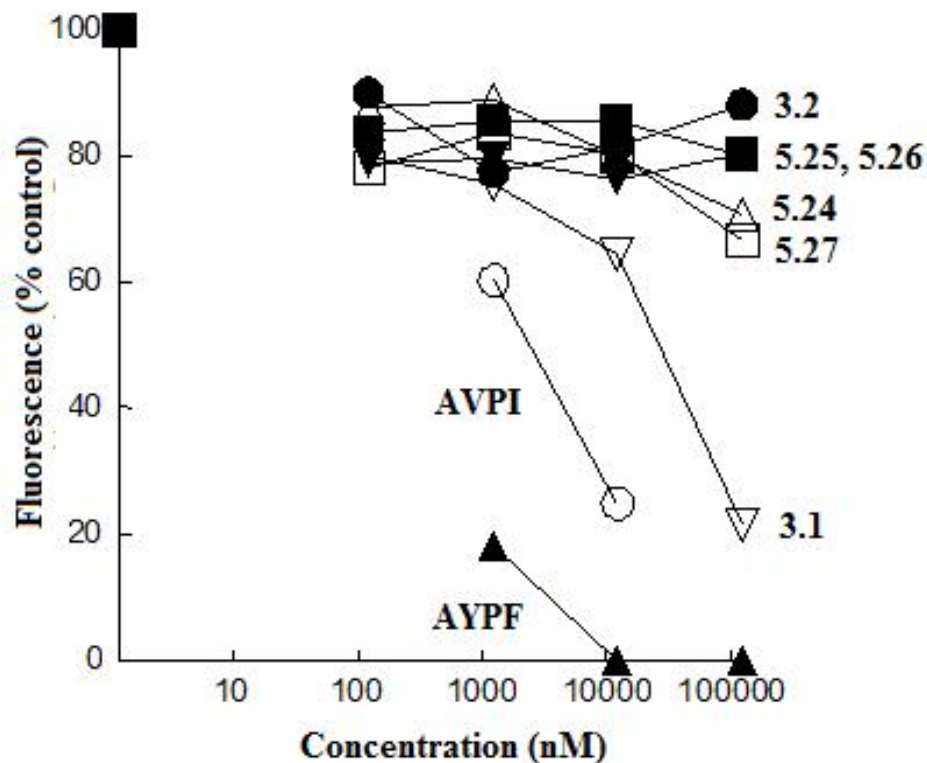


Figure 3.2. Concentration Depend Binding Assay of AVPI Peptidomimetics

The purified fusion protein, DS-red-BIR3-GST, was incubated in the presence or absence of the ψ_1 compounds in concentrations varying from 0.1 μM – 100 μM . After incubation, the plates were washed with buffer to remove free protein and the fluorescence intensity was measured. Fluorescence intensities were compared as a percentage of the control DS-red-BIR3-GST fusion protein when incubated in the absence of competitors. The native caspase-9 AYPF peptide demonstrated an approximated IC_{50} of less than 1 μM while the native terminal tetrapeptide of Smac, AVPI, was $\approx 5 \mu\text{M}$. The methyl ester derivative of the ψ_1 constrained compound **3.1** was the only compound in the entire series for this chapter and **Chapter 5** that showed measurable activity (**Figure 3.2**). The IC_{50} of $\approx 50 \mu\text{M}$ was disappointing but still a more positive result than the greater than 100 μM IC_{50} of the methyl amide derivative. These

slightly disappointing results led once again to further retro – modeling analysis of the compounds in order to glean any further information that was readily available.

3.5. Retro – Modeling Analysis of the ψ_1 Constrained Peptidomimetics

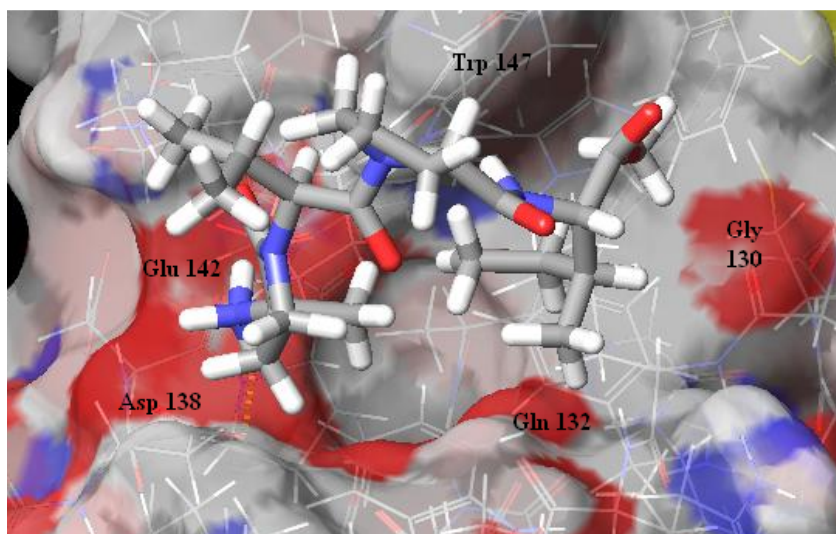


Figure 3.3. Retro-Modeling Analysis of ψ_1 Constrained AVPI Methyl Ester Derivative (3.1)

Modeling analysis of the ψ_1 constrained mimics was performed upon the same *in silico* protein that was built and tested in **Chapter 2**. When the methyl ester derivative of the ψ_1 constrained AVPI mimic was docked into the active site utilizing the Schrödinger flexible docking program (also as described in **Chapter 2**) the methyl ester displayed a unique docking conformation (**Figure 3.3**). The native AVPI peptide utilizes the two hydrophobic pockets within the active site. In the first pocket, AVPI interacts with the key residues through multiple hydrogen bonds to the P1 position. In the second pocket the interaction is through hydrogen bonding to Gly130 and aromatic interactions. The methyl ester derivative displays a tight turn conformation which only interacts within the first pocket. This peptide conformation displays hydrogen bonding interactions to

Asp138, Glu143 and two separate interactions with Gln132 similarly to the native AVPI. Where they differ is that instead of the P2 valine making the critical contacts to Gln132 it is the P4 position of the methyl ester **3.1** derivative which makes the necessary hydrogen bonds. This turn conformation seems to eliminate the steric interference of the ethylene bridge which was observed in the φ_1 constrained mimics and in the methyl amide ψ_1 derivative. The methyl amide derivative **3.2** showed the same hydrogen bonding to Asp138 and Glu143 at the P1 position as well as to Gly130 at the P4 position which are the same hydrogen bonds that AVPI displays (**Figure 3.4**). Where the methyl amide **3.2** differs from AVPI is the absence of the P2 position hydrogen bonds with Gln132. However, the GScore of -5.22 seems to indicate that this compound should have more potent activity as compared the methyl ester instead of significantly less.

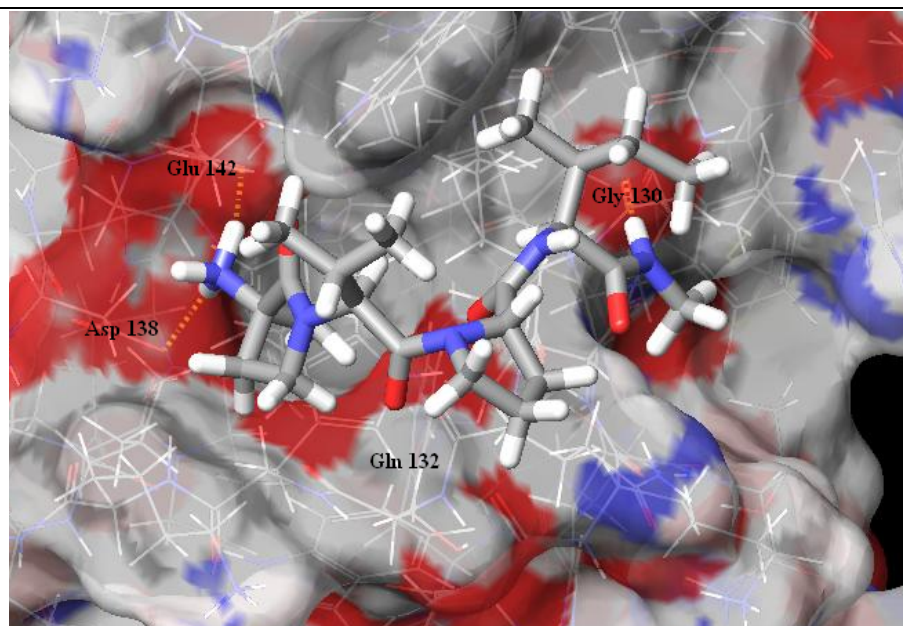
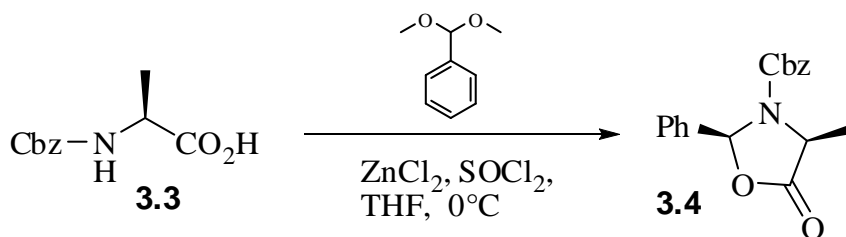


Figure 3.4. Retro-Modeling Analysis of ψ_1 Constrained AVPI Methyl Amide Derivative (3.2)

We explain this disparity with the observation that the GScores differ by less than 0.5 and that the activity of the methyl ester is at the limit of the validation study of 100 μM . Because the *in silico* preferred conformation of the methyl ester is such a radical shift from that observed in AVPI and other compounds we have modeled we constrained the system to resemble the P1 and P2 conformation of the AVPI peptide. These conformations showed drastically lower GScores of -3.72 and -3.24 with 1 and 2 constraints respectively. Placing any further restraints upon the molecule (>3) did not produce valid structures.

3.6. Experimentals

(*S,S*)-4-Methyl-5-oxo-2-phenyl-oxazolidine-3-carboxylic Acid Benzyl Ester (**3.4**)



Thionyl chloride (3.27 mL, 44.8 mmol) was added to Cbz-alanine (**3.3**, 10.0 g, 44.8 mmol) and benzaldehyde dimethyl acetal (6.73 mL, 44.8 mmol) in 75 mL of dry THF at 0°C . After stirring for 5 minutes, anhydrous ZnCl_2 (6.11 g, 44.8 mmol) was added and the reaction mixture was stirred at this temperature for 3 hours. At this stage, 0.2 equivalents each of SOCl_2 (0.6 mL, 9.0 mmol) and anhydrous ZnCl_2 (1.22 g, 9.0 mmol) were added and the reaction mixture was stirred for an additional hour. The

reaction mixture was quenched by dropwise addition of water so that the reaction temperature did not exceed 10 °C. The reaction mixture was then extracted with ethyl ether (200 mL). The ether extract was washed with water until almost neutral (approx. 2 L), with 10% NaHCO₃ (100 mL), water (100 mL), dried with MgSO₄ and evaporated under reduced pressure. The resulting yellow oil was then carefully crystallized from H₂O / EtOH (1: 50) to yield (7.5 g, 54%) of white needles (**3.4**).

Mp 50 – 52 °C

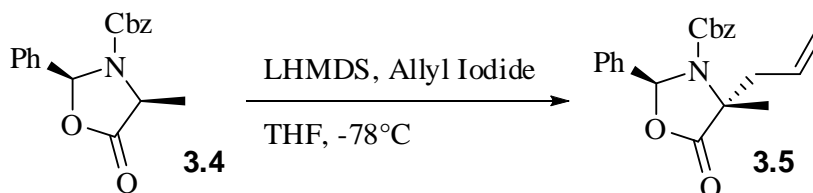
TLC R_f = 0.41 (EtOAc / Hexanes, 1:3)

[α]_D –20.5 (c 0.4, MeOH)

¹H NMR⁹(300 MHz, CDCl₃, COSY) δ 7.41 (s, 5H, Cbz-C₆H₅), 7.34 (s, 5H, C₆H₅), 6.65 (s, 1H, NCHO), 5.17 (t, *J* = 14.7 Hz, 27.3 Hz, 2H, CH₂C₆H₅), 4.49 (q, *J* = 6.9 Hz, 1H, Ala α – CH), 1.58 (d, *J* = 6.9 Hz, 3H, Ala CH₃),

¹³C NMR (75 MHz, CDCl₃) δ 172.2 (Ala CO), 137.1 (C₆H₅), 135.5 (C₆H₅), 130.0 (C₆H₅), 128.9 (C₆H₅), 128.8 (C₆H₅), 128.7 (C₆H₅), 128.3 (C₆H₅), 126.4 (C₆H₅), 89.3 (NCHO), 68.3 (Cbz – CH₂C₆H₅), 52.5 (Ala α-C), 18.6 (Ala CH₃).

4-Allyl-4-methyl-5-oxo-2-phenyl-oxazolidine-3-carboxylic Acid Benzyl Ester (**3.5**)



Allyl iodide (0.88 mL, 9.6 mmol) was added to a stirred solution of the oxazolidinone **3.4** (1.0 g, 3.2 mmol) in THF (7 mL) and the solution was cooled to –78 °C.

A solution of 0.7 M LHMDS (5.8 mL, 3.85 mmol) in THF was then added dropwise to the reaction mixture via cannulation while maintaining an internal temperature no greater than $-70\text{ }^{\circ}\text{C}$. The reaction was monitored for the complete loss of starting material by TLC. Upon completion the reaction was quenched with saturated NH_4Cl (5 mL) and the solvent evaporated under reduced pressure. The resulting yellow oily residue was dissolved in EtOAc (20 mL), washed with brine (20 mL), water (20 mL), dried over MgSO_4 and evaporated under reduced pressure. The residue was then purified by fluorosil column chromatography (3 x 8 cm) eluting with ethyl acetate in hexanes (1:3) to yield 0.55 grams (51%) of the pure product as a clear oil (**3.5**). It should be noted that this product is not stable on silica gel and should normally not be purified.

TLC $R_f = 0.54$ (EtOAc / Hexanes, 1:3)

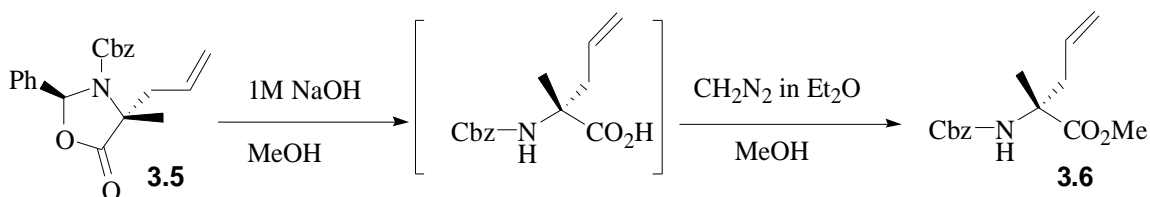
$[\alpha]_D -4.8$ (c 6.2, MeOH)

^1H NMR (300 MHz, CDCl_3 , COSY, *rotamers present*) δ 7.21 – 7.31 (m, 9H, C_6H_5), 6.90 (d, $J = 6.6$ Hz, 1H, C_6H_5), 6.31 and 6.37 (NCHO), 5.58 – 5.75 (m, 1H, $\text{CH}=\text{CH}_2$), 5.05 – 5.29 (m, 2H, $\text{CH}=\text{CH}_2$), 4.98 (s, 2H, $\text{Cbz}-\text{CH}_2\text{C}_6\text{H}_5$), 2.94 and 3.30 (dd, 1H, $J = 9$ Hz, 13.5 Hz, $\text{CH}_2\text{C}_6\text{H}_5$), 2.57 (dd, $J = 6$ Hz, 13.5 Hz, $\text{CH}_2\text{C}_6\text{H}_5$), 1.75 and 1.84 (Ala- CH_3).

^{13}C NMR (75 MHz., CDCl_3 , *rotamers present*) δ 174.1 (Ala CO), 151.9 (Cbz CO), 137.2 (C_6H_5), 135.5 (C_6H_5), 131.2 (C_6H_5), 130.7 (C_6H_5), 130.1 (C_6H_5), 128.9 (C_6H_5), 128.5 (C_6H_5), 128.3 (C_6H_5), 128.0 (C_6H_5), 127.1 ($\text{CH}=\text{CH}_2$), 121.6 ($\text{CH}=\text{CH}_2$), 89.8 (NCHO), 67.5 and 68.2 ($\text{Cbz} - \text{CH}_2\text{C}_6\text{H}_5$), 63.1 and 63.5 (Ala α -C), 39.8 and 41.7 ($\text{CH}_2\text{CH}=\text{CH}_2$), 24.0 and 24.9 (Ala CH_3).

ESI HRMS m/z calcd for $\text{C}_{21}\text{H}_{21}\text{NNaO}_4$ (MNa) $^+$, 374.1368; found, 374.1372.

2-Benzyloxycarbonylamino-2-methyl-pent-4-enoic Acid Methyl Ester (3.6)



A solution of the allyl oxazolidinone **3.5** (0.32 g, 0.91 mmol) in 10 mL of a mixture of 1M NaOH / methanol (1:1) was allowed to stir at room temperature overnight. The mixture was concentrated under reduced pressure and the resulting residue was acidified with 10% NaHSO₄ (50 mL) to pH 1. This mixture was extracted with EtOAc (3 x 50 mL). The combined organic phases were washed with H₂O (50 mL), brine (50 mL), dried over MgSO₄, and concentrated *in vacuo*. The crude Cbz- α -allyl-Ala-OH that was obtained as a light yellow oil was taken forward without further purification.

Crude Cbz- α -allyl-Ala-OH (0.23 g, 0.9 mmol) was dissolved in MeOH (20 mL) and the solution was cooled to 4 °C. To this clear solution was added CH₂N₂ in Et₂O until bubbling ceased and the solution maintained a bright yellow color. The reaction was then evaporated under reduced pressure to yield a clear yellow oil. This residue was then purified by column chromatography (3 x 8 cm) eluting with ethyl acetate in hexanes (1:3) to yield 0.23 g (97%) of the pure product as a clear oil (**3.6**).

TLC R_f = 0.41 (EtOAc / Hexanes, 1:3)

[α]_D 15.6 (*c* 2.4, MeOH)

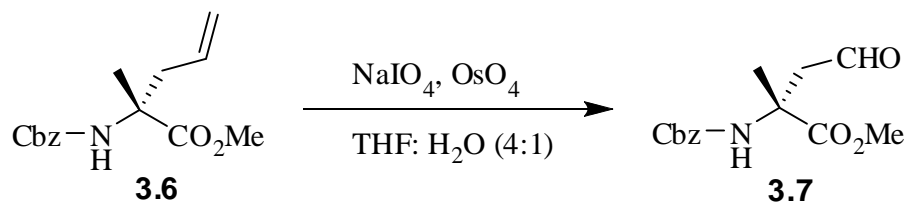
¹H NMR (300 MHz, CDCl₃, COSY) δ 7.26 – 7.39 (m, 5H, Cbz-C₆H₅), 5.55 – 5.71 (m, 2H, CH=CH₂, Ala NH), 5.04 – 5.12 (m, 4H, CH=CH₂, Cbz-CH₂C₆H₅), 3.73 (s, 3H,

CO₂CH₃), 2.77 – 2.83 (m, 1H, CH₂CH=CH₂), 2.54 – 2.61 (dd, *J* = 7.5 Hz, 14.1 Hz, 1H, CH₂CH=CH₂, 1.56 (s, 3H, Ala – CH₃)

¹³C NMR (75 MHz, CDCl₃, HMQC) δ 174.3 (CO₂CH₃), 154.8 (Cbz-CO), 136.6 (CH=CH₂), 132.3 (C₆H₅), 128.7 (C₆H₅), 128.3 (C₆H₅), 128.2 (C₆H₅), 119.8 (CH=CH₂), 66.8 (Cbz – CH₂C₆H₅), 59.8 (Ala α – C), 53.0 (CO₂CH₃), 41.7 (CH₂C₆H₅), 23.5 (Ala β – C)

ESI HRMS *m/z* calcd for C₁₅H₁₉NNaO₄ (MNa)⁺, 300.1212; found, 300.1205.

2-Benzoyloxycarbonylamino-2-methyl-4-oxo-butyrlic Acid Methyl Ester (3.7)



2-Benzoyloxycarbonylamino-2-methyl-pent-4-enoic acid methyl ester (**3.6**, 0.3 g, 1.1 mmol) was dissolved in a 4:1 mixture of THF in H₂O. This solution was stirred under N₂ and it turned dark brown when OsO₄ (15 mg) was added as a 2.5% solution in *t*-BuOH (0.3 mL). After 5 minutes of stirring the solution, NaIO₄ (0.9 g, 4.2 mmol) was added in three batches over a 90 minute period. At this point, the reaction turned light yellow and stirring was continued for 5 hours. The reaction was then diluted with Et₂O until the layers separated and the aqueous phase was extracted three times with successive Et₂O washes (100 mL). The Et₂O layers were combined, washed with H₂O (150 mL), saturated Na₂SO₃ (150 mL) and dried with MgSO₄. Removal of the solvent *in vacuo* gave a tan oil. The oil was purified by silica gel flash chromatography (5 x 8 cm)

and eluted with ethyl acetate in hexanes (3:1). The isolated clear oil yielded 0.26 g (88%) of the pure compound (**3.7**).

TLC R_f = 0.82 (EtOAc / Hexanes, 3:1)

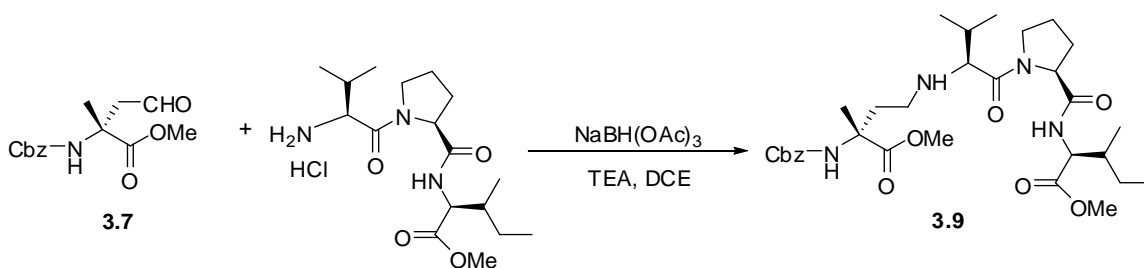
$[\alpha]_D$ 5.9 (*c* 5.4, MeOH)

^1H NMR (300 MHz, CDCl_3 , COSY) δ 9.64 (s, 1H, CHO), 7.25 – 7.37 (m, 5H, Cbz- C_6H_5), 5.93 (br s, 1H, Ala NH), 5.03 (s, 2H, Cbz- $\text{CH}_2\text{C}_6\text{H}_5$), 3.73 (s, 3H, CO_2CH_3), 3.56 (d, J = 18.3 Hz, 1H, CH_2CHO), 3.10 (d, J = 17.7 Hz, 1H, CH_2CHO), 1.56 and 1.58 (s, 3H, Ala – CH_3)

^{13}C NMR (75 MHz, CDCl_3 , HMQC) δ 199.3 (CHO), 173.7 (CO_2CH_3), 154.7 (Cbz-CO), 136.3 (C_6H_5), 128.7 (C_6H_5), 128.3 (C_6H_5), 128.1 (C_6H_5), 66.9 (Cbz – $\text{CH}_2\text{C}_6\text{H}_5$), 56.8 (Ala α -C), 53.4 (CO_2CH_3), 49.5 (CH_2CHO), 24.5 (Ala β -C).

ESI HRMS m/z calcd for $\text{C}_{19}\text{H}_{26}\text{NaN}_2\text{O}_3$ (MNa) $^+$, 302.1004; found, 302.1008.

N-[2(R)-Benzyloxycarbonylamino-2-methoxycarbonyl-4-butyl]-L-Val-L-Pro-L-Ile-OMe (intermediate only) (3.9)



Cbz-2-methyl-4-oxo-butyric acid methyl ester (**3.7**, 0.42 g, 1.5 mmol) and HCl·NH₂-Val-Pro-Ile-OMe (0.62 g, 1.6 mmol) were dissolved in 1,2 dichloroethane (15 mL) and then treated with triethylamine (0.3 mL). After stirring the reaction for 5

minutes, sodium triacetoxyborohydride (0.45 g, 2.1 mmol) was added in one portion and the reaction was stirred at room temperature under N₂ atmosphere for 1.5 – 5 hours. The reaction was monitored by TLC for the disappearance of the starting material. The reaction mixture was then quenched by adding aqueous saturated NaHCO₃, and the product was extracted with EtOAc. The organic layer was dried with MgSO₄ and the solvent was removed under reduced pressure to give the crude free base as a clear oil. The oil was purified by silica gel flash chromatography (5 x 8cm) and eluted with ethyl acetate in hexanes (3:1). The isolated clear oil yielded 0.76 g (83%) of the pure compound (**3.9**).

TLC R_f = 0.42 (EtOAc / Hexanes, 3:1)

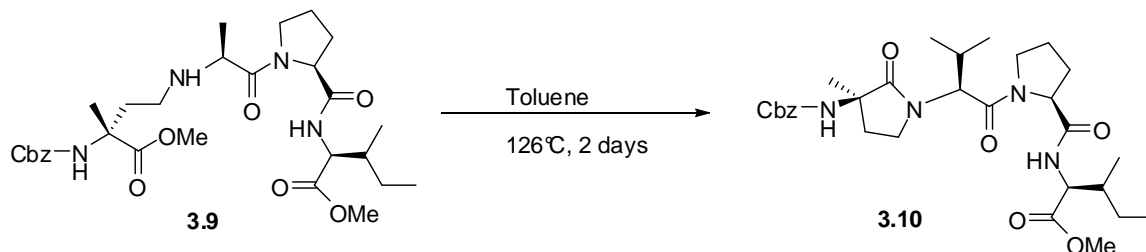
[α]_D – 61.3 (*c* 1.2, MeOH)

¹H NMR (300 MHz, CDCl₃, COSY) δ 8.09 (br s, 1H, Val - NH), 7.38 (d, *J* = 8.1 Hz, 1H, Ala - NH), 7.26 – 7.32 (m, 5H, C₆H₅), 5.04 – 5.05 (m, 2H, Pro α-CH, Ile - NH), 4.62 (d, *J* = 8.1 Hz, 1H, Ile α-CH), 4.43 – 4.74 (m, 1H, Val α-CH), 3.70 (s, 3H, CO₂CH₃), 3.69 (s, 3H, CO₂CH₃), 3.48 – 3.52 (m, 2H, Pro δ-CH₂), 3.09 (d, *J* = 4.5 Hz, 1H, Cbz – CH₂C₆H₅), 2.69 – 2.75 (m, 1H, Cbz – CH₂C₆H₅), 1.77 – 2.35 (m, 10H, Pro β-CH₂, Pro γ-CH₂, Ile β-CH, Val β-CH, NHCH₂CH₂, NHCH₂CH₂), 1.61 (s, 3H, CCH₃), 0.98 – 1.43 (m, 2H, Ile γ-CH₂), 0.83 – 0.95 (m, 12H, Val γ-CH₃, Ile γ-CH₃, Ile δ-CH₃)

¹³C NMR (75 MHz, CDCl₃, HMQC) δ 174.7 (Ile CO₂CH₃), 174.4 (Pro CO), 172.2 (Val CO), 170.9 (Ala CO₂CH₃), 155.9 (Cbz – CO), 136.9 (C₆H₅), 128.5 (C₆H₅), 128.0 (C₆H₅), 128.0 (C₆H₅), 66.5 (Pro α – C), 65.6 (Cbz – CH₂C₆H₅), 60.4 (Ile α – CH), 59.9 (Ala – CCH₃), 57.1 (Val α – CH), 52.8 (Ile CO₂CH₃), 52.3 (Ala CO₂CH₃), 47.7 (Pro δ – CH₂), 44.7 (Pro β – CH₂), 38.6 (CH₂CH₂NH), 38.0 (Ala C(CH₃)), 31.8 (CH₂CH₂NH), 27.4 (Val

$\beta - \text{CH}$), 25.5 (Ile $\beta - \text{CH}$), 25.4 (Pro $\gamma - \text{CH}_2$), 24.6 (Ile $\gamma - \text{CH}_2$), 20.4 (Val CH_3), 18.2 (Val CH_3) 15.8 (Ile CH_3), 11.9 (Ile CH_3).

***N*-[3-(*R*)-[Benzyloxycarbonylamino-3-methyl-2-oxo-1-pyrrolidine-(*S*)-3-methyl-2-butanoyl-Pro-Ile-OMe (3.10)**



N-[2(*R*)-Benzyloxycarbonylamino-2-methoxycarbonyl-3-butyl]-Val-Pro-Ile-OMe (**3.9**, 0.2 g, 0.33 mmol) was dissolved in toluene and the solution was placed within a sealed vessel. The reaction was then heated to 126 °C for 2 days and then it was allowed to cool to room temperature. Toluene was evaporated under reduced pressure to afford the crude product as a slightly orange oil. The oil was purified by silica gel flash chromatography (5 x 8 cm) and eluted with ethyl acetate in hexanes (3:1). The isolated clear oil yielded 0.14 g (74%) of the pure compound (**3.10**).

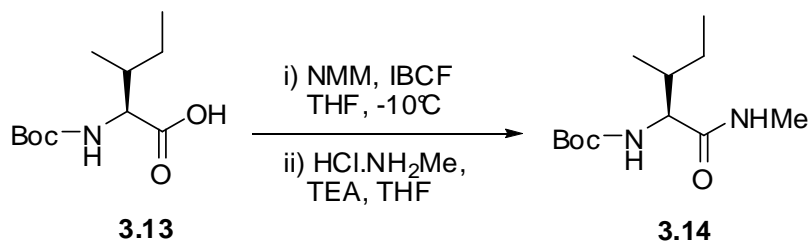
TLC $R_f = 0.23$ (EtOAc / Hexanes, 3:1)

$[\alpha]_D - 156.4$ (c 1.1, MeOH)

$^1\text{H NMR}$ (300 MHz, CDCl_3 , COSY) δ 7.19 – 7.30 (m, 5H, C_6H_5), 7.17 (d, $J = 8.4$ Hz, 1H, Cbz- $\text{CH}_2\text{C}_6\text{H}_5$), 5.36 (s, 1H, NH), 5.00 (m, 2H, NH, Pro $\alpha\text{-CH}$), 4.48 – 4.52 (m, 2H, Val $\alpha\text{-CH}$, Ile $\alpha\text{-CH}$), 3.69 – 3.74 (m, 1H, Pro $\delta\text{-CH}_2$), 3.64 (s, 3H, CO_2CH_3), 3.54 – 3.60 (m, 1H, Pro $\delta\text{-CH}_2$), 3.34 – 3.39 (m, 2H, NHCH_2), 1.73 – 2.41 (m, 8H, NHCH_2CH_2 , Val

β -CH, Pro δ -CH₂, Pro γ -CH₂, Ile β -CH), 1.32 – 1.40 (m, 1H, Ile γ -CH₂), 1.25 (s, 3H, CCH₃), 1.06 – 1.18 (m, 1H, Ile γ -CH₂), 0.80 – 0.92 (m, 12H, Ile-C(CH₃)₂, Val – (CH₃)₂)
¹³C NMR (75 MHz, CDCl₃, HMQC) δ 175.2 (Ile – CO₂CH₃), 172.2 (Pro – CO), 170.8 (Val – CO), 169.8 (Ala – CO), 155.0 (Cbz – CO), 136.4 (Cbz – CH₂C₆H₅), 128.7 (C₆H₅), 128.3 (C₆H₅), 128.2 (C₆H₅), 66.9 (Pro α -C), 60.1 (Val α -C), 59.3 (Ile α -C), 58.3 (Cbz-CH₂C₆H₅), 57.1 (NCH₂CH₂C), 52.3 (CO₂CH₃), 48.1 (Pro δ -C), 41.0 (NCH₂), 38.0 (Pro β – C), 33.1 (Ile β – CH), 27.9 (NCH₂CH₂C), 27.6 (Val β – CH), 25.5 (Pro γ – C), 25.2 (Ile γ – CH₂), 22.2 (CCH₃), 19.4 (Val – CH₃), 19.0 (Val – CH₃), 15.8 (Ile CH₃), 11.9 (Ile CH₃)
 ESI HRMS *m/z* calcd for C₃₀H₄₄N₄NaO₇ (MNa)⁺, 595.3108; found, 595.3130.

Boc-Ile-NHMe (3.14)



To a chilled solution of THF and Boc-Ile-OH (**3.13**), NMM and isobutylchloroformate were added. After stirring the solution for 10 minutes, a pre-cooled solution of HCl·NH₂Me and triethylamine in THF was added. The reaction mixture was stirred at 0 °C for 2 hours and then overnight at room temperature. The solvent was evaporated *in vacuo* and the oil residue was dissolved in ethyl acetate. This solution was washed successively with 5% citric acid, saturated NaHCO₃, and brine. The

EtOAc solution was dried with MgSO₄ and evaporated under reduced pressure to obtain the final product as a white crystalline solid (90.6%). The final product **3.14** was used without further purification.

TLC R_f = 0.56 (EtOAc / Hexanes, 2:1)

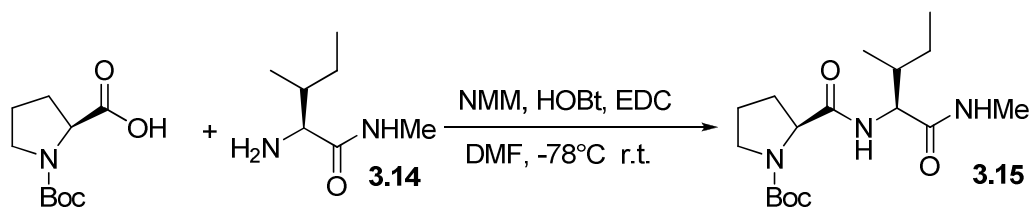
[α]_D 88.0 (c 0.5, CH₂Cl₂)

¹H NMR (300 MHz, CDCl₃, COSY) δ 6.21 (br d, *J* = 2.1 Hz, 1H, Boc – NH), 5.12 (br d, *J* = 8.1 Hz, 1H, NHMe), 3.90 (dd, *J* = 6.6 Hz, 9 Hz., 1H, Ile α-CH), 2.81 (dd, *J* = 1.2 Hz, 5.1 Hz, 3H, NHCH₃), 1.83 – 1.87 (m, 1H, Ile β-CH), 1.39 – 1.54 (m, 9H, Boc – (CH₃)₃), 1.02 – 1.12 (m, 2H, Ile – CH₂C₆H₅), 0.89 – 0.98 (m, 6H, Ile – CH₂CH₃, Ile – CHCH₃)

¹³C NMR (75 MHz., CDCl₃, HMQC) δ 172.5 (CONHCH₃), 148 (), 80.5 (Boc-C(CH₃)₃), 59.7 (α – C), 37.5 (NHCH₃), 28.7 (Boc – C(CH₃)₃), 25.1 and 26.5 (Ile – CHCH₃), 21.2 and 21.4 (Ile – CH₂CH₃), 15.9 (Ile CHCH₃), 11.8 (Ile – CH₂CH₃).

ESI HRMS *m/z* calcd for C₁₂H₂₄N₂NaO₃ (MNa)⁺, 267.1685; found, 267.1693.

Boc-L-Pro-Ile-NHMe (3.15)



Boc-proline (0.27 g, 1.24 mmol) and Ile-NHMe · HCl (**3.14**, 1.4 mmol) were dissolved in DMF which had been dried over 5 Å molecular sieves. While this solution was stirred, HOBT (0.19 g, 1.4 mmol) was added and the solution was cooled to -78 °C. EDC · HCl (0.26 g, 1.4 mmol) and NMM (0.3 mL, 2.72 mmol) were added consecutively

to the cooled solution, which then was allowed to warm slowly to room temperature where upon it was stirred for 3 days. On the third day the reaction mixture was concentrated *in vacuo* to give an orange residue to which a small portion of xylenes was added to azeotropically remove the remaining traces of DMF. The orange residue was then partitioned between H₂O (50 mL) and EtOAc (50 mL). The organic layer was washed consecutively with 0.5 M HCl (50 mL), 1 M NaHCO₃ (50 mL) and brine (50 mL), dried with MgSO₄ and concentrated under reduced pressure to yield 3.5 g of crude product. The crude Boc-Pro-Ile-NHMe (**3.15**) was purified by silica gel chromatography (3 x 5 cm) eluting with ethyl acetate in hexanes (1:1) to give 0.3 g (83 %) of pure product as a clear colorless oil (**3.15**).

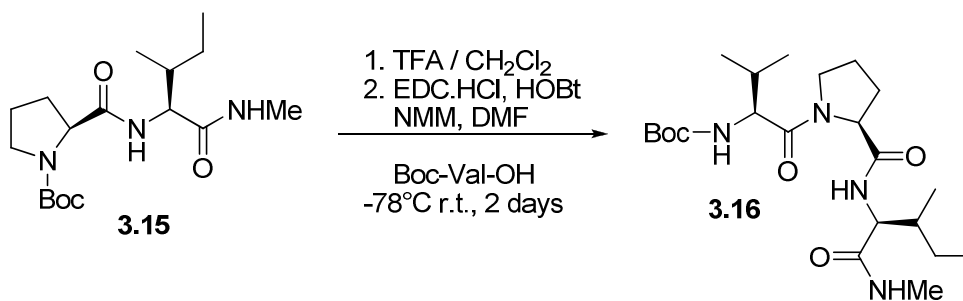
TLC R_f = 0.40 (EtOAc / Hexanes, 3:1)

[α]_D – 89.3 (c 0.7, CH₂Cl₂)

¹H NMR (300 MHz, CDCl₃, COSY) δ 6.88 (br s, 2H, Ile-NH, CONHMe), 4.25 (br s, 2H, Pro δ-CH₂), 2.71 (d, J = 2.7 Hz, 3H, CONHCH₃), 1.83 – 2.10 (br m, 4H, Pro β-CH₂, Pro γ-CH₂), 1.40 (s, 10H, Boc-(CH₃)₃, Ile β-CH), 0.87 – 1.18 (br m, 2H, Ile-CH₂CH₃), 0.79 – 0.87 (m, 6H, Ile – CHCH₃, Ile – CH₂CH₃)

¹³C NMR (75 MHz, CDCl₃, HMQC) δ 172.3 (Ile – CO), 171.7 (Pro – CO), 156.0 (Boc – CO), 81.0 (Boc – C(CH₃)₃), 58.2 and 60.8 (Pro α – C, Ile α – C), 47.5 (Pro δ – CH₂), 36.4 (Pro β – CH₂), 29.1 (Ile γ – CH₂), 28.6 (Boc – (CH₃)₃), 24.5 and 25.0 (Ile β – CH, Pro γ – CH₂), 16.2 (Ile – CH₃), 12.0 (Ile – CH₃).

ESI HRMS *m/z* calcd for C₁₇H₃₁N₃NaO₄ (MNa)⁺, 364.2212; found, 364.2199.

Boc-L-Val-L-Pro-L-Ile-NHMe (3.16)

Boc-Pro-Ile-NHMe (**3.15**, 1.0 g, 2.93 mmol) was dissolved in 4.5 mL of TFA in 5 mL of dry CH₂Cl₂ and the solution was stirred under nitrogen for 24 hours while it was monitored by TLC. Upon completion the reaction was concentrated under reduced pressure. The residue was dissolved in CH₂Cl₂ and evaporated three times to azeotropically remove any last traces of TFA. The orange compound was then allowed to dry under vacuum for 24 – 48 hours. The orange solid was then used in the subsequent coupling reaction without further purification.

L-Pro-L-Ile-NHMe • TFA (2.93 mmol) and Boc-valine (0.63 g, 2.93 mmol) were dissolved in DMF which had been dried over 5 Å molecular sieves. While this solution was stirred HOBT (0.40 g, 2.93 mmol) was added and the solution was cooled to -78 °C. EDC • HCl (0.57 g, 2.93 mmol) and NMM (0.65 mL, 5.85 mmol) were added consecutively to the cooled solution, which then was allowed to warm slowly to room temperature where upon it was stirred for 3 days. On the third day the reaction mixture was concentrated *in vacuo* to give an orange residue to which a small portion of xylenes was added to azeotropically remove the traces of DMF. The orange residue was then partitioned between H₂O (100 mL) and EtOAc (100 mL). The organic layer was washed consecutively with 0.5 M HCl (100 mL), 1 M NaHCO₃ (100 mL) and brine (100 mL),

dried with MgSO_4 and concentrated under reduced pressure to yield 0.96 g of crude product. The crude Boc-Val-Pro-Ile-NHMe (**3.16**) was purified by silica gel chromatography (5 x 15 cm) and eluted with methanol in ethyl acetate (1:50) to yield 0.8 g. (67 %) of pure product as a clear colorless oil **3.16**.

TLC $R_f = 0.33$ (2% MeOH in EtOAc)

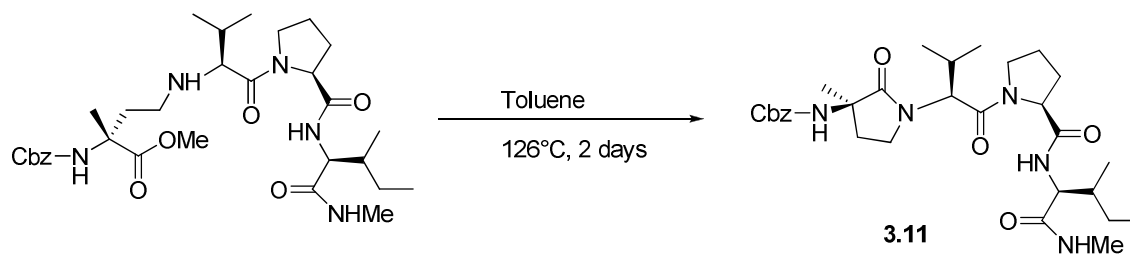
$[\alpha]_D^{25} 75.6$ (c 0.6, CH_2Cl_2)

^1H NMR (300 MHz, CDCl_3 , COSY) δ 6.94 (br s, 1H, Ile-NH), 6.16 (br s, 1H, CONHCH₃), 5.23 (br d, $J = 9$ Hz, 1H, Val – NH), 4.54 – 4.56 (m, 1H, Pro α -CH), 4.30 (dd, $J = 6$ Hz, 9.1 Hz, 1H, Val α – CH), 4.23 (dd, $J = 5.9$ Hz, 8.9 Hz, 1H, Ile α – CH), 3.76 (m, 1H, Pro δ – CH₂), 3.62 (m, 1H, Pro δ – CH₂), 2.89 (d, $J = 4.6$ Hz, 3H, CONHCH₃), 2.25 – 2.26 (m, 0.5 H, Val β – CH), 1.92 – 2.05 (m, 4.5 H, Val β – CH, Pro β – CH₂, Pro γ – CH₂), 1.69 (s, 2H, Ile γ – CH₂), 1.50 (s, 10H, Boc – C(CH₃)₃, Ile β – CH), 0.87 – 1.09 (m, 12H, Val – (CH₃)₂, Ile – (CH₃)₂).

^{13}C NMR (75 MHz, CDCl_3 , HMQC) δ 172.5 (Pro – CO), 171.8 (Val – CO), 171.5 (Ile – CO), 156.0 (Boc – CO), 79.8 (Boc – C(CH₃)₃), 60.6 (Pro α – CH), 58.3 (Ile α – CH), 57.2 (Val α – CH), 48.1 (Pro δ – CH₂), 37.1 (Pro β – CH₂), 31.8 (Val β – CH), 28.7 (C(CH₃)₃), 28.5 (Ile β – CH₂), 26.5 (NHCH₃), 25.6 (Pro γ – CH₂), 24.9 (Ile γ – CH₂), 19.9 (Ile – CH₃), 17.8 (Ile – CH₃), 15.9 (Val – CH₃), 11.7 (Val – CH₃).

ESI HRMS m/z calcd for $\text{C}_{22}\text{H}_{40}\text{N}_4\text{O}_5$ (MH)⁺, 441.3077; found, 441.3073

***N*-[3-(*R*)-[Benzyloxycarbonylamino-3-methyl-2-oxo-1-pyrrolidine]-(*S*)-3-methyl-2-butanoyl]-Pro-Ile-NHMe (3.11)**



N-[Cbz-(*R*)-2-amino-2-methyl-butanoyl]-L-Val-L-Pro-L-Ile-NHMe **3.17** (0.2 g, 0.33 mmol) was dissolved in toluene and placed within a sealed vessel. The reaction was then heated to 126°C for 2 days and allowed to cool to room temperature. Toluene was evaporated under reduced pressure to afford the crude product as a slightly orange oil. The oil was purified by silica gel flash chromatography (5 x 8cm) and eluted with ethyl acetate in hexanes (3:1). The isolated clear oil yielded 0.14 g (74%) of the pure compound.

TLC R_f = 0.20 (EtOAc / Hexanes, 3:1)

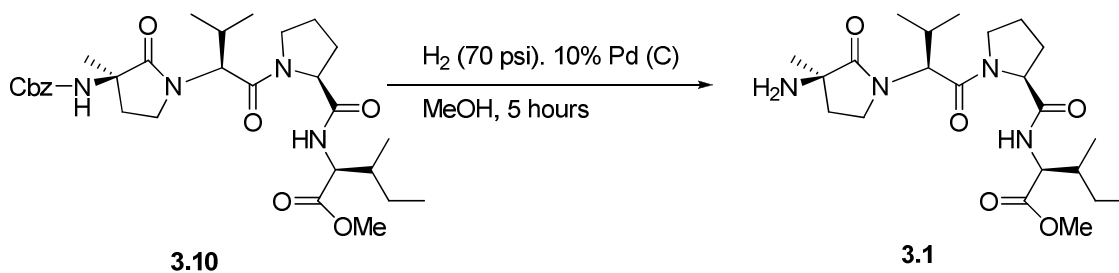
$[\alpha]_D - 140.20$ (c 0.5, MeOH)

^1H NMR (300 MHz, CDCl_3 , COSY) δ 7.21 – 7.31 (m, 5H, C_6H_5), 6.88 (d, J = 9 Hz, 1H, Ile NH), 6.42 (s, 1H, Ile NHCH_3), 4.93 – 5.04 (m, 2H, $\text{CH}_2\text{C}_6\text{H}_5$), 4.50 (d, J = 10.8 Hz, 1H, Ile α – CH), 3.71 – 3.76 (m, 1H, Pro δ – CH_2), 3.56 – 3.63 (m, 1H, Pro δ – CH_2), 3.30 – 3.38 (m, 2H, NCH_2CH_2), 2.71 (d, J = 4.8Hz, 3H, NHCH_3), 1.80 – 2.67 (m, 8H, Pro γ – CH_2 , Pro β – CH_2 , NCH_2CH_2 , Ile β – CH, Val β – CH), 1.33 – 1.44 (m, 1H, Ile γ – CH_2), 1.25 (s, 3H, γ – Lac CH_3), 0.97 – 1.03 (m, 1H, Ile γ – CH_2), 0.80 – 0.97 (m, 12H, Ile CH_3 , Val CH_3)

^{13}C NMR (75 MHz, CDCl_3 , HMQC) δ 175.3 (γ – Lac CO), 171.6 (Val CO), 171.1 (Pro CO), 168.8 (Ile CO), 155.0 (Boc CO), 136.3 (C_6H_5), 128.7 (C_6H_5), 128.3 (C_6H_5), 66.9 (C_6H_5), 60.7 (Pro α – C), 59.4 (Val α – C), 58.4 (Ile α – C), 58.3 (γ – Lac α – C), 48.2 (Pro δ – C), 41.0 (NCH_2CH_2), 37.2 (NCH_2CH_2), 28.7 (Pro β – C), 27.5 (Pro γ – C), 26.5 (Ile β – C), 25.4 (NHCH_3), 25.1 (Val β – C), 22.3 (γ – Lac CH_3), 21.4 (Ile γ – CH_2), 19.4 (Val CH_3), 19.0 (Val CH_3), 15.9 (Ile CH_3), 11.8 (Ile CH_3)

ESI HRMS m/z calcd for $\text{C}_{30}\text{H}_{46}\text{N}_5\text{O}_6 + \text{Na}^+$, 572.3448; found, 572.3447.

***N*-[(*R*)-3-amino-3-methyl-2-oxo-1-pyrrolidine-(*S*)-3-methyl-2-butanoyl]-*L*-Pro-*L*-Ile-OMe Trifluoroacetate Salt (3.1)**



Cbz-NH-(*R*)- α Me- γ -Lactam-L-Val-L-Pro-L-Ile-OMe (**3.10**) was dissolved in MeOH and palladium on carbon was added to the reaction mixture. The palladium was initially wetted with MeOH in a 2 dram vial under inert environment before addition to the reaction mixture which prevents ignition of the MeOH within the solvent flask. The mixture was stirred for 5 hours under a 70 psi H_2 atmosphere. Filtration of the reaction mixture followed *in vacuo* evaporation of the solvents yielded pure product in a 98% yield.

TLC $R_f = 0.71$ (Propanol / NH_4OH , 4:1)

$[\alpha]_D -154.8$ (c 0.09, MeOH)

^1H NMR (300 MHz, CDCl_3 , COSY) δ 4.46 – 4.56 (m, 2H, Ile α – CH, Pro α – CH), 4.35 (d, $J = 5.7\text{Hz}$, 1H, Val α – CH), 3.63 – 3.78 (m, 1H, Pro δ – CH_2), 3.70 (s, 3H, CO_2CH_3).

3.30 – 3.40 (m, 1H, Pro δ – CH_2), 1.81 – 2.29 (m, 4H, Pro β – CH_2 , Pro γ – CH_2 ,

NCH_2CH_2 , NCH_2CH_2), 1.47 – 1.53 (m, 1H, Ile γ – CH_2), 1.23 – 1.33 (m, 1H, Ile γ –

CH_2). 1.17 (s, 3H, γ – Lac CH_3), 0.84 – 1.01 (m, 12H, Ile CH_3 , Val CH_3)

^{13}C NMR (75 MHz, CDCl_3 , HMQC) δ 179.6 (γ – Lac CO), 175.3 (Val CO), 174.7 (Ile

CO), 170.9 (Pro CO), 64.1 (γ – Lac α – C), 62.4 (Ile α – C), 61.9 (Pro α – C), 59.7 (Val α

– C), 42.7 (NCH_2CH_2), 39.8 (Pro δ – C), 37.6 (Pro β – C), 32.0 (Ile β – C), 29.5

(NCH_2CH_2), 27.8 (Ile γ – CH_2), 27.2 (Pro γ – C), 21.0 (Val CH_3), 20.7 (Val CH_3), 20.5 (γ

– Lac CH_3), 17.4 (Ile CH_3), 13.3 (Ile CH_3)

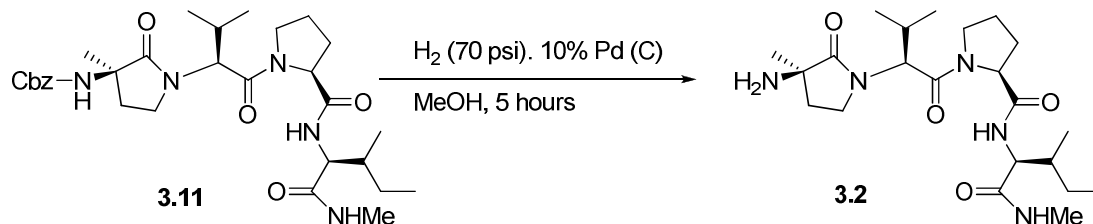
HRMS (ESI) m/z calcd for $\text{C}_{22}\text{H}_{38}\text{N}_4\text{O}_5 + \text{Na}^+$, 461.2740; found, 461.2720.

HPLC: t_R : (2% H_2O in 98% CH_3CN) 9.12 minutes; (2% MeOH in 98% CH_3CN) 7.26

minutes. Sample dissolved in CHCl_3 and MeOH

***N*-[(*R*)-3-amino-3-methyl-2-oxo-1-pyrrolidine-(*S*)-3-methyl-2-butanoyl]-*L*-Pro-*L*-Ile-**

NHMe Trifluoroacetate Salt (3.2)



Cbz-NH-(*R*)- α -Me- γ -Lactam-L-Val-L-Pro-L-Ile-NHMe was dissolved in MeOH and palladium on carbon was added to the reaction mixture. The palladium was initially wetted with MeOH in a 2 dram vial under inert environment before addition to the reaction mixture which prevents ignition of the MeOH within the solvent flask. The mixture was stirred for 5 hours under a 70 psi H₂ atmosphere. Filtration of the reaction mixture followed *in vacuo* evaporation of the solvents yielded pure product in a 98% yield.

TLC R_f = 0.64 (Propanol / NH₄OH, 4:1)

[α]_D -179.5 (c 0.04, MeOH)

¹H NMR (300 MHz, CDCl₃, COSY) δ 4.54 (d, *J* = 10.8 Hz, 1H, Ile α - CH), 4.43 – 4.47 (m, 1H, Pro α - CH), 4.10 (d, *J* = 8.1 Hz, 1H, Val α - CH), 3.63 – 3.83 (m, 2H, γ - Lac NH₂), 3.36 – 3.47 (m, 2H, Pro δ - CH₂), 2.72 (s, 3H, NHCH₃), 1.75 – 2.35 (m, 10H, Pro β - CH₂, Pro γ - CH₂, NCH₂CH₂, NCH₂CH₂, Ile β - CH, Val β - CH), 1.55 – 1.64 (m, 1H, Ile γ - CH₂), 1.13 – 1.30 (m, 4H, Ile γ - CH₂, γ - Lac CH₃), 0.89 – 1.02 (m, 12H, Ile CH₃, Val CH₃)

¹³C NMR (75 MHz, CDCl₃, HMQC) δ 178.8 (γ - Lac CO), 175.3 (Pro CO), 175.0 (Ile CO), 170.9 (Val CO), 68.4 (γ - Lac α - C), 62.6 (Pro α - C), 61.9 (Ile α - C), 60.7 (Val α - C), 42.7 (NCH₂CH₂), 40.8 (Pro δ - C), 39.6 (Pro β - C), 31.9 (Val β - C), 29.4 (NCH₂CH₂), 27.5 (Ile β - C), 27.3 (Pro γ - C), 27.2 (NHCH₃), 23.7 (Ile γ - CH₂), 22.5 (γ - Lac CH₃), 20.9 (Val CH₃), 20.5 (Val CH₃), 17.2 (Ile CH₃), 12.8 (Ile CH₃)

ESI HRMS *m/z* calcd for C₂₂H₃₉N₅O₄ + Na⁺, 460.2900; found, 460.2889.

HPLC: t_R (2% H₂O in 98% CH₃CN) 7.89 minutes; t_R (2% MeOH in 98% CH₃CN) 15.90 minutes. Sample was dissolved in CHCl₃ and MeOH.

3.7. References

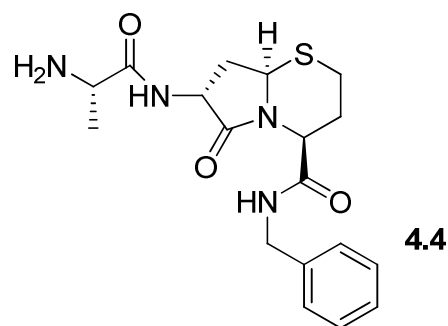
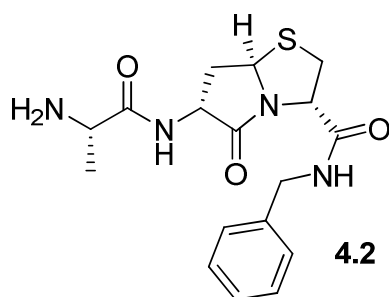
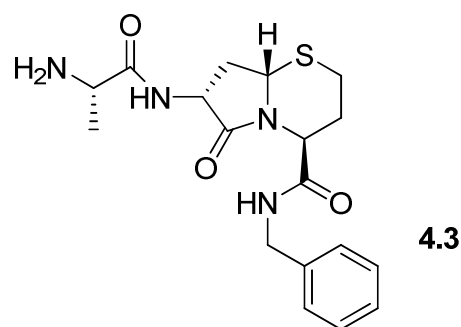
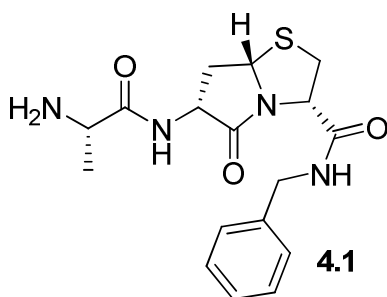
1. Kipp, R. A.; Case, M. A.; Wist, A. D.; Cresson, C. M.; Carrel, M.; Gringer, E.; Wiita, A.; Albinia, P. A.; Chai, J. J.; Shi, Y. G.; Semmelhack, M. F.; McLendon, G. L. *Biochemistry* **2002**, *41*, 7344 – 7349.
2. Wist, A. D.; Gu, L.; Riedl, S. J.; Shi, Y.; McLendon, G. L. Structure-activity based study of the Smac-binding pocket within the BIR3 domain of XIAP. *Bioorg. Med. Chem.* **2007**, *15*, 2935 – 2943.
3. Pang, Y. P.; Perola, E.; Xu, K.; Prenderast, F. G. EUDOC: A computer program for identification of drug interaction sites in macromolecules and drug leads from chemical databases. *J. Comp. Chem.* **2001**, *22*, 1750 – 1771.
4. Freidinger, R. M.; Schwenk, D.; Veber, D. F. Protected lactam bridged dipeptides for use as conformational constraints in peptides. *J. Org. Chem.* **1982**, *67*, 104 – 109.
5. Zydowsky, T. M.; Dellaria, Jr. J. F.; Nellans, H. N. Efficient and versatile synthesis of dipeptide isosteres containing γ - or δ -lactams. *J. Org. Chem.* **1988**, *53*, 5607 – 5616.
6. Genin, M.J.; Gleason, W.B.; Johnson, R.L. Design, synthesis, and X-ray crystallographic analysis of two novel spriolactam systems as β -turn mimics. *J. Org. Chem.* **1993**, *58*, 860 – 866.

7. Genin, M. J.; Ojala, W. H.; Gleason, W. B.; Johnson, R.L. Synthesis and crystal structure of a peptidomimetic containing the (*R*)-4.4-sprio lactam type-II β – turn mimic. *J. Org. Chem.* **1993**, *58*, 2334 – 2337.

8. Palomo, C.; Aizpurua, J. M.; Benito, A; Miranda, J. I.; Fratila, R. M.; Matute, C.; Domercq, M.; Gago, F.; Martin-Santamaria, S.; Linden, A. α -Alkyl- α -amino- β -lactam peptides: design, synthesis and conformational features. *Angew. Chem., Int. Ed.* **1999**, *38*, 3056 – 3058.

9. Kapadia, S. R.; Spero, D. M.; Eriksson, M. An improved synthesis of chiral α -(4-Bromobenzyl)alanine Ethyl Ester and its application to the synthesis of LFA-1 antagonist BIRT-377. *J. Org. Chem.* **2001**, *66*, 1903 – 1905.

Chapter 4. The Stereoselective Synthesis of ψ_2 , ϕ_3 Constrained AVPI Mimics



4.1 Design and Scope

In further attempts to constrain the active AVPI peptide to its bioactive conformation we have designed a bicyclic ring system which will maintain or hopefully enhance the hydrophobic and hydrogen bonding interactions with the active site of XIAP. Based upon initial modeling studies we hypothesize that the sulfur atom within the bicyclic structure will form *d*-orbital π interactions not present in the native AVPI ligand. This chapter will focus upon the synthesis and testing of the bicyclic lactam structures illustrated above.

These thiazabicycloalkane ring systems constrain the ψ_2 and ϕ_3 torsion angles which correspond to those in AVPI that are constrained by the proline residue. Initial modeling suggests that the bicyclic ring structure will mimic the specific angles present in the native peptide.¹ In **Chapter 2** we discussed the compounds synthesized by the

Wang group of the University of Michigan. Dr. Wang's compounds were used as our test compounds for the modeling confidence study.^{2,3} The indolizidinone templates designed by Dr. Wang were active within the low μM range. Our compounds are similar to the template of Dr. Wang's compounds with several significant differences that should enhance the affinity active site interactions. The first difference is the sulfur atom in the bicyclic lactams. The *d* orbital of the sulfur atom should be able to interact with the pi electron of the Trp and Tyr residues near the active site.¹ The second difference is that the stereochemistry at the 2 and 7 positions of the bicycle differ from the Wang indolizidinone system and should allow our bicyclic lactam to more accurately mimic the extended conformation of the native AVPI peptide. The indolizidinone, in contrast, favors a turn like conformation.^{2,3} The stereochemistry at the bridgehead directs whether or not the ring structure will fold into the S2 pocket. The pocket would normally accommodate the P2 valine side chain. This orientation of the bicyclic structure, unlike the indolizidinone which projects into the pocket, will allow future modifications to be made to the thiazabicycloalkane template.

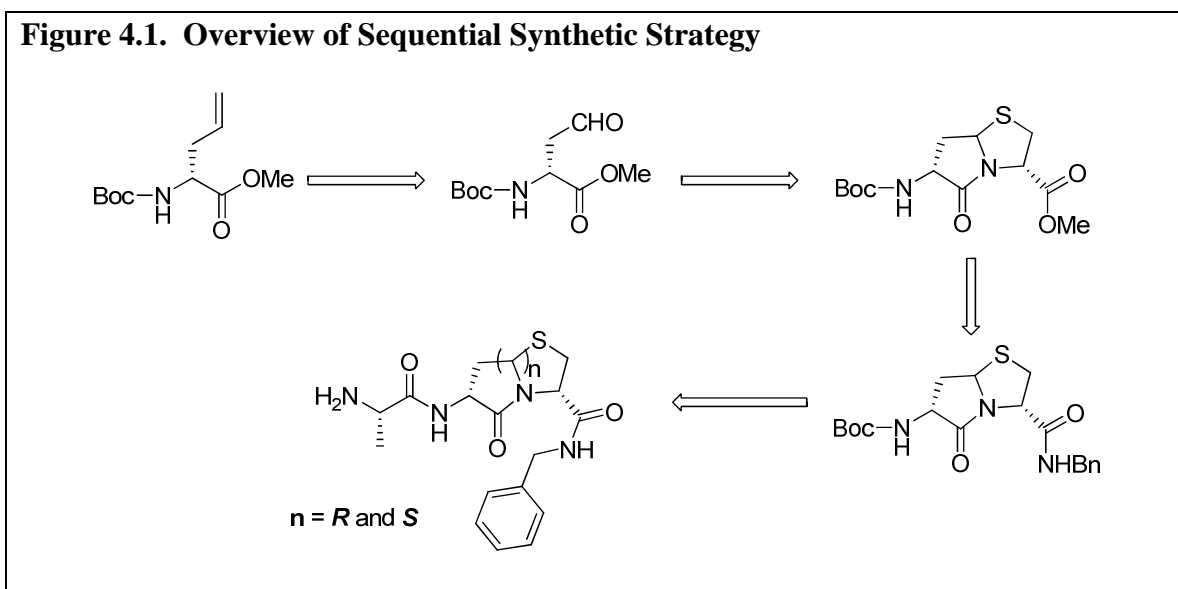
We proposed to synthesize the 5,5, 5,6, and 6,5 bicyclic ring system with both the *R* and *S* stereochemistry at the bridgehead position for each compound. We proposed that the *R* stereochemistry would be the most active since it would fold the bicycle into the S2 pocket. The *S* stereochemistry was synthesized as a negative control to validate our bicyclic model. Synthesis of this series of 6 compounds should help up to determine which ring size is optimal to interact with the XIAP – BIR3 binding pocket. In addition, the 5,5 system will be made with stereochemistry identical to the Wang compounds at the bridgehead position (**7a**) utilizing D-Cys-OMe, thus acting as a negative control for

testing our hypothesis that the extended conformation of our compounds will have greater activity than the turn conformation of the Wang compounds.

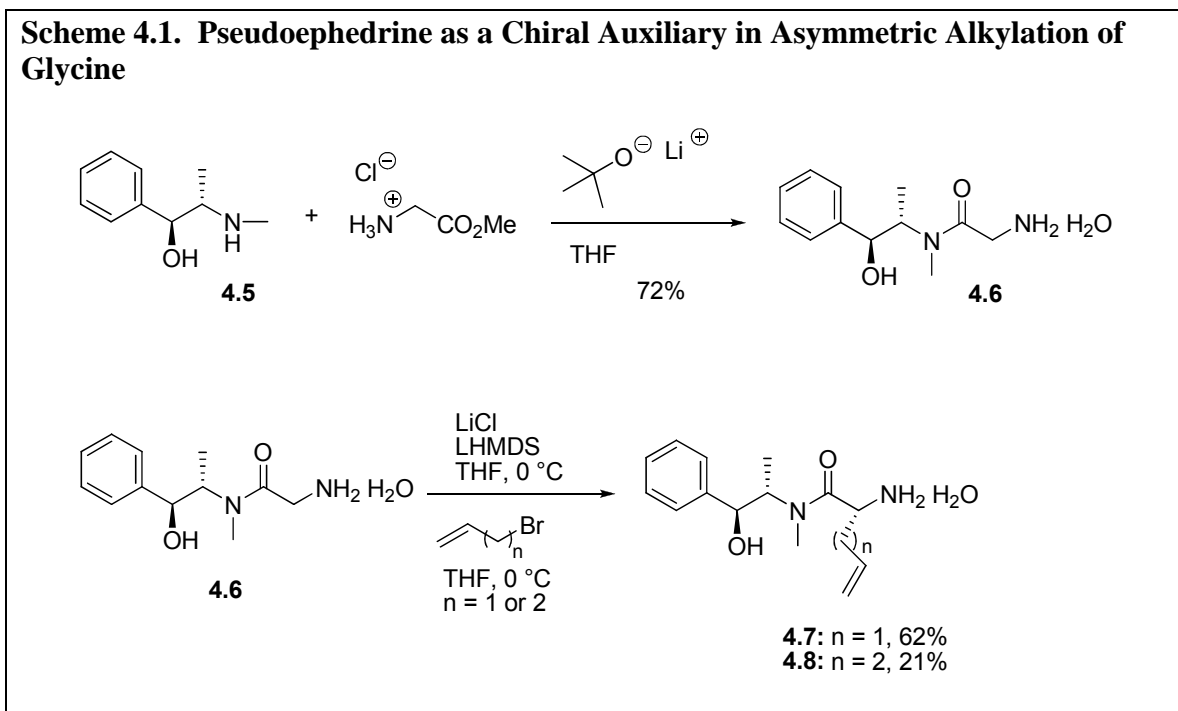
4.2 Synthetic Strategy: Sequential

Analogous bicyclic thiazolidine lactams derivatives have been synthesized before in our lab in an attempt to mimic the bioactive conformation of PLG.⁴⁻⁷ In general these bicyclic lactams were synthesized by stereoselectively alkylating an amino acid to yield an aldehyde amino acid as illustrated in **Figure 4.1**.⁸ These aldehydes were then subjected to a Schiff base condensation with a cysteine methyl ester derivative.

Subsequent cyclization utilizing an appropriate coupling reagent such as Mukaiyama's reagent afforded the final bicyclic lactam. Analogous diastereomers which result from this methodology are easily separated by silica gel flash chromatography.⁷ Assignment of the diastereomers can be accomplished by NOE analysis after the condensation or at a future intermediate depending on the difficulty of separation and assignment.

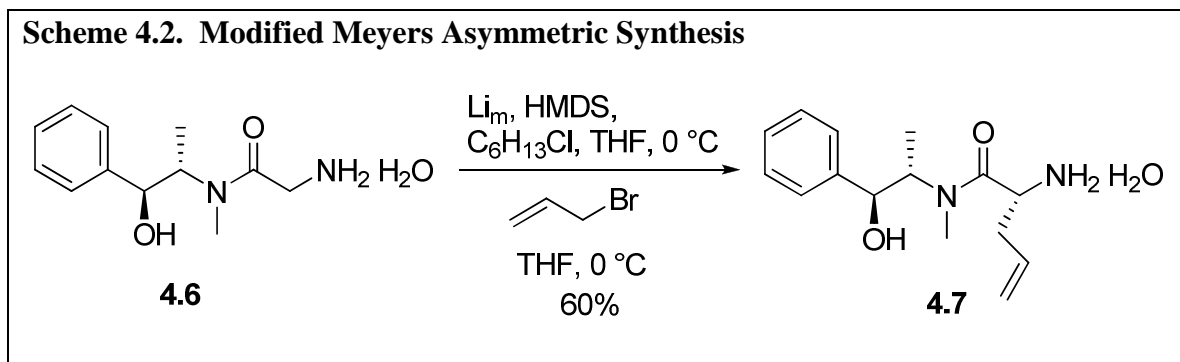


The initial synthetic challenge we faced was the stereoselective alkylation of an amino acid, in our case the stereoselective alkylation of glycine. Multiple methods have been developed for alkylation of amino acids at the α carbon.⁹⁻¹² Dr. Subasinghe followed a modified version of the synthesis originally described by Lee and Miller.¹³ whereas Dr. Khalil followed a method envisioned by Dr. Karady.¹⁴ Both of these methods involved the cyclization of the amino acid to an oxazolidinone which was then selectively alkylated. These methods, although effective, involved multiple steps with moderate yields. In recent years, the alkylation of a glycine enolate has been thoroughly explored by many research labs.¹² The method that we chose to employ is the use of pseudoephedrine as a chiral auxiliary to promote the asymmetric alkylation of the aforementioned enolate. The Myers group developed and optimized this 2-3 step synthesis which contains only one step with a moderate yield, inexpensive starting material and readily available enantiomers.^{15,16}



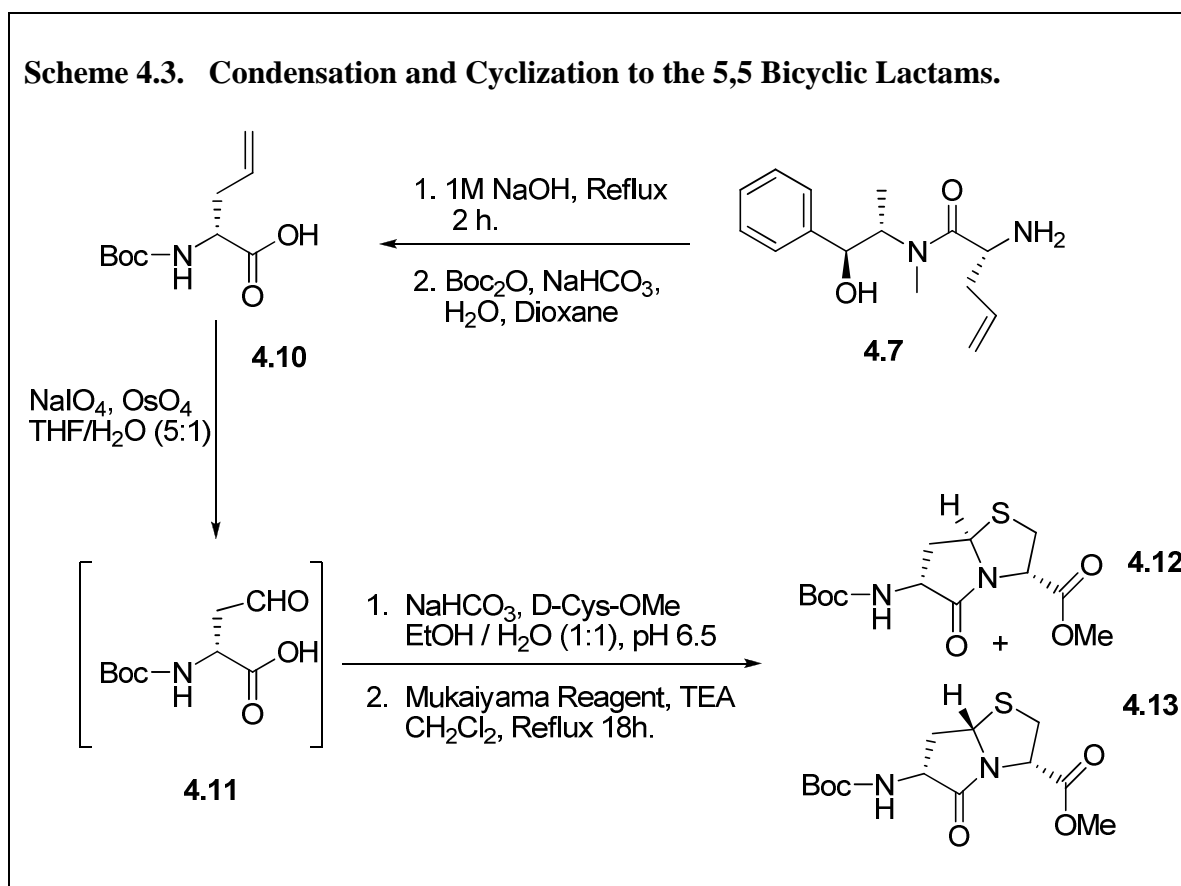
The attachment of the pseudoephedrine chiral auxiliary (**4.5**) proceeds through a lithium *tert*-butoxide mediated base catalysis. Dr. Myers proposes that this reaction proceeds through an $\text{N} \rightarrow \text{O}$ acyl transfer.¹⁵ In our hands this reaction proceeded in similar yields to the published data of 72% to yield pseudoephedrine glycinate (**4.6**). The alkylation was performed utilizing both allyl (**4.7**) and butenyl (**4.8**) electrophiles. The enolates were formed (**Scheme 4.1**) through the use of 3 equivalents of LHMDS and in both cases the alkylation was greater than 99% stereoselective. This high degree of facial selectivity is proposed to be due to the blocking of one face of the enolate by solvent.¹⁵ The alkyl halides would then be attacked from the face opposite the solvent hindered face. Once again, the allyl (**4.7**) reaction proceeded well in our laboratory with a yield of 62% and poorly for the butenyl (**4.8**) derivative with a yield of 21%. This procedure produced good results for the allyl side chain but not the butenyl. The modified version of the Myer's asymmetric synthesis did not yield any butenyl product

whatsoever and had only comparable yields to the original method when the allyl bromide electrophile was used. (**Scheme 4.2**)



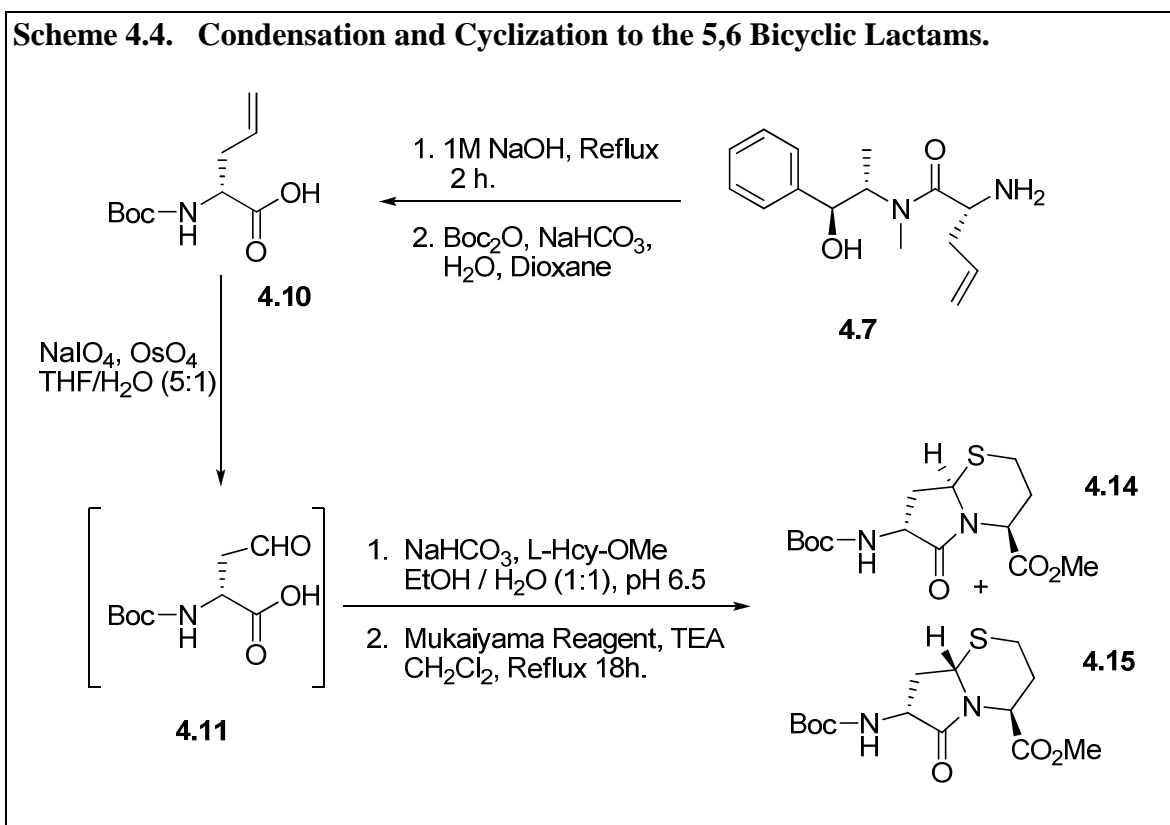
The modified Myers synthesis was developed because of the need for completely anhydrous LiCl. LiCl is notoriously hard to keep dry. However, we found that heating the salt over a gas flame under house vacuum (30 mmHg) for 5 – 10 minutes provided the moderate yields listed above in **Scheme 4.1**. The modified synthesis however, produces anhydrous LiCl from lithium metal and 1-chloro-hexane in a solution of anhydrous THF and HMDS. The obvious intended side reaction is the production of LHMDS *in situ* as well. After stirring overnight the addition of starting material produced the allyl derivative of pseudoephedrine glycineamide (**4.7**) in a 60% yield.

Once the alkylation was performed successfully, the hydrolysis of the chiral auxillary (**4.7**) proceeds quantitatively in a 1M solution of NaOH. (**Scheme 4.3**) This reaction also allows for the recovery and recrystallization of the pseudoephedrine. Boc protection is then effected after a quick workup to yield the protected amino acid in near quantitative yield (**4.10**). Oxidative cleavage of the allyl glycine analogue was accomplished efficiently by the use of NaIO₄ / OsO₄ to yield the corresponding aldehyde, **4.11**. These compounds predominately reside in the form of hydroxy-lactones.

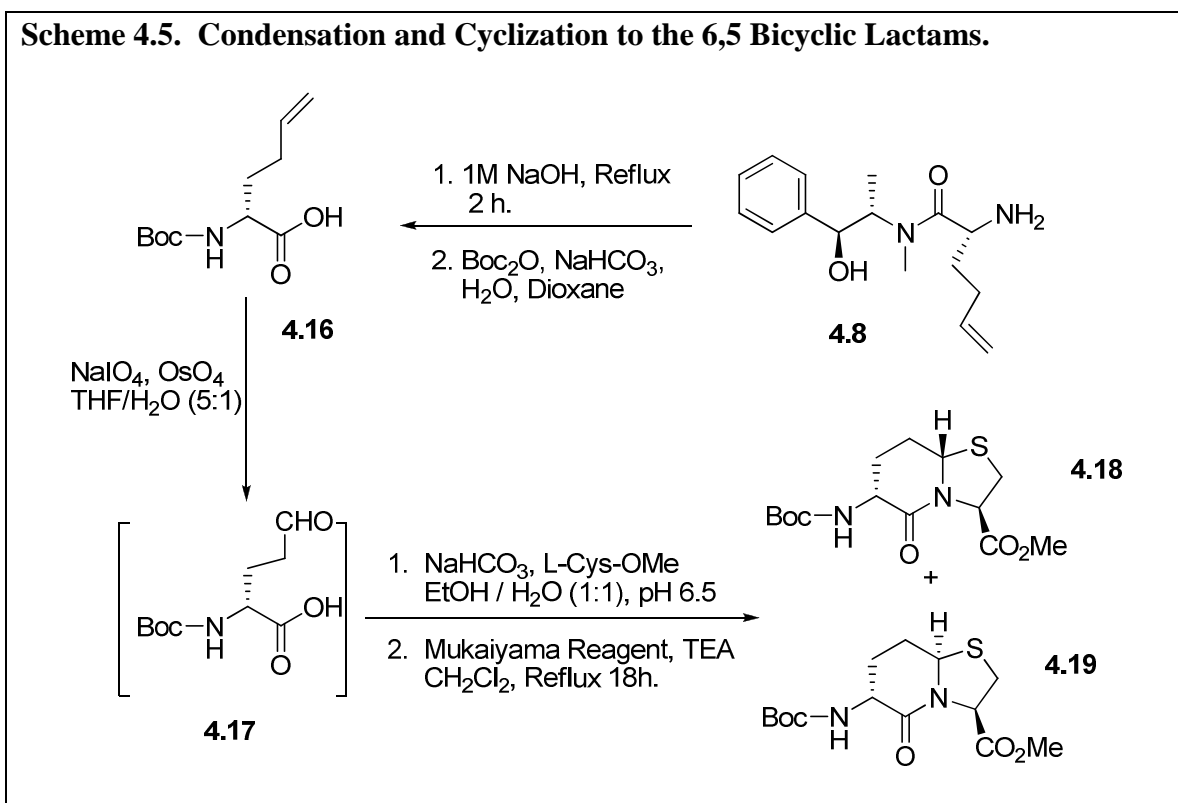


The aldehyde / hydroxyl lactone (**4.11**) was exposed to Schiff base condensation conditions which have previously been described by Khalil in our lab.⁷ The condensed product was then cyclized utilizing Mukaiyama's reagent and as expected both

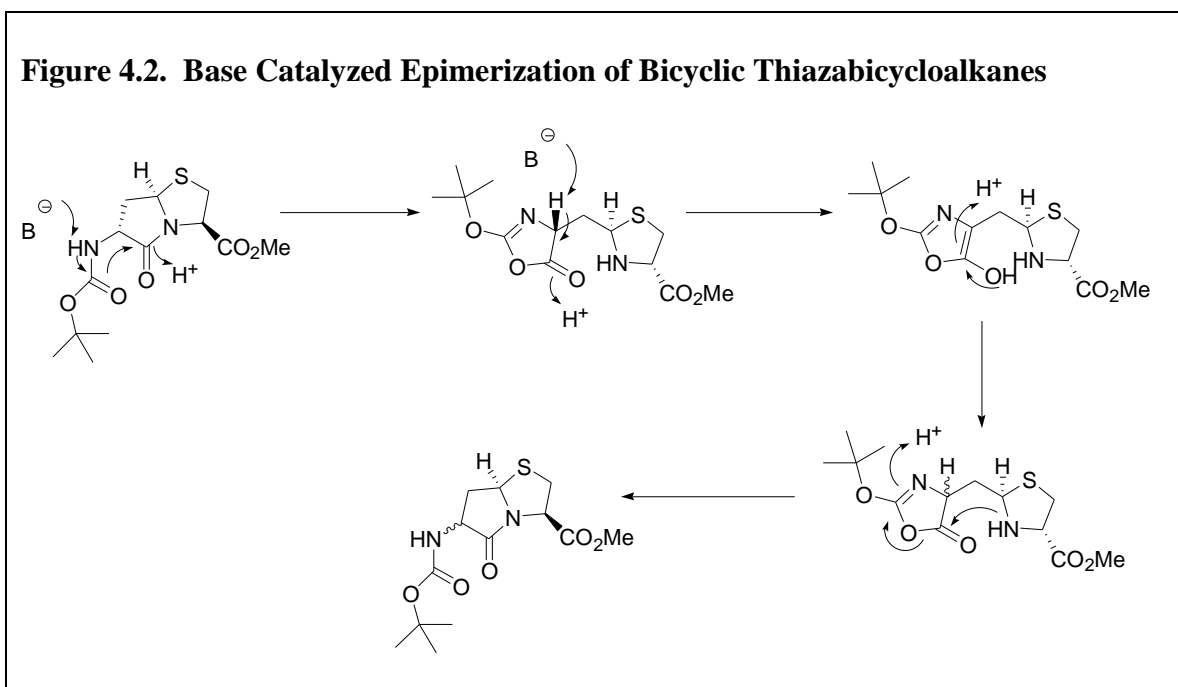
diastereomers were present within the reaction mixture (**4.12** and **4.13**). The diastereomers at the position 7 bridgehead were easily separable by flash chromatography. NOE analysis of these compounds did not provide definitive proof of *R* or *S* stereochemistry at this point.



Condensation and cyclization reactions utilizing the same methodology as the 5,5 lactams were performed in parallel to yield the 5,6 (**4.14** and **4.15**) and 6,5 ring systems (**4.18** and **4.19**) as well (**Schemes 4.4** and **4.5**). Ring size did not seem to factor into the efficacy of the reaction as similar yields of between 19% and 31% were obtained for the major diastereomer and between 7% - 14% for the minor diastereomer.



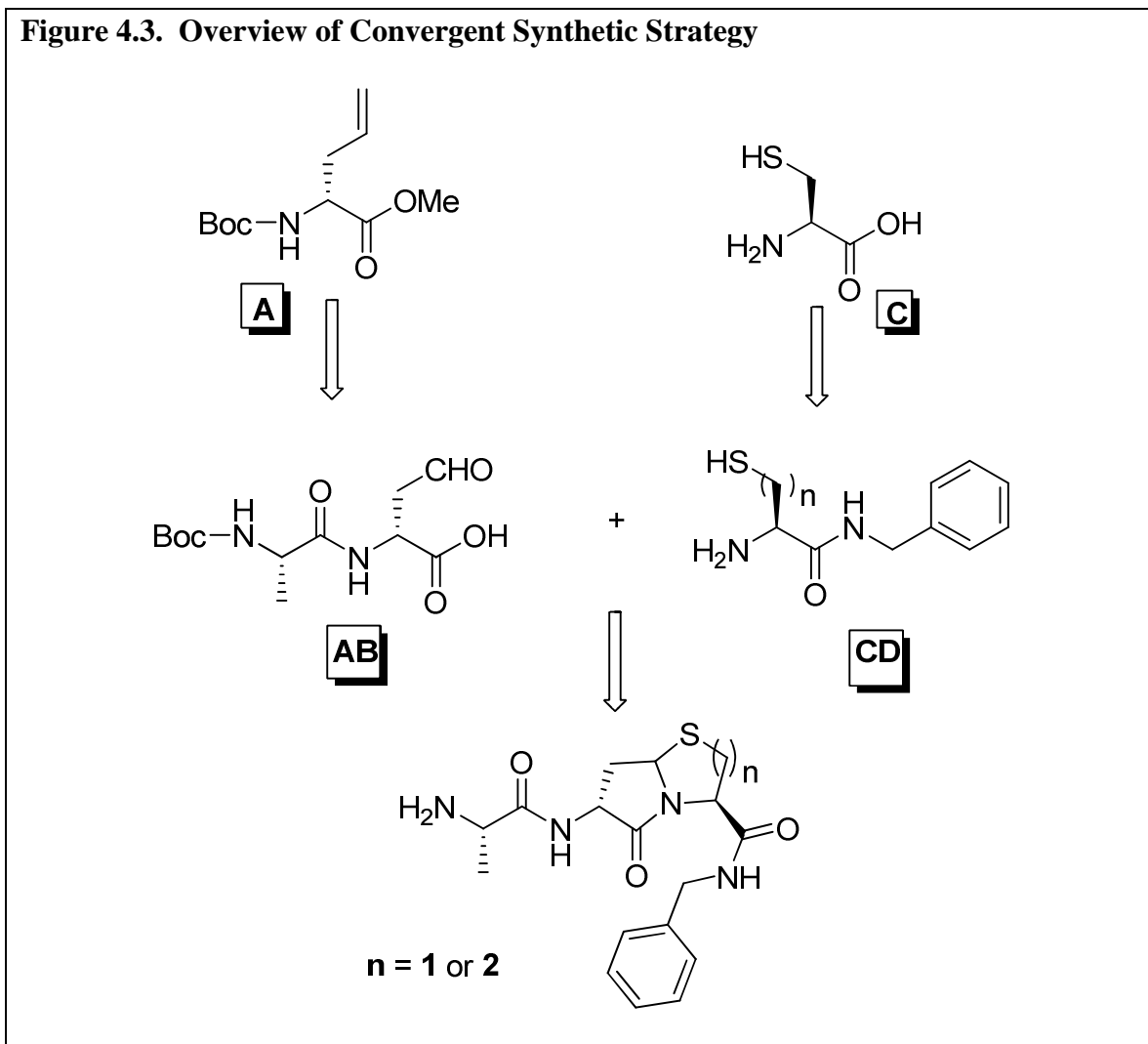
The 5,6 thiazolidine methyl ester (**4.14** and **4.15**) was hydrolyzed using 2 equivalents of LiOH in a 0.05 M THF/MeOH/H₂O system. The free carboxylic acid was then coupled to benzyl amine utilizing standard solution phase coupling chemistry. Analysis of the product by TLC analysis showed epimerization, at the C6 position presumably, due to base catalyzed ring breakdown. This result was not unanticipated based upon previous results by Dr. Subasinghe.⁶ He proposed that the epimerization at position 2 occurs through the formation of an oxazolone intermediate as shown in **Figure 4.2**.



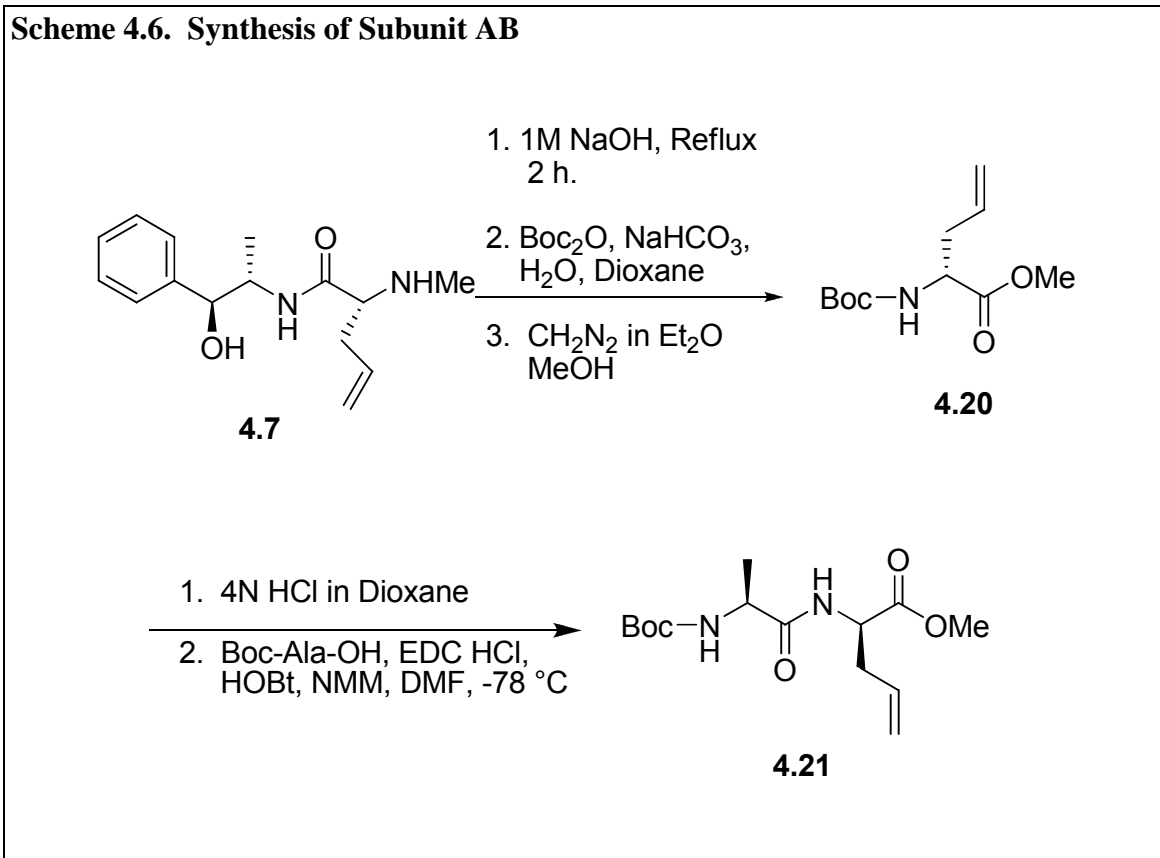
We have encountered an analogous method of racemization in peptide coupling as evidenced by the valine epimerization in **Chapter 2**. We propose that the energy necessary to promote the epimerization is the release of ring strain inherent in the bicyclic system. Although the base-catalyzed epimerization was anticipated we did not anticipate that the mild conditions of a LiOH hydrolysis would be strong enough to cause the ring to break down. Dr. Subashinge found this epimerization after harshly refluxing the same material in pyridine. The sensitivity of this group complicated matters in the final two steps and caused significant alternative methods to be explored to avoid this problem of racemization.

4.3 Synthetic Strategy: Convergent

Since, previous research has indicated the potential for epimerization of the bridgehead position and the C7- α -glycine center,^{7,8} an alternative synthetic strategy (**Figure 4.3**) was explored in parallel with the original sequential strategy, shown in **Figure 4.1**. The alternative methodology illustrated in **Figure 4.3** was based upon postponing the condensation and cyclization step until later in the synthesis to minimize or eliminate the amount of steps that were subject to the epimerization driving ring strain. To this end we synthesized the cysteine benzyl amide, **CD**, to avoid the previous described epimerization producing base hydrolysis in **Scheme 4.5**. Within this strategy the benzyl amide was envisioned to be condensed with the dipeptide aldehyde, subunit **AB**. This should afford the protected final compound while subjecting the intermediates to a minimum of potential for racemization.

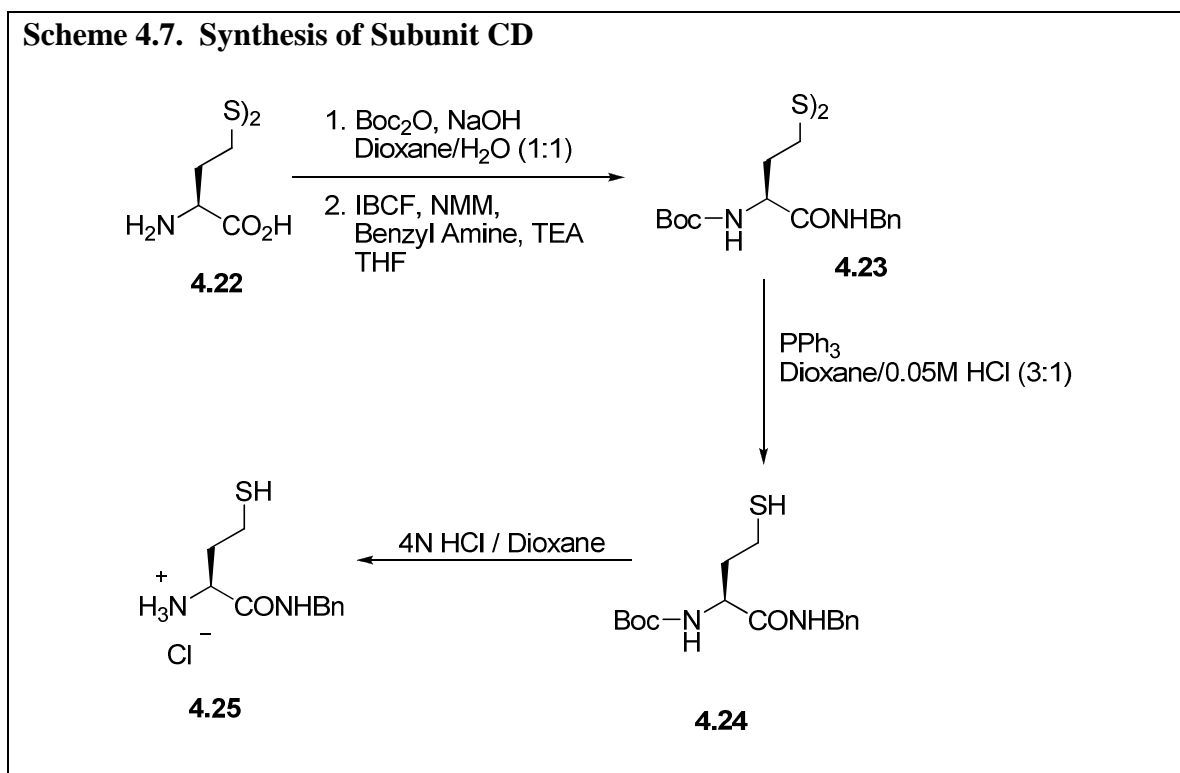


Subunit **AB** was synthesized in a manner similar to **Scheme 4.3** with the exception that prior to oxidative cleavage of the alkene the Boc- α -allyl-glycine was esterified to the methyl ester (**4.20**). This compound was easily purified by flash chromatography and coupled to Boc-Ala-OH to yield **4.21**. Oxidative cleavage of the alkene produced Boc-Ala- α -(CH₂CHO)-Gly-OMe which was also purified by column chromatography to yield subunit **AB**.



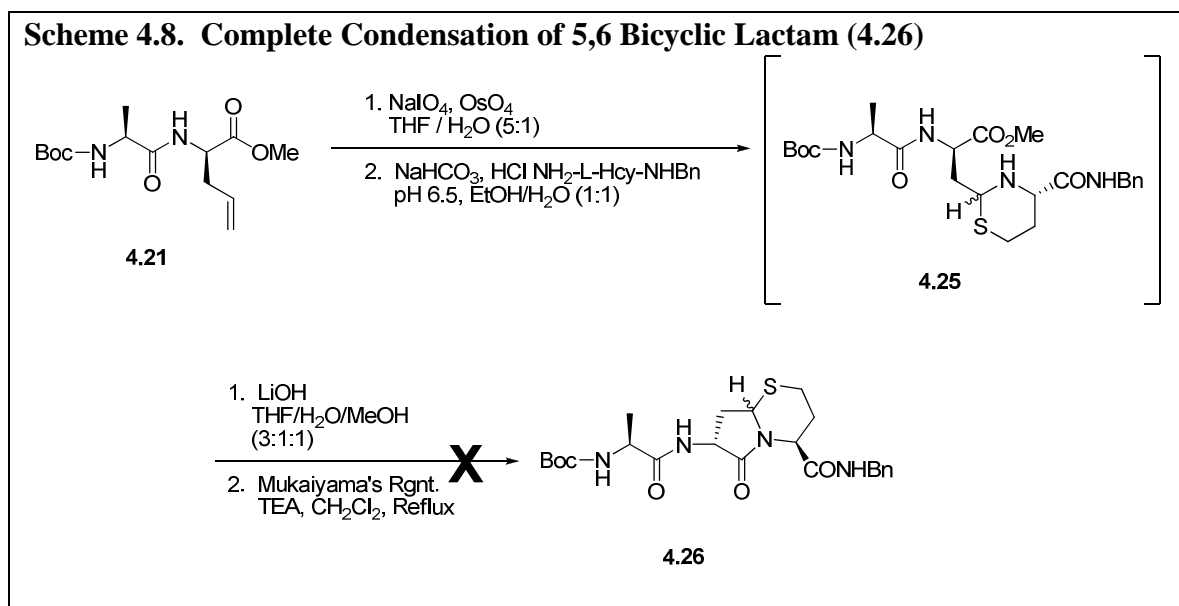
In parallel with the synthesis of subunit **AB**, subunit **CD** was being synthesized using the appropriate starting D-Cys and L-homo cystine amino acids as illustrated in **Scheme 4.7**. Boc protection of the amine proceeded in satisfactory yields utilizing standard chemistry. The coupling of benzyl amine to the free acid was not efficient with standard solution phase coupling chemistry. However, the use of isobutylchloroformate and the hydrochloride salt of benzyl amine produced the cystine benzyl amide in near quantitative yields. Deprotection and disulfide reduction following a methodology

initially described by the Overmann group allowed the attainment of subunit **B** in its various derivatives.¹⁷

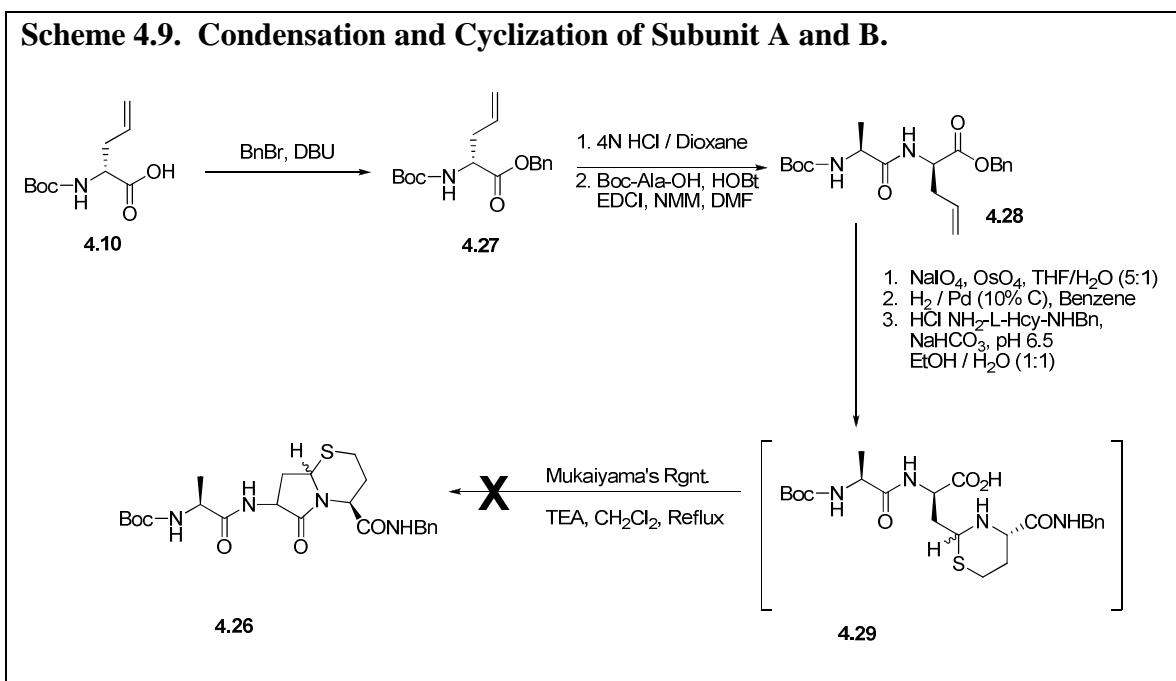


Subunit **AB** and subunit **CD** were condensed utilizing the chemistry in **Scheme 4.8**. The anticipated problem was that the steric bulk of the two subunits, **4.17** and **4.24**, would make the condensation or cyclization problematic. This proved to be the case as the condensation of the subunits did not yield an isolatable amount of final product (**4.26**) of either the major or the minor diastereomer.

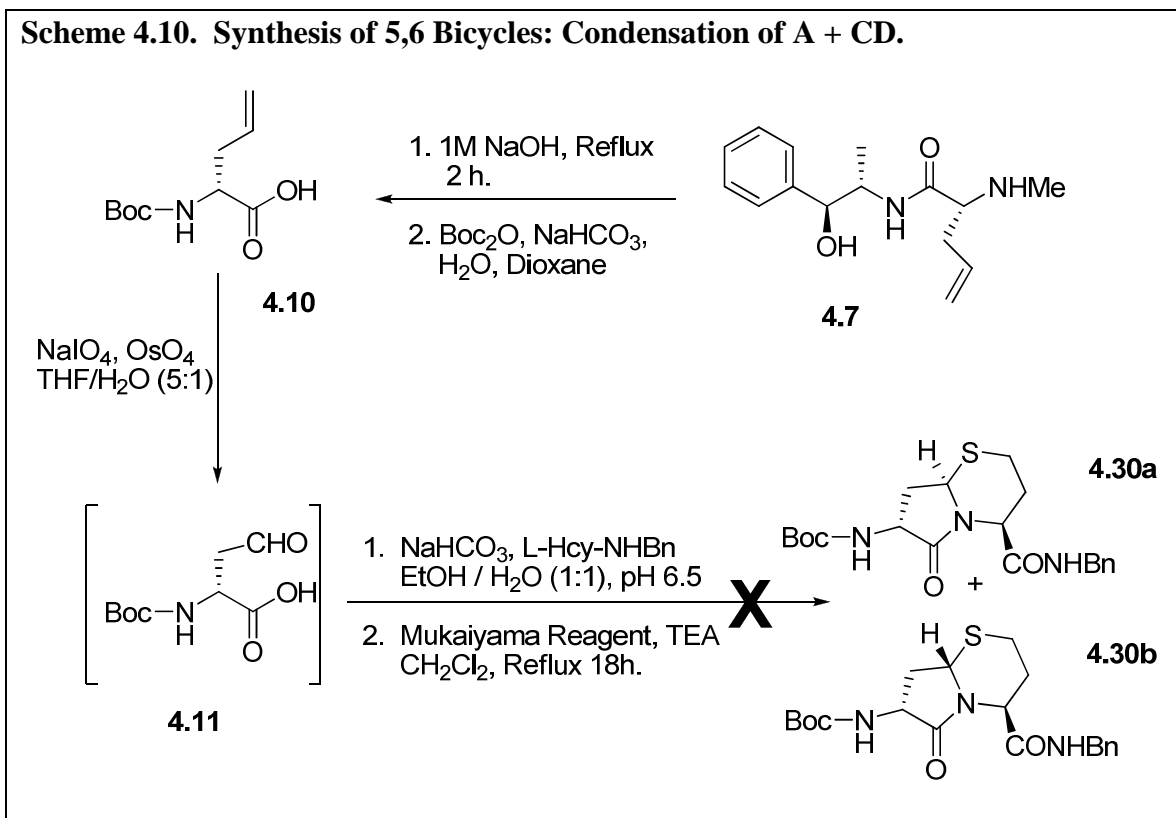
Two other synthetic methods were explored in parallel with this method in anticipation of the potential steric problem. Subjecting the thiazine to basic conditions may cause degradation back to the two starting materials and could have been a potential cause other than sterics for the failure of the reactions in **Scheme 4.8**.



In order to prevent the exposure of the condensation intermediate (**4.25**) to basic condition the benzyl ester of **4.10** was synthesized in hopes that reductive de-esterification before the condensation would circumvent the breakdown of the condensed product. In order to synthesize the benzyl ester derivative, **4.10** was stirred in a mixture of DBU and benzyl bromide to yield the final product **4.27** in a quantitative yield. Standard solution phase coupling with Boc-Ala-OH provided the dipeptide, **4.28**. Conversion to the aldehyde and subsequent reduction of the benzyl ester did not improve the yields of the final product **4.26**. The reaction once again did not yield any isolatable product. This affirmed the previous hypothesis that steric bulk and not the reversibility of the condensation was the problem within the reaction scheme.



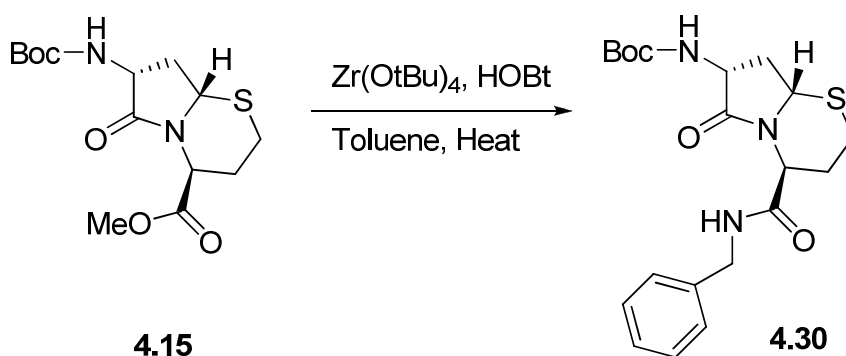
The second of the contingency synthetic plans was to eliminate the steric bulk from the alanine residue on subunit **AB** by coupling just subunit **B** (**4.11**) to the deprotected derivative of the homo-cysteine benzyl amide (**4.24**) as illustrated in **Scheme 4.10**. Condensation and cyclization still did not provide an isolatable amount of the cyclized product **4.30** and **4.31**.



4.4 Sequential Strategy Revisited: Zirconium Trans-Amidation and LiOH

Hydrolysis.

The Porco group reported the development of an ester-amide exchange process catalyzed by zirconium (IV) *tert*-butoxide in the presence of coupling reagents such as 1-hydroxy-7-azabenzotriazole (HOAt).¹⁸ In order to circumvent the problems of the base sensitive groups and to afford conversion of the methyl ester to the benzyl amine we utilized the Porco zirconium chemistry. We were initially rewarded by this straight forward, simple reaction (**Scheme 4.11**) with the desired benzyl amide (**4.30**) in 20% yield with 70% recovery of the starting material.

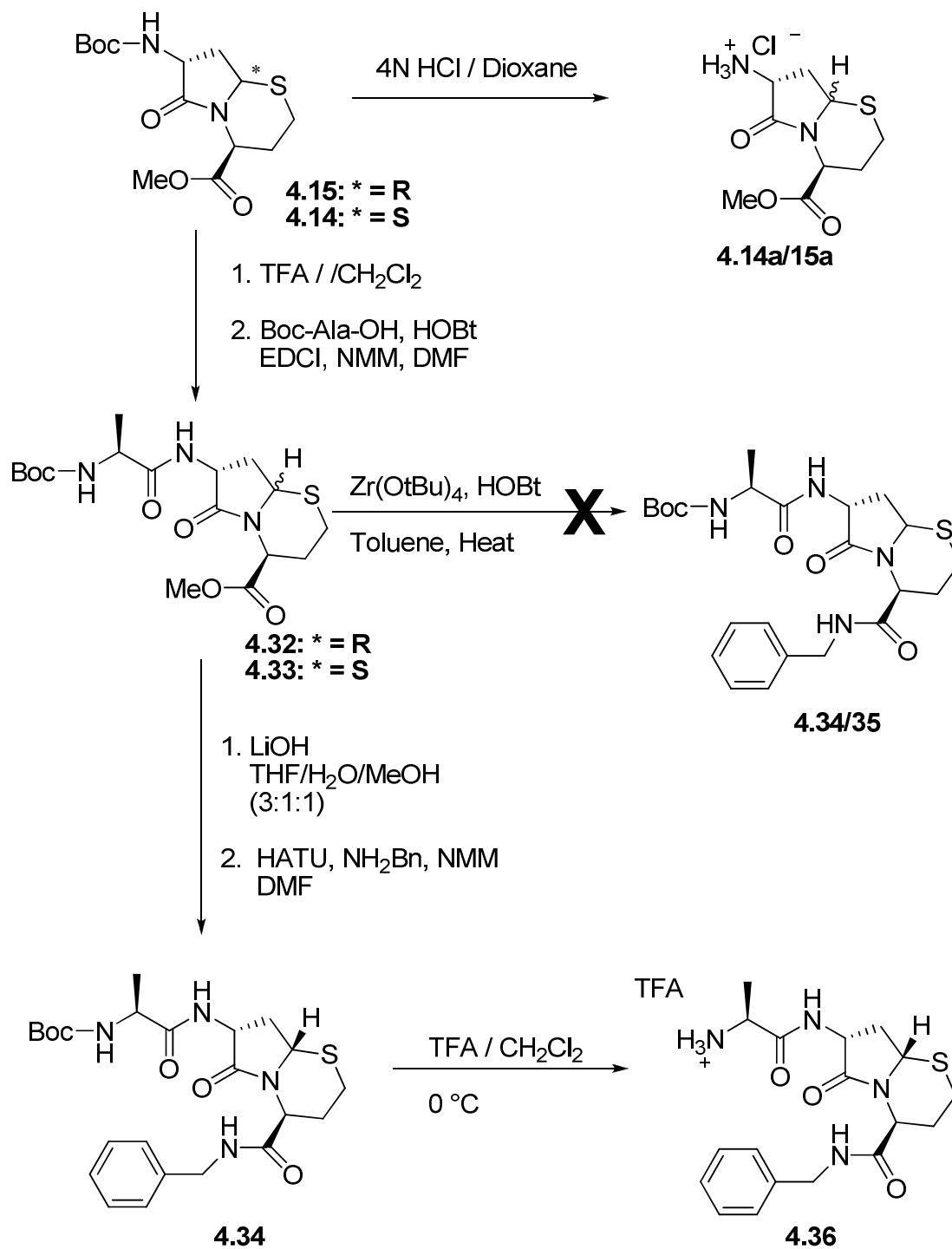
Scheme 4.11. Zirconium Mediated Trans-Amidation


Subsequent reaction upon the alanine derivatives of the bicycle with zirconium (**Scheme 4.12** and **Scheme 4.13**) presented us with a singular and frustrating problem. The esters and the amides (**4.32/33** and **4.34/4.35**) were inseparable by silica gel chromatography and the obvious strategy of hydrolyzing the remaining starting material would lead to epimerization of the base sensitive center thus leading to an intractable synthetic situation.

After having tried many strategies to work around the problems inherent in the bicyclic ring system, we revisited the initial sequential coupling method with the renewed vision of merely minimizing the epimerization versus abolishing it altogether. With minimized epimerization the hope was to monitor the reaction closely in order to separate the diastereomers at the crucial stage through silica gel chromatography.

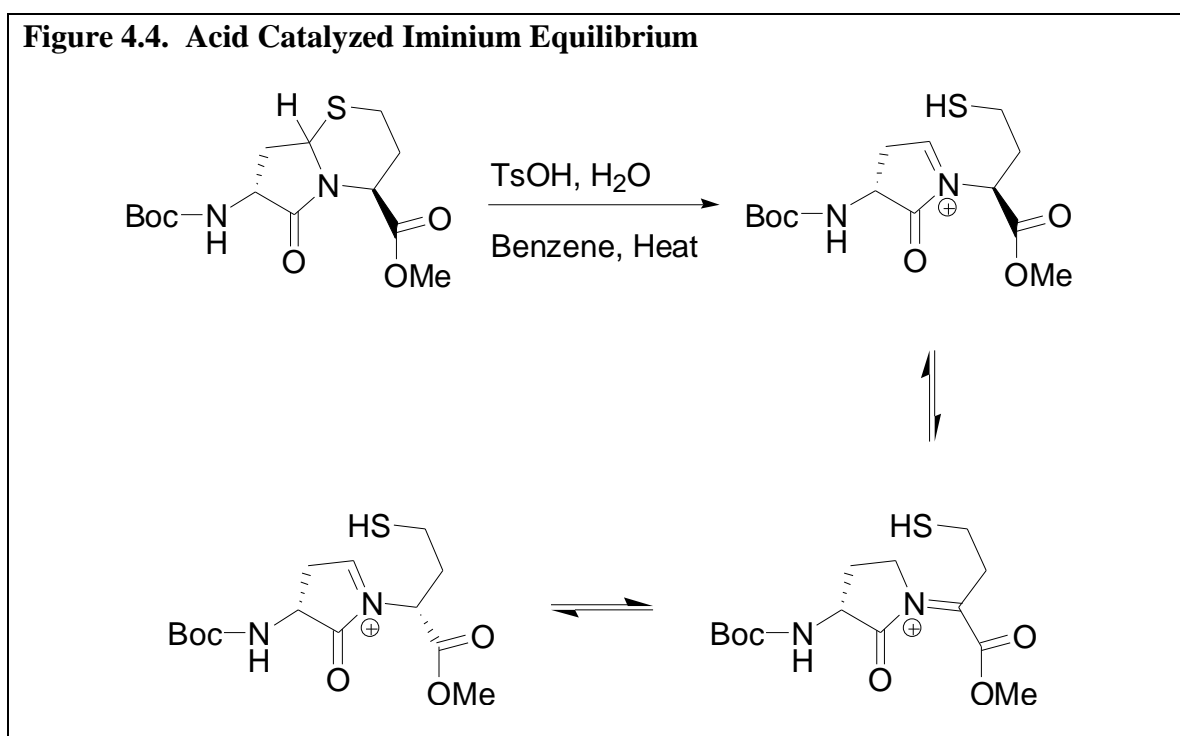
Scheme 4.12. Synthesis of the 5,6 Tetrapeptides via Standard Sequential Coupling

Chemistry



The bicyclic system **4.14/15** was deprotected initially utilizing the standard 4N HCl / dioxane conditions and to complicate matters further not only was there a base sensitive group but the bridgehead carbon was also epimerizable under acidic conditions as illustrated in **Figure 4.4**. This also was anticipated since Dr. Khalil initially discovered the potential for acidic racemization while synthesizing structurally analogous Pro-Leu-Gly peptidomimetics.⁸ The use of TFA at 0 °C for 45 minutes proved to be an effective way to remove the Boc protecting group without affecting the bridgehead center.

(Scheme 4.12 and Scheme 4.13)

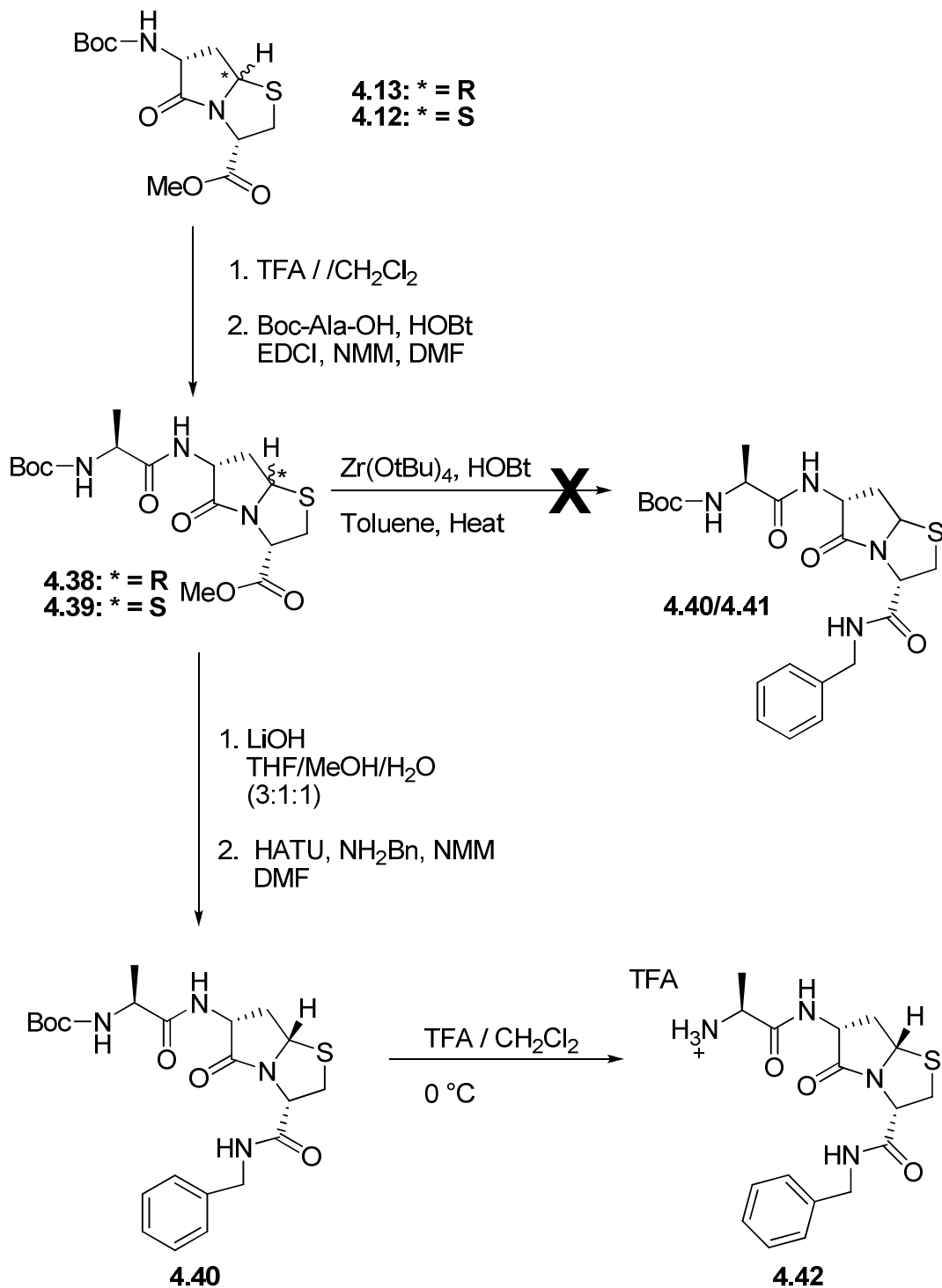


After successfully deprotecting the strained bicyclic structures, standard solution phase coupling conditions linked alanine to the structures in an efficient yields of 77 – 90%.

(**4.32, 4.33, 4.38, 4.39**).

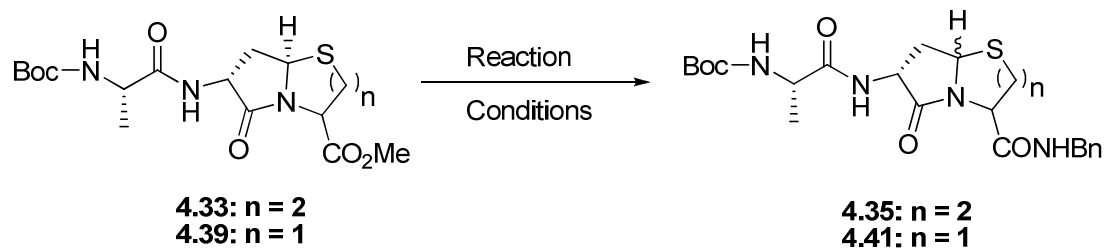
Scheme 4.13. Synthesis of the 5,5 Tetrapeptides via Standard Sequential Coupling

Chemistry



Gentle hydrolysis with LiOH and constant monitoring showed a minor conversion of the bicycles to the corresponding epimerized diastereomer. This was monitored carefully and the reaction was neutralized to pH 6.8 as soon as the TLC indicated that the ester had been fully hydrolyzed which was generally within 30 – 40 minutes of adding the LiOH solution. After workup to obtain the free acid, benzyl amine hydrochloride was coupled to the ring structure utilizing HATU to obtain the Boc protected final intermediate (**4.34**, **4.40**). Once again gentle TFA deprotection at 0 °C provided the TFA salts **4.36** and **4.42** respectively.

Synthesis of the *R* stereochemistry at the bridgehead position was problematic in several respects. The first problem was the lack of material which was obtained from the initial cyclization as illustrated in **Schemes 4.3** and **Scheme 4.4**. **4.12** was obtained as 7% of the overall yield and **4.14** was 3% of the overall yield. Several conditions were attempted to convert **4.33** and **4.39** to **4.35** and **4.41** respectively. Sn(OH)₂ was first attempted as a mild non-basic hydrolysis, however, no detectable reaction occurred (**Table 4.1**). The zirconium *tert*-butoxide converted the methyl ester to the benzyl amine without racemization of the bridgehead center, however, the reaction could not be forced to completion and the starting material could not be separated from the product. The last conditions were the LiOH hydrolysis which did not cause racemization of the *S* stereochemistry. The minor *R* diastereomer is, not unexpectedly, more unstable than the *S* stereochemistry and racemizes under the LiOH hydrolysis conditions. The racemization problem was compounded by the difficulty of the benzylamine coupling. Several coupling reagents and conditions were attempted the best of which produced a 26% overall yield. The racemization compounded with the low yields of both **Scheme**

Table 4.1. Reaction Conditions and Yield in the Synthesis of 4.35 and 4.41

Reaction	Reaction Conditions	Result
1.	Sn(OH) ₂ ,	No Reaction
2.	Zr(OtBu) ₄ , HOBt, Toluene, Heat Benzylamine (3 eq.), 1 day	Inseparable from Starting Material (~50% complete)
3.	Zr(OtBu) ₄ , HOBt, Toluene, Heat Benzylamine (6eq.), 1 day	Inseparable from Starting Material (~80% complete)
4.	Zr(OtBu) ₄ , HOBt, Toluene, Heat Benzylamine (6 eq.), 3 days	Inseparable from Starting Material (80% complete)
5.	a. LiOH, THF/MeOH/H ₂ O b. Benzylamine, HOBt, EDC, NMM DMF	1:1 Racemization; 12% overall yield
6.	a. LiOH, THF/MeOH/H ₂ O b. Benzylamine, HOBt, EDC, NMM HATU, DMF	1:1 Racemization; 26% overall yield
7.	a. LiOH, THF/MeOH/H ₂ O b. Benzylamine, HATU, TEA DMF	1:1 Racemization; 8% overall yield

4.3/4.4 and the benzyl amine coupling (**Table 4.1.**) and since the compounds were being synthesized as a negative control led us to abandon these molecules and focus upon the molecules which were predicted by the initial modeling studies to have biological activity.

4.5 Modeling Analysis

Modeling analysis of the ϕ_2 , ψ_3 , constrained AVPI mimics was performed upon the same *in silico* protein that was built and tested in **Chapter 2**. The terminal tetrapeptide of Smac binds to a surface groove, 892 Å total surface area,^{19,20} on BIR3 formed by the β -strand and the α_3 helix. Val2 and Pro3 form a short anti-parallel β -strand.²⁰ The native AVPI forms a total of eight inter-molecular hydrogen bonds with the BIR3 domain.^{19,20} Ala 1 of the tetrapeptide forms 5 of the eight hydrogen bonds with Glu 142 and Asp 138 as well as with Glu 132, thus, demonstrating the critical nature of the Ala1 in the tight binding of the peptide to the surface groove.²⁰ These modeling data correlate well with data obtained from other BIR3 domains such as survivin.²¹⁻²⁴

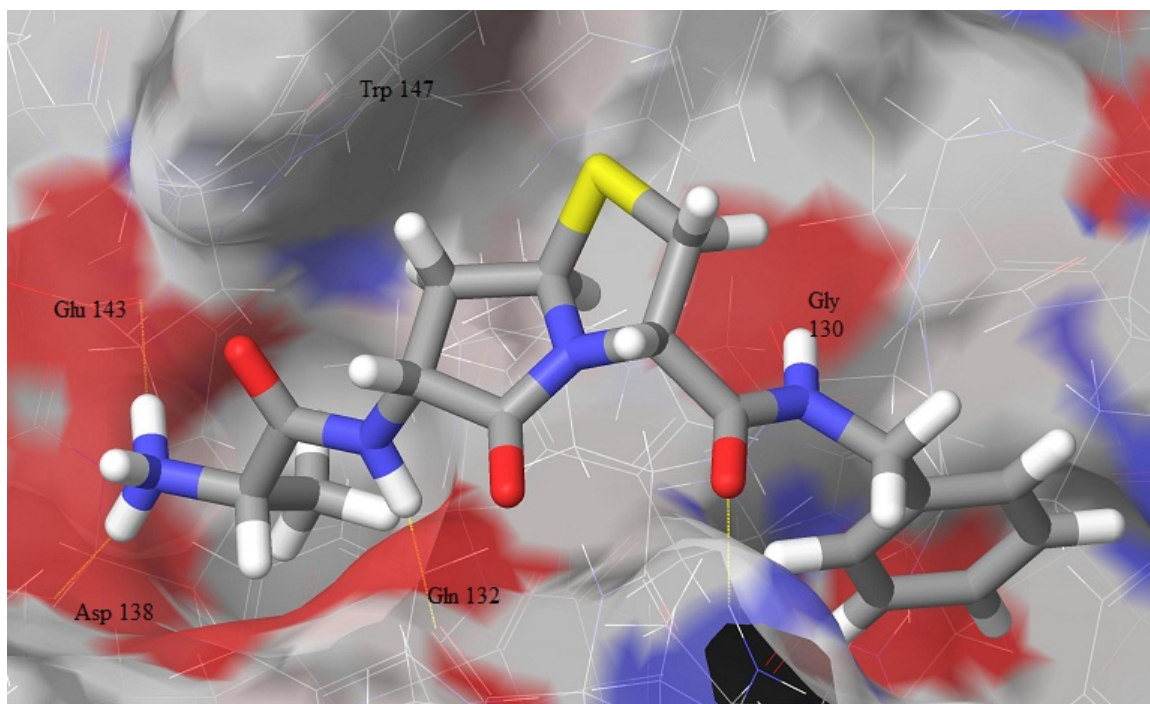


Figure 4.5. Ala-[(3*S*,6*R*,7*aR*)-6-amino-*N*-benzyl-5-oxohexahydropyrrolo[2,1-*b*]thiazole-3-carboxamide]•TFA **4.42**

The ϕ_3 , ψ_3 benzyl derivative (**4.42**) was modeled first (**Figure 4.5**) and docked into the active site using a flexible docking option of the Glide software with 1000

iterations of possible conformations being selected for all modeling attempts. The gross morphology of the docking of **4.42** is the same as that for AVPI at the P1 pocket. The bicyclic structure of the 5,5 system mimics the native AVPI binding at the S1 pocket. The bicycle forms the same hydrogen bonds to Glu 143 and Asp 138 as the native ligand. The P2 nitrogen of valine also forms a hydrogen bond with Gln 132, which is also similar to AVPI. The benzyl group does not enter into the expected hydrophobic-aromatic interactions that we initially predicted. Taken together the Glide program assigned a GScore value of -8.91 as compared to the -8.01 value it assigned to the native ligand, AVPI. This promising GScore value should correlate to an even greater activity than that of the native peptide.

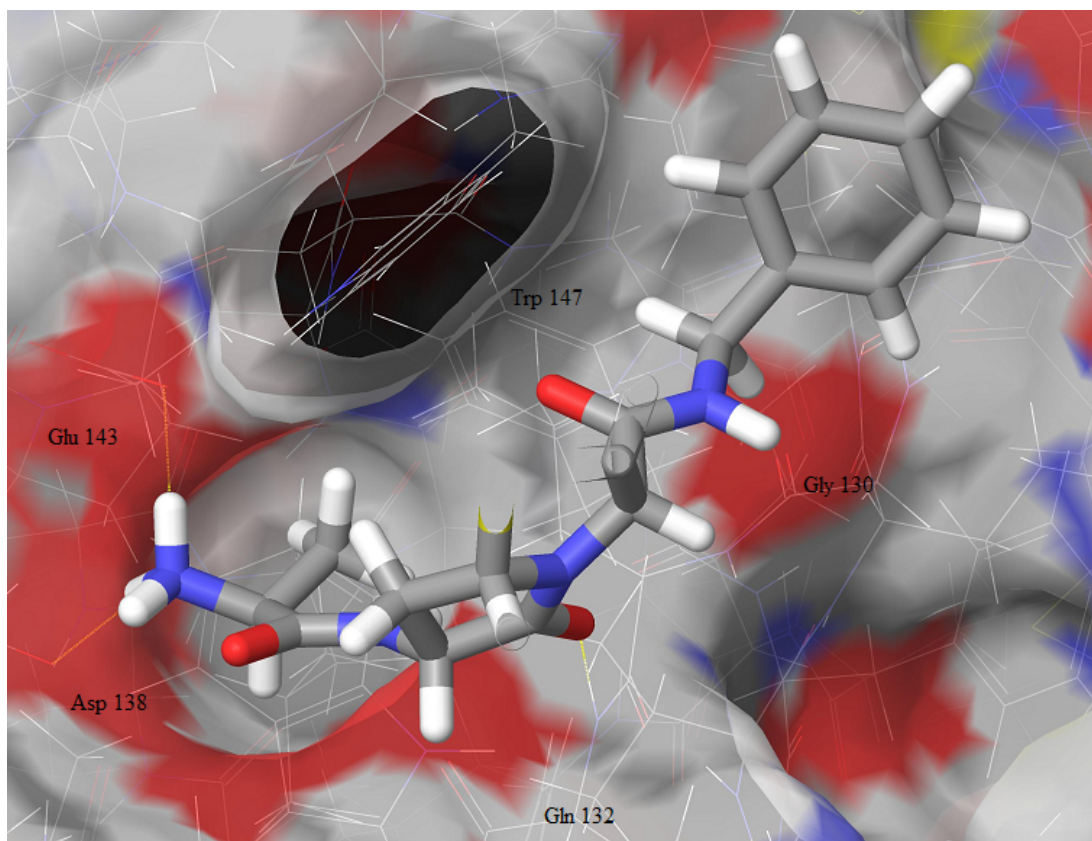


Figure 4.6. Ala-[(3*S*,6*R*,7*aS*)-6-amino-*N*-benzyl-5-oxohexahydropyrrolo[2,1-*b*]thiazole-3-carboxamide]•TFA **4.43**

The (3*S*, 6*R*, 7*aS*) isomer of the 5,5 bicyclic structure (**4.43**) was modeled next (**Figure 4.6**) and docked into the active site using the same modeling parameters as **4.42**. The gross morphology of the docking of the **7S** is the same as that for **4.42**. The constraints at the P1 position places the molecule into the same hydrophobic pocket as well as having the same hydrogen bonding as in the case of **4.42** with the exception that **4.43** differs from the *R* form at the P2 nitrogen which does not form any hydrogen bonding interactions. It is this difference which presumably makes the difference in the assigned GScore value of -5.67 as compared to the -8.91 value it assigned to **4.42** and the -8.01 value to the native ligand, AVPI. The GScore value should correlate to an activity within the Wang assay of greater than a 100 μM K_i .

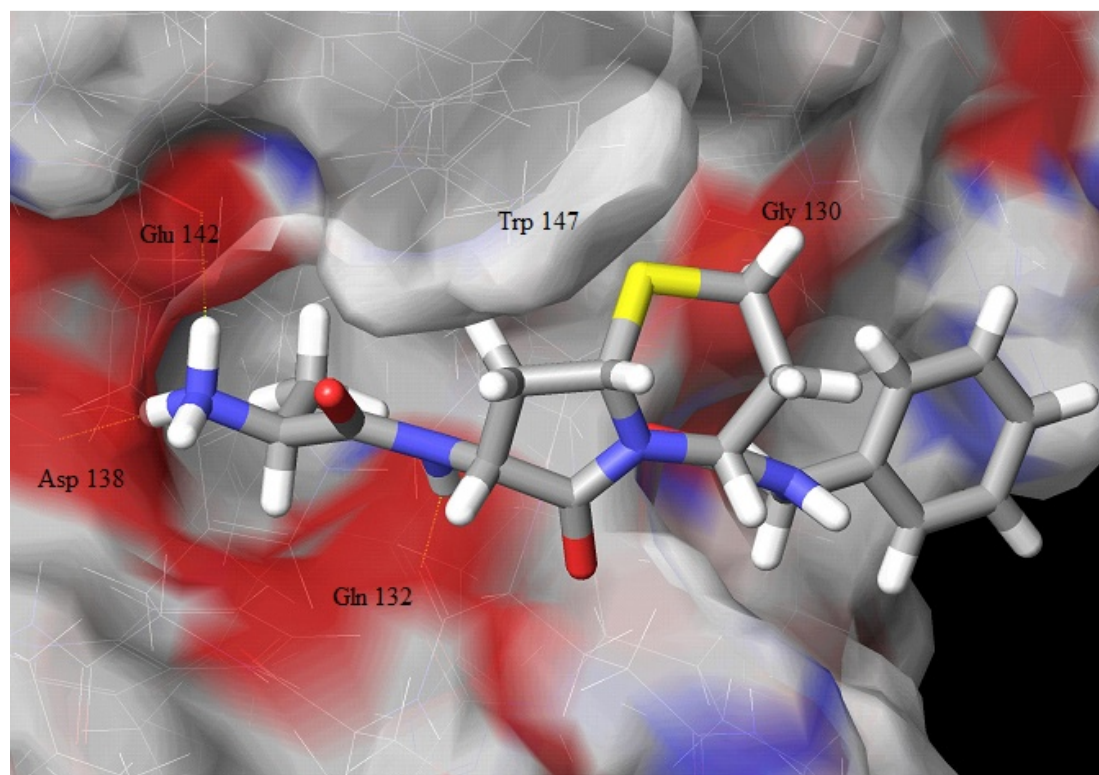


Figure 4.7. Ala-[(4*R*,7*R*,8*aS*)-7-amino-*N*-benzyl-6-oxohexahydro-2*H*-pyrrolo[2,1-*b*][1,3]thiazine-4-carboxamide]•TFA **4.37**

When the (*4R*, *7R*, *8aS*) 5,6 bicyclic derivative (**4.37**) was docked into the active site utilizing the Schrödinger flexible docking program (also as described in **Chapter 2**) the φ_2 , ψ_3 constrained mimic gave a very favorable GScore of -7.34 (**Figure 4.7**). The hydrogen bonding was precisely the same as the native peptide binding to Glu 143, Asp 138 and Gln 132 at the amine group and the carbonyl of Gln 132.

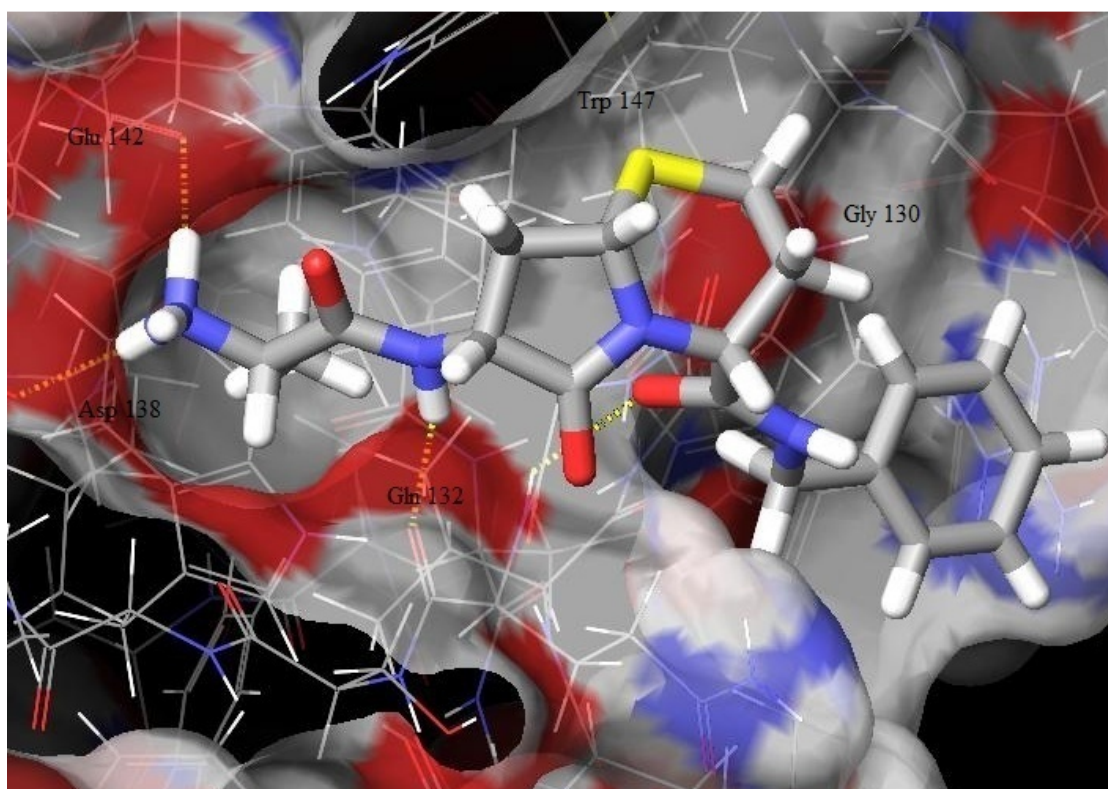


Figure 4.8. Ala-[(*4R*,*7R*,*8aR*)-7-amino-N-benzyl-6-oxohexahydro-2*H*-pyrrolo[2,1-*b*][1,3]thiazine-4-carboxamide]•TFA **4.36**

The 8*R* position (**4.36**), surprisingly had the same interactions as the 8*S* orientation and the exact same GScore as **4.37**. The GScore data of both of the φ_2 , ψ_3 constrained 5,6 bicyclic derivatives suggests an activity slightly lower than that of the native peptide.

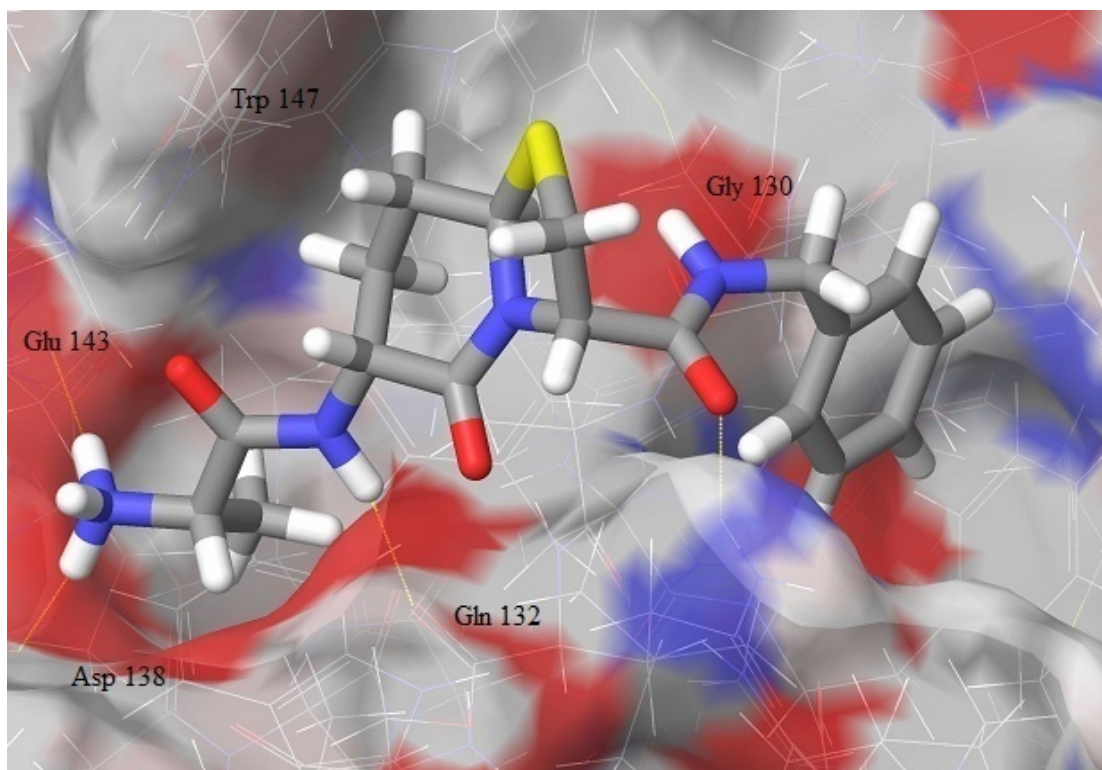


Figure 4.9. Ala-[(3*R*,6*R*,8*aR*)-6-amino-*N*-benzyl-5-oxohexahydro-2*H*-thiazolo[3,2-*a*]pyridine-3-carboxamide]•TFA

Although the 6,5 bicyclic derivatives were never fully synthesized, the compounds were initially modeled to determine their potential efficacy in the biological assays. The Glide program predicted that the 8*R* stereochemistry would have the same hydrogen bonding interactions as AVPI at the Glu 143, Asp 138 and Gln 132 residues and correspondingly assigned a GScore of -7.75. This GScore combined with the potential hydrogen bonding interactions lends support to the hypothesis that the 6,5 system will have similar activity to the native ligand in the Wang assay.

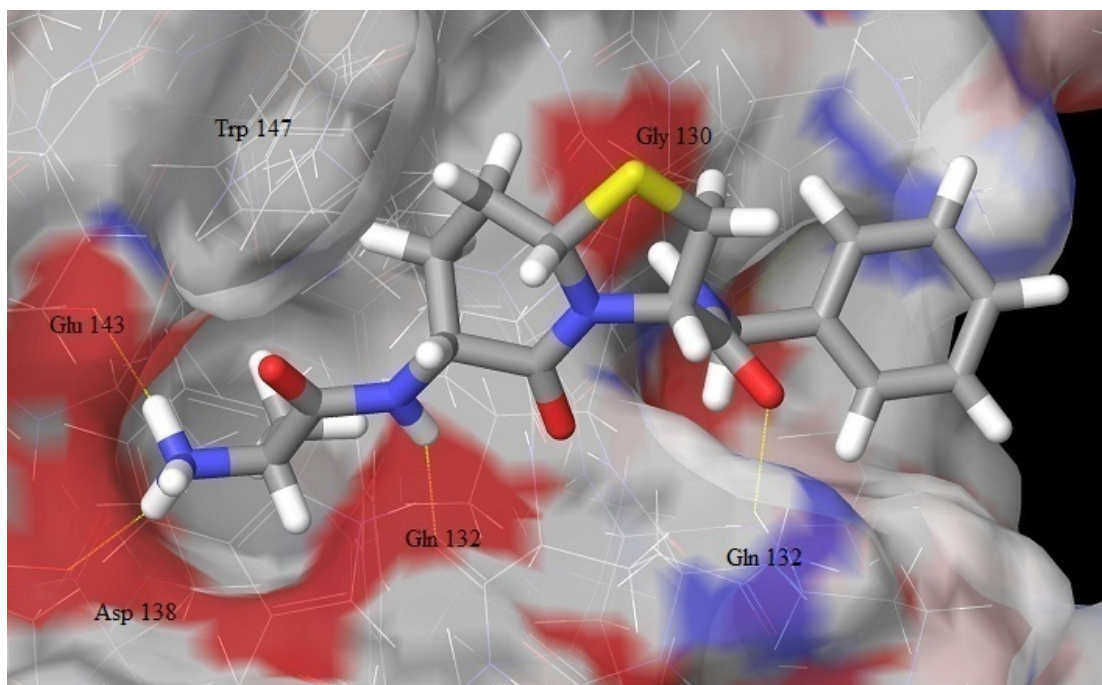


Figure 4.10. Ala-[(3*R*,6*R*,8*aS*)-6-amino-*N*-benzyl-5-oxohexahydro-2*H*-thiazolo[3,2-*a*]pyridine-3-carboxamide]•TFA

The 8*S* compound was also not synthesized but like the other analogues it mimics the native hydrogen bonding interactions of AVPI. Glide predicted a GScore of -6.89 which correlates to a potential K_i within the Wang assay of slightly less than the native peptide.

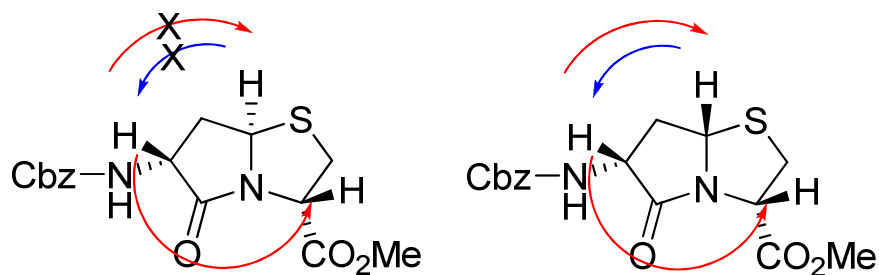


Figure 4.11 NOE Structure Confirmation of (3*S*, 6*R*, 7*aR*)-6-tert-Butoxycarbonylamino-5-oxo-hexahydro-pyrrolo[2,1-*b*]thiazole-3-carboxylic Acid Methyl Ester and (3*S*, 6*R*, 7*aS*)-6-tert-Butoxycarbonylamino-5-oxo-hexahydro-pyrrolo[2,1-*b*]thiazole-3-carboxylic Acid Methyl Ester.

The structures of compounds **4.12**, **4.13**, **4.14**, and **4.15** were determined utilizing NOE spectroscopy. The bridgehead proton of both the 6,5 and 5,5 bicyclic compounds showed correlations to the known alpha proton at position 7. The correlation or lack thereof was used to determine whether or not the proton was in the bridgehead up or down position as shown in **Figure 4.11** and **Figure 4.12**.

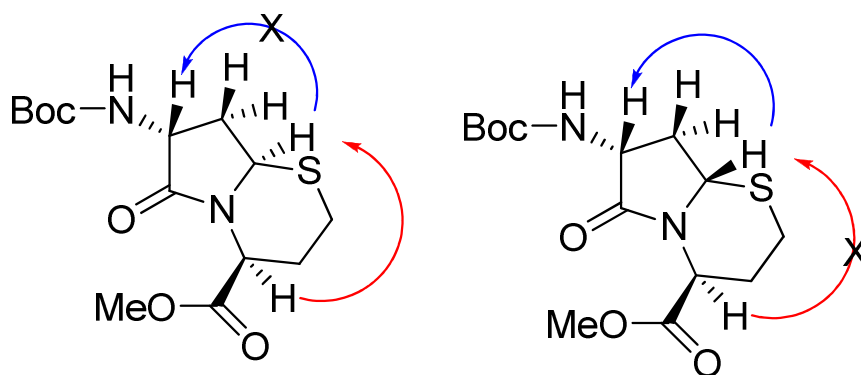
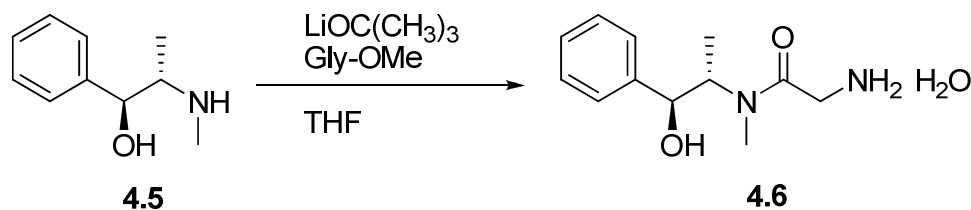


Figure 4.12 NOE Structure Confirmation of (4*S*, 7*R*, 8*aR*)-7-tert-Butoxycarbonylamino-6-oxo-hexahydro-pyrrolo[2,1-*b*][1,3]thiazine-4-carboxylic Acid Methyl Ester (**4.14**) and (4*S*, 7*R*, 8*aS*)-7-tert-Butoxycarbonylamino-6-oxo-hexahydro-pyrrolo[2,1-*b*][1,3]thiazine-4-carboxylic Acid Methyl Ester (**4.15**).

4.6 Experimentals

(*S,S*)-(+)-Pseudoephedrine Glycinamide (**4.6**)



A round bottom flask was charged with (*1S*, *2S*) pseudoephedrine (**4.5**, 10 g, 79 mmol) and glycine methyl ester hydrochloride (10 g, 61 mmol). Tetrahydrofuran (80 mL) was added to the solid mixture and the reaction was stirred at room temperature for 15 – 60 minutes producing a fine suspension. Lithium *tert*-butoxide powder (6.83 g, 85.4 mmol) was added to the suspension in a single portion. This addition caused the mixture to become a homogenous yellow solution in 5 – 10 minutes. After stirring at ambient temperature for 2 hours, water (80 mL) was added and the mixture was concentrated *in vacuo* to remove the bulk of the THF. The largely aqueous concentrate was then extracted with a portion of DCM (160 mL). Solid NaCl was added to the aqueous layer to the point of saturation and the resulting layer was washed with DCM (4 x 60 mL). The combined organic extracts were dried over anhydrous K₂CO₃ and then filtered and concentrated by rotary evaporation. The liquid residue was further concentrated under high vacuum overnight. The resulting dark orange syrup was dissolved in 250 mL of a mixture of THF / H₂O (25:1). Upon cooling to room temperature white crystals formed immediately (**4.6**, 9.2 g, 63 %). Concentration of the mother liquor provided another 1.9 g of crystals for a total yield of 76%.

mp = 84 – 87 °C [lit.¹⁵ 84 – 86 °C]

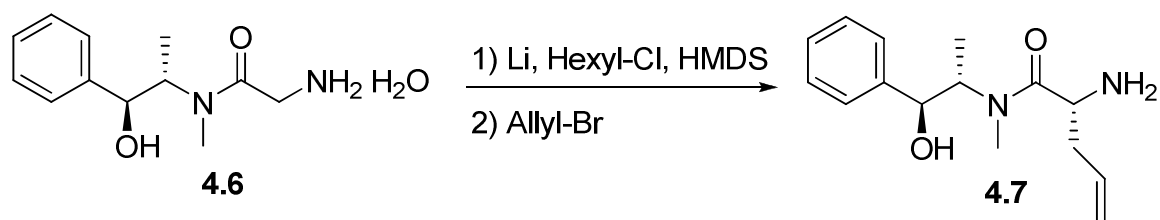
TLC R_f = 0.38 (Propanol / NH_4OH , 4:1)

$[\alpha]_D^{25}$ 98.5 (c 0.01, CH_2Cl_2) [lit.¹⁵ 102 (c 1.1, MeOH)]

^1H NMR (300 MHz, CDCl_3 , COSY)^{15,16} δ 7.21 – 7.34 (m, 5H, C_6H_5), 4.58 – 4.65 (m, 1H, CHCH_3 , CHOH), 4.42 – 4.51 (dd, J = 8.7 Hz, 0.8H, CHCH_3 , CHOH), 3.60 – 3.68 (m, 0.7H, CH_2) and 3.18 – 3.34 (m, 1.3H, CH_2), 3.01 (H_2O), 2.87 (s, 1.5H, NCH_3) and 2.79 (s, 1.5h, NCH_3), 2.55 – 2.64 (m, 0.5H, CHCH_3), 0.82 – 0.94 (m, 3H, CHCH_3).

^{13}C NMR (75 MHz, CDCl_3 , HMQC, rotamers present) δ 173.4 and 173.6 (CO), 142.4 and 142.5 (C_6H_5), 128.7 (C_6H_5), 128.5 (C_6H_5), 128.2 (C_6H_5), 127.9 (C_6H_5), 127.0 (C_6H_5), 127.0 (C_6H_5), 74.9 and 75.6 (CHOH), 56.8 and 57.6 (NCH_3), 43.3 and 43.6 (CH_2NH_2), 27.3 and 30.0 (CHCH_3), 14.6 and 15.7 (CHCH_3)

Pseudoephedrine D-Allyl Glycinamide (4.7)



A round bottom flask was filled with 15 mL of THF and then flushed with argon. Lithium wire (0.18 g, 25.8 mmol) was freed of oil by briefly dipping it in hexanes. It was then cut into 1 – 2 cm pieces which were subsequently added to the reaction vessel. HMDS (2.95 mL, 14.1 mmol) and 1-chlorohexane were added sequentially to the

reaction mixture, and the reaction vessel was immersed in a water bath at 23 °C. The reaction became cloudy due to the precipitation of LiCl after a few minutes. Ice was added to the water bath and the reaction was allowed to gradually warm to room temperature where it was stirred overnight. After approximately 16 hours, the Li wire was fully consumed and the resulting suspension was cooled to 0 °C in an ice-water bath. Solid pseudoephedrine glycinamide (**4.6**, 0.91 g, 3.8 mmol) was added in one portion. The reaction mixture was stirred vigorously for 2.5 hours until it formed a bright orange enolate suspension. Allyl bromide (0.26 mL, 4 mmol) was added dropwise via syringe over a period of 10 minutes. After complete addition, the resulting solution was stirred in an ice bath for 1 hour. Ice-water (10 mL) was added slowly to the reaction mixture, which then was acidified to pH 0 by the addition of 1M HCl. The mixture was transferred to a separation funnel and ethyl acetate (10 mL) was added to the mixture. The organic layer was extracted three times with 1M HCl (3 x 10 mL). The aqueous layers were combined and cooled to 5 °C by the addition of ice chunks of distilled H₂O. The aqueous solution was treated with 50% NaOH and the basic solution was then extracted with dichloromethane (4 x 30 mL). The organic extracts were dried with K₂CO₃, filtered, and concentrated *in vacuo*. Toluene was added and rotovapped off to yield a yellow semi-solid oil which was then placed under high vacuum for 1 hour. The solid was then crystallized from toluene and ether. The resulting white crystals were washed with Et₂O and taken forward to yield 48% of **4.7**. (0.48 g).

mp = 82 – 84 °C [lit¹. 79 – 83 °C]

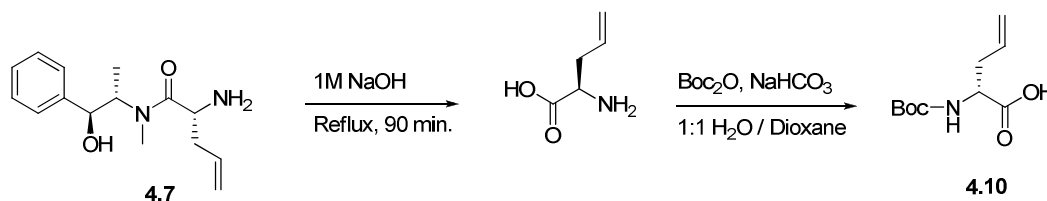
TLC R_f = 0.55 (Propanol / NH₄OH, 4:1)

[α]_D 80 (c 0.01, CH₂Cl₂)

^1H NMR (300 MHz, CDCl_3 , COSY, 3:1 *rotamer ratio present*)^{15,16} δ 7.16 – 7.28 (m, 5H, C_6H_5), 5.56 – 5.76 (m, 1H, CHCH_2), 4.99 – 5.11 (CHCH_2), 4.49 and 4.64 (br m, 2H, α CH, CHOH), 3.53 – 3.61 (m, 1H, CHCH_3), 2.79 and 2.85 (NCH_3), 1.99 – 2.24 (m, 2H, CH_2CHCH_2), 0.88 – 0.94 (d, $J = 6.3$ Hz., 3H, CHCH_3).

^{13}C NMR (75 MHz, CDCl_3 , HMQC, *rotamers present*) δ 175.3 and 176.4 (CO), 142.1 and 142.4 (C_6H_5), 134.0 and 135.0 (CHCH_2), 128.8 (C_6H_5), 128.5 (C_6H_5), 128.4 (C_6H_5), 127.9 (C_6H_5), 127.1 (C_6H_5), 126.7 (C_6H_5), 118.3 and 118.5 (CHCH_2), 75.2 and 75.9 (CHOH), 58.1 (NCH_3), 51.5 and 51.6 (α CH), 40.0 and 40.3 (CHCH_3), 31.9 (CH_2CHCH_2), 14.9 and 16.0 (CHCH_3).

Boc- α -Allyl-D-Gly-OH (4.10)



An aqueous solution of NaOH (1M, 7.6 mL, 7.6 mmol) was added to a solution of (*S,S*)-pseudoephedrine-(*R*)-allyl glycine (**4.7**, 1.0 g, 3.8 mmol) in water (7.6 mL). The resulting solution was heated at reflux for 90 minutes. Upon cooling to room temperature we observed the formation of a white precipitate which was pseudoephedrine crystals. Water (20 mL) was added and the aqueous mixture was extracted with dichloromethane (2 x 20 mL). The organic layers were combined and washed once again with water (20 mL). The aqueous layers were combined and concentrated to approximately 10 mL.

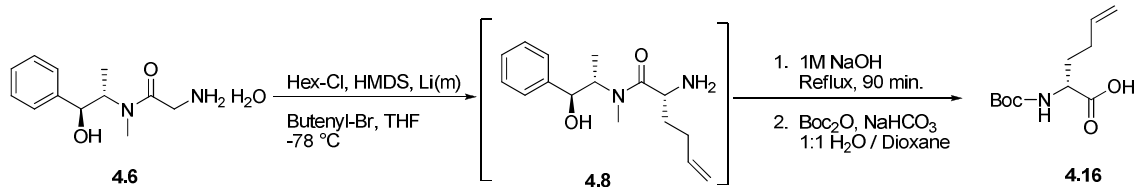
Solid NaHCO₃ (0.3 g, 7.6 mmol) was added to the concentrated aqueous layer, which was then allowed to stir for 5 minutes. Boc₂O (1.0 g, 4.6 mmol) was dissolved in 1,4-dioxane (10 mL) and this solution was added in one portion to the reaction flask. The reaction was stirred at room temperature for 90 minutes. Water (20 mL) was added and the aqueous solution was extracted with ethyl acetate (30 mL). The organic layer was washed with saturated NaHCO₃ (20 mL). The aqueous layers were combined and the resulting solution was carefully acidified to pH 2 – 3 by the addition of 1M HCl. The acidified solution was extracted with four portions of dichloromethane (30 – 50 mL each). The combined organic layers were dried with MgSO₄ and concentrated under reduced pressure to yield 0.81 g (99%) of **4.10** as a clear oil.

TLC R_f = 0.63 (NH₄OH / Propanol, 1:4)

[α]_D 14.1 (*c* 0.4, CH₂Cl₂)

¹H NMR (300 MHz, CDCl₃, COSY) δ 11.62 (s, 1H, CO₂H), 6.48 (br s, 1H, NH), 5.66 – 5.77 (m, 1H, CHCH₂), 5.10 – 5.16 (CHCH₂), 4.35 – 4.41 (α CH), 2.44 – 2.60 (m, 2H, CH₂CHCH₂), 1.41 (s, 9H, Boc C(CH₃)₃).

¹³C NMR (75 MHz, CDCl₃, HMQC, rotamers present) δ 176.3 (CO₂H), 155.6 and 156.9 (Boc CO), 132.3 (CHCH₂), 119.5 (CHCH₂), 80.5 and 82.0 (Boc C(CH₃)₃), 53.0 and 54.6 (α C), 36.8 (CH₂CHCH₂), 28.6 and 28.7 (Boc C(CH₃)₃).

(R)-2-(tert-Butoxycarbonylamino)hex-5-enoic Acid (4.16)

A round bottom flask was filled with 15 mL of THF and flushed with argon. Lithium wire (0.18 g, 25.8 mmol) was freed of oil by briefly dipping it in hexanes. It was then cut into 1 – 2 cm pieces which were subsequently added to the reaction vessel. HMDS (2.95 mL, 14.1 mmol) and 1-chlorohexane were added sequentially to the reaction mixture, and the reaction vessel was immersed in a water bath at 23 °C. The reaction became cloudy due to the precipitation of LiCl after a few minutes. Ice was added to the water bath and the reaction was allowed to gradually warm to room temperature where it was stirred overnight. After approximately 16 hours, the Li wire was fully consumed and the resulting suspension was cooled to 0 °C in an ice-water bath, whereupon solid pseudoephedrine glycinamide (**4.6**, 0.91 g, 3.8 mmol) was added in one portion. The reaction mixture was stirred vigorously for 2.5 hours until it formed a bright orange enolate suspension. Butenyl bromide (0.41 mL, 4 mmol) was added dropwise via syringe over a period of 10 minutes. After complete addition, the resulting solution was stirred in an ice bath for 1 hour. Ice-water (10 mL) was added slowly to the reaction mixture and then it was acidified to pH 0 by the addition of 1M HCl. The mixture was transferred to a separation funnel, and ethyl acetate (10 mL) was added to the mixture. The organic layer was extracted three times with 1M HCl (3 x 10 mL). The aqueous layers were combined and cooled to 5 °C by the addition of ice chunks of distilled H₂O. The aqueous solution was treated with 50% NaOH and the basic solution was then

extracted with dichloromethane (4 x 30 mL). The organic extracts were dried with K_2CO_3 , filtered, and concentrated *in vacuo*. Toluene was added and rotovapped off to yield a yellow semi-solid oil which was then placed under high vacuum for 1 hour. The crude solid was analyzed and taken forward without further purification.

TLC R_f = 0.68 (Propanol / NH_4OH , 4:1)

1H NMR (300 MHz, $CDCl_3$, COSY) δ 7.16 – 7.21 (m, 5H, C_6H_5), 5.61 – 5.67 (m, 1H, $CHCH_2$), 4.87 – 4.95 (m, 2H, $CHCH_2$), 4.36 – 4.48 (m, 2H, NH_2 , $\alpha - CH$), 3.46 – 3.50 (m, 1H, $CHOH$), 3.13 – 3.18 (m, 3H, $CHOH$, $CHCH_3$, NH_2), 2.83 (impurity), 2.74 (s, 3H, NCH_3), 1.97 – 2.12 (m, 2H, CH_2CHCH_2), 1.29 – 1.46 ($CH_2CH_2CHCH_2$), 0.82 – 0.98 (m, 3H, $CHCH_3$).

An aqueous solution of NaOH (1M, 7.6 mL, 7.6 mmol) was added to a solution of (*S,S*)-pseudoephedrine-(*R*)-allyl glycine (**4.8**, 1.0 g, 3.8 mmol) in water (7.6 mL). The resulting solution was heated at reflux for 90 minutes. Upon cooling to room temperature we observed the formation of a white precipitate which was pseudoephedrine crystals. Water (20 mL) was added and the aqueous mixture was extracted with dichloromethane (2 x 20 mL). The organic layers were combined and washed once again with water (20 mL). The aqueous layers were combined and concentrated to approximately 10 mL. Solid $NaHCO_3$ (0.3 g, 7.6 mmol) was added to the concentrated aqueous layer which was then allowed to stir for 5 minutes. Boc_2O (1.0 g, 4.6 mmol) was dissolved in 1,4-dioxane (10 mL) and this solution was added in one portion to the above stirring aqueous solution. The reaction was stirred at room temperature for 90 minutes. Water (20 mL) was added

and the aqueous solution was extracted with ethyl acetate (30 mL). The organic layer was washed with saturated NaHCO₃ (20 mL). The aqueous layers were combined and the resulting solution was carefully acidified to pH 2 – 3 by the addition of 1M HCl. The acidified solution was extracted with four portions of dichloromethane (30 – 50 mL each). The combined organic layers were dried with MgSO₄ and concentrated under reduced pressure to yield 0.81 g, 99%, of **4.16** as a clear oil.

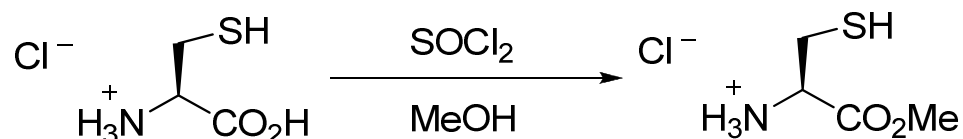
TLC R_f = 0.74 (Propanol / NH₄OH, 4:1)

[α]_D 11.2 (c 5, MeOH)

¹H NMR (300 MHz, CDCl₃, COSY) δ 5.75 – 5.86 (m, 1H, CHCH₂), 3.93 – 4.08 (m, 1H, α – CH), 2.29 – 2.31 (m, 0.5H, CH₂CHCH₂), 2.10 – 2.27 (m, 1.5H, CH₂CHCH₂), 1.84 – 1.89 (m, 1H, CH₂CH₂CHCH₂), 1.68 – 1.77 (m, 1H, CH₂CH₂CHCH₂), 1.44 (s, 9H, Boc – (CH₃)₃).

¹³C NMR (75 MHz, CDCl₃, HMQC, rotamers present) δ 177.3 and 174.6 (CO), 158.2 and 159.1 (Boc – CO), 137.9 and 139.5 (CHCH₂), 117.2 and 118.2 (CHCH₂), 81.6 and 82.7 (Boc – C(CH₃)₃), 55.5 and 56.0 (α – C), 35.0 and 35.4 (CH₂CHCH₂), 32.0 and 32.3 (CH₂CH₂CHCH₂), 29.8 and 29.9 (Boc C(CH₃)₃).

D-Cys-OMe•HCl



D-Cys (0.5 g, 2.8 mmol) was added to 20 mL of MeOH and the suspension was cooled to $-78\text{ }^{\circ}\text{C}$. Thionyl chloride (0.61 mL, 8.5 mmol) was added dropwise to the reaction mixture which was allowed to warm slowly to room temperature overnight. After 16 hours the solvent was removed under reduced pressure to yield a white solid. The solid was suspended in CH_2Cl_2 to dissolve any further traces of thionyl chloride. The CH_2Cl_2 was removed under reduced pressure and the process was repeated 5 – 6 times until the product was a free flowing white solid (0.4 g, 98% yield).

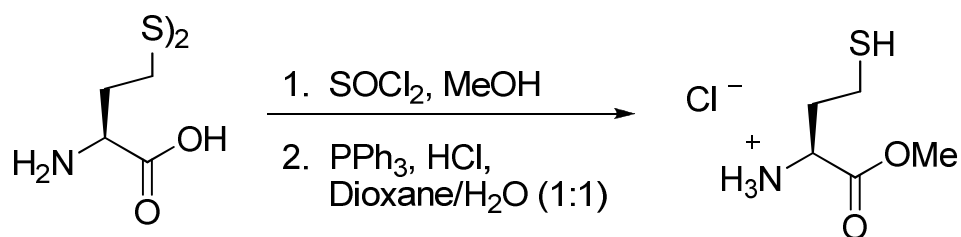
$R_f = 0.69$ (Propanol/ NH_4OH , 4:1)

$[\alpha]_D 2.6$ (c 0.4, MeOH)

$^1\text{H NMR}$ (300 MHz, CD_3OD , COSY) δ 4.33 – 4.35 (m, 1H, α -H), 3.87 (s, 3H, CO_2CH_3), 3.07 – 3.09 (m, 2H, CH_2SH).

$^{13}\text{C NMR}$ (75 MHz, CD_3OD , HMQC) δ 170.4 (CO), 57.0 (CO_2CH_3), 55.2 (α -C), 26.4 (CH_2SH).

L-Hcy-OMe•HCl



L-Homocysteine-OH (1.5 g, 5.4 mmol) was added to 100 mL of MeOH and the suspension was cooled to $-78\text{ }^{\circ}\text{C}$. Thionyl chloride (7.3 mL, 0.1 mol) was added dropwise to the reaction mixture which was allowed to warm slowly to room temperature overnight. After 16 hours the solvent was removed under reduced pressure to yield a white solid. The solid was suspended in CH_2Cl_2 to dissolve any further traces of thionyl

chloride. The CH_2Cl_2 was removed under reduced pressure and the process was repeated 5 – 6 times until the product was a free flowing white solid (1.8 g, 98% yield).

L-Hcy-OMe (1.8 g, 5.4 mmol) was dissolved in 200 mL of dioxane / H_2O (3:1) and PPh_3 (2.84 g, 10.7 mmol) was added in one portion to the reaction mixture. The reaction was allowed to stir at room temperature overnight. Upon completion of the reaction the solvents were removed under reduced pressure to yield a semi-solid oil. The oil was partitioned between H_2O (100 mL) and Et_2O (100 mL) and the aqueous layer was separated and concentrated *in vacuo* to provide the product as a white solid (1.75 g, 10.5 mmol) in 94% yield.

TLC $R_f = 0.72$ (Propanol / NH_4OH , 4:1)

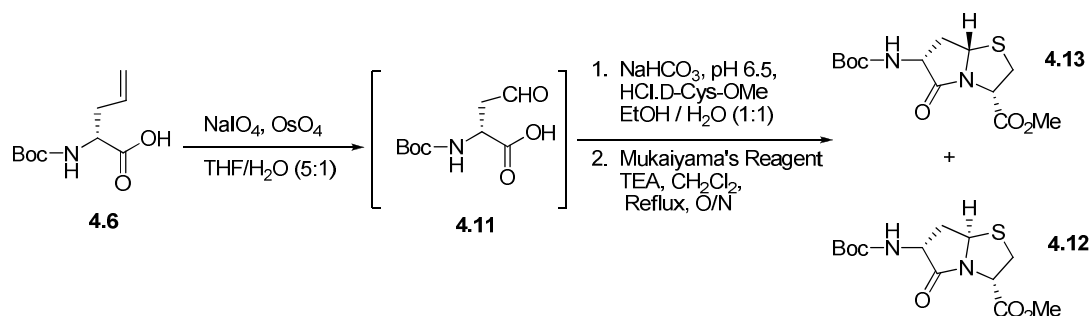
$[\alpha]_D 17.5$ (*c* 0.9, MeOH)

^{13}C NMR (75 MHz, CDCl_3 , HMQC) δ 171.7 (CO), 60.4 (CO_2CH_3), 55.0 (α CH), 53.8 (CH_2Cl_2), 36.7 (CH_2SH), 31.6 ($\text{CH}_2\text{CH}_2\text{SH}$), 29.8 (Boc – $\text{C}(\text{CH}_3)_3$).

(3S, 6R, 7aR)-6-tert-Butoxycarbonylamino-5-oxo-hexahydro-pyrrolo[2,1-b]thiazole-3-carboxylic Acid Methyl Ester (4.12)

and

(3S, 6R, 7aS)-6-tert-Butoxycarbonylamino-5-oxo-hexahydro-pyrrolo[2,1-b]thiazole-3-carboxylic Acid Methyl Ester (4.13)



Boc- D- α -allyl-Gly-OH (**4.6**, 1.3 g, 6.3 mmol) was dissolved in a 4:1 mixture of THF in H₂O. This solution was stirred under N₂ and it turned dark brown when OsO₄ was added as a 2.5% solution in t-BuOH (2.7 mL). After 5 minutes of stirring the solution NaIO₄ (4.0 g) was added in three batches over a 90 minute period. At this point, the reaction turned light yellow and stirring was continued for 5 hours. Upon completion the reaction was filtered to remove the excess salts and the filtrate was concentrated under reduced pressure. The resulting light yellow semi-solid / oil mixture was dissolved in EtOAc and filtered once more through Whatman filter paper and secondly through a 0.45 μm filter disk. The solvent was then concentrated under reduced pressure to yield the desired product (**4.11**).

TLC R_f = 0.77 (Propanol / NH₄OH, 4:1)

^{13}C NMR (75 MHz, CDCl_3) δ 174.8 (CO), 162.6 (CO), 156.0 (Boc-CO), 97.2 ($\text{CH}_2\text{C}(\text{OH})\text{O}$), 81.2 (Boc - $\text{C}(\text{CH}_3)_3$), 80.9 (Boc- $\text{C}(\text{CH}_3)_3$), 49.9 (α - C), 36.8 (α - C), 30.6 (CH_2CHO), 30.0 (CH_2CHO), 28.6 (Boc- $\text{C}(\text{CH}_3)_3$), 28.2 (Boc- $\text{C}(\text{CH}_3)_3$),

The resulting aldehyde (**4.11**, 0.4 g, 1.8 mmol) was dissolved in 50 mL of H_2O / EtOH (1:1) and the solution was cooled to 0 °C in an ice-salt bath. D-Cys-OMe (0.3 g, 1.8 mmol) was then added to the cooled solution and the pH was adjusted with solid NaHCO_3 to 6.5 while the reaction was stirred. While the reaction warmed to room temperature the solution was degassed with Ar for 20 minutes and allowed to stir overnight. After 18 hours the solvents were removed under reduced pressure and the residue was redissolved in H_2O . The solution was extracted with EtOAc. The pH of the aqueous layer was adjusted to 6.5 using 1N HCl, and then the aqueous layer was extracted with EtOAc. To facilitate the partitioning of the layers, NaCl was added to the aqueous layer followed by extractions into Et_2O . This process was repeated 5-6 times with adjustment of the pH to 6.5 between extractions. The organic layers were combined and dried with MgSO_4 . Removal of the solvent under vacuum gave a light orange oil (0.4 g, 1.2 mmol) which was dried under a high vacuum and then dissolved in dry CH_2Cl_2 . To the solution 2-chloro-1-methylpyridinium iodide (0.4 g, 1.4 mmol) and NEt_3 (0.15 g, 0.2 mL) was added. The resulting solution was refluxed overnight. The reaction mixture was allowed to cool, and then was extracted with 1N HCl (100 mL), saturated NaHCO_3 (100 mL), and brine (100 mL). Drying with MgSO_4 and subsequent removal of the solvents under vacuum resulted in an orange oil. The mixture of products was separated

by silica gel chromatography (EtOAc / Hexanes, 1:1) to yield 0.11 g (29%) of the 7aS diastereomer (**4.13**) and 42 mg (11%) of the 7aR diastereomer (**4.12**) both as clear oils.

4.13: Top / Major (7aS)-isomer

TLC R_f = 0.67 (EtOAc / Hexanes, 1:1)

$[\alpha]_D$ 140.4 (*c* 5.0, CH₂Cl₂)

¹H NMR (300 MHz, CDCl₃, COSY) δ 5.52 – 5.53 (br m, 1H, Boc – NH), 5.10 (d, *J* = 6.6 Hz, 1H, CHS), 4.96 – 5.00 (q, *J* = 4.5 Hz, 8.4 Hz, 1H, C2 α CH), 4.33 (d, *J* = 7.5 Hz, 1H, NCHCO₂Me), 3.71 (s, 3H, CO₂CH₃), 3.27 – 3.45 (m, 2H, SCH₂), 2.36 – 3.04 (br m, 2H, CH₂CHS), 1.38 (Boc – C(CH₃)₃).

¹³C NMR (75 MHz, CDCl₃, HMQC) δ 175.5 (CO), 170.4 (CO), 155.7 (Boc – CO), 80.6 (Boc – C(CH₃)₃), 64.2 (CHS), 58.8 (NCHCO₂Me), 53.1 (CO₂CH₃), 52.1 (C2 α – CH), 37.2 (SCH₂), 30.4 (C3 CH₂), 28.5 (Boc-C(CH₃)₃).

ESI HRMS *m/z* calcd for C₁₃H₂₀N₂O₅S + H⁺, 317.1171; found, 317.1176.

4.12: Bottom/Minor (7aR)-isomer

TLC R_f = 0.38 (EtOAc / Hexanes, 1:1)

$[\alpha]_D$ 45.6 (*c* 0.5, CH₂Cl₂)

¹H NMR (300 MHz, CDCl₃, COSY) δ 5.18 – 5.24 (br m, 1H, Boc – NH), 4.99 (dd, *J* = 5.1 Hz, 9.6 Hz, 1H, CHS), 4.66 – 4.70 (m, 1H, C2 α CH), 4.35 (d, *J* = 10.2 Hz, 1H, NCHCO₂Me), 3.73 (s, 3H, CO₂CH₃), 3.59 – 3.73 (m, 1H, SCH₂), 3.30 – 3.35 (m, 1H, SCH₂), 3.00 – 3.04 (m, 1H, CH₂CHS), 2.00 – 2.11 (m, 1H, CH₂CHS), 1.38 (Boc – C(CH₃)₃).

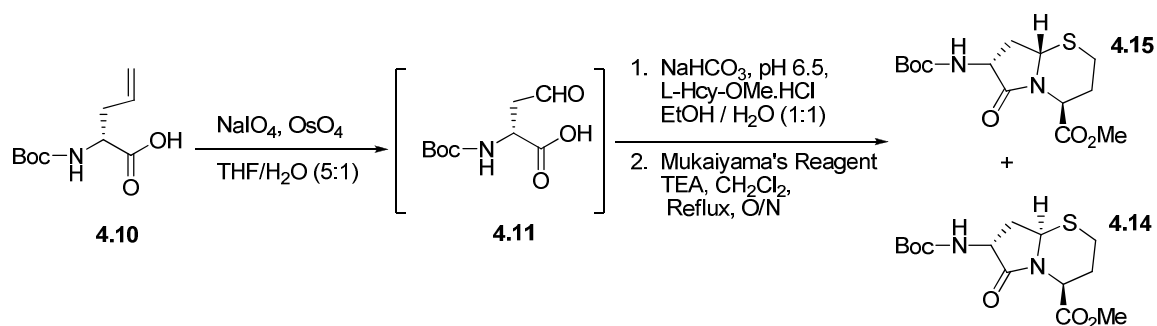
^{13}C NMR (75 MHz, CDCl_3 , HMQC) δ 174.2 (CO), 170.0 (CO), 154.2 (Boc – CO), 79.0 (Boc – $\text{C}(\text{CH}_3)_3$), 62.8 (CHS), 57.5 (NCHCO₂Me), 51.8 (CO₂CH₃), 50.6 (C2 α – CH), 35.9 (SCH₂), 28.9 (C3 CH₂), 27.2 (Boc-C(CH₃)₃).

ESI HRMS m/z calcd for $\text{C}_{13}\text{H}_{20}\text{N}_2\text{O}_5\text{S} + \text{Na}^+$, 339.0974; found, 339.0978.

**(4*S*, 7*R*, 8*aR*)-7-tert-Butoxycarbonylamino-6-oxo-hexahydro-pyrrolo[2,1-
b][1,3]thiazine-4-carboxylic Acid Methyl Ester (4.14)**

and

**(4*S*, 7*R*, 8*aS*)-7-tert-Butoxycarbonylamino-6-oxo-hexahydro-pyrrolo[2,1-
b][1,3]thiazine-4-carboxylic Acid Methyl Ester (4.15)**



Boc- D- α -allyl-Gly-OH (**4.10**, 1.3 g, 6.3 mmol) was dissolved in a 4:1 mixture of THF in H_2O . This solution was stirred under N_2 and it turned dark brown when OsO_4 was added as a 2.5% solution in *t*-BuOH (2.7 mL). After 5 minutes of stirring the solution, NaIO_4 (4.0 g) was added in three batches over a 90 minute period. At this point, the reaction turned light yellow and stirring was continued for 5 hours. Upon completion the reaction was filtered to remove the excess salts and concentrated under

reduced pressure. The resulting light yellow semi-solid / oil mixture was dissolved in EtOAc and filtered once more through Whatman filter paper and secondly through a 0.45 μm filter disk. The solvent was then concentrated under reduced pressure to yield the desired product (**4.11**).

TLC $R_f = 0.77$ (Propanol / NH_4OH , 4:1)

^{13}C NMR (75 MHz, CDCl_3) δ 174.8 (CO), 162.6 (CO), 156.0 (Boc-CO), 97.2 ($\text{CH}_2\text{C}(\text{OH})\text{O}$), 81.2 (Boc - $\text{C}(\text{CH}_3)_3$), 80.9 (Boc- $\text{C}(\text{CH}_3)_3$), 49.9 (α - C), 36.8 (α - C), 30.6 (CH_2CHO), 30.0 (CH_2CHO), 28.6 (Boc- $\text{C}(\text{CH}_3)_3$), 28.2 (Boc- $\text{C}(\text{CH}_3)_3$),

The resulting aldehyde (**4.11**, 1.9 g, 8.8 mmol) was dissolved in 200 mL of H_2O / EtOH (1:1) and the solution was cooled to 0 $^\circ\text{C}$ in an ice-salt bath. L-Hcy-OMe (1.63 g, 8.8 mmol) was then added to the cooled solution and the pH was adjusted with solid NaHCO_3 to 6.5 while the reaction stirred. While the reaction warmed to room temperature the solution was degassed with Ar for 20 minutes and allowed to stir overnight. After 18 hours the solvents were removed under reduced pressure and the residue was redissolved in H_2O (50 mL). The solution was extracted with EtOAc (100 mL). The pH of the aqueous layer was adjusted to 6.5 using 1N HCl, and then the aqueous layer was extracted with EtOAc (4 x 250 mL). To facilitate the partitioning of the layers, NaCl was added to the aqueous layer followed by extractions into Et_2O (2 x 250 mL). In between each extraction the aqueous layer was adjusted pH 6.5. The organic layers were combined and dried with MgSO_4 . Removal of the solvent under vacuum gave a light orange oil (2.2 g, 6.3 mmol) which was dried under hard vacuum

and then dissolved in dry CH_2Cl_2 (300 mL). To the solution 2-chloro-1-methylpyridinium iodide (1.94 g, 7.6 mmol) and NEt_3 (1.95 mL, 13.9 mmol) was added. The resulting solution was refluxed overnight. The reaction mixture was allowed to cool, and then was extracted with 1N HCl (200 mL), saturated NaHCO_3 (200 mL), and brine (200 mL). Drying with MgSO_4 and subsequent removal of the solvents under vacuum resulted in an orange oil. The mixture of products was separated by silica gel chromatography (EtOAc / Hexanes, 1:1) to yield 0.52 g (24.4 %) of the major product **4.15** and 0.23 g (10.7 %) of the minor spot **4.14**.

4.15: Top/Major (8aS)-isomer

TLC R_f = 0.34 (EtOAc / Hexanes, 1:2)

$[\alpha]_D$ 111.5 (c 1.4, CH_2Cl_2)

^1H NMR (300 MHz, CDCl_3 , COSY) δ 5.12 (br d, J = 6.6 Hz, 1H, CHS), 4.83 (d, J = 7.8 Hz, 1H, NCHCO₂Me), 4.31 – 4.33 (m, 1H, C2 α CH), 3.71 (s, 3H, CO₂CH₃), 3.68 – 3.74 (m, 1H, NH), 2.93 – 3.03 (m, 1H, SCH₂), 2.76 – 2.84 (m, 1H, SCH₂), 2.23 – 2.39 (m, 2H, CH₂CHS), 2.05 – 2.12 (m, 1H, SCH₂CH₂), 1.81 – 1.91 (m, 1H, SCH₂CH₂), 1.38 (Boc – C(CH₃)₃).

^{13}C NMR (75 MHz, CDCl_3 , HMQC) δ 171.7 (CO), 168.9 (CO), 155.8 (Boc – CO), 80.3 (Boc – C(CH₃)₃), 59.2 (CHS), 57.7 (NCHCO₂Me), 52.7 (CO₂CH₃), 51.6 (C2 α – CH), 33.9 (SCH₂), 28.5 (Boc-C(CH₃)₃), 28.1 (C3 CH₂), 26.1 (SCH₂CH₂).

ESI HRMS m/z calcd for $\text{C}_{14}\text{H}_{22}\text{N}_2\text{O}_5 + \text{Na}^+$, 353.1147; found, 353.1176.

4.14: Bottom/Minor (8aR)-isomerTLC $R_f = 0.13$ (EtOAc / Hexanes, 1:2) $[\alpha]_D^{25} 21.8$ (c 2.0, CH_2Cl_2)

^1H NMR (300 MHz, CDCl_3 , COSY) δ 5.05 (br s, 1H, Boc – NH), 4.75 (t, $J = 6.6$ Hz, 12.6 Hz, 1H, CH_2CHS), 4.32 – 4.34 (br m, 1H, NCHCO_2Me), 3.93 – 3.97 (m, 1H, $\text{C2 } \alpha$ CH), 3.71 (CO_2CH_3), 2.72 – 2.97 (m, 3H, SCH_2 , SCH_2CH_2), 2.11 – 2.22 (m, 2H, SCH_2CH_2 , C3 CH_2), 1.71 – 1.75 (m, 1H, C3 CH_2), 1.41 (s, 9H, Boc – $\text{C}(\text{CH}_3)_3$).

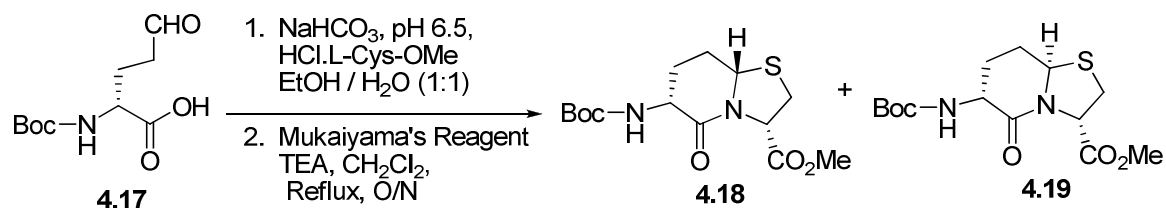
^{13}C NMR (75 MHz, CDCl_3) δ 171.7 (CO), 169.6 (CO), 155.9 (Boc – CO), 80.4 (Boc – $\text{C}(\text{CH}_3)_3$), 56.6 (CHS), 55.7 (NCHCO_2Me), 52.9 (CO_2CH_3), 50.8 ($\text{C2 } \alpha$ CH), 35.0 (SCH_2), 28.5 (Boc – $\text{C}(\text{CH}_3)_3$), 26.2 (SCH_2CH_2), 26.1 (CH_2CHS).

ESI HRMS m/z calcd for $\text{C}_{14}\text{H}_{22}\text{N}_2\text{O}_5 + \text{Na}^+$, 353.1147; found, 353.1157

(3S,6R,8aS)-6-tert-Butoxycarbonylamino-5-oxo-hexahydro-thiazolo[3,2-a]pyridine-3-carboxylic Acid Methyl Ester (4.18)

and

(3S,6R,8aR)-6-tert-Butoxycarbonylamino-5-oxo-hexahydro-thiazolo[3,2-a]pyridine-3-carboxylic Acid Methyl Ester (4.19)



The butenyl aldehyde (**4.17**, 0.48 g, 2.1 mmol) was dissolved in 50 mL of H_2O / EtOH (1:1) and the solution was cooled to 0°C in an ice-salt bath. $\text{HCl}\cdot\text{NH}_2\text{-L-Cys-OMe}$

(0.36 g, 2.1 mmol) was then added to the cooled solution and the pH was adjusted with solid NaHCO₃ to 6.5 while the reaction stirred. While the reaction warmed to room temperature the solution was degassed with Ar for 20 minutes and allowed to stir overnight. After 18 hours the solvents were removed under reduced pressure and the residue was redissolved in H₂O. The solution was extracted with EtOAc. The pH of the aqueous layer was adjusted to 6.5 using 1N HCl, and then the aqueous layer was extracted with EtOAc. To facilitate the partitioning of the layers, NaCl was added to the aqueous layer followed by extractions into Et₂O. This process was repeated 5-6 times with adjustment of the pH to 6.5 between extractions. The organic layers were combined and dried with MgSO₄. Removal of the solvent under vacuum gave a light orange oil (0.36 g, 1.0 mmol) which was dried under hard vacuum and then dissolved in dry CH₂Cl₂. To the solution 2-chloro-1-methylpyridinium iodide (0.32 g, 1.24 mmol) and NEt₃ (0.32 mL, 2.3 mmol) was added. The resulting solution was refluxed overnight. The reaction mixture was allowed to cool, and then was extracted with 1N HCl, saturated NaHCO₃, and brine. Drying with MgSO₄ and subsequent removal of the solvents under vacuum resulted in an orange oil. The mixture of products was separated by silica gel chromatography (EtOAc / Hexanes, 1:1) to yield the final products in 0.08 g (23%) of the major product **4.18** and 0.04 g (11%) of the minor product **4.19**.

4.18: Top/ Major (8a*S*)-isomer

TLC R_f = 0.52 (EtOAc / Hexanes, 1:1)

[α]_D 25.7 (c 0.4, CH₂Cl₂)

^1H NMR (300 MHz, CDCl_3 , COSY) δ 5.42 (br s, 1H, NH), 5.28 – 5.32 (m, 1H, CHS), 4.88 (br t, $J = 5.1$ Hz, 10.5 Hz, 1H, NCHCO₂Me), 4.12 – 4.17 (m, 1H, C2 α CH), 3.71 (s, 3H, CO₂CH₃), 3.12 – 3.32 (m, 2H, SCH₂), 1.71 – 2.40 (m, 4H, C3 CH₂, C4 CH₂), 1.38 (Boc – C(CH₃)₃).

^{13}C NMR (75 MHz, CDCl_3 , HMQC) δ 168.9 (CON), 167.4 (CO₂Me), 154.3 (Boc – CO), 78.7 (Boc – C(CH₃)₃), 59.5 (C2 α C), 52.4 (CO₂CH₃), 51.8 (C5-CH), 49.6 (NCHCO₂Me), 31.2 (SCH₂), 30.7 (C3 CH₂), 27.3 (Boc – C(CH₃)₃), 25.2 (C4 CH₂).

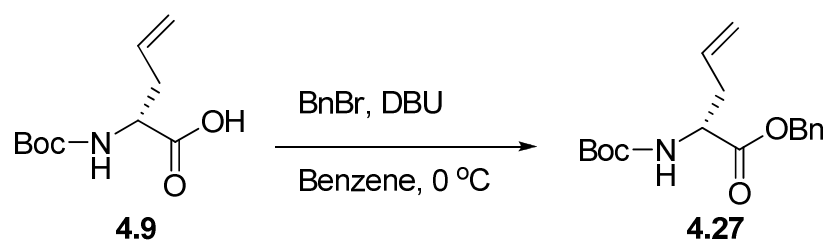
ESI HRMS m/z calcd for C₁₄H₂₂N₂O₅S⁺ Na⁺, 353.1147; found, 353.1125.

4.19: Bottom/Minor (8aR)-isomer:

TLC R_f = 0.36 (EtOAc / Hexanes, 1:1)

No further data is present due to the drop of the NMR tube containing the only 40 mg of sample. The compound was not remade due to a parallel synthesis which provided a better method.

2-tert-Butoxycarbonylamino-pent-4-enoic Acid Benzyl Ester (4.27)



To a solution of 2-*tert*-butoxycarbonylamino-pent-4-enoic acid (**4.9**, 0.4 g, 1.8 mmol) in benzene (10 mL) at 0 °C was added 1,8-diazabicyclo[5.4.0]undec-7-ene (0.27 mL, 1.8 mmol), followed by the dropwise addition of benzyl bromide (0.23 mL, 1.93 mmol). A white precipitant formed after 5 minutes. The mixture was refluxed overnight after which time the reaction mixture was cooled to room temperature and filtered to

removed the DBU•HBr salt. The salt was washed with benzene (50 mL) and ethyl acetate (50 mL) and the combined filtrates were washed with 1M HCl (50 mL), sat. NaHCO₃ (50 mL), and brine (50 mL). The organic layer was dried over MgSO₄ and it was concentrated to give 2-*tert*-butoxycarbonylamino-pent-4-enoic acid benzyl ester (**4.27**) as a light brown oil. The oil was purified through flash chromatography using a 6 cm x 3 cm silica gel plug with EtOAc / hexanes (20:1) as the eluting solvent. The pure final product, 0.52 g, was obtained as a clear oil in 98% yield.

TLC R_f = 0.41 (EtOAc / Hexanes, 1:20)

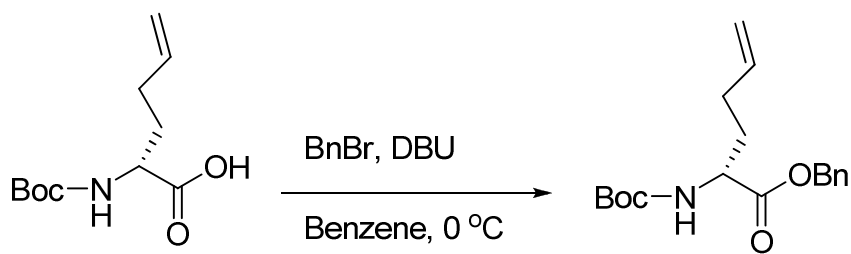
[α]_D 32.6 (*c* 0.05, CH₂Cl₂)

¹H NMR (300 MHz, CDCl₃, COSY) δ 7.26 (s, 5H, C₆H₅), 5.50 – 5.61 (m, 1H, CH₂CHCH₂), 4.96 – 5.14 (m, 5H, CH₂C₆H₅, CH₂CHCH₂, NH), 4.30 – 4.37 (m, 1H, α-CH), 2.36 – 2.47 (m, 2H, CH₂CHCH₂), 1.35 (Boc C(CH₃)₃)

¹³C NMR (75 MHz, CDCl₃, HMQC) δ 172.0 (COBn), 155.3 (Boc CO), 135.5 (C₆H₅), 132.4 (CH₂CHCH₂), 128.8 (C₆H₅), 128.6 (C₆H₅), 128.5 (C₆H₅), 119.4 (CH₂CHCH₂), 80.1 (Boc C(CH₃)₃), 67.3 (CH₂C₆H₅), 53.3 (α-C), 37.0 (CH₂CHCH₂), 28.7 (Boc C(CH₃)₃)

ESI HRMS *m/z* calcd for C₁₇H₂₃NO₄+ Na⁺, 328.1525; found, 328.1528.

2-*tert*-Butoxycarbonylamino-hex-5-enoic Acid Benzyl Ester



To a solution of (*R*)-2-(*tert*-butoxycarbonylamino)hex-5-enoic acid (0.4 g, 1.8 mmol) in benzene (10 mL) at 0 °C was added 1,8-diazabicyclo[5.4.0]undec-7-ene (0.27 mL, 1.8 mmol), followed by the dropwise addition of benzyl bromide (0.23 mL, 1.93 mmol). A white precipitant formed after 5 minutes. The mixture was refluxed overnight after which time the reaction mixture was cooled to room temperature and filtered to removed the DBU•HBr salt. The salt was washed with benzene (50 mL) and ethyl acetate (50 mL) and the combined filtrates were washed with 1M HCl (50 mL), sat. NaHCO₃ (50 mL), and brine (50 mL). The organic layer was dried over MgSO₄ and it was concentrated to give 2-*tert*-butoxycarbonylamino-pent-4-enoic acid benzyl ester as a light brown oil. The oil was purified through flash chromatography using a 6 cm x 3 cm silica gel plug with EtOAc / hexanes (20:1) as the eluting solvent. The pure final product, 0.52 g, was obtained as a clear oil in 98% yield.

TLC R_f = 0.29 (EtOAc / Hexanes, 1:9)

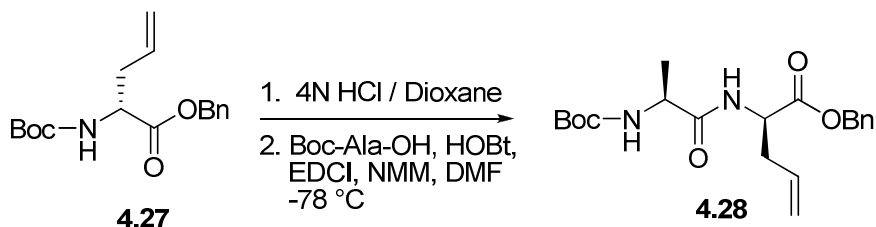
[α]_D -3.42 (*c* 0.7, CH₂Cl₂)

¹H NMR (300 MHz, CDCl₃, COSY) δ 7.22 (s, 5H, C₆H₅), 5.70 – 5.57 (m, 1H, CH₂CHCH₂), 4.84 – 5.20 (m, 5H, CH₂C₆H₅, CH₂CHCH₂, NH), 4.23 – 4.27 (m, 1H, α – CH), 1.94 – 1.98 (m, 2H, CH₂CHCH₂), 1.77 – 1.83 (m, 1H, CH₂CH₂CHCH₂), 1.58 – 1.67 (m, 1H, CH₂CH₂CHCH₂), 1.33 (s, 9H, Boc C(CH₃)₃).

¹³C NMR (75 MHz, CDCl₃, HMQC) δ 172.7 (COBn), 155.5 (Boc CO), 137.1 (C₆H₅), 135.6 (CH₂CHCH₂), 128.7 (C₆H₅), 128.5 (C₆H₅), 128.4 (C₆H₅), 115.9 (CH₂CHCH₂), 79.9 (Boc C(CH₃)₃), 67.2 (CH₂C₆H₅), 53.4 (α – C), 32.1 (CH₂CHCH₂), 29.8 (CH₂CH₂CHCH₂), 28.7 (Boc C(CH₃)₃).

ESI HRMS m/z calcd for $C_{18}H_{25}NO_4 + Na^+$, 342.1681; found, 342.1705.

(R)-Benzyl 2-((S)-2-(tert-Butoxycarbonylamino)propanamido)pent-4-enoate (4.28)



Boc- α -allyl-Gly-OBn (**4.27**, 0.3 g, 1.2 mmol) was dissolved in 1 mL of 4N HCl / dioxane and the solution was stirred under nitrogen for 24 hours while it was monitored by TLC. Upon completion the reaction was concentrated under reduced pressure. The residue was dissolved in CH_2Cl_2 and evaporated three times to azeotropically remove any last traces of dioxane. The orange compound was then allowed to dry under vacuum for 24 – 48 hours. The light yellow solid was then used in the subsequent coupling reaction without further purification.

α -Allyl-Gly-OBn \cdot HCl (1.2 mmol) and Boc-alanine (0.2 g, 1.1 mmol) were dissolved in DMF which had been dried over 5 Å molecular sieves. While this solution was stirred HOBT (0.2 g, 1.4 mmol) was added and the solution was cooled to -78 °C. EDC \cdot HCl (0.26 g, 1.4 mmol) and NMM (0.35 mL, 2.5 mmol) were added consecutively to the cooled solution, which then was allowed to warm slowly to room temperature where upon it was stirred for 3 days. On the third day, the reaction mixture was concentrated *in vacuo* to give an orange residue to which a small portion of xylenes was added to azeotropically remove the traces of DMF. The orange residue was then partitioned between H_2O (100 mL) and EtOAc (100 mL). The organic layer was washed

consecutively with 0.5 M HCl (100 mL), 1 M NaHCO₃ (100 mL) and brine (100 mL), dried with MgSO₄ and concentrated under reduced pressure to yield 0.96 g of crude product. The crude Boc-Ala- α -allyl-Gly-Bn (**4.28**) was purified by silica gel chromatography (5 x 15 cm) by elution with ethyl acetate in hexanes (1:2) to yield 0.38 g. (83%) of pure product as a clear colorless oil.

TLC R_f = 0.46 (EtOAc / Hexanes, 1:2)

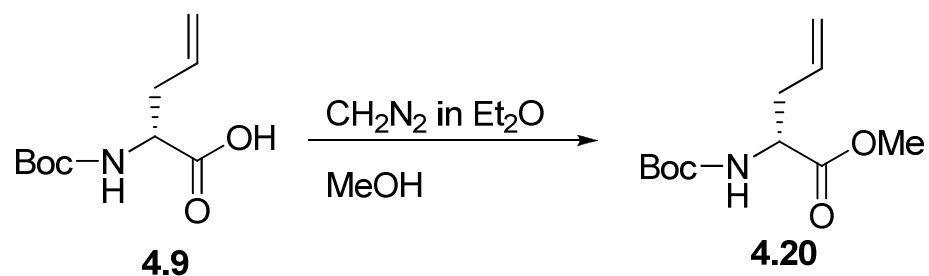
[α]_D – 19.3 (*c* 1.6, CH₂Cl₂)

¹H NMR (300 MHz, CDCl₃, COSY) δ 7.32 (s, 5H, C₆H₅), 6.60 – 6.61 (m, 1H, CH₂C₆H₅), 5.48 – 5.59 (m, 1H, Boc-NH), 4.93 – 5.15 (m, 5H, CH₂C₆H₅, CHCH₂, CONH), 4.62 (dd, 1H, Ala α -CH), 4.11 – 4.13 (m, 1H, Gly α -CH), 2.39 – 2.55 (m, 2H, CH₂CHCH₂), 1.37 (s, 9H, Boc CH₃), 1.27 (d, *J* = 6.9 Hz, 3H, Ala CH₃).

¹³C NMR (75 MHz, CDCl₃) δ 172.4 (CO₂CH₂Bn), 171.4 (Ala CO), 155.5 (Boc CO), 141.8 (C₆H₅), 135.4 (C₆H₅), 132.0 (CHCH₂), 128.8 (C₆H₅), 128.7 (C₆H₅), 128.5 (C₆H₅), 119.7 (CHCH₂), 80.5 (Boc C(CH₃)₃), 67.5 (CH₂C₆H₅), 51.8 (Ala α -C), 50.8 (Gly α -C), 36.7 (CH₂CHCH₂), 28.7 (Boc C(CH₃)₃).

ESI HRMS *m/z* calcd for C₂₀H₂₈N₂O₅ + Na⁺, 399.1896; found, 399.1898.

Boc- α -Allyl-Gly-OMe (**4.20**)



Boc- α -Allyl-Gly-OH (**4.9**, 0.34 g, 1.6 mmol) was dissolved in MeOH (20 mL) and the solution was cooled to 4°C. To this clear solution was added CH₂N₂ in Et₂O until bubbling ceased and the solution maintained a bright yellow color. The reaction was then evaporated under reduced pressure to yield a clear yellow oil. This residue was then purified by column chromatography (3 x 8cm) eluting with ethyl acetate in hexanes (1:3) to yield 0.35 g, 97%, of the pure product **4.20** as a clear oil.

TLC R_f = 0.72 (EtOAc / Hexanes, 1:3)

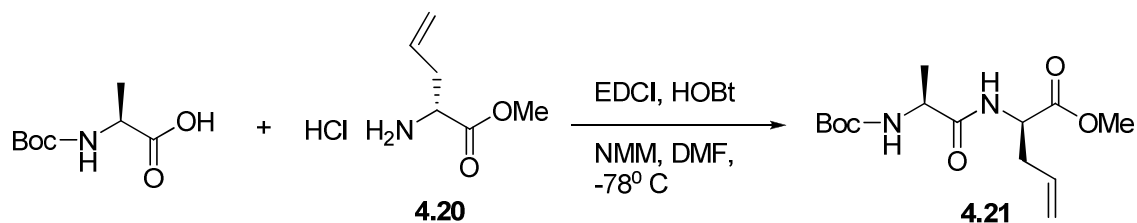
[α]_D – 8.7 (*c* 0.8, CH₂Cl₂)

¹H NMR (300 MHz, CDCl₃, COSY) δ 5.58 – 5.67 (m, 1H, CHCH₂), 5.03 – 5.08 (m, 3H, NH, CHCH₂), 4.29 – 4.32 (m, 1H, α – CH), 3.66 (s, 3H, CO₂CH₃), 2.38 – 2.48 (m, 2H, CH₂CHCH₂), 1.37 (s, 9H, Boc – C(CH₃)₃).

¹³C NMR (75 MHz, CDCl₃) δ 172.5 (CO), 155.2 (Boc – CO), 132.4 (CHCH₂), 119.1 (CHCH₂), 80.0 (Boc C(CH₃)₃), 53.1 (α – CH), 52.4 (CO₂CH₃), 37.0 (CH₂CHCH₂), 28.5 (Boc – C(CH₃)₃).

ESI HRMS *m/z* calcd for C₁₁H₁₉NO₄ + Na⁺, 252.1212; found, 252.1210.

Boc-L-Ala-(R)- α -allyl-Gly-OMe (**4.21**).



Boc-alanine (0.52 g, 2.74 mmol) and 2-amino-pent-4-enoic acid methyl ester•HCl (**4.20**, 0.5 g, 3 mmol) were dissolved in DMF which had been dried over 5Å

molecular sieves. While this solution was stirred, HOBt (0.45 g, 3.3 mmol) was added and the solution was cooled to -78°C . EDC \cdot HCl (0.64 g, 3.3 mmol) and NMM (847 μL , 6 mmol) were added consecutively to the cooled solution, which then was allowed to warm slowly to room temperature where upon it was stirred overnight. Upon completion the reaction mixture was concentrated *in vacuo* to give an orange residue to which a small portion of xylenes was added to remove the remaining traces of DMF. The orange residue was then partitioned between H_2O (50 mL) and EtOAc (50 mL). The organic layer was washed consecutively with 1.0 M HCl (50 mL), 1M NaHCO_3 (50 mL) and brine (50 mL), dried with MgSO_4 and concentrated under reduced pressure to yield 0.8 grams of crude product. The crude Boc-L-Ala-(R)- α -allyl-Gly-OMe was purified by silica gel chromatography (3 x 5cm) and eluted with ethyl acetate in hexanes (1:1) to yield 0.7 g (82 %) of pure **4.21** as a clear colorless oil.

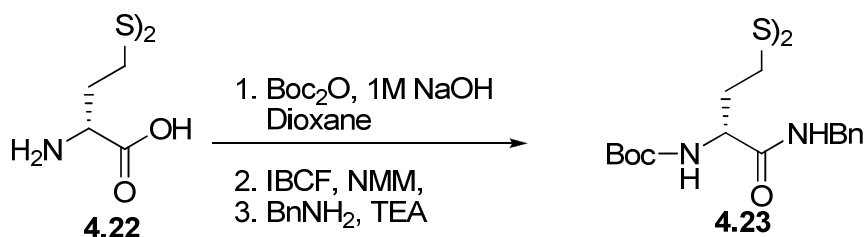
TLC R_f = 0.52 (EtOAc / Hexanes, 1:1)

$[\alpha]_D - 43.5$ (*c* 5.7, CH_2Cl_2)

^1H NMR (300 MHz, CDCl_3 , COSY) δ 6.97 (d, J = 6 Hz, 1H, Allyl – Gly NH), 5.53 – 5.67 (m, 1H, CH_2CHCH_2), 5.35 (d, J = 7.2 Hz, 1H, Ala NH), 5.00 – 5.06 (CH_2CHCH_2), 4.54 – 4.60 (m, 1H, Ala α – CH), 4.15 – 4.19 (m, 1H, Allyl – Gly α – CH), 3.64 (s, 3H, CO_2CH_3), 2.38 – 2.53 (m, 2H, CH_2CHCH_2), 1.35 (s, 9H, Boc $\text{C}(\text{CH}_3)_3$), 1.27 (d, J = 7.2 Hz, 3H, Ala CH_3).

^{13}C NMR (75 MHz, CDCl_3) δ 172.7 (COCH_3), 172.0 (Ala CO), 155.5 (Boc CO), 132.3 (CH_2CHCH_2), 119.3 (CH_2CHCH_2), 80.0 (Boc $\text{C}(\text{CH}_3)_3$), 52.6 (CO_2CH_3), 51.8 (Ala α – C), 50.2 (Allyl – Gly α – C), 36.6 (CH_2CHCH_2), 28.6 (Boc $\text{C}(\text{CH}_3)_3$), 18.8 (Ala CH_3).

HRMS (FAB) m/z calcd for $\text{C}_{14}\text{H}_{24}\text{N}_2\text{O}_5 + \text{Na}^+$, 323.1583; found, 323.1576.

Boc-Homocystine-NHBn (4.23)

To a solution of homocystine (**4.22**, 1.0 g, 3.72 mmol) in aq. NaOH (1M, 8 mL), was added di-*tert*-butyldicarbonate (3.27 g, 15 mmol) in dioxane (4 mL) at 0 °C. The reaction mixture was allowed to gradually warm to room temperature where it was stirred for 2 days. Solvents were evaporated *in vacuo* and the mixture was then diluted with H₂O and extracted with EtOAc (50 mL). The combined aq. phases were acidified (pH 1) with aq HCl (1M) and extracted with EtOAc (3 x 50 mL). The combined organic layers were washed with brine, dried with MgSO₄, filtered and concentrated under reduced pressure to afford the protected homocystine, 1.1 g, 66%.

To a chilled solution of Boc-homocystine-OH in THF, NMM and isobutylchloroformate were added. After stirring for 10 minutes a pre-cooled solution of HCl·NH₂Bn and triethylamine in THF was added. The reaction mixture was stirred at 0°C for 2 hours and then overnight at room temperature. The solvent was evaporated *in vacuo* and the oil residue was dissolved in ethyl acetate and was washed successively

with 1M HCl, saturated NaHCO₃, brine and dried with MgSO₄, then evaporated under reduced pressure. The final product was purified by silica gel flash chromatography with EtOAc / hexanes (1:1) as the eluting solvent to yield 0.54 g (96%) of **4.23** as white solid.

TLC R_f = 0.61 (EtOAc / hexanes, 1:1)

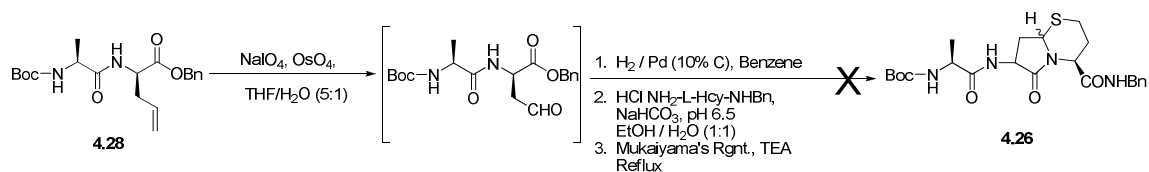
[α]_D – 13.5 (c 0.05, CH₂Cl₂)

¹H NMR (300 MHz, CDCl₃, COSY) δ 7.27 (s, 10H, (C₆H₅)₂), 4.16 – 4.45 (m, 6H, CH₂C₆H₅, α – CH), 2.68 – 2.73 (m, 4H, CH₂CH₂S), 2.13 – 2.17 (m, 2H, CH₂CH₂S), 1.93 – 2.02 (m, 2H, CH₂CH₂S), 1.44 (Boc C(CH₃)₃)

¹³C NMR (75 MHz, CDCl₃) δ 171.5 (CO), 155.8 (Boc CO), 138.2 (C₆H₅), 128.8 (C₆H₅), 127.7 (C₆H₅), 127.5 (C₆H₅), 80.4 (Boc C(CH₃)₃), 67.4 and 68.3 (CH₂C₆H₅), 43.7 (α – C), 32.7 and 34.9 (CH₂CH₂S), 28.6 (Boc C(CH₃)₃), 21.4 and 26.0 (CH₂CH₂S).

HRMS (FAB) *m/z* calcd for C₃₂H₄₆N₄O₆ + Na⁺, 669.2756; found, 669.2770.

(4*S*,7*R*,8*aR*)-7-(2-(*S*)-*tert*-Butoxycarbonylamino-propanoyl)-6-oxohexahydro-2*H*-pyrrolo[2,1-*b*][1,3]thiazine-4-*N*-benzyl-carboxamide (4.26**).**



Boc-Ala-D-allyl-Gly-OBn (**4.28**, 0.12 g, 0.3 mmol) was dissolved in a 4:1 mixture of THF in H₂O. This solution was stirred under N₂ and it turned dark brown when OsO₄ was added as a 2.5% solution in *t*-BuOH (0.24 mL). After 5 minutes of

stirring the solution NaIO₄ (0.36 g) was added in three batches over a 90 minute period. At this point, the reaction turned light yellow and stirring was continued for 5 hours. Upon completion the reaction was filtered to remove the excess salts and concentrated under reduced pressure. The reaction was then diluted with Et₂O until the layers separated and the aqueous phase was extracted three times with successive Et₂O washes (100 mL). The Et₂O layers were combined, washed with H₂O (150 mL), saturated Na₂SO₃ (150 mL) and dried with MgSO₄. Removal of the solvent *in vacuo* gave a tan oil. The oil was purified by silica gel flash chromatography (5 x 8 cm) and eluted with ethyl acetate in hexanes (1:1). The isolated clear oil yielded 0.1 g (94%) of the pure aldehyde.

TLC R_f = 0.45 (EtOAc / Hexanes, 1:1)

¹H NMR (300 MHz, CDCl₃, COSY) δ 9.60 (CHO), 7.20 – 7.32 (m, 5H, C₆H₅), 7.09 – 7.11 (br m, 1H, Boc – NH), 5.09 (s, 2H, CH₂C₆H₅), 4.96 – 5.09 (m, 1H, Gly – NH), 4.10 (br s, 1H, Ala α-CH), 2.93 – 3.11 (m, 2H, CH₂CHO), 1.36 (Boc – C(CH₃)₃), 1.24 (d, J = 7.5 Hz, 3H, Ala – CH₃).

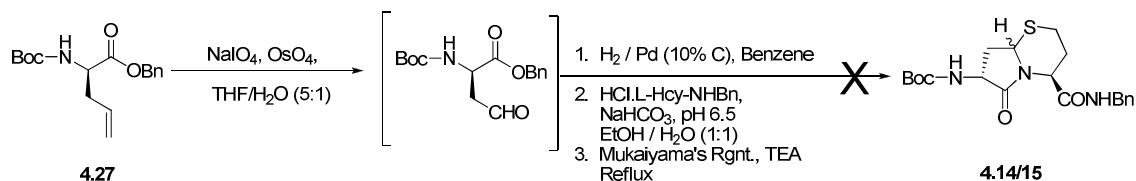
¹³C NMR (75 MHz, CDCl₃, HMQC) δ 199.2 (CHO), 172.8 (CO₂CH₂C₆H₅), 170.5 (Ala CO), 155.5 (Boc-CO), 135.2 (C₆H₅), 128.8 (C₆H₅), 128.7 (C₆H₅), 128.5 (C₆H₅), 128.4 (C₆H₅), 80.6 (Boc-C(CH₃)₃), 68.0 (CH₂C₆H₅), 50.6 (Ala α-CH), 47.7 (Gly α-CH), 45.7 (CH₂CHO), 28.6 (Boc-C(CH₃)₃), 18.6 (Ala CH₃).

The compound was dissolved in benzene in an Ar-purged pressure bottle. To that solution 10% Pd/C catalyst (10 mol %) was added, and the mixture was placed on a Parr shaker under 35 psi of H₂ for 18 hours. The mixture was gravity filtered, and the filtrate

was passed through a 0.45 μm filter disk. Concentration of the resulting clear solution resulted in a white foam which was taken forward without further purification.

The resulting aldehyde (0.1 g, 0.35 mmol) was dissolved in 100 mL of H_2O / EtOH (1:1) and the solution was cooled to 0 $^\circ\text{C}$ in an ice-salt bath. L-Hcy-NHBn (**4.25**, 0.62 g, 0.35 mmol) was then added to the cooled solution and the pH was adjusted with solid NaHCO_3 to 6.5 while the reaction stirred. While the reaction warmed to room temperature the solution was degassed with Ar for 20 minutes and allowed to stir overnight. After 18 hours the solvents were removed under reduced pressure and the residue was redissolved in H_2O . The solution was extracted with EtOAc. The pH of the aqueous layer was adjusted to 6.5 using 1N HCl, and then the aqueous layer was extracted with EtOAc. To facilitate the partitioning of the layers, NaCl was added to the aqueous layer followed by extractions into Et_2O . This process was repeated 5-6 times with adjustment of the pH to 6.5 between extractions. The organic layers were combined and dried with MgSO_4 . Removal of the solvent under vacuum gave a light orange oil which was dried under a high vacuum and then dissolved in dry CH_2Cl_2 . To the dichloromethane solution 2-chloro-1-methylpyridinium iodide (90 mg, 0.35 mmol) and NEt_3 (0.1 mL, 0.7 mmol) were added. The resulting solution was refluxed overnight. The reaction mixture was allowed to cool, and then was extracted with 1N HCl, saturated NaHCO_3 , and brine. Drying with MgSO_4 and subsequent removal of the solvents under vacuum resulted in a orange oil. The mixture of products was separated by silica gel chromatography (EtOAc / hexanes, 1:1). The resulting fractions did not yield the desired product after extensive concentration and analysis with ESI HR-MS.

**(4*S*, 7*R*, 8*aR*)-7-tert-Butoxycarbonylamino-6-oxo-hexahydro-pyrrolo[2,1-
b][1,3]thiazine-4-*N*-benzyl-carboxamide (4.30)**



Boc- D-allyl-Gly-OBn (**4.27**, 0.3 g, 1.0 mmol) was dissolved in a 4:1 mixture of THF in H₂O. This solution was stirred under N₂ and it turned dark brown when OsO₄ was added as a 2.5% solution in t-BuOH (0.6 mL). After 5 minutes of stirring the solution, NaIO₄ (0.9 g, 4.2 mmol) was added in three batches over a 90 minute period. At this point, the reaction turned light yellow and stirring was continued for 5 hours. Upon completion, the reaction was filtered to remove the excess salts and concentrated under reduced pressure. The reaction was then diluted with Et₂O until the layers separated and the aqueous phase was extracted three times with successive Et₂O washes (100 mL). The Et₂O layers were combined, washed with H₂O (150 mL), saturated Na₂SO₃ (150 mL) and dried with MgSO₄. Removal of the solvent *in vacuo* gave a tan oil. The oil was purified by silica gel flash chromatography (5 x 8 cm) and eluted with ethyl acetate in hexanes (1:1). The isolated clear oil yielded 0.27 g (93%) of the pure aldehyde.

TLC R_f = 0.23 (EtOAc / Hexanes, 1:3)

^1H NMR (300 MHz, CDCl_3 , COSY) δ 9.63 (s, 1H, CHO), 7.19 – 7.33 (m, 5H, C_6H_5), 5.36 (br d, $J = 9$ Hz, 1H, NH), 5.10 (s, 2H, $\text{CH}_2\text{C}_6\text{H}_5$), 4.55 – 4.57 (m, 1H, α – CH), 2.92 – 3.02 (m, 2H, CH_2CHO), 1.35 (s, 9H, Boc-C(CH_3) $_3$).

^{13}C NMR (75 MHz, CDCl_3 , HMQC) δ 199.5 (CHO), 171.0 ($\text{CO}_2\text{C}_6\text{H}_5$), 155.5 (Boc – CO), 135.3 (C_6H_5), 128.8 (C_6H_5), 128.7 (C_6H_5), 128.5 (C_6H_5), 80.6 (Boc-C(CH_3) $_3$), 67.9 ($\text{CH}_2\text{C}_6\text{H}_5$), 49.1 (α C), 46.3 (CH_2CHO), 28.6 (Boc – C(CH_3) $_3$).

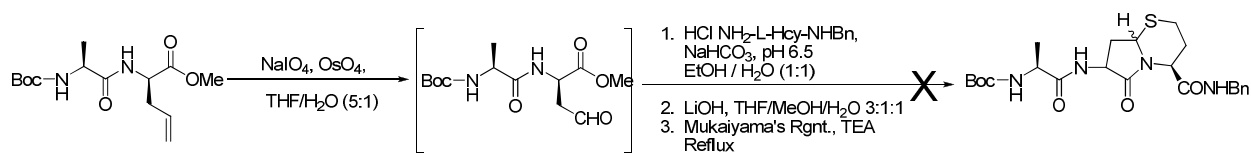
ESI HRMS m/z calcd for $\text{C}_{16}\text{H}_{25}\text{NO}_5 + \text{Na}^+$, 308.1498; found, 308.1525.

The aldehyde was dissolved in benzene in an Ar-purged pressure bottle. To that solution 10% Pd/C catalyst was added, and the mixture was placed on a Parr shaker under 35 psi of H_2 for 18 hours. The mixture was gravity filtered, and the filtrate was passed through a 0.45 μm filter disk. Concentration of the resulting clear solution resulted in a white foam which was taken forward without further purification.

The resulting aldehyde (0.1 g, 0.35 mmol) was dissolved in 100 mL of H_2O / EtOH (1:1) and the solution was cooled to 0 $^\circ\text{C}$ in an ice-salt bath. L-Hcy-NHBn (0.62 g, 0.35 mmol) was then added to the cooled solution and the pH was adjusted with solid NaHCO_3 to 6.5 while the reaction was stirred overnight. After 18 hours, the solvent was removed under reduced pressure and the residue obtained was redissolved in H_2O . The solution was extracted with EtOAc. The pH of the aqueous layer was adjusted to 6.5 using 1N HCl, and then the aqueous layer was extracted with EtOAc. To facilitate the partitioning of the layers, NaCl was added to the aqueous layer followed by extractions into Et_2O . This process was repeated 5-6 times with adjustment of the pH to 6.5 between extraction. The organic layers were combined and dried with MgSO_4 . Removal of the

solvent under vacuum gave a light orange oil which was dried under hard vacuum and then dissolved in dry CH_2Cl_2 . To the dichloromethane solution 2-chloro-1-methylpyridinium iodide (90 mg, 0.35 mmol) and NEt_3 (0.1 mL, 0.7 mmol) were added. The resulting solution was refluxed overnight. The reaction mixture was allowed to cool, and then was extracted with 1N HCl, saturated NaHCO_3 , and brine. Drying with MgSO_4 and subsequent removal of the solvents under vacuum resulted in a orange oil. The mixture of products was separated by silica gel chromatography (EtOAc / hexanes, 1:1). The resulting fractions did not yield the desired product after extensive concentration and analysis with ESI HR-MS.

(4*S*,7*R*,8*aR*)-7-(2-(*S*)-*tert*-Butoxycarbonylamino-propanoyl)-6-oxohexahydro-2*H*-pyrrolo[2,1-*b*][1,3]thiazine-4-benzyl-carboxamide (4.26).



Boc-Ala-D- α -allyl-Gly-OMe (0.5 g, 1.7 mmol) was dissolved in a 4:1 mixture of THF in H_2O . This solution was stirred under N_2 and it turned dark brown when OsO_4 was added as a 2.5% solution in *t*-BuOH (1.0 mL). After 5 minutes of stirring the solution, NaIO_4 (1.5 g) was added in three batches over a 90 minute period. At this point, the reaction turned light yellow and stirring was continued for 5 hours. The

reaction was then diluted with Et₂O, until the layers separated, and the aqueous phase was extracted three times with successive Et₂O washes (100 mL). The Et₂O layers were combined, washed with H₂O (150 mL), saturated Na₂SO₃ (150 mL) and dried with MgSO₄. Removal of the solvent *in vacuo* gave a tan oil. The oil was purified by silica gel flash chromatography (5 x 8 cm) and eluted with ethyl acetate in hexanes (1:1). The isolated clear oil yielded 0.47 g (93%) of the pure aldehyde.

TLC R_f = 0.20 (EtOAc / Hexanes, 1:1)

¹H NMR (300 MHz, CDCl₃, COSY) δ 9.66 (s, 1H, CHO), 7.21 – 7.26 (br d, 1H, NH), 5.27 (br s, 1H, Gly – NH), 4.80 – 4.86 (m, 1H, Gly α-CH), 4.13 – 4.31 (m, 1H, Ala α-CH), 3.70 (s, 3H, CO₂CH₃), 2.97 – 3.14 (m, 2H, CH₂CHO), 1.40 (Boc-C(CH₃)₃), 1.21 (d, *J* = 7.2 Hz, 3H, Ala-CH₃).

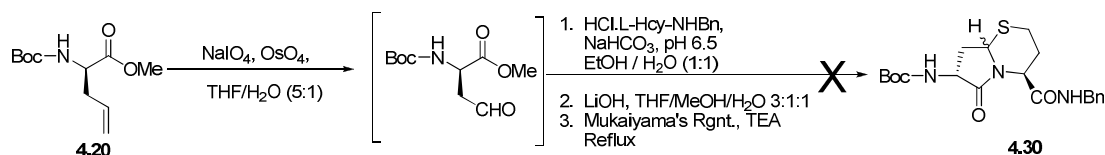
¹³C NMR (75 MHz, CDCl₃) δ 199.3 (CHO), 172.9 (Gly – CO), 171.2 (Ala – CO), 155.6 (Boc – CO), 80.5 (Boc-C(CH₃)₃), 53.1 (CO₂CH₃), 50.4 (Gly α-CH), 47.4 (Ala α-CH), 45.7 (CH₂CHO), 28.6 (Boc – C(CH₃)₃), 18.5 (Ala – CH₃).

The resulting aldehyde (0.1 g, 0.35 mmol) was dissolved in 100 mL of H₂O / EtOH (1:1) and the solution was cooled to 0 °C in an ice-salt bath. L-Hcy-NHBn (**4.25**, 0.62 g, 0.35 mmol) was then added to the cooled solution and the pH was adjusted with solid NaHCO₃ to 6.5 while the reaction stirred overnight. After 18 hours the solvents were removed under reduced pressure and the residue was redissolved in H₂O. The solution was extracted with EtOAc. The pH of the aqueous layer was adjusted to 6.5 using 1N HCl, and then the aqueous layer was extracted with EtOAc. To facilitate the

partitioning of the layers, NaCl was added to the aqueous layer followed by extraction into Et₂O. This process was repeated 5-6 times with adjustment of the pH to 6.5 between extractions. The organic layers were combined and dried with MgSO₄. Removal of the solvent under vacuum gave a light orange oil which was dried under a high vacuum.

The condensed product was dissolved in THF/MeOH/H₂O (3:1:1, 0.3 M total concentration). To the solution was added 14.4 mg of LiOH and it was then allowed to stir for 16 hours. Upon completion, the solvent was evaporated under reduced pressure to give a white solid. The solid was then resuspended in a 1:1 mixture of H₂O and EtOAc whereupon the two layers were separated. The aqueous layer was then acidified to pH 3 with 0.5 M HCl and extracted with EtOAc, dried with MgSO₄ and concentrated under reduced pressure. The free acid was then dissolved in freshly distilled CH₂Cl₂. To the dichloromethane solution 2-chloro-1-methylpyridinium iodide (90 mg, 0.35 mmol) and NEt₃ (0.1 mL, 0.7 mmol) were added. The resulting solution was refluxed overnight. The reaction mixture was allowed to cool, and then was extracted with 1N HCl, saturated NaHCO₃, and brine. Drying with MgSO₄ and subsequent removal of the solvents under vacuum resulted in an orange oil. The mixture of products was separated by silica gel chromatography (EtOAc / Hexanes, 1:1). The resulting fractions did not yield the desired product after extensive concentration and analysis with ESI HR-MS.

**(4*S*, 7*R*, 8*aR*)-7-tert-Butoxycarbonylamino-6-oxo-hexahydro-pyrrolo[2,1-
b][1,3]thiazine-4-*N*-benzyl-carboxamide (4.30)**



Boc-D- α -allyl-Gly-OMe (**4.20**, 0.24 g, 1.0 mmol) was dissolved in a 4:1 mixture of THF in H₂O. This solution was stirred under N₂ and it turned dark brown when OsO₄ was added as a 2.5% solution in t-BuOH (0.5 mL). After 5 minutes of stirring the solution, NaIO₄ (0.72 g) was added in three batches over a 90 minute period. At this point, the reaction turned light yellow and stirring of the reaction was continued for 5 hours. The reaction was then diluted with Et₂O until the layers separated. The aqueous phase was extracted three times with successive Et₂O washes (100 mL). The Et₂O layers were combined, washed with H₂O (150 mL), saturated Na₂SO₃ (150 mL) and dried with MgSO₄. Removal of the solvent *in vacuo* gave a tan oil. The oil was purified by silica gel flash chromatography (5 x 8 cm) with elution carried out with ethyl acetate in hexanes (3:1). The isolated clear oil yielded 0.21 g (88%) of the pure aldehyde.

TLC R_f = 0.28 (EtOAc / Hexanes, 1:3)

¹H NMR (300 MHz, CDCl₃, COSY) δ 9.67 (s, 1H, CHO), 5.35 (br d, *J* = 7.2 Hz, 1H, Boc – NH), 4.52 – 4.55 (m, 1H, α -CH), 3.69 (CO₂CH₃), 2.92 – 3.02 (m, 2H, CH₂CHO), 1.37 (Boc – C(CH₃)₃).

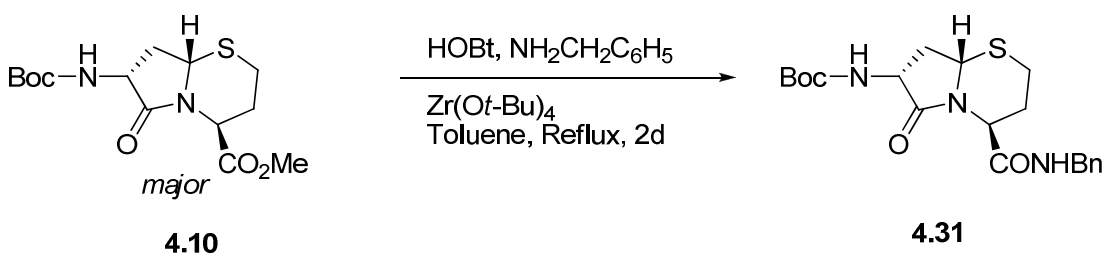
¹³C NMR (75 MHz, CDCl₃) δ 199.5 (CHO), 171.6 (CO₂Me), 155.5 (Boc – CO), 80.6 (Boc – C(CH₃)₃), 53.1 (α – CH), 48.9 (CO₂CH₃), 46.4 (CH₂CHO), 28.5 (Boc – C(CH₃)₃).

The resulting aldehyde was dissolved in H₂O / EtOH (1:1) and the solution was cooled to 0 °C in an ice-salt bath. L-HoCys-NHBn was then added to the cooled solution and the pH was adjusted with solid NaHCO₃ to 6.5 while the reaction was stirred. While the reaction warmed to room temperature, the solution was degassed with Ar for 20 minutes and allowed to stir overnight. After 18 hours the solvents were removed under reduced pressure and the residue was redissolved in H₂O. The solution was extracted with EtOAc. The pH of the aqueous layer was adjusted to 6.5 using 1N HCl, and then the aqueous layer was extracted with EtOAc. To facilitate the partitioning of the layers, NaCl was added to the aqueous layer followed by extractions into Et₂O. This process was repeated 5-6 times with adjustment of the pH to 6.5 between extractions. The organic layers were combined and dried with MgSO₄. Removal of the solvent under vacuum gave a light orange oil which was dried under hard vacuum.

The condensed product was dissolved in THF/MeOH/H₂O (3:1:1, 0.3 M total concentration). To the solution was added 14.4 mg of LiOH and it was then allowed to stir for 16 hours. Upon completion, the solvent was evaporated under reduced pressure to give a white solid. The solid was then resuspended in a 1:1 mixture of H₂O and EtOAc whereupon the two layers were separated. The aqueous layer was then acidified to pH 3 with 0.5 M HCl and extracted with EtOAc, dried with MgSO₄ and concentrated under reduced pressure. The free acid was then dissolved in freshly distilled CH₂Cl₂. To the dichloromethane solution, 2-chloro-1-methylpyridinium iodide (90 mg, 0.35 mmol) and NEt₃ (0.1 mL, 0.7 mmol) were added. The resulting solution was refluxed overnight. The resulting solution was refluxed overnight. The reaction mixture was allowed to cool, and then was extracted with 1N HCl, saturated NaHCO₃, and brine. Drying with MgSO₄ and

subsequent removal of the solvents under vacuum resulted in an orange oil. The mixture of products was separated by silica gel chromatography (EtOAc / hexanes, 1:1). The resulting fractions did not yield the desired product after extensive concentration and analysis with ESI HR-MS.

**(4*S*, 7*R*, 8*aR*)-7-tert-Butoxycarbonylamino-6-oxo-hexahydro-pyrrolo[2,1-
b][1,3]thiazine-4-*N*-benzyl-carboxamide (**4.31**).**



To a solution of methyl ester **4.10** (0.3 g, 0.97 mmol) and benzyl amine (0.11 mL, 1.1 mmol) in 2 mL of toluene was added HOBt (41 mg, 0.3 mmol) followed by Zr(O*t*-Bu)₄ (0.11 mL, 0.3 mmol). The reaction was stirred under reflux conditions for two days. At the completion of two days the reaction was evaporated under reduced pressure and loaded onto a silica gel column. The final product was purified by silica gel flash chromatography with EtOAc / hexanes (1:1) as the eluting solvent to yield 0.08 g (19%) of **4.31** as a clear oil.

TLC R_f = 0.22 (EtOAc / Hexanes, 1:1)

[α]_D 14.7 (*c* 0.3, CH₂Cl₂)

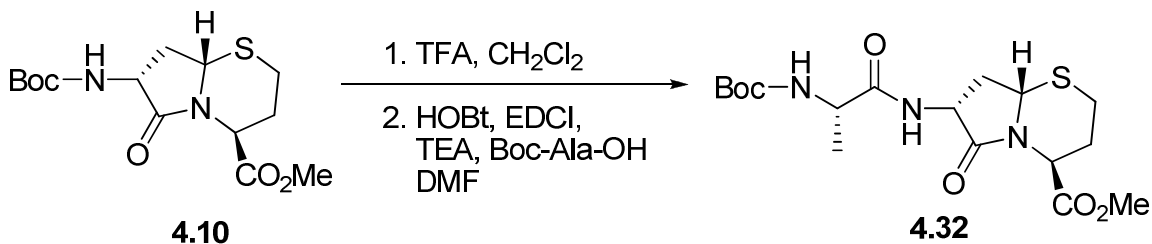
¹H NMR (300 MHz, CDCl₃, COSY) δ 7.16 – 7.27 (m, 5H, C₆H₅), 6.72 (br s, 1H, NHCH₂C₆H₅), 5.14 (d, *J* = 6 Hz, 1H, Boc-NH), 4.88 (d, *J* = 7.2 Hz, 1H, CH₂CHS), 4.55 (dd, *J* = 6.3 Hz, 15 Hz, 1H, NHCH₂C₆H₅), 4.27 (dd, *J* = 6.3 Hz, 15 Hz, 1H,

NHCH₂C₆H₅), 3.99 (d, *J* = 7.2 Hz, 1H, C4 CH), 3.70 (d, *J* = 10.8 Hz, C7 CH), 2.98 – 3.06 (m, 1H, SCH₂CH₂), 2.79 – 2.85 (m, 1H, SCH₂CH₂), 2.14 – 2.38 (m, 3H, SCH₂CH₂, C3-CH₂), 1.83 – 1.98 (m, 1H, SCH₂CH₂), 1.29 (s, 9H, Boc – C(CH₃)₃).

¹³C NMR (75 MHz, CDCl₃, HMQC) δ 172.5 (CON), 168.1(CONHBn), 155.6 (Boc-CO), 138.5 (C₆H₅), 128.6(C₆H₅), 128.1(C₆H₅), 127.5(C₆H₅), 80.7 (Boc C(CH₃)₃), 76.8 (NH₂CH₂C₆H₅), 59.7 (CH₂CHS), 52.3 (C4 C), 44.1 (C7 C), 32.9 (CHCH₂CH₂), 28.8 (CHCH₂CH), 28.5 (Boc C(CH₃)₃), 24.6 (CHCH₂CH₂)

ESI HRMS *m/z* calcd for C₂₀H₂₇N₃O₄S + Na⁺, 428.1620; found, 428.1652.

Methyl (4*S*,7*R*,8*aR*)-7-(2-(*S*)-*tert*-Butoxycarbonylamino-propanoyl)amino-6-oxohexahydro-2*H*-pyrrolo[2,1-*b*][1,3]thiazine-4-carboxylate (4.32).



Methyl (4*S*,7*R*,8*aR*)-7-*tert*-butoxycarbonylamino-6-oxohexahydro-2*H*-pyrrolo[2,1-*b*][1,3]thiazine-4-carboxylate (**4.10**, 0.04 g, 0.12 mmol) was dissolved in 3 mL of CH₂Cl₂ and 185 μL (2.4 mmol) of TFA. This solution was stirred under nitrogen for 4-24 hours while it was monitored by TLC. Upon completion, the reaction was concentrated under reduced pressure. The residue was dissolved in CH₂Cl₂ and then evaporated three times to azeotropically remove any last traces of dioxane. The white compound was then allowed to dry under vacuum for 24 – 48 hours. The white solid was then used in the subsequent coupling reaction without further purification.

(4*S*,7*R*,8*aR*)-Methyl 7-amino-6-oxohexahydro-2*H*-pyrrolo[2,1-*b*][1,3]thiazine-4-carboxylate • HCl (0.12 mmol) and Boc-Ala-OH (23 mg, 0.12 mmol) were dissolved in DMF which had been dried over 5 Å molecular sieves. While this solution was stirred HOBt (18 mg, 0.13 mmol) was added and the solution was cooled to -78 °C. EDC • HCl (25 mg, 0.13 mmol) and NMM (37 µL, 0.26 mmol) were added consecutively to the cooled solution, which then was allowed to warm slowly to room temperature whereupon it was stirred for 3 days. On the third day, the reaction mixture was concentrated *in vacuo* to give an orange residue to which a small portion of xylenes was added to assist in the removal of the traces of DMF. The orange residue was then partitioned between H₂O (100 mL) and EtOAc (100 mL). The organic layer was washed consecutively with 1.2 M HCl (100 mL), 1 M NaHCO₃ (100 mL) and brine (100 mL), dried with MgSO₄ and concentrated under reduced pressure to yield 1.48 g of crude product (**4.32**). The crude methyl-(4*S*,7*R*,8*aR*)-7-(2-*tert*-butoxycarbonylamino-propanoyl)amino-6-oxohexahydro-2*H*-pyrrolo[2,1-*b*][1,3]thiazine-4-carboxylate was purified by silica gel chromatography using 5 cm of silica gel within a 3 cm diameter column which was eluted with 3:1 ethyl acetate in hexanes to yield 51 mg (89 %) of pure **4.32**.

TLC R_f = 0.33 (EtOAc / Hexanes, 3:1)

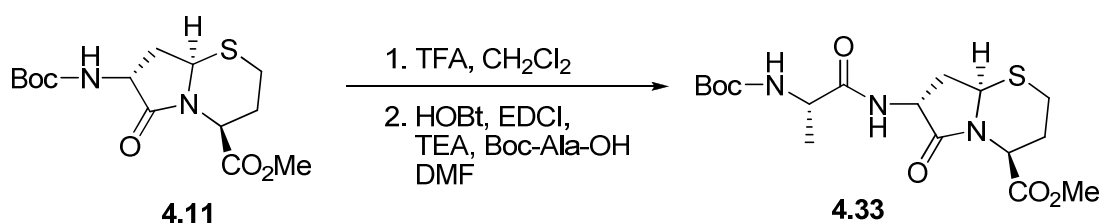
[α]_D 37.2 (*c* 0.9, CH₂Cl₂)

¹H NMR (300 MHz, CDCl₃, COSY) δ 4.82 – 4.98 (m, 2H, *CHS*, *NCHCO*₂Me), 4.49 – 4.58 (m, 1H, *C7 CH*), 4.14 (br s, 1H, Ala α-*CH*), 3.72 (*CO*₂*CH*₃), 2.85 – 3.00 (m, 1H, *SCH*₂), 2.77 - 2.83 (m, 1H, *SCH*₂), 2.45 – 2.60 (m, 1H, *CH*₂*CHS*), 2.07 – 2.21 (m, 1H, *CH*₂*CHS*), 1.84 – 1.98 (*SCH*₂*CH*₂), 1.64 – 1.71 (*SCH*₂*CH*₂), 1.38 (Boc – C(*CH*₃)₃), 1.26 (d, *J* = 9.9 Hz, 3H, Ala *CH*₃).

^{13}C NMR (75 MHz, CDCl_3 , HMQC) δ 173.4 (CO), 171.4 (CO), 168.9 (CO), 155.8 (Boc – CO), 80.5 (Boc – $\text{C}(\text{CH}_3)_3$), 59.4 (CHS), 57.9 (NCHCO₂Me), 55.2 (Ala α -CH), 52.8 (CO₂CH₃), 50.4 (NHCHCON), 33.6 (SCH₂), 28.5 (Boc – $\text{C}(\text{CH}_3)_3$), 28.0 (CH₂CHS), 26.4 (SCH₂CH₂), 18.5 (Ala – CH₃).

ESI HRMS m/z calcd for $\text{C}_{17}\text{H}_{27}\text{N}_3\text{O}_6\text{S} + \text{Na}^+$, 428.1518; found, 428.1517.

Methyl (4*S*,7*R*,8*aS*)-7-(2-(*S*)-tert-Butoxycarbonylamino-propanoyl)amino-6-oxohexahydro-2*H*-pyrrolo[2,1-*b*][1,3]thiazine-4-carboxylate (4.33).



Methyl (4*S*,7*R*,8*aS*)-7-tert-butoxycarbonylamino-6-oxohexahydro-2*H*-pyrrolo[2,1-*b*][1,3]thiazine-4-carboxylate **4.11** (0.04 g, 0.12 mmol) was dissolved in 3 mL of CH_2Cl_2 and 185 μL (2.4 mmol) of TFA. This solution was stirred under nitrogen for 4-24 hours while it was monitored by TLC. Upon completion, the reaction was concentrated under reduced pressure. The residue was dissolved in CH_2Cl_2 and evaporated three times to azeotropically remove any last traces of dioxane. The white compound was then allowed to dry under vacuum for 24 – 48 hours. The white solid was then used in the subsequent coupling reaction without further purification.

Methyl (4*S*,7*R*,8*aS*)-7-amino-6-oxohexahydro-2*H*-pyrrolo[2,1-*b*][1,3]thiazine-4-carboxylate • HCl (0.12 mmol) and Boc-Ala-OH (23 mg, 0.12 mmol) were dissolved in

DMF which had been dried over 5 Å molecular sieves. While this solution was stirred HOBt (18 mg, 0.13 mmol) was added and the solution was cooled to -78°C . EDC • HCl (25 mg, 0.13 mmol) and NMM (37 μL , 0.26 mmol) were added consecutively to the cooled solution, which then was allowed to warm slowly to room temperature whereupon it was stirred for 3 days. On the third day, the reaction mixture was concentrated *in vacuo* to give an orange residue to which a small portion of xylenes was added to assist in the removal of the traces of DMF. The orange residue was then partitioned between H_2O (100 mL) and EtOAc (100 mL). The organic layer was washed consecutively with 1.2 M HCl (100 mL), 1 M NaHCO_3 (100 mL) and brine (100 mL), dried with MgSO_4 and concentrated under reduced pressure to yield 1.48 g of crude product. The crude methyl (4*S*,7*R*,8*aS*)-7-(2-(*S*)-*tert*-butoxycarbonylamino-propanoyl)amino-6-oxohexahydro-2*H*-pyrrolo[2,1-*b*][1,3]thiazine-4-carboxylate (**4.33**) was purified by silica gel chromatography using 5 cm of silica gel within a 3 cm diameter column which was eluted with 3:1 ethyl acetate in hexanes to yield 51 mg (**4.33**, 89 %) of pure product.

TLC $R_f = 0.17$ (EtOAc / Hexanes, 3:1)

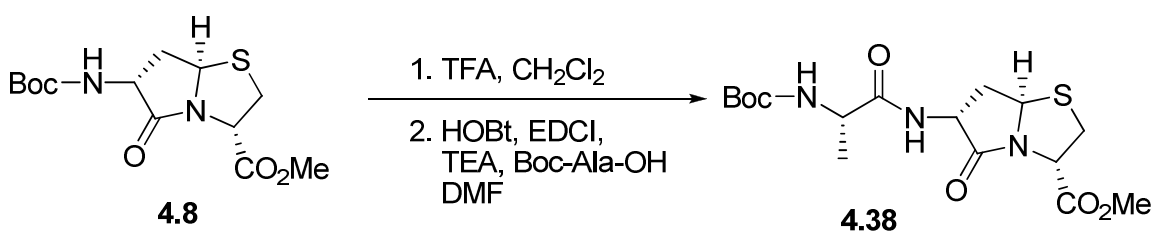
$[\alpha]_D 30.4$ (*c* 0.3, CH_2Cl_2)

^1H NMR (300 MHz, CDCl_3 , COSY) δ 5.09 – 5.12 (m, 1H, *CHS*), 5.01 – 5.03 (m, C4 *CH*), 4.86 (br s, 1H, *NH*), 4.49 – 4.57 (m, 1H, C7 *CH*), 4.17 (br s, Ala α -*CH*), 3.72 (s, 3H, CO_2CH_3), 3.42 (br s, 1H, *NH*), 2.82 – 2.92 (m, 1H, *SCH}_2*), 1.98 – 2.64 (m, 4H, *SCH}_2*, C3 *CH}_2*, C8 *CH}_2*), 1.80 – 1.91 (m, C3 *CH}_2*), 1.39 (s, 9H, Boc – $\text{C}(\text{CH}_3)_3$), 1.27 (d, $J = 16.2$ Hz, 3H, Ala *CH}_3*).

^{13}C NMR (75 MHz, CDCl_3) δ 171.7 (CO), 170.4 (CO), 169.1 (CO), 79.7 (Boc – $\text{C}(\text{CH}_3)_3$), 55.2 (CHS), 53.0 (C4 C), 52.0 (CO_2CH_3), 50.2 (Ala α -C), 33.1 (SCH_2), 28.5 (Boc – $\text{C}(\text{CH}_3)_3$), 26.8 (C8 C), 26.0 (7-C), 25.5 (C3 C), 17.1 (Ala CH_3).

ESI HRMS m/z calcd for $\text{C}_{17}\text{H}_{27}\text{N}_3\text{O}_6\text{S} + \text{Na}^+$, 424.1518; found, 424.1523.

Methyl (3*S*,6*R*,7*aR*)-6-(2-(*S*)-*tert*-Butoxycarbonylamino-propanoyl)amino-5-oxohexahydropyrrolo[2,1-*b*]thiazole-3-carboxylate (4.38)



Methyl (3*S*,6*R*,7*aR*)-6-*tert*-butoxycarbonylamino-5-oxohexahydropyrrolo[2,1-*b*]thiazole-3-carboxylate (**4.8**, 0.1 g, 0.4 mmol) was dissolved in 4.8 mL of CH_2Cl_2 and 1.2 mL (16 mmol) of TFA and the solution was stirred under nitrogen for 4-24 hours while it was monitored by TLC. Upon completion, the reaction was concentrated under reduced pressure. The residue was dissolved in CH_2Cl_2 and evaporated three times to azeotropically remove any last traces of dioxane. The white compound was then allowed to dry under vacuum for 24 – 48 hours. The white solid was then used in the subsequent coupling reaction without further purification.

Methyl (3*S*,6*R*,7*aR*)-6-amino-5-oxohexahydropyrrolo[2,1-*b*]thiazole-3-carboxylate • HCl (0.4 mmol) and Boc-Ala-OH (80 mg, 0.4 mmol) were dissolved in DMF (5 mL) which had been dried over 5 Å molecular sieves. While this solution was stirred HOBt (61 mg, 0.44 mmol) was added and the solution was cooled to -78 °C. EDC • HCl (85 mg, 0.44 mmol) and NMM (124 µL, 0.88 mmol) were added consecutively to the cooled solution, which then was allowed to warm slowly to room temperature, whereupon it was stirred for 3 days. On the third day, the reaction mixture was concentrated *in vacuo* to give an orange residue to which a small portion of xylenes was added to assist in the removal of traces of DMF. The orange residue was then partitioned between H₂O (100 mL) and EtOAc (100 mL). The organic layer was washed consecutively with 1.2 M HCl (100 mL), 1 M NaHCO₃ (100 mL) and brine (100 mL), dried with MgSO₄ and concentrated under reduced pressure to yield 150 mg of crude product. The crude methyl (3*S*,6*R*,7*aR*)-6-(2-(*S*)-*tert*-butoxycarbonylamino)amino-5-oxohexahydropyrrolo[2,1-*b*]thiazole-3-carboxylate (**4.38**) was purified by silica gel chromatography using 5 cm of silica gel within a 3 cm diameter column which was eluted with 3:1 ethyl acetate in hexanes to yield 120 mg (77 %) of pure **4.38**.

TLC R_f = 0.18 (EtOAc / Hexanes, 3:1)

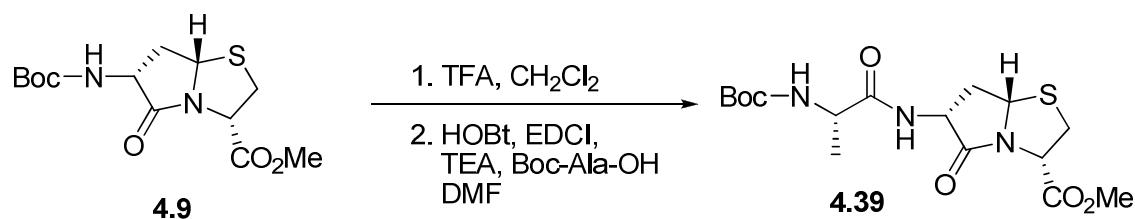
[α]_D - 18.0 (*c* 0.9, CH₂Cl₂)

¹H NMR (300 MHz, CDCl₃, COSY) δ 6.99 (d, *J* = 7.2 Hz, 1H, NH), 4.94 – 5.10 (m, 3H, CHS, 6-CH, 3-CH), 4.34 (d, *J* = 6.6 Hz, 1H, Ala α-CH), 4.22 (br s, 1H, NH), 3.73 (s, 3H, CO₂CH₃), 3.63 (dd, *J* = 6.6 Hz, 12.6 Hz, 1H, SCH₂), 3.34 (d, *J* = 16.4 Hz, 1H, SCH₂), 2.98 – 3.04 (m, 1H, CH₂CHS), 1.98 – 2.11 (m, 1H, CH₂CHS), 1.38 (s, 9H, Boc-C(CH₃)₃), 1.31 (d, *J* = 4.2 Hz, 3H, Ala CH₃).

^{13}C NMR (75 MHz, CDCl_3 , HMQC) δ 173.6 (CO), 170.5 (CO), 168.7 (CO), 155.7 (Boc – CO), 81.8 (Boc – $\text{C}(\text{CH}_3)_3$), 63.9 (CHS), 57.3 (Ala α -C), 55.2 ($\text{NCHCO}_2\text{CH}_3$), 53.2 (CO_2CH_3), 50.3 (6-CH), 39.1 (SCH_2), 37.6 (CH_2CHS), 28.5 (Boc – $\text{C}(\text{CH}_3)_3$), 18.8 (Ala CH_3).

ESI HRMS m/z calcd for $\text{C}_{16}\text{H}_{25}\text{N}_3\text{O}_6\text{S} + \text{Na}^+$, 410.1362; found, 410.1351.

Methyl (3*S*,6*R*,7*aS*)-6-(2-(*S*)-*tert*-Butoxycarbonylamino-propanoyl)amino-5-oxohexahydropyrrolo[2,1-*b*]thiazole-3-carboxylate (4.39)



Methyl (3*S*,6*R*,7*aS*)-6-*tert*-butoxycarbonylamino-5-oxohexahydropyrrolo[2,1-*b*]thiazole-3-carboxylate (**4.9**, 0.1 g, 0.4 mmol) was dissolved in 4.8 mL of CH_2Cl_2 and 1.2 mL (16 mmol) of TFA and the solution was stirred under nitrogen for 4-24 hours while it was monitored by TLC. Upon completion, the reaction was concentrated under reduced pressure. The residue was dissolved in CH_2Cl_2 and evaporated three times to azeotropically remove any last traces of dioxane. The white compound was then allowed to dry under vacuum for 24 – 48 hours. The white solid was then used in the subsequent coupling reaction without further purification.

Methyl-(3*S*,6*R*,7*aS*)-6-amino-5-oxohexahydropyrrolo[2,1-*b*]thiazole-3-carboxylate • HCl (0.4 mmol) and Boc-Ala-OH (80 mg, 0.4 mmol) were dissolved in DMF (5 mL) which had been dried over 5 Å molecular sieves. While this solution was stirred HOBt (61 mg, 0.44 mmol) was added and the solution was cooled to -78 °C. EDC • HCl (85 mg, 0.44 mmol) and NMM (124 µL, 0.88 mmol) were added consecutively to the cooled solution, which then was allowed to warm slowly to room temperature whereupon it was stirred for 3 days. On the third day, the reaction mixture was concentrated *in vacuo* to give an orange residue to which a small portion of xylenes was added to assist in the removal of traces of DMF. The orange residue was then partitioned between H₂O (100 mL) and EtOAc (100 mL). The organic layer was washed consecutively with 1.2 M HCl (100 mL), 1 M NaHCO₃ (100 mL) and brine (100 mL), dried with MgSO₄ and concentrated under reduced pressure to yield 120 mg of crude product. The crude methyl (3*S*,6*R*,7*aS*)-6-(2-(*S*)-*tert*-butoxycarbonylamino-propanoyl)amino-5-oxohexahydropyrrolo[2,1-*b*]thiazole-3-carboxylate (**4.39**) was purified by silica gel chromatography using 5 cm of silica gel within a 3 cm diameter column which was eluted with 3:1 ethyl acetate in hexanes to yield 126 mg (81 %) of pure **4.39**.

TLC R_f = 0.42 (EtOAc / Hexanes, 3:1)

[α]_D 124.2 (*c* 0.6, CH₂Cl₂)

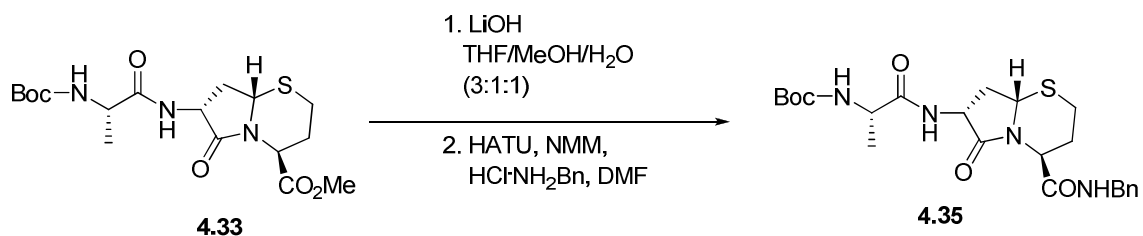
¹H NMR (300 MHz, CDCl₃, COSY) δ 5.33 (d, *J* = 8.4 Hz, 1H, *CHS*) 5.06 – 5.09 (m, 1H, 6-*CH*), (dd, *J* = 4.8 Hz, 8.4 Hz, 1H, 3-*CH*), 4.70 – 4.73 (br m, 1H, *NH*), 4.20 (br s, 1H, Ala α-*CH*), 3.72 (s, 3H, CO₂CH₃), 3.30 – 3.46 (m, 2H, SCH₂), 2.59 – 2.68 (m, 1H,

CH_2CHS), 2.27 – 2.36 (m, 1H, CH_2CHS), 1.37 (s, 9H, $\text{Boc-C}(\text{CH}_3)_3$), 1.31 (d, $J = 6.6$ Hz, 3H, Ala CH_3).

^{13}C NMR (75 MHz, CDCl_3 , HMQC) δ 175.0 (CO), 173.5 (CO), 170.4 (CO), 155.9 (Boc – CO), 80.4 (Boc – $\text{C}(\text{CH}_3)_3$), 64.3 (CHS), 58.5 ($\text{NCHCO}_2\text{CH}_3$), 53.3 (CO_2CH_3), 50.9 (Ala α -CH), 50.3 (6-CH), 37.0 (SCH_2), 30.6 (CH_2CHS), 28.6 (Boc – $\text{C}(\text{CH}_3)_3$), 18.4 (Ala CH_3).

ESI HRMS m/z calcd for $\text{C}_{16}\text{H}_{25}\text{N}_3\text{O}_6 \text{ S} + \text{H}^+$, 388.1542; found, 388.1524.

(4*S*,7*R*,8*aR*)-7-(2-(*S*)-*tert*-butoxycarbonylamino-propanoyl)amino-6-oxohexahydro-2*H*-pyrrolo[2,1-*b*][1,3]thiazine-4-*N*-benzyl-carboxamide (4.35)



Methyl (4*S*,7*R*,8*aR*)-7-(2-(*S*)-*tert*-butoxycarbonylamino-propanoyl)amino-6-oxohexahydro-2*H*-pyrrolo[2,1-*b*][1,3]thiazine-4-carboxylate (**4.33**) was dissolved in THF/MeOH/H₂O (3:1:1, 0.3 M total concentration). To the solution was added 14.4 mg of LiOH and it was then allowed to stir for 16 hours. Upon completion, the solvent was evaporated under reduced pressure to give a white solid. The solid was then resuspended in a 1:1 mixture of H₂O and EtOAc whereupon the two layers were separated. The aqueous layer was then acidified to pH 3 with 0.5 M HCl and extracted with EtOAc, dried with MgSO_4 and concentrated under reduced pressure.

(4*S*,7*R*,8*aR*)-7-(2-(*S*)-*tert*-Butoxycarbonylamino-propanoyl)amino-6-oxohexahydro-2*H*-pyrrolo[2,1-*b*][1,3]thiazine-4-carboxylic acid (0.4 mmol) and benzyl amine hydrochloride (80 mg, 0.4 mmol) were dissolved in DMF (5 mL) which had been dried over 5 Å molecular sieves and the solution was cooled to -78°C . While this solution was stirred HATU (61 mg, 0.44 mmol) and NMM (124 μL , 0.88 mmol) were added consecutively to the cooled solution which then was allowed to warm slowly to room temperature whereupon it was stirred for 26 hours. Upon completion the reaction mixture was concentrated *in vacuo* to give an orange residue to which a small portion of xylenes was added to assist in the removal of the traces of DMF. The orange residue was then partitioned between H_2O (100 mL) and EtOAc (100 mL). The organic layer was washed consecutively with 1.2 M HCl (100 mL), 1 M NaHCO_3 (100 mL) and brine (100 mL), dried with MgSO_4 and concentrated under reduced pressure to yield 120 mg of crude product. The crude (4*S*,7*R*,8*aR*)-7-(2-(*S*)-*tert*-butoxycarbonylamino-propanoyl)amino-6-oxohexahydro-2*H*-pyrrolo[2,1-*b*][1,3]thiazine-4-*N*-benzyl-carboxamide (**4.35**) was purified by silica gel chromatography using 5 cm of silica gel within a 3 cm diameter column which was eluted with 3:1 ethyl acetate in hexanes to yield 126 mg (81 %) of pure **4.35**.

TLC $R_f = 0.27$ (EtOAc / Hexanes, 3:1)

$[\alpha]_D 40.1$ (*c* 0.5, CH_2Cl_2)

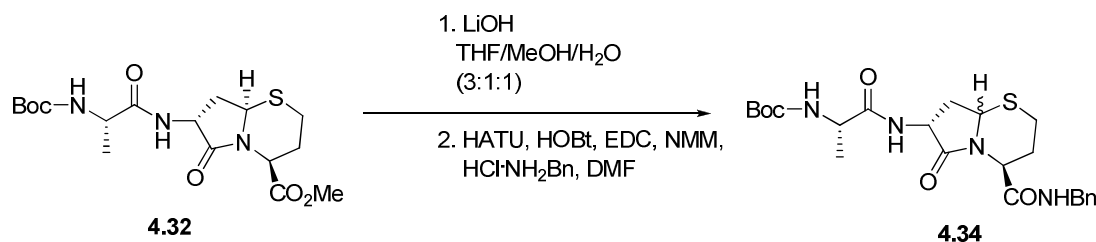
$^1\text{H NMR}$ (300 MHz, CDCl_3 , COSY) δ 7.18 – 7.25 (m, 7H, C_6H_5 , NH), 4.85 – 4.91 (m, 2H, CHS, NH), 4.62 (d, $J = 7.8$ Hz, 1H, $\text{CH}_2\text{C}_6\text{H}_5$), 4.38 – 4.44 (m, 2H, $\text{CH}_2\text{C}_6\text{H}_5$, 4-CH), 3.96 – 3.99 (m, 2H, 7-CH, Ala α -CH), 2.72 – 2.87 (m, 2H, SCH_2), 2.55 – 2.60 (m, 1H,

C3 CH₂), 2.31 – 2.33 (m, 1H, 8-CH₂), 2.11 – 2.17 (m, 1H, 8-CH₂), 1.81 – 1.90 (m, 1H, 3-CH₂), 1.38 (s, 9H, Boc – C(CH₃)₃), 1.08 (d, *J* = 6.9 Hz, 3H, Ala CH₃).

¹³C NMR (75 MHz, CDCl₃, HMQC) δ 173.6 (CO), 170.8 (CO), 168.1 (CO), 155.5 (Boc – CO), 138.7 (C₆H₅), 128.8 (C₆H₅), 128.7 (C₆H₅), 128.4 (C₆H₅), 128.3 (C₆H₅), 127.5 (C₆H₅), 80.2 (Boc – C(CH₃)₃), 55.8 (CHS), 52.7 (4-C), 50.7 (Ala α-C), 44.2 (7-C), 38.8 (CH₂C₆H₅), 32.0 (SCH₂), 28.5 (Boc – C(CH₃)₃), 26.0 (8-C), 25.6 (3-C), 17.1 (Ala CH₃).

ESI HRMS *m/z* calcd for C₂₃H₃₂N₄O₅S + Na⁺, 499.1991; found, 499.1967.

(4*S*,7*R*,8*aS*)-7-(2-(*S*)-*tert*-Butoxycarbonylamino-propanoyl)amino-6-oxohexahydro-2*H*-pyrrolo[2,1-*b*][1,3]thiazine-4-*N*-benzyl-carboxamide (4.34)



Methyl-(4*S*,7*R*,8*aS*)-7-(2-(*S*)-*tert*-butoxycarbonylamino-propanoyl)amino-6-oxohexahydro-2*H*-pyrrolo[2,1-*b*][1,3]thiazine-4-carboxylate **4.32** was dissolved in THF/MeOH/H₂O (3:1:1, 0.3 M total concentration). To the solution was added 14.4 mg of LiOH and it was then allowed to stir for 16 hours. Upon completion, the solvent was evaporated under reduced pressure to give a white solid. The solid was then resuspended in a 1:1 mixture of H₂O and EtOAc whereupon the two layers were separated. The aqueous layer was then acidified to pH 3 with 0.5 M HCl and extracted with EtOAc, dried with MgSO₄ and concentrated under reduced pressure.

(4*S*,7*R*,8*aS*)-7-(2-(*S*)-*tert*-butoxycarbonylamino-propanoyl)amino-6-oxohexahydro-2*H*-pyrrolo[2,1-*b*][1,3]thiazine-4-carboxylic acid (0.4 mmol) and benzyl amine hydrochloride (80 mg, 0.4 mmol) were dissolved in DMF (5 mL) which had been dried over 5 Å molecular sieves and the solution was cooled to -78 °C. While this solution was stirred HATU (61 mg, 0.44 mmol), HOBT (0.44 mmol), EDC•HCl (0.44 mmol) and NMM (124 µL, 0.88 mmol) were added consecutively to the cooled solution which then was allowed to warm slowly to room temperature whereupon it was stirred for 26 hours. Upon completion the reaction mixture was concentrated *in vacuo* to give an orange residue to which a small portion of xylenes was added to assist in the removal of the traces of DMF. The orange residue was then partitioned between H₂O (100 mL) and EtOAc (100 mL). The organic layer was washed consecutively with 1.2 M HCl (100 mL), 1 M NaHCO₃ (100 mL) and brine (100 mL), dried with MgSO₄ and concentrated under reduced pressure to yield 20 mg of crude product. The crude Boc-Ala(4*S*,7*R*,8*aS*)-7-(2-(*S*)-*tert*-butoxycarbonylamino-propanoyl)amino-6-oxohexahydro-2*H*-pyrrolo[2,1-*b*][1,3]thiazine-4-*N*-benzyl-carboxamide **4.34** was purified by silica gel chromatography using 5 cm of silica gel within a 3 cm diameter column which was eluted with 3:1 ethyl acetate in hexanes to yield 15 mg (12%) of mixture of diastereomers, one of which was **4.35**.

TLC R_f = 0.27 and 0.18 (EtOAc / Hexanes, 3:1)

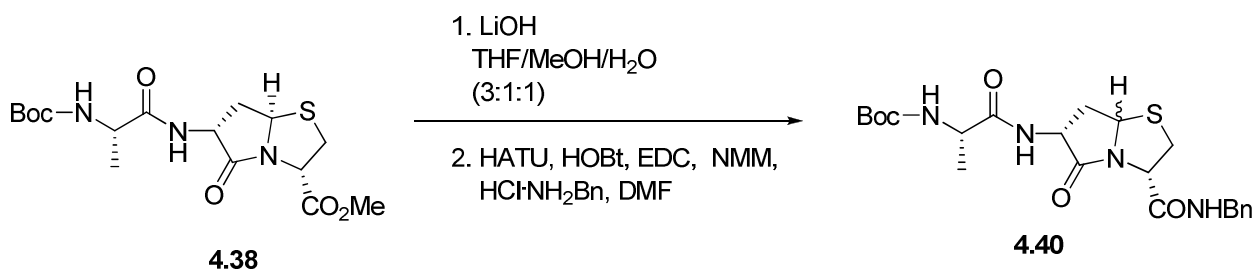
¹H NMR (300 MHz, CDCl₃, COSY) δ 7.09 – 7.24 (m, 7H, C₆H₅, NH), 4.85 – 4.91 (m, 2H, CHS, NH), 4.62 (d, *J* = 7.8 Hz, 1H, CH₂C₆H₅), 4.38 – 4.44 (m, 2H, CH₂C₆H₅, C4 CH), 3.96 – 3.99 (m, 2H, C7 CH, Ala-α CH), 2.72 – 2.87 (m, 2H, SCH₂), 2.55 – 2.60 (m, 1H, C3 CH₂), 2.31 – 2.33 (m, 1H, C8 CH₂), 2.11 – 2.17 (m, 1H, C8 CH₂), 1.81 – 1.90 (m,

1H, C3 CH₂), 1.58 (s, 1.5 H, Boc – C(CH₃)₃) and 1.38 (s, 7H, Boc – C(CH₃)₃), 1.19 (s, 1H, Ala CH₃) and 1.08 (d, *J* = 6.9 Hz, 2H, Ala CH₃).

¹³C NMR (75 MHz, CDCl₃, HMQC) δ 173.6 and 174.5 (CO), 170.8 and 171.4 (CO), 168.1 (CO), 155.5 (Boc – CO), 138.7 (C₆H₅), 128.8 (C₆H₅), 128.7 (C₆H₅), 128.4 (C₆H₅), 128.3 (C₆H₅), 127.5 (C₆H₅), 80.2 (Boc – C(CH₃)₃), 55.8 (CHS), 52.7 (C4 α C), 50.7 (Ala α-C), 49.9 (C7 C), 38.8 (CH₂C₆H₅), 33.6 and 34.0 (SCH₂), 28.0 and 28.5 (Boc – C(CH₃)₃), 26.0 and 26.8 (C8 C), 25.1 and 25.6 (C3 C), 18.5 (Ala CH₃).

ESI HRMS *m/z* calcd for C₂₃H₃₂N₄O₅S + Na⁺, 499.1991; found, 499.1967.

[(3*S*,6*R*,7*aR*)-6-(2-(*S*)-tert-Butoxycarbonylamino-propanoyl)amino-5-oxohexahydropyrrolo[2,1-*b*]thiazole-3-*N*-benzyl-carboxamide (4.40)



Methyl (3*S*,6*R*,7*aS*)-6-(2-(*S*)-tert-butoxycarbonylamino-propanoyl)amino-5-oxohexahydropyrrolo[2,1-*b*]thiazole-3-carboxylate **4.38** was dissolved in THF/MeOH/H₂O (3:1:1, 0.3 M total concentration). To the solution was added 14.4 mg of LiOH and it was then allowed to stir for 16 hours. Upon completion, the solvent was evaporated under reduced pressure to give a white solid. The solid was then resuspended

in a 1:1 mixture of H₂O and EtOAc whereupon the two layers were separated. The aqueous layer was then acidified to pH 3 with 0.5 M HCl and extracted with EtOAc, dried with MgSO₄ and concentrated under reduced pressure.

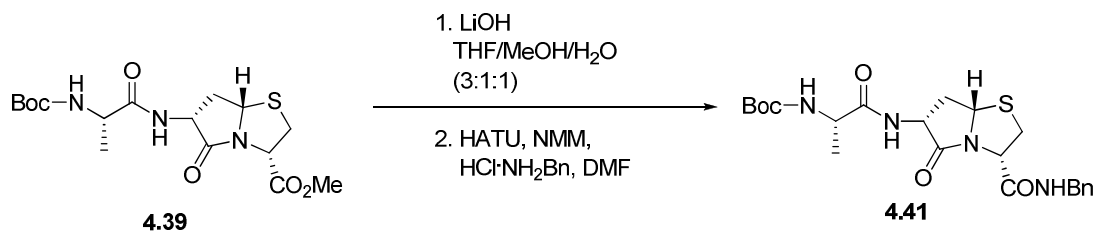
(3*S*,6*R*,7*aS*)-6-(2-(*S*)-*tert*-Butoxycarbonylamino-propanoyl)amino-5-oxohexahydropyrrolo[2,1-*b*]thiazole-3-carboxylic acid (0.4 mmol) and benzyl amine hydrochloride (80 mg, 0.4 mmol) were dissolved in DMF (5 mL) which had been dried over 5 Å molecular sieves and the solution was cooled to -78 °C. While this solution was stirred HATU (61 mg, 0.44 mmol) and NMM (124 µL, 0.88 mmol) were added consecutively to the cooled solution which then was allowed to warm slowly to room temperature whereupon it was stirred for 26 hours. Upon completion the reaction mixture was concentrated *in vacuo* to give an orange residue to which a small portion of xylenes was added to assist in the removal of the traces of DMF. The orange residue was then partitioned between H₂O (100 mL) and EtOAc (100 mL). The organic layer was washed consecutively with 1.2 M HCl (100 mL), 1 M NaHCO₃ (100 mL) and brine (100 mL), dried with MgSO₄ and concentrated under reduced pressure to yield 40 mg of crude product. The crude (3*S*,6*R*,7*aS*)-6-(2-(*S*)-*tert*-Butoxycarbonylamino-propanoyl)amino-5-oxohexahydropyrrolo[2,1-*b*]thiazole-3-*N*-benzyl-carboxamide **4.40** was purified by silica gel chromatography using 5 cm of silica gel within a 3 cm diameter column which was eluted with 3:1 ethyl acetate in hexanes to yield 6 mg (4 %) of a mixture of epimers at the bridgehead carbon.

TLC R_f = 0.51 and 0.46 (EtOAc)

^1H NMR (300 MHz, CDCl_3) δ ^1H NMR (300 MHz, CDCl_3 , COSY) δ 7.17 – 7.30 (m, 5H, C_6H_5), 6.97 (br s, 1H, NH), 6.79 (br s, 1H, NH), 4.93 – 4.97 (m, 2H, NH, CHS), 4.67 – 4.83 (m, C3 CH, Ala α -CH), 4.35 – 4.37 ($\text{CH}_2\text{C}_6\text{H}_5$), 4.02 – 4.10 (br m, C6 CH), 3.67 – 3.73 (m, 1H, SCH_2), 3.24 – 3.30 (m, 1H, SCH_2), 3.01 – 3.05 (CH_2CHS), 1.63 – 2.03 (CH_2CHS), 1.36 and 1.48 (s, 9H, Boc – $\text{C}(\text{CH}_3)_3$), 1.14 – 1.16 and 1.19 – 1.31 (m, 3H, Ala CH_3).

ESI HRMS m/z calcd for $\text{C}_{22}\text{H}_{30}\text{N}_4\text{O}_5\text{S} + \text{Na}^+$, 485.1846; found, 485.1835.

(3*S*,6*R*,7*aS*)-6-(2-(*S*)-tert-Butoxycarbonylamino-propanoyl)amino-5-oxohexahydropyrrolo[2,1-*b*]thiazole-3-*N*-benzyl-carboxamide (4.41).



Methyl (3*S*,6*R*,7*aS*)-6-(2-(*S*)-tert-Butoxycarbonylamino-propanoyl)amino-5-oxohexahydropyrrolo[2,1-*b*]thiazole-3-carboxylate (**4.39**) was dissolved in THF/MeOH/H₂O (3:1:1, 0.3 M total concentration). To the solution was added 14.4 mg of LiOH and it was then allowed to stir for 16 hours. Upon completion, the solvent was evaporated under reduced pressure to give a white solid. The solid was then resuspended in a 1:1 mixture of H₂O and EtOAc whereupon the two layers were separated. The

aqueous layer was then acidified to pH 3 with 0.5 M HCl and extracted with EtOAc, dried with MgSO₄ and concentrated under reduced pressure.

(3*S*,6*R*,7*aR*)-6-(2-(*S*)-tert-Butoxycarbonylamino-propanoyl)amino-5-oxohexahydropyrrolo[2,1-*b*]thiazole-3-carboxylic acid (0.4 mmol) and benzyl amine hydrochloride (80 mg, 0.4 mmol) were dissolved in DMF (5 mL) which had been dried over 5 Å molecular sieves and the solution was cooled to -78 °C. While this solution was stirred HATU (61 mg, 0.44 mmol) and NMM (124 µL, 0.88 mmol) were added consecutively to the cooled solution which then was allowed to warm slowly to room temperature whereupon it was stirred for 26 hours. Upon completion the reaction mixture was concentrated *in vacuo* to give an orange residue to which a small portion of xylenes was added to assist in the removal of the traces of DMF. The orange residue was then partitioned between H₂O (100 mL) and EtOAc (100 mL). The organic layer was washed consecutively with 1.2 M HCl (100 mL), 1 M NaHCO₃ (100 mL) and brine (100 mL), dried with MgSO₄ and concentrated under reduced pressure to yield 120 mg of crude product. The crude [(3*S*,6*R*,7*aS*)-6-(2-(*S*)-tert-Butoxycarbonylamino-propanoyl)amino-5-oxohexahydropyrrolo[2,1-*b*]thiazole-3-*N*-benzyl-carboxamide] (**4.41**) was purified by silica gel chromatography using 5 cm of silica gel within a 3 cm diameter column which was eluted with 3:1 ethyl acetate in hexanes to yield 126 mg (81 %) of pure **4.41**.

TLC R_f = 0.51 (EtOAc)

[α]_D 70.1 (*c* 0.4, CH₂Cl₂)

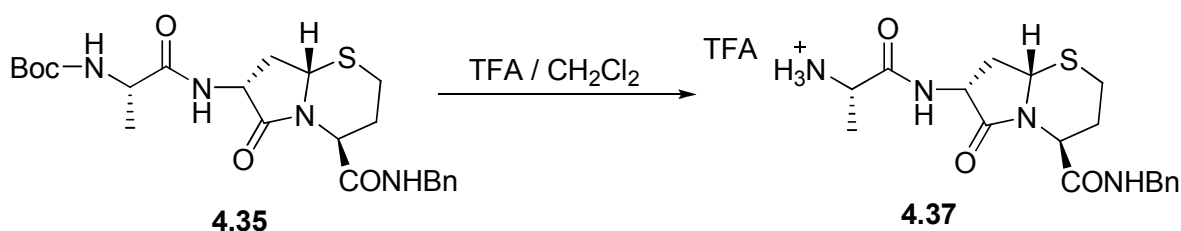
¹H NMR (300 MHz, CDCl₃, COSY) δ 7.17 – 7.30 (m, 5H, C₆H₅), 6.97 (br s, 1H, NH), 6.79 (br s, 1H, NH), 4.93 – 4.97 (m, 2H, NH, CHS), 4.67 – 4.83 (m, 3-CH, Ala α-CH), 4.35 – 4.37 (CH₂C₆H₅), 4.02 – 4.10 (br m, 6-CH), 3.67 – 3.73 (SCH₂), 3.24 – 3.30

(SCH₂), 3.01 – 3.05 (CH₂CHS), 1.63 – 2.03 (CH₂CHS), 1.36 (Boc – C(CH₃)₃), 1.19 – 1.31 (m, 3H, Ala CH₃).

¹³C NMR (75 MHz, CDCl₃, HMQC) δ 173.1 (CO), 173.1 (CO), 168.2 (CO), 155.3 (Boc – CO), 137.9 (C₆H₅), 129.0 (C₆H₅), 128.1 (C₆H₅), 127.9 (C₆H₅), 80.2 (Boc – C(CH₃)₃), 62.8 (CHS), 59.8 (NCHCON), 53.7 (Ala α-C), 50.7 (7-C), 44.0 (NHCHC₆H₅), 37.2 (SCH₂), 34.9 (CH₂CHS), 28.5 (Boc – C(CH₃)₃), 18.4 (Ala CH₃).

ESI HRMS *m/z* calcd for C₂₂H₃₀N₄O₅S + Na⁺, 485.1846; found, 485.1835.

(4*S*,7*R*,8*aR*)-7-(2-(*S*)-Amino-propanoyl)amino-6-oxohexahydro-2*H*-pyrrolo[2,1-*b*][1,3]thiazine-4-*N*-benzyl-carboxamide Trifluoroacetate Salt. (4.37)



(4*S*,7*R*,8*aR*)-7-(2-(*S*)-tert-Butoxycarbonylamino-propanoyl)amino-6-

oxohexahydro-2*H*-pyrrolo[2,1-*b*][1,3]thiazine-4-*N*-benzyl-carboxamide **4.35** (1.0 g, 2.93 mmol) was dissolved in 4.5 mL of TFA in 5 mL of dry CH₂Cl₂ and the solution was stirred under nitrogen for 24 hours while it was monitored by TLC. Upon completion the reaction was concentrated under reduced pressure. The residue was dissolved in CH₂Cl₂ and evaporated three times to azeotropically remove any last traces of TFA. The light orange compound (**4.37**) was then allowed to dry under vacuum for 24 – 48 hours.

TLC R_f = 0.46 (Propanol / NH₄OH, 4:1)

[α]_D 93.9 (*c* 0.15, MeOH)

¹H NMR (300 MHz, CD₃OD, COSY) δ 7.15 – 7.26 (m, 5H, C₆H₅), 5.13 – 5.17 (m, 1H, CHS), 4.82 – 4.84 (m, 1H, 4-CH), 4.34 – 4.41 (m, 3H, CH₂C₆H₅, 7-CH), 3.83 – 3.85 (m,

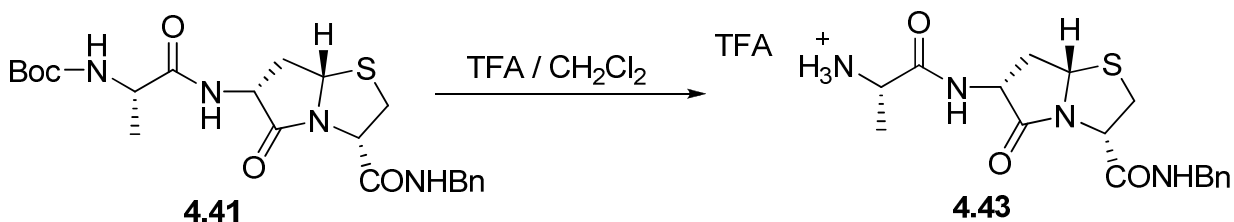
¹H, Ala α -CH), 2.86 – 2.90 (m, 1H, SCH₂), 2.20 – 2.61 (m, 4H, SCH₂, SCH₂CH₂, C8 CH₂), 1.71 – 1.86 (m, 1H, 8-CH₂), 1.39 (d, *J* = 7.2 Hz, 3H, Ala CH₃).

¹³C NMR (75 MHz, CD₃OD, HMQC) δ 174.4 (CO), 172.7 (CO), 172.2 (CO), 141.2 (C₆H₅), 130.8 (C₆H₅), 129.7 (C₆H₅), 129.5 (C₆H₅), 57.6 (CHS), 55.0 (4-C), 52.5 (7-C), 51.3 (Ala α -C), 45.6 (CH₂C₆CH₅), 33.7 (SCH₂), 28.7 (8-C), 27.0 (3-C), 18.4 (Ala CH₃).

ESI HRMS *m/z* calcd for C₁₈H₂₄N₄O₃S + H⁺, 337.1647; found, 337.1619.

HPLC: *t*_R (2% MeOH in 98% CH₃CN) 4.89 minutes; *t*_R (2% H₂O in CH₃CN) 8.39 minutes. Sample was dissolved in MeOH

[(3*S*,6*R*,7*aS*)-6-(2-(*S*)-Amino-propanoyl)amino-5-oxohexahydropyrrolo[2,1-*b*]thiazole-3-*N*-benzyl-carboxamide] Trifluoroacetate Salt. (4.43)



[(3*S*,6*R*,7*aS*)-6-(2-(*S*)-tert-butoxycarbonylamino-propanoyl)amino-5-oxohexahydropyrrolo[2,1-*b*]thiazole-3-*N*-benzyl-carboxamide] (**4.41**, 1.0 g, 2.93 mmol) was dissolved in 4.5 mL of TFA in 5 mL of dry CH₂Cl₂ and the solution was stirred under nitrogen for 24 hours while it was monitored by TLC. Upon completion the reaction was concentrated under reduced pressure. The residue was dissolved in CH₂Cl₂

and evaporated three times to azeotropically remove any last traces of TFA. The white-orange compound (**4.43**) was then allowed to dry under vacuum for 24 – 48 hours.

TLC $R_f = 0.33$ (Propanol / NH_4OH , 4:1)

$[\alpha]_D 108.3$ (c 0.2, MeOH)

^1H NMR (300 MHz, CD_3OD , COSY) δ 7.11 – 7.24 (m, 5H, C_6H_5), 5.00 – 5.05 (t, $J = 6.3$ Hz, 14.1 Hz, 1H, CHS), 4.81 – 4.89 (m, 2H, NCHCONHBn, 7-CH), 4.25 – 4.39 (m, 3H, Ala α -CH, $\text{CH}_2\text{C}_6\text{H}_5$), 3.78 – 3.85 (m, 1H, SCH₂), 3.28 – 3.44 (m, 1H, SCH₂), 2.86 – 2.95 (m, 1H, CH₂CHS), 1.96 – 2.06 (m, 1H, CH₂CHS), 1.43 (d, $J = 7.2$ Hz, 3H, Ala CH₃).

^{13}C NMR (75 MHz, CD_3OD , HMQC) δ 173.0 (CO), 170.4 (CO), 170.3 (CO), 138.9 (C_6H_5), 128.9 (C_6H_5), 127.9 (C_6H_5), 127.6 (C_6H_5), 127.6 (C_6H_5), 62.7 (CHS), 60.4 (NCHCO₂NHBn), 54.0 (Ala α -CH), 49.6 (7-CH), 43.5 (NHCH₂C₆H₅), 36.6 (SCH₂), 35.6 (CH₂CHS), 16.7 (Ala CH₃).

ESI HRMS m/z calcd for $\text{C}_{17}\text{H}_{22}\text{N}_3\text{O}_4\text{S} + \text{H}^+$, 363.1491; found, 363.1491.

HPLC: t_R (2% MeOH in 98% CH_3CN) 5.12 minutes; t_R (2% H_2O in CH_3CN) 5.43 minutes. Sample was dissolved in MeOH

4.7 References:

1. Initial modeling studies were prepared by Dr. Pang's group utilizing the EUDOC modeling program

Pang, Y.P.; Perola, E.; Xu, K.; Prenderast, F. G. EUDOC: A computer program for identification of drug interaction sites in macromolecules and drug leads from chemical databases. *J. Comp. Chem.* **2001**, *22*, 1750 – 1771.

2. Nikolovska-Coleska, Z.; Wang, R.; Fang, X.; Pan, H.; Tomita, Y.; Li, P.; Roller, P. P.; Krajewski, K.; Saito, N. G.; Stuckey, J. A.; Wang, S. Development and optimization of a binding assay for the XIAP – BIR3 domain assay fluorescence polarization. *Anal. Biochem.* **2004**, *332*, 261 – 273.

3. Sun, H.; Nikolovska-Coleska, Z.; Chen, J.; Yang, C.; Tomita, Y.; Pan, H.; Yoskioka, Y.; Krajewski, K.; Roller, P. P.; Wang, S. Structure – based design, synthesis and biochemical testing of novel and potent Smac peptido-mimetics. *Biorganic Med. Chem. Lett.* **2005**, *15*, 793 – 797.

4. Genin, M. J.; Ojala, W. H.; Gleason, W. B.; Johnson, R.L. Synthesis and crystal structure of a peptidomimetic containing the (*R*)-4.4-sprio lactam type-II β – turn mimic. *J. Org. Chem.* **1993**, *58*, 2334 – 2337.

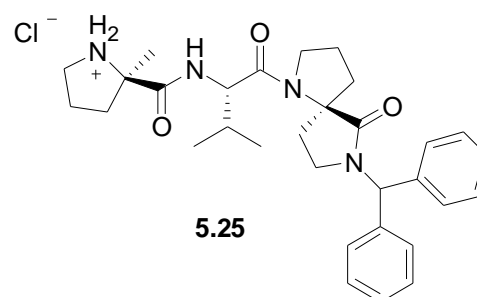
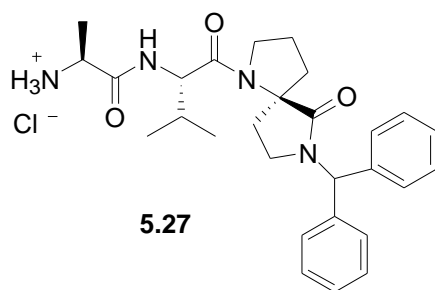
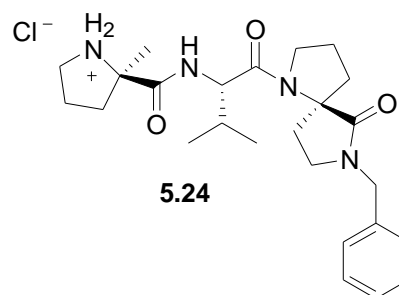
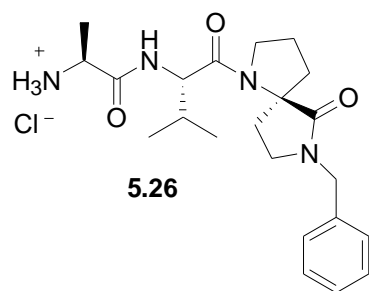
5. Somu, R. V.; Johnson, R. L. Synthesis of pipercolic acid based spiro bicyclic lactam scaffolds as β – turn mimics. *J. Org. Chem.* **2005**, *70*, 5954 – 5963.
6. Subashinge, N. L.; Bontems, R. J.; McIntee, E.; Mishra, R. K.; Johnson, R. L. Bicyclic thiazolidine lactam peptidomimetics of the dopamine receptor modulating peptide Pro-Leu-Gly-NH₂. *J. Med. Chem.* **1993**, *36*, 2356 – 2361.
7. Khalil, E. M.; Pradhan, A.; Ojala, W. J.; Gleason, W. B.; Mishra, R. K.; Johnson, R. L.; Nair, V.; Design, synthesis and dopamine receptor modulating activity of spiro bicyclic peptidomimetics of L-prolyl-L-leucyl-glycinamine. *J. Med. Chem.* **1999**, *42*, 628 – 637.
8. Seebach, D.; Does, M.; Naef, R.; Schwizer, B. Alkylation of amino acids without loss of the optical activity: preparation of *R* – substituted proline derivatives. A case of self-reproduction of chirality. *J. Am. Chem. Soc.* **1983**, *105*, 5390 – 5398.
9. Coppola, G. N. Schuster, H. F. Asymmetric synthesis: construction of chiral molecules using amino acids; Wiley: New York, 1987.
10. Duthaler, R. O. Recent developments in the stereoselective synthesis of α -amino acids. *Tetrahedron* **1994**, *50*, 1539-1650.

11. O'Donnell, M. J.; Bennett, W. D.; Wu, S. The stereoselective synthesis of alpha-amino acids by phase-transfer catalysis. *J. Am. Chem. Soc.* **1989**, *111*, 2353-2355.
12. Myers, A. G.; Gleason, J. L.; Yoon, T. Practical method for the synthesis of D- or L- alpha-amino acids by the alkylation of (+)- or (-)-pseudoephedrine glycinamide. *J. Am. Chem. Soc.* **1995**, *117*, 8488.
13. Lee, B. H.; Miller, M. J.; Constituents of microbial iron chelators. The synthesis of optically active derivatives of δ -N-hydroxy-L-ornithine. *Tetrahedron Lett.* **1984**, *25*, 927 – 930.
14. Karady, S.; Amato, J. S.; Weinstock, I. M. Enantioselective alkylation of acyclic amino acids. *Tetrahedron Lett.* **1984**, *25*, 4337 – 4340.
15. Myers, A. G.; Gleason, J. L.; Yoon, T.; Kung, D. W. Highly practical methodology for the synthesis of D- and L- α -amino acids, N-protected α -amino acids, and N-methyl- α -amino acids. *J. Amer. Chem. Soc.* **1997**, *119*, 656- 673.
16. Myers, A. G.; Schnider, P.; Kwon, S.; Kung, D. W. Greatly simplified procedures for the synthesis of α -amino acids by the direct alkylation of pseudoephedrine glycinamide hydrate. *J. Org. Chem.* **1999**, *64*, 3322 – 3327.
17. Overman, L. E.; Smool, J.; Overman, J. D. The reduction of aryl disulfides with triphenyl phosphine. *Synthesis*, **1974**, 59 – 60.

18. Han, C.; Lee, J. P.; Lobkovsky, E.; Porco, J. A. Catalytic ester – amide exchange using group (IV) metal alkoxide – activator complexes. *J. Am. Chem. Soc.* **2005**, *127*, 10039 – 10044.
19. Chai, J. Structural and biochemical basis of apoptotic activation by Smac/DIABLO. *Nature*, **2000**, *406*, 855 – 862.
20. Wu, G.; Chai, J.; Suber, T. L.; Wu, J.; Du, C.; Wang, X.; Shi, Y. Structural Basis of IAP Recognition by Smac / DIABLO. *Nature* **2000**, *408*, 1008-1012.
21. Sun, C. NMR structure and mutagenesis of the inhibitor of apoptosis protein XIAP. *Nature*, **1999**, *401*, 818 – 822.
22. Shi, Y. Survivin structure: crystal unclear. *Nature Struct. Biol.* **2000**, *7*, 620 – 623.
23. Verdecia, M.A. Structure of the human anti-apoptotic protein surviving reveals a dimeric arrangement. *Nature Struct. Biol.* **2000**, *7*, 602 – 608.
24. Chantalat, L. Crystal structure of human surviving reveals a bow tie shaped dimer with two unusual alpha helical extensions. *Mol. Cell* **2000**, *6*, 183 – 189.

Chapter 5. The Stereoselective Synthesis of ϕ_1 , ϕ_3 , ψ_3 , and ϕ_3 , ψ_3 Constrained AVPI

Mimics.



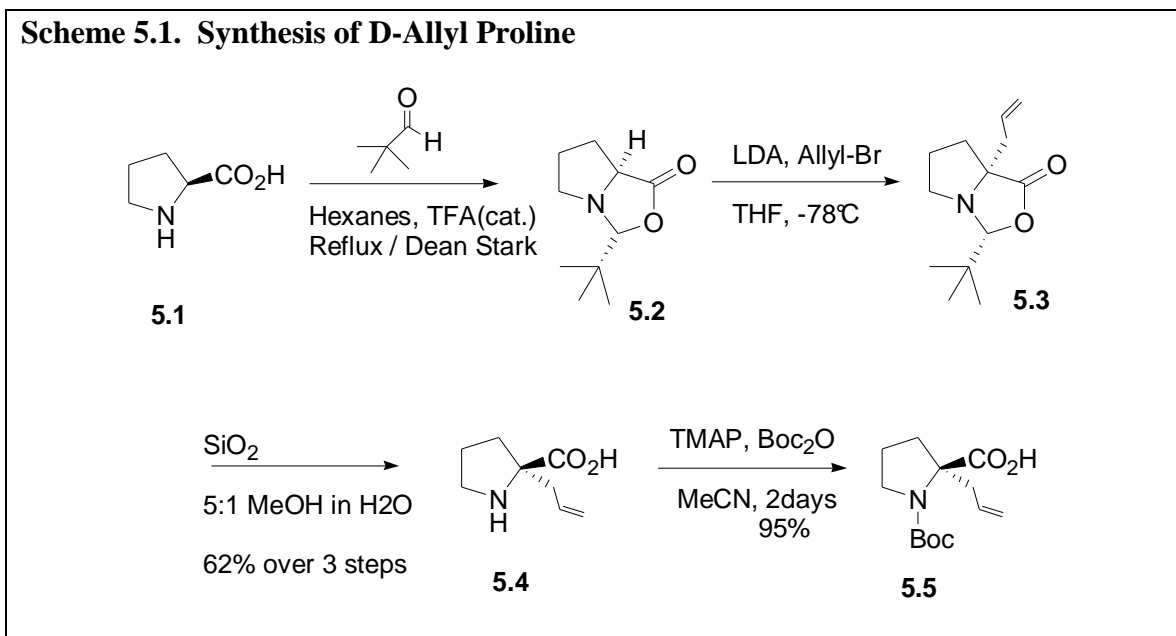
5.1 Design and Scope

The last set of constraints that were imposed upon the AVPI peptide were designed to constrain the ϕ_1 , ϕ_3 , ψ_3 and ϕ_3 , ψ_3 torsion angles. These angles correspond to the ϕ_3 angle at the P3 position of AVPI which is constrained by proline in the native peptide. Previous research by Dr. Genin in our lab suggests that incorporation of a 4.4 spirocycle will constrict the ϕ_3 , ψ_3 torsion angles to roughly -50° and 130° respectively.^{1,2} Initial modeling suggested that the AVPI peptide backbone will coincide with the spatial positioning of the spirocyclic compounds.³ The modeling studies also suggest that the restriction of these torsion angles may maximize the interactions of the P4 position of AVPI. In the native AVPI peptide, the P4 side chain interacts with a hydrophobic pocket

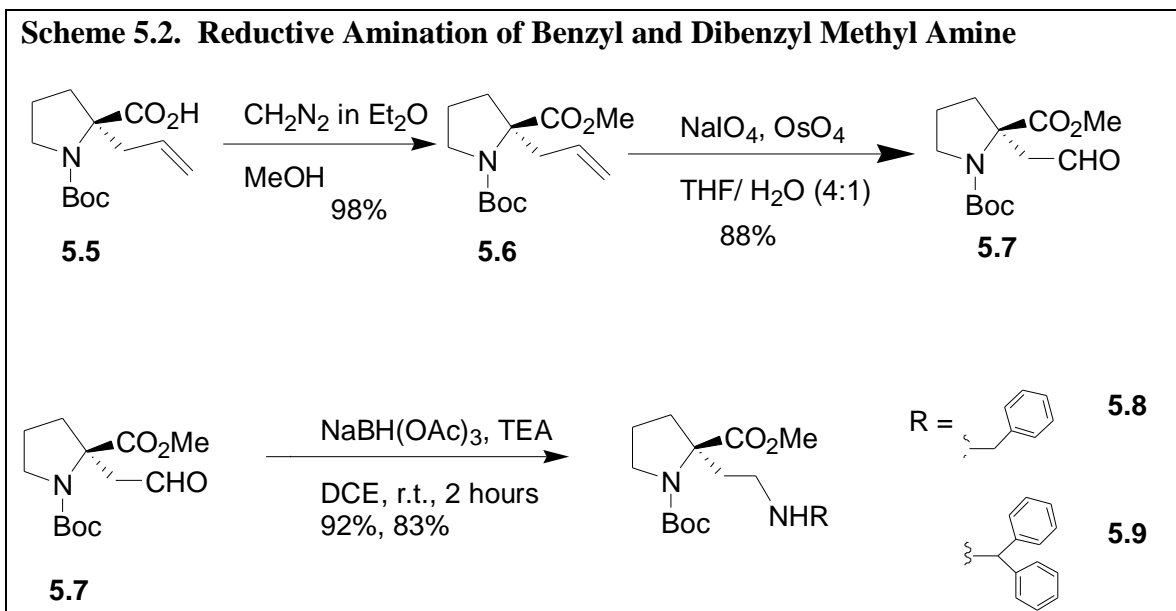
which previous research has shown may be neatly mimicked by the replacement of the isoleucine side chain with the benzyl moiety.^{4,5} Modeling suggests that the benzyl amide group will interact with the hydrophobic residues as well as form the requisite hydrogen bonding interactions.³ Similar compounds lacking the spirocyclic structure of our compounds but with the P4 benzyl amide showed a 28 nM K_i in a study by the Wang group that was discussed in **Chapter 2**.^{5,6} This chapter will focus on the synthesis and biological testing of the spirocyclic compounds illustrated above.

5.2. Synthetic Strategy

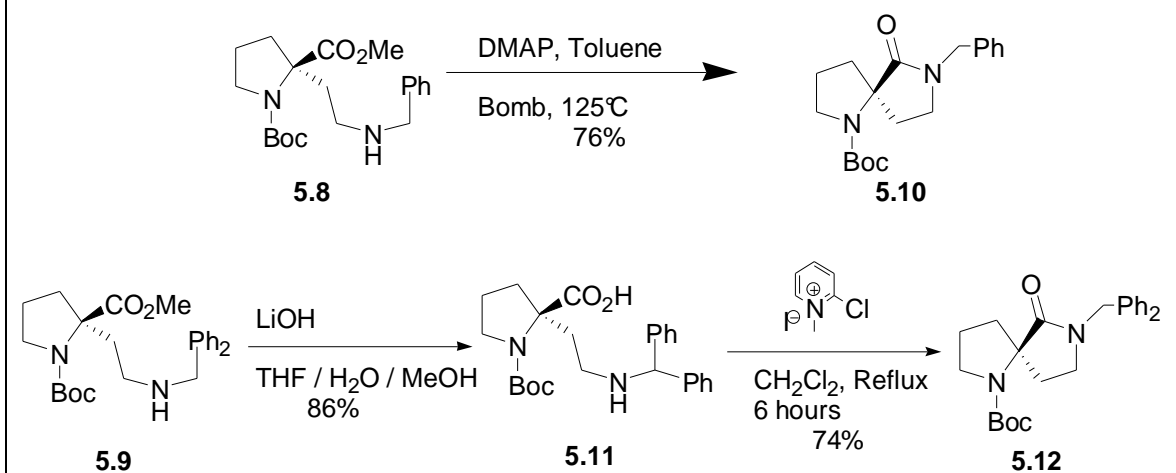
4.4-Spirocycle derivatives have generally been synthesized through two strategies. The original strategy was utilized by Ward *et. al.* for the production of L-Pro-L-Leu derivatives.⁷ The methodology involves reductive *N*-alkylation of the C-terminal amino acid followed by formation of a lactam. The second method was developed within our laboratory to synthesize L-Pro-L-Gly derivatives by Dr. Khalil and Dr. Genin utilized a strategy developed by the Hind lab.^{2,8,9,10} For this synthesis we started by synthesizing the Boc protected α -alkylated proline using the Seebach methodology¹¹⁻¹⁴ shown in **Scheme 5.1** and described in detail in **Chapter 3**.



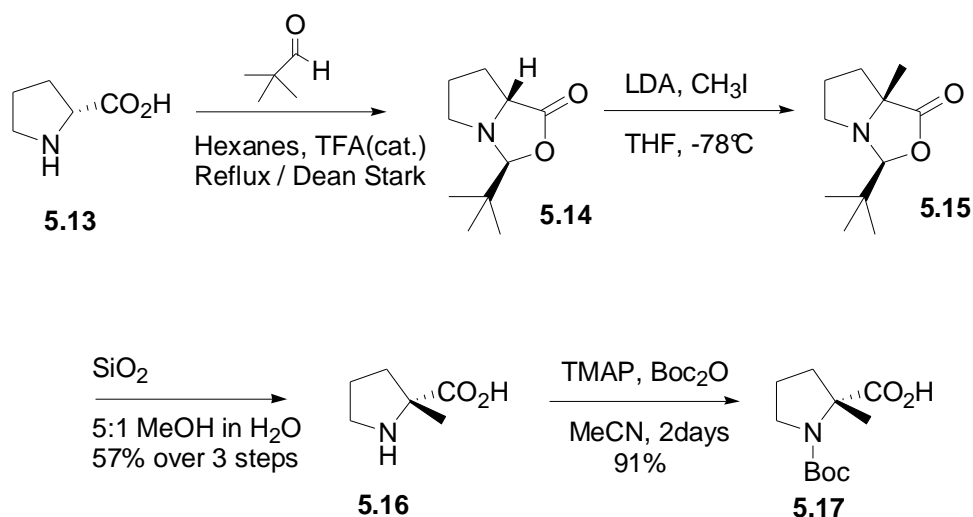
The alkylated proline (**5.5**) was converted to the methyl ester (**5.6**) utilizing standard diazomethane conditions and subsequently converted to the aldehyde (**5.7**) through oxidative cleavage of the double bond (**Scheme 5.2**). This compound was then purified through silica gel chromatography and taken forward. Reductive amination of the aldehyde with both benzyl amine (**5.8**) and diphenyl methyl amine (**5.9**) proceeded smoothly to the desired product (**Scheme 5.2**).



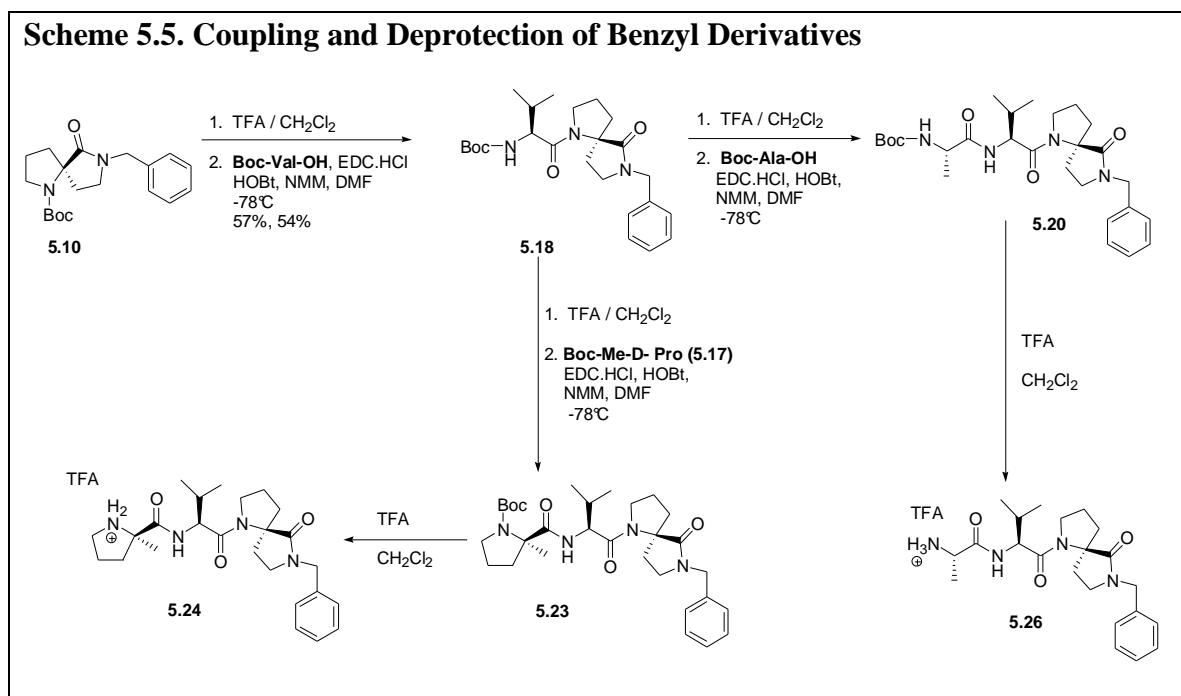
To form the 4.4 spirocycle (**5.10**, **5.12**) we initially pursued the direct heat induced cyclization in toluene at 125 °C in the presence of DMAP. This methodology proceeded smoothly with the benzyl derivative (**5.10**) in a clean 76% yield (**Scheme 5.3**). The diphenyl methyl derivative (**5.9**), however, was resistant to the thermal cyclization and did not yield any product. Hydrolysis of the methyl ester (**5.11**) and subsequent cyclization with Mukaiyama's coupling reagent provided the spirocycle (**5.12**) in 74% after 6 hours of reflux and purification through silica gel flash chromatography (**Scheme 5.3**).

Scheme 5.3. Synthesis of Benzyl and Dibenzyl 4.4 Spirocycles


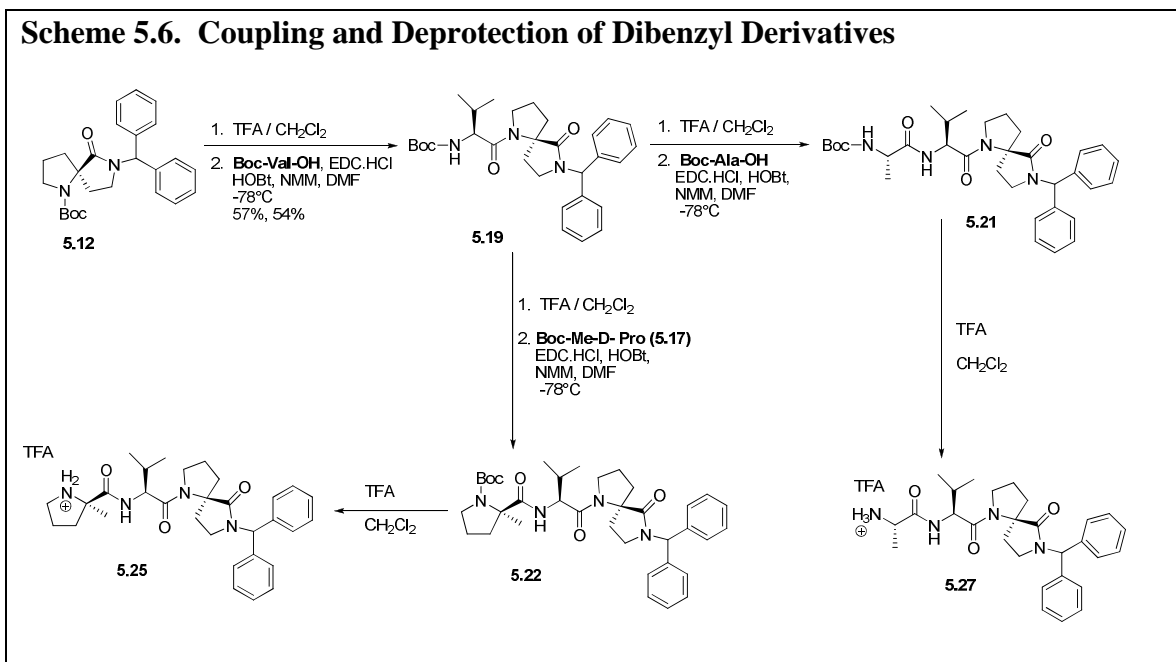
The last building block that was made was α -Me-D-proline (**5.16**) utilizing the now familiar Seebach methodology.¹¹⁻¹⁴ In this case, D-proline (**5.13**) was used in place of the the L-proline as the starting material. Alkylation of this derivative was accomplished using methyl iodide as the alkylating agent to yield the α -Me-D-proline (**5.16**) which was then Boc protected (**5.17**) using the phase transfer methodology developed by Dr. Khalil (**Scheme 5.4**).¹⁴

Scheme 5.4. Synthesis of α -Me-D-Proline


Deprotection of the spirocycle derivatives followed by coupling with Boc-valine using standard solution phase coupling conditions of HOBt and EDC•HCl in DMF while letting it warm gradually from $-78\text{ }^{\circ}\text{C}$ to room temperature produced the tripeptide mimics (**5.18**, **5.19**).



The two valine derivatives (**5.18**, **5.19**) were both deprotected again and coupled to both Boc-alanine and Boc- α -Me-D-proline which produced the four final compounds (**5.24** - **5.27**) after purification and subsequent deprotection (**Scheme 5.5** and **5.6**).



5.3 Biological Testing

The final molecules were shipped to our collaborator Dr. Scott Kauffman at the Mayo Medical Clinic. For these compounds as well as the compounds from **Chapter 3**, Dr. Kaufmann's group investigated a new assay method. Unlike the biological assay in **Chapter 2**, this assay is a direct binding assay utilizing a competitively binding fluorescent protein. The fluorescent protein was generated by expressing a DS-red-BIR3-GST fusion protein in *E. coli* bacteria and purified with glutathione agarose. DS-red is the fluorescence generating segment of our fusion protein which is coupled to the caspase 9 binding domain, BIR3. This segment was then fused to the GST selection sequence which allowed this fusion protein to be purified on glutathione agarose before use in the binding assay. The completed fusion protein was over expressed with *E. coli* bacteria and subsequently purified and used in the biological assay as the competitive binding agent and complete binding negative control.

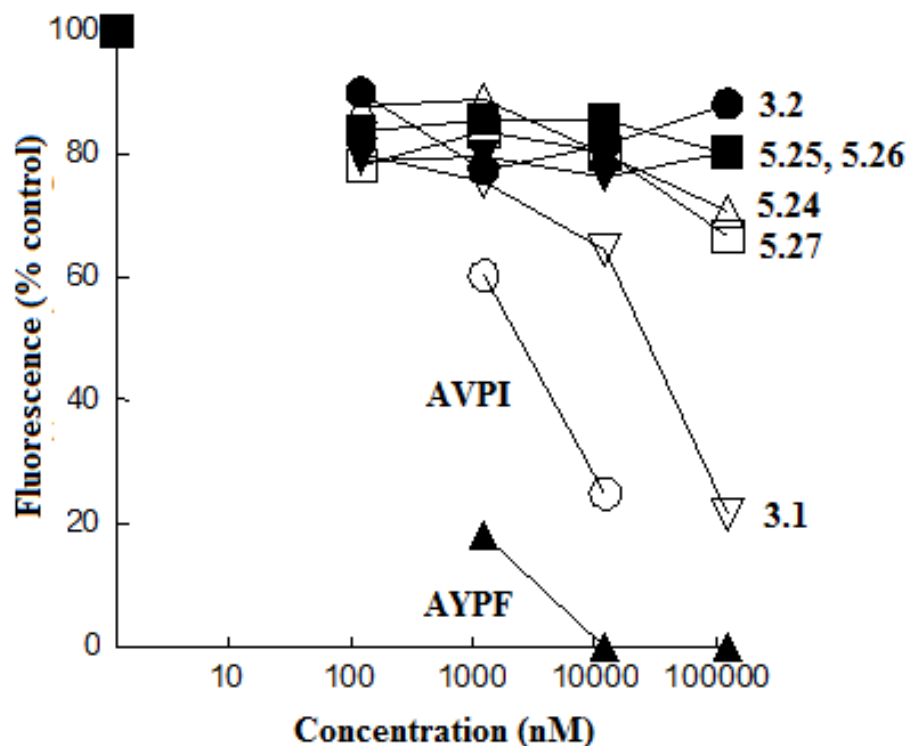


Figure 5.1. Concentration Depend Binding Assay of AVPI Peptidomimetics

The purified fusion protein, DS-red-BIR3-GST, was incubated in the presence or absence of the ϕ_1 , ϕ_3 , ψ_3 , and ϕ_3 , ψ_3 constrained compounds in concentration varying from 0.1 μM – 100 μM . After incubation the plates were washed with buffer to remove free protein and the fluorescence intensity was measured. Fluorescence intensities were compared as a percentage of the control DS-red-BIR3-GST fusion protein when incubated in the absence of competitors. The native caspase 9 AYPF peptide demonstrated an approximated IC_{50} of less than 1 μM while the native terminal tetrapeptide of Smac, AVPI, was $\approx 5 \mu\text{M}$. The methyl ester derivative of the ϕ_1 , ϕ_3 , ψ_3 , and ϕ_3 , ψ_3 constrained compounds was the only compound in the entire series for this chapter and **Chapter 3** that showed measurable activity. The IC_{50} of $\approx 50 \mu\text{M}$ was disappointing but still a more positive result than the greater than 100 μM IC_{50} of the

methyl amide derivative. These slightly disappointing results led once again to further retro – modeling analysis of the compounds in order to glean any further information that was readily available.

5.4. Retrosynthetic Modeling Analysis of the Constrained Peptidomimetics

Modeling analysis of the ϕ_1 , ϕ_3 , ψ_3 , and ϕ_3 , ψ_3 constrained AVPI mimics was performed upon the same *in silico* protein that was built and tested in **Chapter 2**. The terminal tetrapeptide of Smac binds to a surface groove, 892 Å total surface area,^{4, 15} on BIR3 formed by the β -strand and the α_3 helix. Val2 and Pro3 form a short anti-parallel β -strand.¹⁵ The native AVPI forms a total of eight inter-molecular hydrogen bonds with the BIR3 domain.^{4, 15} Ala 1 of the tetrapeptide forms 5 of the eight hydrogen bonds with Glu 142 and Asp 138 as well as with Glu 132, thus, demonstrating the critical nature of the Ala1 in the tight binding of the peptide to the surface groove.¹⁵ These modeling data correlate well with data obtained from other BIR3 domains such as survivin.¹⁶⁻¹⁹

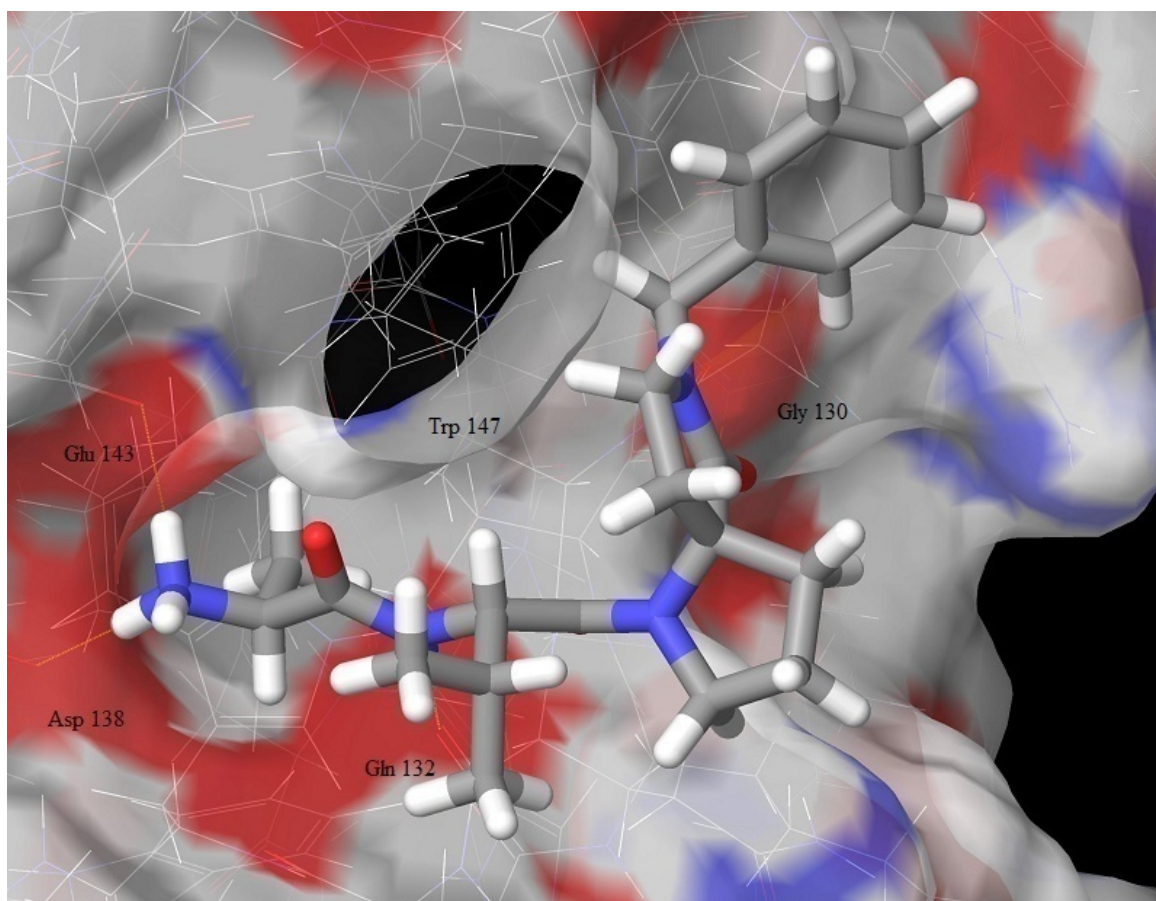


Figure 5.2. Retrosynthetic Modeling of Ala-Val-[7-Benzyl-6-oxo-1,7-diazaspiro[4.4]nonane] (5.26)

The φ_3 , ψ_3 benzyl derivative (**5.26**) was modeled first (**Figure 5.2**) and docked into the active site using a flexible docking option of the Glide software with 1000 iterations of possible conformations being selected for all modeling attempts. The gross morphology of the docking of **5.26** is the same as that for AVPI at the P1 pocket. The constraints at the P1 position places the side chain into the same hydrophobic pocket as well as having the same hydrogen bonding at P1 to Glu 142. The molecule also forms the second H-bond to Asp 138 that AVPI displays. The P2 nitrogen of valine forms a hydrogen bond with Gln 132, which is similar to AVPI. The P4 position in the secondary pocket does not enter into the expected hydrophobic-aromatic interactions that we

initially predicted. Taken together the Glide program assigned a GScore value of -7.39 as compared to the -8.01 value it assigned to the native ligand, AVPI. The GScore value should correlate to an activity near that of the native peptide.

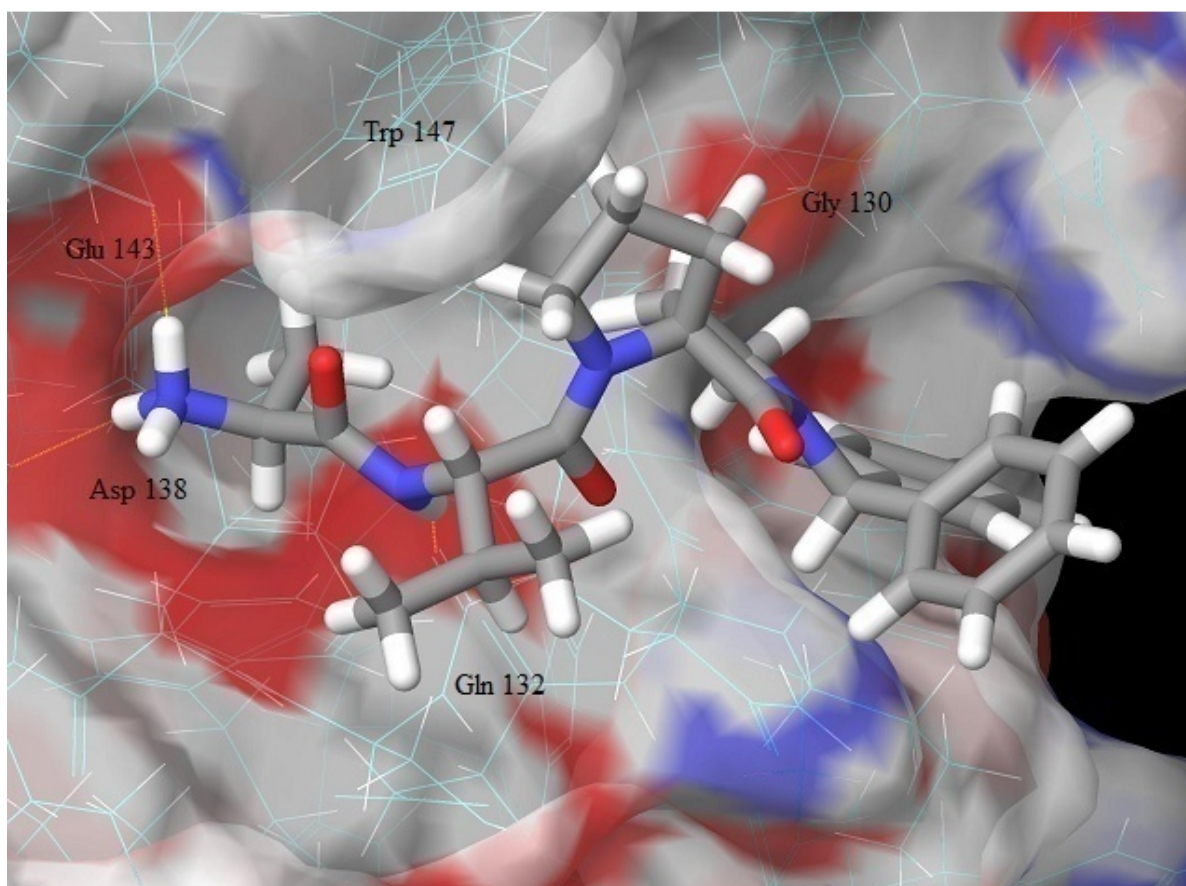


Figure 5.3. Retrosynthetic Modeling of Ala-Val-7-Benzhydryl-6-oxo-1,7-diaza-spiro[4.4]nonane (5.27)

The ϕ_3, ψ_3 dibenzyl derivative (**5.27**) was modeled next (**Figure 5.3**) and docked into the active site using the same modeling parameters as **5.26**. The gross morphology of the docking of the dibenzyl is the same as that for AVPI. The constraints at the P1 position places the side chain into the same hydrophobic pocket as well as having the same hydrogen bonding as the native peptide. The dibenzyl derivative (**5.27**) differs from the benzyl (**5.26**) in the interaction at the P4 position. Compound **5.27** does favor

the aromatic interactions with the secondary pocket while **5.26** did not favor them. Taken together the Glide program assigned a GScore value of -7.00 as compared to the -8.01 value it assigned to the native ligand, AVPI. The GScore value should correlate to an activity within the Wang assay of greater than a 100 μM K_i . Within the biological assay performed by the Kauffman laboratory this predictor would correlate to baseline activity.

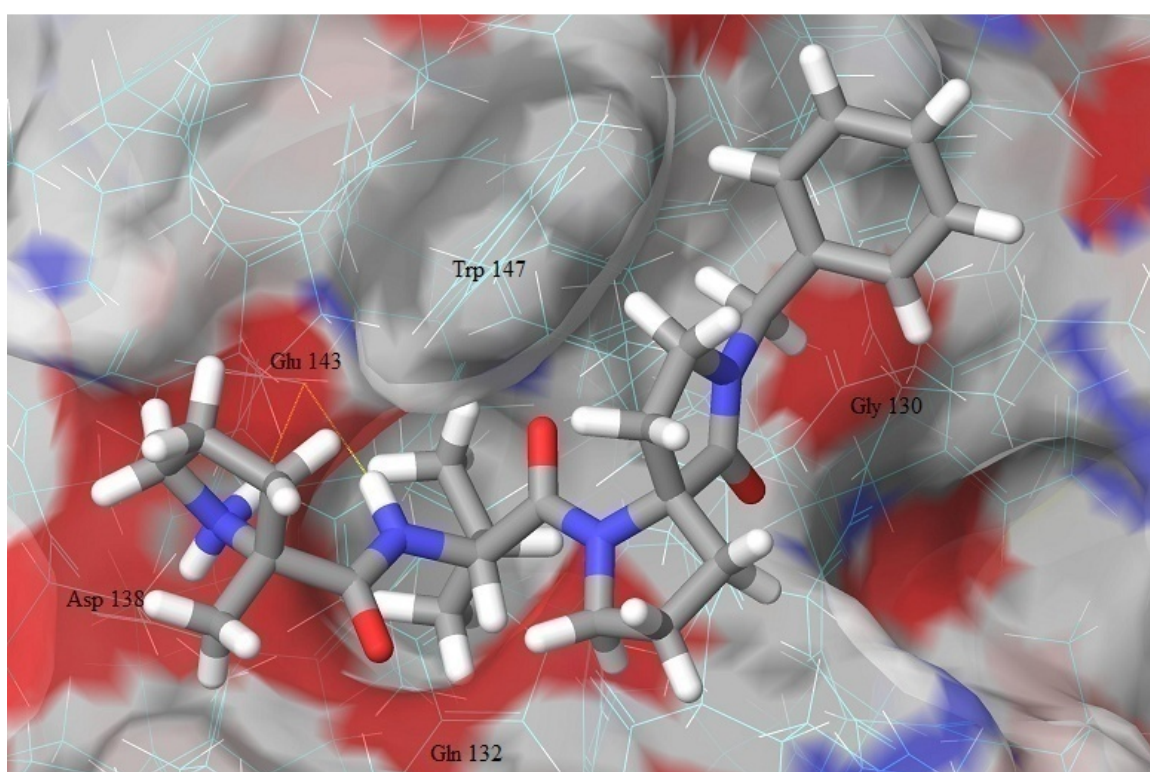


Figure 5.4. Retrosynthetic Modeling of α -Me-D-Pro-Val-[7-Benzyl-6-oxo-1,7-diazaspiro[4.4]nonane](5.24)

The φ_1 , φ_3 , ψ_3 benzyl derivative (**5.24**) was modeled next (**Figure 5.4**) and docked into the active site using the same parameters as compound **5.26**. The gross morphology of the docking of **5.24** is the same as that for **5.26** at the P1 pocket as well as for the P4

interactions. The constraints of the more highly constrained α -Me-D-Proline at the P1 position places the side chain outside of the hydrophobic pocket the is accessed by AVPW. **5.24** is also missing the H-bonding at the P1 position to Asp 138 as seen in the native peptide and **5.26**. Like **5.26** the benzyl side chain does not favor the aromatic interaction that we predicted. Taken together the Glide program assigned a GScore value of -5.03 as compared to the -8.01 value it assigned to the native ligand, AVPI. The GScore value should correlate to an activity within the Wang assay of greater than a 100 μM K_i . Within the biological assay performed by the Kauffman laboratory this predictor would correlate to baseline activity.

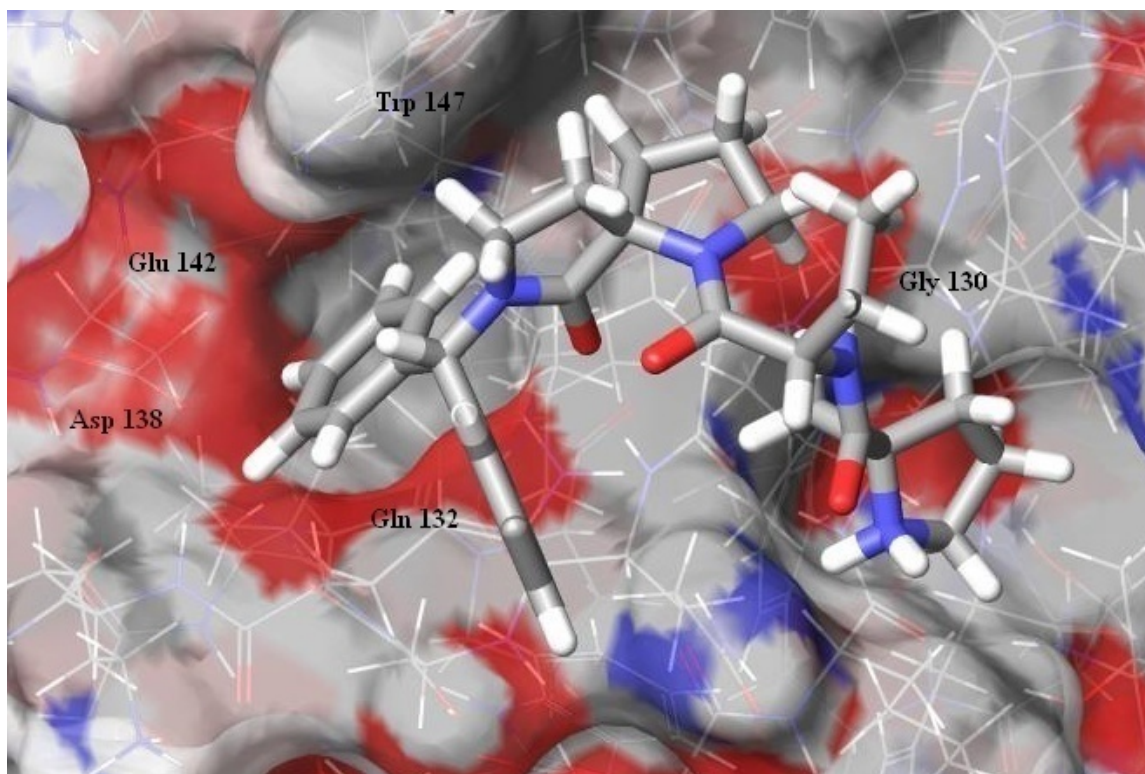
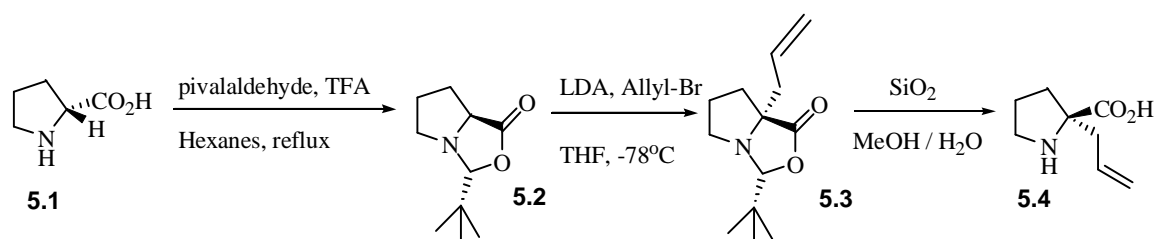


Figure 5.5. Retrosynthetic Modeling of α -Me-D-Pro-Val-[1-(7-benzhydryl-6-oxo-1,7-diaza-spiro[4.4]nonane)] (5.25)

. When the ϕ_1 , ϕ_3 , ψ_3 dibenzyl derivative was docked into the active site of utilizing the Schrödinger flexible docking program (also as described in **Chapter 2**) the ϕ_1 , ϕ_3 , ψ_3 dibenzyl derivative docked in the reverse orientation of what we would have initially proposed. The native peptide utilizes the two binding pockets through multiple hydrogen bonds to the P1 position in the first pocket and through Gly 130 hydrogen bonding and aromatic interaction in the second pocket. The ϕ_1 , ϕ_3 , ψ_3 dibenzyl derivative displays no hydrogen bonding interactions and this orientation with GScore of -2.89 and taken together will have a K_i greater than $100 \mu\text{M}$. Within the biological assay performed by the Kauffman laboratory this predictor would correlate to baseline activity.

5.5. Experimentals

α -Allyl-L-Pro-OH (5.4)



L-Proline (**5.1**) (10 g, 86.7 mmol) was dried under heat and vacuum for 10-15 minutes and then pulverized into a fine powder. To this powder was added 1 drop of TFA mixed in hexanes. The hexanes were evaporated under a light stream of N_2 . To the resulting white powder was added 50 mL of hexanes and pivalaldehyde (28.3 mL, 260 mmols). The reaction was then heated overnight using a Dean Stark trap for water capture. In the morning the reaction was carefully concentrated *in vacuo* to a yellow oil.

The resultant oxazolidinone (**5.2**) was then carried on to the alkylation reaction without any further purification.

Freshly distilled THF (200 mL) was added to the round bottom flask containing the oxazolidinone. The solution was then cooled to $-78\text{ }^{\circ}\text{C}$ before a 1M solution of LDA (95.4 mL) was cannulated into the reaction with vigorous stirring. After 10 minutes of stirring, allyl bromide (8.1 mL, 95.4 mmol) was added via syringe to the solution and it was then allowed to rise to room temperature over 2-3 hours. The reaction was concentrated under reduced pressure with minimal heat and partitioned between Et_2O and water. The pH of the water layer was checked to confirm basicity and then washed 2 more times with Et_2O . The organic layers were concentrated under reduced pressure after being dried over MgSO_4 . The product (**5.3**) was taken forward to the next step without further purification.

The alkylated oxazolidinone (**5.3**) was hydrolyzed by dissolving it in a 5:1 MeOH / H_2O with a total volume of 250 mL. Silica gel (20 g) was added to that solution and the resulting suspension was stirred at room temperature for 48-72 hours. The reaction mixture was filtered on a fritted Buchner funnel and the filtrate was evaporated *in vacuo* to a yellowish solid. This solid was then boiled in ethyl acetate until a white solid resulted and the ethyl acetate turned yellow. The resulting white solid (**5.4**) was then crystallized from methanol/isopropyl alcohol to yield 7.73 g of clear crystals (57.4%).

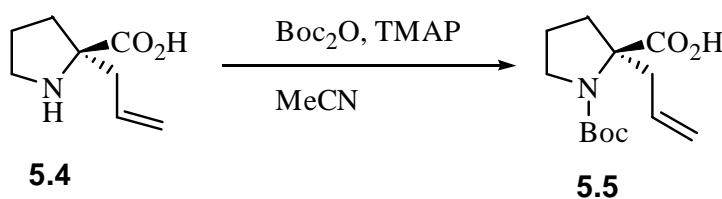
TLC $R_f = 0.16$ (Propanol/ NH_4OH , 4:1)

$[\alpha]_D^{25} 70.3$ (c 1.0, MeOH)

^1H NMR (300 MHz, CD_3OD): ^{13}C δ 4.94 (1H, d, NH), 3.32-3.47 (1H, m, $\delta\text{-CH}_2$), 3.25-3.31 (1H, m, $\delta\text{-CH}_2$), 2.38-2.45 (1H, dd, $\beta\text{-CH}_2$), 1.80-2.10 (3H, m, $\beta\text{-CH}_2$, $\gamma\text{-CH}_2$), 1.59 (3H, s, $\alpha\text{-CH}_3$).

^{13}C NMR (75 MHz, CDCl_3): δ 175.5 (CO_2H), 70.5 ($\alpha\text{-C}$), 45.2 ($\delta\text{-CH}_2$), 35.9 ($\alpha\text{-C}(\text{CH}_3)$), 23.4 ($\beta\text{-CH}_2$), 21.1 ($\gamma\text{-CH}_2$).

Boc- α -Allyl-L-Pro-OH (5.5)



α -Allyl proline (**5.4**) (7 g, 45.1 mmol) and tetramethylammonium pentahydrate (9.0 g, 49.6 mmol) were added to MeCN (150 mL) which had been freshly distilled from CaH_2 . The mixture was stirred at room temperature until a clear solution formed. Boc_2O (19.69 g, 90.2 mmols) was added to the solution and allowed to continue stirring for 1 day. On the second day another equivalent of Boc_2O (4.93 g, 22.6 mmols) was added and the solution was stirred for another day after which MeCN was removed *in vacuo*. The residue was then partitioned between H_2O (100 mL) and Et_2O (100 mL). The aqueous layer was washed with an additional portion of ether and then acidified with solid citric acid to pH 3–4. The aqueous fraction was then extracted 3 times with ethyl acetate (100 mL). The combined organic fractions were then washed with H_2O (150 mL) and brine (150 mL), dried with MgSO_4 , and then concentrated *in vacuo* to give N-Boc- α -allyl-L-proline as a white solid. (**5.5**) The white solid was crystallized from boiling ethyl acetate to yield 11.1 grams of product as white crystalline needles (96.4%).

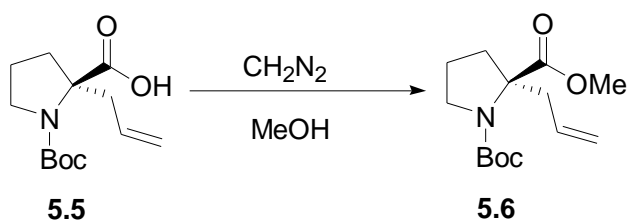
TLC $R_f = 0.54$ (MeOH / EtOAc, 1:50)

$[\alpha]_D 70.7$ (c 1.0, CHCl_3)

$^1\text{H NMR}$ (300 MHz, CDCl_3 , COSY, *rotamers present*):²⁰ δ 5.61 - 5.75 (m, 1H, $\text{CH}=\text{CH}_2$), 5.09 - 5.17 (m, 2H, $\text{CH}=\text{CH}_2$), 3.65 - 3.71 and 3.48 - 3.56 (m, 1H, $\delta\text{-CH}_2$), 3.24 - 3.40 (m, 1H, $\delta\text{-CH}_2$), 2.88 - 3.00 (m, 1H, $\text{CH}_2\text{CH}=\text{CH}_2$), 2.52 - 2.69 (m, 1H, $\text{CH}_2\text{CH}=\text{CH}_2$), 2.40 - 2.48 and 2.12 - 2.16 (m, 1H, $\beta\text{-CH}_2$), 1.73 - 2.03 (m, 3H, $\gamma\text{-CH}_2$, $\beta\text{-CH}_2$), 1.41 - 1.46 (s, 9H, $\text{Boc}(\text{CH}_3)_3$).

$^{13}\text{C NMR}$ (75 MHz, CDCl_3 , *rotamers present*): δ 180.8 and 176.7 (CO), 153.8 and 156.2 (Boc-CO), 132.2 and 133.2 ($\text{CH}=\text{CH}_2$), 119.4 and 120.0 ($\text{CH}=\text{CH}_2$), 80.8 and 81.6 (Boc-C(CH_3)₃), 67.2 and 69.4 ($\alpha\text{-C}$), 48.8 and 49.5 ($\delta\text{-C}$), 38.4 and 39.5 ($\text{CH}_2\text{CH}=\text{CH}_2$), 35.2 and 37.4 ($\beta\text{-C}$), 28.7 (Boc-C(CH_3)₃), 22.9 and 23.1 ($\gamma\text{-C}$).

N-Boc- α -Allyl-L-Pro-OMe (**5.6**)



Boc-allyl-L-proline (**5.5**) (2.0 g, 7.83 mmol) was dissolved in MeOH (50 mL) and this solution was cooled in an ice bath. A solution of CH_2N_2 in Et_2O was poured into the reaction vessel until a light yellow color persisted. The reaction was then concentrated *in vacuo* to yield a light yellow oil which was purified by flash chromatography (5 x 15 cm) eluting with ethyl acetate in hexanes (1:3), to yield 2.09 g (99.1%) of a light yellow oil which was the desired methyl ester (**5.6**).

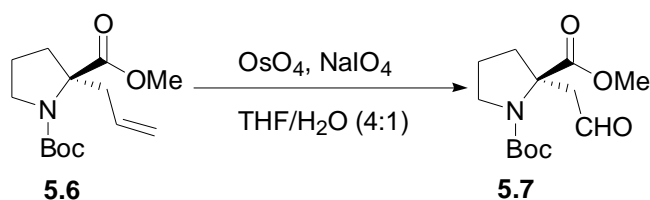
TLC: $R_f = 0.35$ (EtOAc / Hexanes, 1:9)

$[\alpha]_D^{25}$ 73.1 (*c* 0.2, MeOH)

^1H NMR (300 MHz, CDCl_3 , COSY, *rotamers present*)²⁰: δ 5.62 - 5.76 (m, 1H, $\text{CH}=\text{CH}_2$), 5.02 - 5.08 (m, 2H, $\text{CH}=\text{CH}_2$), 3.65 (s, 3H, CO_2CH_3), 3.49 - 3.67 (m, 1H, $\delta\text{-CH}_2$), 3.23 - 3.35 (m, 1H, $\delta\text{-CH}_2$), 3.35 and 2.86 (dd, $J = 6.9$ Hz, 14.1 Hz, 1H, $\text{CH}_2\text{CH}=\text{CH}_2$), 2.54 (dd, $J = 8.4$ Hz, 14.1 Hz, 1H, $\text{CH}_2\text{CH}=\text{CH}_2$), 1.94 - 2.09 (m, 2H, $\beta\text{-CH}_2$), 1.69 - 1.87 (m, 2H, $\gamma\text{-CH}_2$), 1.35 - 1.39 (s, 9H, $\text{Boc-C}(\text{CH}_3)_3$).

^{13}C NMR (75 MHz, CDCl_3 , *rotamers present*): δ 174.9 and 175.1 (CO), 153.6 and 153.9 (Boc-CO), 133.4 and 133.7 ($\text{CH}=\text{CH}_2$), 118.8 and 119.1 ($\text{CH}=\text{CH}_2$), 79.6 and 80.2 (Boc- $\text{C}(\text{CH}_3)_3$), 67.1 and 67.7 ($\alpha\text{-C}$), 52.3 (COCH_3), 48.6 and 48.7 ($\delta\text{-C}$), 38.6 and 39.9 ($\text{CH}_2\text{CH}=\text{CH}_2$), 35.9 and 37.2 ($\beta\text{-C}$), 28.6 and 28.7 (Boc- $(\text{CH}_3)_3$), 22.9 and 23.4 ($\gamma\text{-C}$).

(R)-N-(tert-Butoxycarbonyl)-2-(formylmethyl)proline Methyl Ester (5.7)



Boc-allyl-L-proline-OMe (**5.6**) (1.0 g, 3.71 mmol) was dissolved in a 4:1 mixture of THF in H_2O . This solution was stirred under N_2 and turned dark brown when OsO_4 (50mg) was added as a 2.5% solution in *t*-BuOH. After 5 minutes of stirring, NaIO_4 (2.0 g, 7.42 mmol) was added in three batches over a 90 minute period. At this point the reaction turned light yellow and stirring was continued for 5 hours. The reaction was then diluted with Et_2O and extracted three times with successive Et_2O washes (100 mL). The Et_2O layers were combined, washed with H_2O (150 mL), saturated Na_2SO_3 (150 mL)

and dried with MgSO_4 . Removal of the solvent *in vacuo* gave a tan oil. The oil was purified by silica gel flash chromatography (5 x 8cm) and eluted with ethyl acetate in hexanes (1:3). The isolated clear oil yielded 0.89 g (89%) of the pure compound (**5.7**).

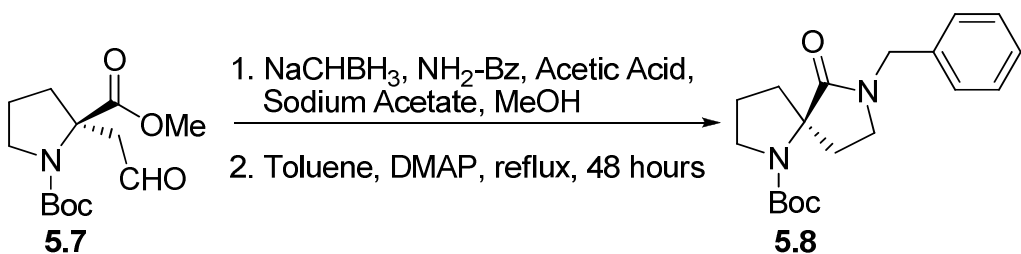
TLC: $R_f = 0.60$ (EtOAc / Hexanes, 1:3)

$[\alpha]_D^{25}$: +35.2 (*c* 0.89, MeOH)

^1H NMR (300 MHz, CDCl_3 , rotamers present)²⁰: δ 9.57 and 9.58 (s, 1H, CHO), 3.49 and 3.52 (s, 3H, OCH_3), 3.21 - 3.46 (m, 2H, δ - CH_2), 2.52 - 2.86 (m, 2H, CH_2CHO), 1.92 - 2.08 (m, 2H, β - CH_2) 1.64 - 1.80 (m, 2H, γ - CH_2), 1.17 and 1.19 (s, 9H, Boc $\text{C}(\text{CH}_3)_3$).

^{13}C NMR (75 MHz, CDCl_3 , rotamers present): δ 199.5 and 199.6 (CHO), 173.6 and 173.8 (CO), 152.8 and 154.1 (Boc-CO), 80.1 and 80.8 (Boc- $\text{C}(\text{CH}_3)_3$), 65.8 and 66.2 (α -C), 52.5 and 52.6 (COCH_3), 48.7 and 49.2 (CH_2CHO), 48.0 (δ -C), 37.2 and 38.2 (β -C), 28.3 and 28.4 (Boc- $\text{C}(\text{CH}_3)_3$), 22.8 and 23.3 (γ -C).

(R)-tert-Butoxycarbonyl-7-Benzyl-6-oxo-1,7-diaza-spiro[4.4]nonane (5.8)



(R)-tert-butyl 7-benzyl-6-oxo-1,7-diazaspiro[4.4]nonane-1-carboxylate

The aldehyde (**5.7**) (1.0 g, 3.7 mmol) was dissolved in a solution of MeOH buffered with acetic acid (0.22 g, 3.67 mmol) and sodium acetate (0.6 g, 7.3 mmol), 4Å molecular sieves (3.7 g) and benzyl amine (0.48 g, 4.44 mmol). The sodium

cyanoborohydride (0.47 g, 7.4 mmol) was then added in a single addition and the reaction was stirred at room temperature until the aldehyde was consumed (~1-3 hours). Once the reaction was complete 10% aqueous HCl was added carefully to a pH of 2 to destroy any excess sodium cyanoborohydride. The aqueous layer was adjusted to pH 10 with saturated NaHCO₃ and extracted twice with ethyl acetate (150 mL). The combined organic layers were washed twice with brine (100 mL), dried with MgSO₄, filtered and concentrated *in vacuo* to provide the reductive amination product as a light yellow oil which was taken forward without further purification.

The light yellow oily residue was dissolved in 200 mL of toluene with a catalytic amount of DMAP (0.08 mmol) and refluxed for 48 hours. The reaction vessel was then cooled and the mixture was concentrated to remove toluene. The concentrate was then partitioned between water (150 mL) and ethyl acetate (150 mL). The ethyl acetate layer was then washed with brine (100 mL), dried over MgSO₄ and concentrated *in vacuo*. The residue was then purified by column chromatography (3 x 8cm) eluting with ethyl acetate in hexanes (1:1) to yield 0.5 grams (78%) of pure **5.10** as a clear oil.

TLC: R_f = 0.21 (EtOAc / Hexanes, 1:1)

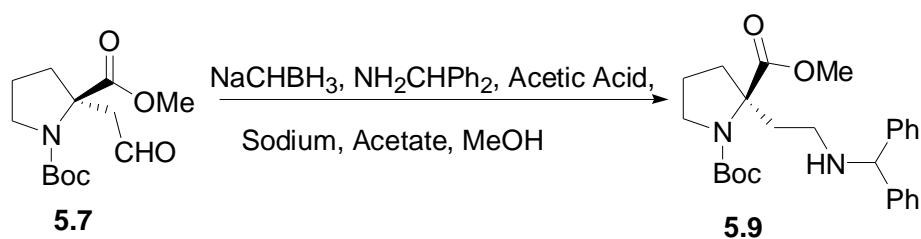
[α]_D -73.3 (c 0.15, MeOH)

¹H NMR (300 MHz., CDCl₃, COSY, *rotamers present*): δ 7.15-7.28 (m, 5H, C₆H₅), 3.95 and 4.82 (1H, J = 14.4 Hz, d, CH₂C₆H₅), 4.22 and 4.67 (1H, J = 14.4 Hz, d, CH₂C₆H₅), 3.42 - 3.63 (2H, m, Pro δ-CH₂), 2.72 - 2.96 (m, 2H, CONCH₂), 2.37 and 2.54 (1H, J = 9.0 Hz, dd, COCH₂), 1.72 - 2.11 (5H, m, COCH₂, Pro β-CH₂, Pro γ-CH₂), 1.32 and 1.40 (9H, s, Boc-C(CH₃)₃)

^{13}C NMR (75 MHz, CDCl_3 , HMQC, *rotamers present*): δ 174.6 (Pro-CO), 174.5 (CON), 153.6 (Boc-CO), 136.7 and 136.4 (C_6H_5), 128.9 (C_6H_5), 128.8 (C_6H_5), 128.6 (C_6H_5), 128.3 (C_6H_5), 127.8 (C_6H_5), 127.6 (C_6H_5), 79.8 and 80.2 (Boc- $\text{C}(\text{CH}_3)_3$), 67.1 and 67.3 (Pro α -C), 48.1 and 48.3 (Pro δ -C), 47.7 and 47.8 ($\text{CH}_2\text{C}_6\text{H}_5$), 43.0 and 43.3 (CONCH $_2$), 37.4 and 38.1 (CH_2CON), 30.4 and 31.2 (Pro β -C), 28.7 and 28.9 (Boc- $\text{C}(\text{CH}_3)_3$), 23.1 and 23.8 (Pro γ -C).

ESI HRMS m/z calcd for $\text{C}_{19}\text{H}_{26}\text{N}_2\text{O}_3$ (MNa^+), 353.1840; found, 353.1836.

N-Boc- 2-[2-(*R*)-(Benzhydryl-amino)-ethyl]-Pro-OMe (5.9)



Aldehyde **5.7** (1.0g, 3.7mmol) was dissolved in a solution of MeOH buffered with acetic acid (0.22 g, 3.67 mmol) and sodium acetate (0.6 g, 7.3 mmol) to which was added 4Å molecular sieves (3.7 g) and diphenylmethanamine (0.48 g, 4.44 mmol). Sodium cyanoborohydride (0.47 g, 7.4 mmol) is then added in a single addition and the reaction was stirred at room temperature until the aldehyde was consumed (~1-3 hours). Once the reaction was complete, 10% aqueous HCl was added carefully to a pH of 2 to destroy any excess sodium cyanoborohydride. The aqueous layer was adjusted to pH 10 with saturated NaHCO₃ and extracted with ethyl acetate (2x). The combined organic layers were washed twice with brine, dried with MgSO₄, filtered and concentrated *in vacuo* to provide the reductive amination product **5.9**.

TLC $R_f = 0.87$ (EtOAc / Hexanes, 1:1)

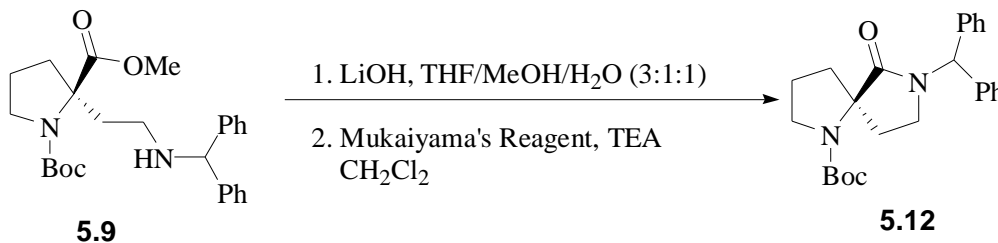
$[\alpha]_D^{25} 27.6$ (c 2, CH_2Cl_2)

^1H NMR (300 MHz, CDCl_3 , COSY, *rotamers present*) δ 7.17 – 7.40 (m, 10H, C_6H_5), 5.28 (d, $J = 2.1\text{Hz}$, 0.5H, $\text{CH}(\text{C}_6\text{H}_5)_2$), 4.82 (d, $J = 2.1\text{Hz}$, 0.5H, $\text{CH}(\text{C}_6\text{H}_5)_2$), 3.71 (s, 3H, CO_2CH_3), 3.53 – 3.71 (m, 1H, Pro $\delta - \text{CH}_2$), 3.28 – 3.36 (m, 1H, Pro $\delta - \text{CH}_2$), 2.55 – 2.65 (m, 2H, $\text{CH}_2\text{CH}_2\text{NH}$), 2.36 – 2.39 (m, 1H, Pro $\beta - \text{CH}_2$), 2.00 – 2.15 (m, 3H, Pro $\gamma - \text{CH}_2$, Pro $\beta - \text{CH}_2$), 1.69 – 1.87 (m, 2H, $\text{CH}_2\text{CH}_2\text{NH}$), 1.34 – 1.40 (s, 9H, Boc – $\text{C}(\text{CH}_3)_3$)

^{13}C NMR (75 MHz, CDCl_3 , HMQC, *rotamers present*) δ 175.1 and 175.3 (COCH_3), 153.9 (Boc – CO), 144.2 (C_6H_5), 128.7 (C_6H_5), 128.7 (C_6H_5), 127.5 (C_6H_5), 127.4 (C_6H_5), 127.2 (C_6H_5), 127.1 (C_6H_5), 127.1 (C_6H_5), 79.9 and 80.3 (Boc – $\text{C}(\text{CH}_3)_3$), 67.6 and 67.9 ($\text{CH}(\text{C}_6\text{H}_5)_2$), 52.4 (CO_2CH_3), 48.7 (Pro $\alpha - \text{C}$), 43.7 (Pro $\delta - \text{C}$), 38.3 ($\text{CH}_2\text{CH}_2\text{NH}$), 36.3 (Pro $\beta - \text{C}$), 28.6 and 28.7 (Boc – $\text{C}(\text{CH}_3)_3$), 23.5 (Pro $\gamma - \text{C}$), 23.0 ($\text{CH}_2\text{CH}_2\text{NH}$)

ESI HRMS m/z calcd for $\text{C}_{26}\text{H}_{35}\text{N}_2\text{O}_4$ (MNa^+), 461.2416; found, 461.2409.

5-(R)-1-tert-Butoxycarbonyl-7-benzhydryl-6-oxo-1,7-diaza-spiro[4.4]nonane-1-carboxylic Acid tert-Butyl Ester (5.12)



The condensed product (**5.9**) was dissolved in THF/MeOH/ H_2O (3:1:1, 0.3 M total concentration). To the solution was added 14.4 mg of LiOH and the solution was then allowed to stir for 16 hours. Upon completion, the solvent was evaporated under

reduced pressure to give a white solid. The solid was then resuspended in a 1:1 mixture of H₂O and EtOAc whereupon the two layers were separated. The aqueous layer was then acidified to pH 3 with 0.5 M HCl and extracted with EtOAc, dried with MgSO₄ and concentrated under reduced pressure. The free acid was then dissolved in freshly distilled CH₂Cl₂. To the dichloromethane solution 2-chloro-1-methylpyridinium iodide (90 mg, 0.35 mmol) and NEt₃ (0.1 mL, 0.7 mmol) were added. The resulting solution was refluxed overnight. The reaction mixture was allowed to cool, and then was extracted with 1N HCl, saturated NaHCO₃, and brine. Drying with MgSO₄ and subsequent removal of the solvents under vacuum resulted in an orange mixture of products, which we separated by silica gel chromatography (EtOAc / Hexanes, 1:1) to yield pure **5.12** in 63% yield.

TLC R_f = 0.36 (EtOAc / Hexanes, 1:1)

[α]_D 1.0 (c 1.8, CH₂Cl₂)

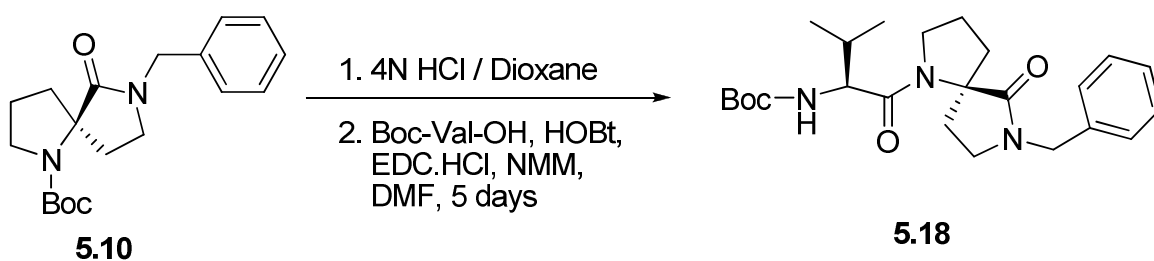
¹H NMR (300 MHz, CDCl₃, COSY, *rotamers present*) δ 7.13-7.26 (m, 9H, C₆H₅), 7.00-7.01 (m, 1H, C₆H₅), 6.52 (s, 1H, CH(C₆H₅)₂), 3.41-3.51 (m, 2H, Pro δ-CH₂), 3.15-3.29 (m, 1H, NCH₂CH₂), 2.92-2.95 (m, 0.5H, NCH₂CH₂), 2.70-2.82 (m, 0.5H, NCH₂CH₂), 2.62-2.65 (m, 0.5H, NCH₂CH₂), 2.39-2.42 (m, 0.5H, NCH₂CH₂), 1.68-2.01 (m, 5H, Pro β-CH₂, Pro γ-CH₂, NCH₂CH₂), 1.40 (s, 4.5H, Boc C(CH₃)₃), 1.26 (s, 4.5H, Boc C(CH₃)₃)

¹³C NMR (75 MHz, CDCl₃, HMQC, *rotamers present*) δ 174.7 and 174.9 (CON), 153.6 and 153.7 (Boc - CO), 138.1 and 138.4 (C₆H₅), 138.2 (C₆H₅), 129.5 (C₆H₅), 129.3 (C₆H₅), 128.6 (C₆H₅), 128.5 (C₆H₅), 128.4 (C₆H₅), 128.2 (C₆H₅), 127.9 (C₆H₅), 127.8 (C₆H₅), 127.6 (C₆H₅), 127.2 (C₆H₅), 79.6 and 80.5 (Boc - C(CH₃)₃), 67.3 and 67.4 (Pro α-

C), 59.5 and 59.6 ($\text{CH}_2(\text{C}_6\text{H}_5)_2$), 48.4 and 48.5 (Pro δ -C), 40.4 and 41.0 (CONCH_2), 37.3 and 37.4 (Pro β -C), 30.2 and 30.7 ($\text{CONCH}_2\text{CH}_2$), 28.8 and 28.9 (Boc - $\text{C}(\text{CH}_3)_3$), 22.8 and 23.7 (Pro γ -C)

ESI HRMS m/z calcd for $\text{C}_{25}\text{H}_{30}\text{N}_2\text{O}_3 + \text{H}^+$, 407.2335; found, 407.2356.

5-(R)-1-(2-(S)-(tert-Butoxycarbonyl)amino-3-methyl-butanoyl)-7-benzyl-6-oxo-1,7-diazaspiro[4.4]nonane (5.18)



Boc-7-benzyl-6-oxo-1,7-diaza-spiro[4.4]nonane (**5.10**) (0.45 g, 1.4 mmol) was dissolved in 10 mL of 4N HCl in dioxane and the solution was stirred under nitrogen for 4-24 hours while it was monitored by TLC. Upon completion the reaction was concentrated under reduced pressure. The residue was dissolved in CH_2Cl_2 and evaporated three times to azeotropically remove any last traces of dioxane. The white compound was then allowed to dry under vacuum for 24 – 48 hours. The white solid was then used in the subsequent coupling reaction without further purification.

Boc-L-valine (0.27 g, 1.24 mmol) and 7-benzyl-6-oxo-1,7-diaza-spiro[4.4]nonane • HCl (1.4 mmol) were dissolved in DMF which had been dried over 5 Å molecular sieves. While this solution was stirred, HOBT (0.19 g, 1.4 mmol) was added and the solution was cooled to -78°C . EDC • HCl (0.26 g, 1.4 mmol) and NMM (0.3 mL, 2.72 mmol) were added consecutively to the cooled solution, which then was allowed to warm

slowly to room temperature whereupon it was stirred for 3 days. On the third day the reaction mixture was concentrated *in vacuo* to give an orange residue to which a small portion of xylenes was added to remove the remaining traces of DMF. The orange residue was then partitioned between H₂O (50 mL) and EtOAc (50 mL). The organic layer was washed consecutively with 0.5 M HCl (50 mL), 1M NaHCO₃ (50 mL) and brine (50 mL), dried with MgSO₄ and concentrated under reduced pressure to yield 3.5 grams of crude product. The crude 5-(*R*)-1-(2-(*S*)-(tert-butoxycarbonyl)amino-3-methylbutanoyl)-7-benzyl-6-oxo-1,7-diazaspiro[4.4]nonane (**5.18**) was purified by silica gel chromatography (3 x 5 cm) eluting with ethyl acetate in hexanes (1:1), to yield 0.3 g. (58 %) of pure **5.18** as a clear colorless oil.

TLC R_f = 0.27 (EtOAc / Hexanes, 1:1)

[α]_D -33.3 (c 0.6, MeOH)

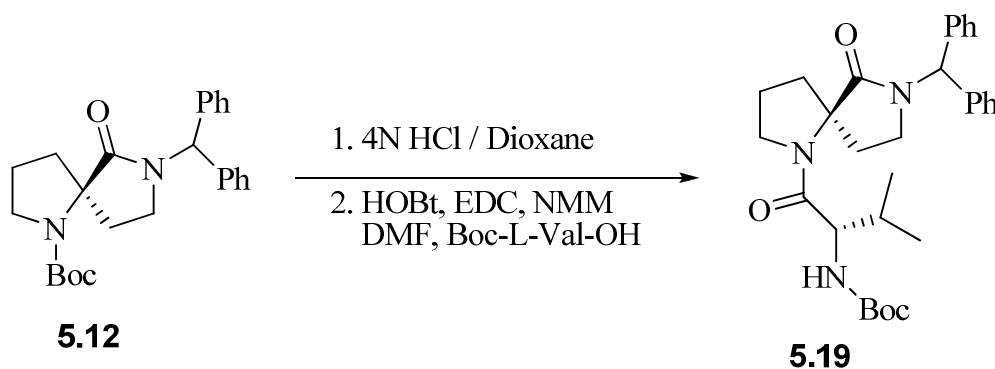
¹H NMR (300 MHz, CDCl₃, COSY): δ 7.17 - 7.28 (m, 5H, C₆H₅), 5.13 (d, *J* = 9.3 Hz, 1H, Val-NH), 4.57 (d, *J* = 15 Hz, 1H, CH₂C₆H₅), 4.28 (d, *J* = 15 Hz, 1H, CH₂C₆H₅), 4.18 (dd, *J* = 6.6 Hz, 9.3 Hz, 1H, Val α -CH), 3.84 (t, *J* = 8.1 Hz, 1H, Pro δ -CH₂), 3.55 - 3.63 (m, 1H, Pro δ -CH₂), 3.24 - 3.31 (m, 1H, CONCH₂), 3.05 (dd, *J* = 7.8 Hz, 17.4 Hz, 1H, CONCH₂), 2.45 - 2.55 (m, 1H, CH₂CON), 1.70 - 2.13 (m, 6H, Val β -CH₂, Pro γ -CH₂, Pro β -CH₂, CH₂CON), 1.36 (s, 9H, Boc-C(CH₃)₃), 1.00 (d, *J* = 6.9 Hz, 3H, Val γ -CH₃), 0.89 (d, *J* = 6.6 Hz, 3H, Val γ -CH₃).

¹³C NMR (75 MHz, CDCl₃, HMQC): 173.5 (Pro-CO, Val-CO), 170.7 (CON), 156.1 (Boc-CO), 136.6 (C₆H₅), 128.8 (C₆H₅), 128.2 (C₆H₅), 127.6 (C₆H₅), 79.7 (Boc-C(CH₃)₃), 68.6 (Pro α -C), 57.5 (Val α -C), 48.6 (Pro δ -C), 47.7 (CH₂C₆H₅), 43.5 (CONCH₂), 36.9

(CH₂CON), 31.7 (Val β-C), 30.0 (Pro β-C), 28.7 (Boc-C(CH₃)₃), 24.5 (Pro γ-C), 19.8 (Val γ-C), 17.9 (Val γ-C).

ESI HRMS *m/z* calcd for C₂₄H₃₅N₃O₄ (MNa)⁺, 430.2706; found, 430.2694

5-(*R*)-1-(2-(*S*)-(tert-Butoxycarbonyl)amino-3-methyl-butanoyl)-7-benzhydryl-6-oxo-1,7-diazaspiro[4.4]nonane (5.19)



(*R*)-tert-Butoxycarbonyl-7-benzhydryl-6-oxo-1,7-diazaspiro[4.4]nonane (**5.12**)

(0.24 g, 0.6 mmol) was dissolved in 10 mL of 4N HCl in dioxane and the solution was stirred under nitrogen for 4-24 hours while it was monitored by TLC. Upon completion the reaction was concentrated under reduced pressure. The residue was dissolved in CH₂Cl₂ and evaporated three times to azeotropically remove any last traces of dioxane. The white compound was then allowed to dry under vacuum for 24 - 48 hours. The white solid was then used in the subsequent coupling reaction without further purification.

Boc-L-valine (120 mg, 0.55 mmol) and (*R*)-7-benzhydryl-6-oxo-1,7-diazaspiro[4.4]nonane (0.6 mmol) were dissolved in DMF which had been dried over 5Å molecular sieves. While this solution was stirred, HOBt (82.3 mg, 0.6 mmol) was added and the solution was cooled to -78° C. EDC • HCl (120 mg, 0.6 mmol) and NMM (130 μL, 1.2 mmol) were added consecutively to the cooled solution, which then was allowed

to warm slowly to room temperature where upon it was stirred for 3 days. On the third day the reaction mixture was concentrated *in vacuo* to give an orange residue to which a small portion of xylenes was added to remove the remaining traces of DMF. The orange residue was then partitioned between H₂O (50 mL) and EtOAc (50 mL). The organic layer was washed consecutively with 0.5 M HCl (50 mL), 1M NaHCO₃ (50 mL) and brine (50 mL), dried with MgSO₄ and concentrated under reduced pressure to yield 0.1 grams of crude product. The crude 5-(*R*)-1-(2-(*S*)-(tert-butoxycarbonyl)amino-3-methylbutanoyl)--6-oxo-1,7-diazaspiro[4.4]nonane (**5.19**) was purified by silica gel chromatography (3 x 5cm) eluting with ethyl acetate in hexanes (3:1) to yield 170 mg. (61 %) of pure **5.19** as a clear colorless oil.

TLC R_f = 0.63 (EtOAc / Hexanes, 3:1)

[α]_D -28.6 (c 3.4, CH₂Cl₂)

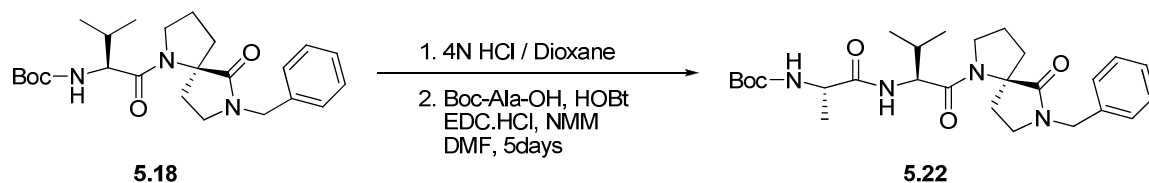
¹H NMR (300 MHz, CDCl₃, COSY) δ 7.13-7.30 (m, 10H, C₆H₅), 6.52 (s, 1H, CH(C₆H₅)₂), 5.18 (br s, 1H, Val-NH), 4.20 (dd, *J* = 6.9 Hz, 9.3 Hz, 1H, Val α-C), 3.83 (t, *J* = 8.4 Hz, 16.2 Hz, 1H, Pro δ-C), 3.54 - 3.63 (m, 1H, Pro δ-C), 3.28 (dd, *J* = 8.4 Hz, 9.9 Hz, NCH₂), 2.85 (dd, *J* = 7.8 Hz, 16.2 Hz, 1H, NCH₂), 2.65 (dd, *J* = 9.3 Hz, 12 Hz, 1H, NCH₂CH₂), 1.36 (s, 9H, Boc-C(CH₃)₃), 1.00 (d, *J* = 6.9 Hz, 3H, Val CH₃), 0.88 (d, *J* = 6.9 Hz, 3H, Val CH₃)

¹³C NMR (75 MHz, CDCl₃, HMQC, rotamers present) δ 173.6 (Val-CO), 170.6 (γ-Lac CO), 156.0 (Boc-CO), 139.0 (C₆H₅), 138.3 (C₆H₅), 129.4 (C₆H₅), 128.7 (C₆H₅), 128.6 (C₆H₅), 128.4 (C₆H₅), 127.9 (C₆H₅), 127.3 (C₆H₅), 79.6 Boc-C(CH₃)₃, 68.8 (Pro α-C), 59.6 (CH(C₆H₅)₂), 57.5 (Val α-C), 48.8 (Pro δ-C), 40.9 (NCH₂CH₂), 36.2 (Pro β-C), 31.8

(Pro γ -C), 29.6 (NCH₂CH₂), 28.7 (Boc-C(CH₃)₃), 24.4 (Val β -C), 19.8 (Val-CH₃), 18.0 (Val-CH₃)

ESI HRMS m/z calcd for C₃₀H₃₉N₃O₄ + Na⁺, 528.2838; found, 528.2867.

Boc-L-Ala-L-Val-(R)-7-benzyl-6-oxo-1,7-diazaspiro[4.4]nonane (5.20)



Boc-L-Val-7-benzyl-6-oxo-1,7-diazaspiro[4.4]nonane **5.18** (0.12 g, 0.3 mmol)

was dissolved in 10 mL of 4N HCl in dioxane and the solution was stirred under nitrogen for 4-24 hours while it was monitored by TLC. Upon completion, the reaction was concentrated under reduced pressure. The residue was dissolved in CH₂Cl₂ and evaporated three times to azeotropically remove any last traces of dioxane. The white compound was then allowed to dry under vacuum for 24 – 48 hours. The white solid was then used in the subsequent coupling reaction without further purification.

Boc-L-alanine (47.3 mg, 0.25 mmol) and L-Val-7-benzyl-6-oxo-1,7-diazaspiro[4.4]nonane•HCl (0.3 mmol) were dissolved in DMF which had been dried over 5Å molecular sieves. While this solution was stirred, HOBt (38.4 mg, 0.3 mmol) was added and the solution was cooled to -78° C. EDC • HCl (54.2 mg, 0.3 mmol) and NMM (61.5 μ L, 0.6 mmol) were added consecutively to the cooled solution, which then was allowed to warm slowly to room temperature where upon it was stirred for 3 days. On the third day the reaction mixture was concentrated *in vacuo* to give an orange residue to which a small portion of xylenes was added to remove the remaining traces of DMF.

The orange residue was then partitioned between H₂O (50 mL) and EtOAc (50 mL). The organic layer was washed consecutively with 0.5 M HCl (50 mL), 1M NaHCO₃ (50 mL) and brine (50 mL), dried with MgSO₄ and concentrated under reduced pressure to yield 0.1 grams of crude product. The crude Boc-L-Ala-L-Val-7-benzyl-6-oxo-1,7-diazaspiro[4.4]nonane (**5.20**) was purified by silica gel chromatography (3 x 5cm) and eluted with ethyl acetate in hexanes (3:1) to yield 75 mg (61 %) of pure product as a clear colorless oil. (**5.20**)

TLC: R_f = 0.24 (EtOAc / Hexanes, 3:1)

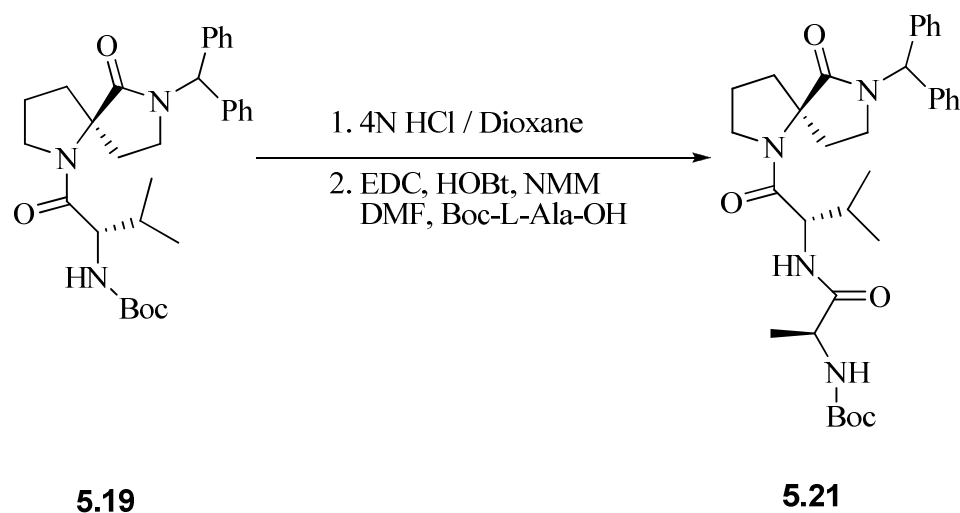
[α]_D -91.6 (c 0.5, MeOH)

¹H NMR (300 MHz, CDCl₃, COSY): δ 7.16-7.28 (m, 5H, C₆H₅), 6.72 (d, *J* = 6.6 Hz, Ala-NH), 5.01 (d, *J* = 6.6 Hz, 1H, Val-NH), 4.46-4.60 (m, 2H, CH₂C₆H₅, Val α-CH), 4.26 (d, *J* = 15.3 Hz, 1H, CH₂C₆H₅), 4.10 (br s, 1H, Ala α-CH), 3.85 (m, 1H, Pro δ-CH₂), 3.60 (m, 1H, Pro δ-CH₂), 3.22-3.28 (m, 1H, CONCH₂), 2.99-3.07 (m, 1H, CONCH₂), 2.42 - 2.52 (m, 1H, CH₂CON), 1.68-2.11 (m, 6H, Pro β-CH₂, Pro γ-CH₂, Val β-CH, CH₂CON), 1.36 (s, 9H, Boc-C(CH₃)₃), 1.28 (d, *J* = 9.9 Hz, 3H, Ala-CH₃), 1.0 (d, *J* = 9.7 Hz, 3H, Val-CH₃), 0.88 (d, *J* = 9.7 Hz, 3H, Val-CH₃).

¹³C NMR (75 MHz., CDCl₃, HMQC): δ 172.6 (Val-CO), 169.8 (Ala-CO), 155.4 (Boc-CO), 136.6 (C₆H₅), 128.8 (C₆H₅), 128.2 (C₆H₅), 127.6 (C₆H₅), 80.2 (Boc-C(CH₃)₃), 68.6 (Pro α-C), 56.1 (Val α-C), 50.6 (Ala α-C), 48.7 (Pro δ-C), 47.6 (CH₂C₆H₅), 43.4 (CONCH₂), 36.7 (Pro β-C), 31.7 (Val β-C), 29.9 (CH₂CON), 28.6 (Boc-C(CH₃)₃), 24.4 (Pro γ-C), 19.7 (Val γ-C), 18.5 (Ala-CH₃), 18.1 (Val-CH₃).

ESI HRMS *m/z* calcd for C₂₇H₄₀N₄O₅ (MH)⁺, 501.3072; found, 501.3099.

Boc-L-Ala-L-Val- (*R*)-7-benzhydryl-6-oxo-1,7-diazaspiro[4.4]nonane (5.21)



Boc-L-Val- (*R*)-7-benzhydryl-6-oxo-1,7-diazaspiro[4.4]nonan-1-yl (**5.19**) (0.18g, 0.36mmol) was dissolved in 10 mL of 4N HCl in dioxane and the solution was stirred under nitrogen for 4-24 hours while it was monitored by TLC. Upon completion the reaction was concentrated under reduced pressure. The residue was dissolved in CH₂Cl₂ and evaporated three times to azeotropically remove any last traces of dioxane. The white compound was then allowed to dry under vacuum for 24 - 48 hours. The white solid was then used in the subsequent coupling reaction without further purification.

Boc-L-alanine (61mg, 0.32mmol) and L-Val- (*R*)-7-benzhydryl-6-oxo-1,7-diazaspiro[4.4]nonane•HCl (0.36mmol) were dissolved in DMF which had been dried over 5Å molecular sieves. While this solution was stirred, HOBT (49.3 mg, 0.36 mmol) was added and the solution was cooled to -78 °C. EDC • HCl (69 mg, 0.36 mmol) and NMM (79 µL, 0.72 mmol) were added consecutively to the cooled solution, which then

was allowed to warm slowly to room temperature where upon it was stirred for 3 days. On the third day the reaction mixture was concentrated *in vacuo* to give an orange residue to which a small portion of xylenes was added to remove the remaining traces of DMF. The orange residue was then partitioned between H₂O (50 mL) and EtOAc (50 mL). The organic layer was washed consecutively with 0.5 M HCl (50 mL), 1M NaHCO₃ (50 mL) and brine (50 mL), dried with MgSO₄ and concentrated under reduced pressure to yield 0.1 grams of crude product. The crude Boc-L-Ala-L-Val- (*R*)-7-benzhydryl-6-oxo-1,7-diazaspiro[4.4]nonan-1-yl (**5.21**) was purified by silica gel chromatography (3 x 5cm) and eluted with ethyl acetate in hexanes (3:1) to yield 126 mg. (61 %) of pure product **5.21** as a clear colorless oil.

TLC R_f = 0.77 (2% MeOH in EtOAc)

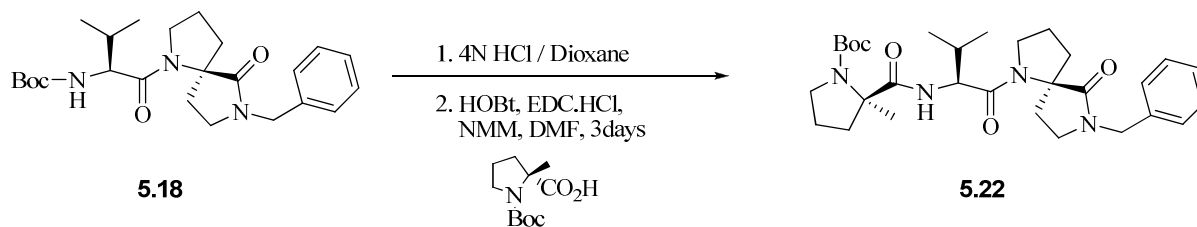
[α]_D -57.05 (c 1.1, CH₂Cl₂)

¹H NMR (300 MHz, CDCl₃, COSY) δ 7.14-7.30 (m, 10H, C₆H₅), 6.71 (d, *J* = 8.4 Hz, 1H, Val-NH), 6.59 (s, 1H, CH(C₆H₅)₂), 4.92 (br s, 1H, Ala-NH), 4.49 (t, *J* = 7.8 Hz, 16.2 Hz, 1H, Val α -CH), 4.10 (br s, 1h, Ala α -CH), 3.86 (t, *J* = 7.1 Hz, 1H, Pro δ -CH₂), 3.60 (dd, *J* = 5.1 Hz, 12.3 Hz, 1H, NCH₂), 3.26 (t, *J* = 9.3 Hz, 1H, NCH₂), 2.60 (dd, *J* = 6.6 Hz, 15.3 Hz, 1H, NCH₂CH₂), 1.64 - 2.06 (m, 6H, Pro γ -CH₂, Pro β -CH₂), Val β -CH, NCH₂CH₂), 1.38 (s, 9H, Boc - C(CH₃)₃), 1.29 (d, *J* = 7.2 Hz, 3H, Ala-CH₃), 1.00 (d, *J* = 6.9 Hz, 3H, Val-CH₃), 0.87 (d, *J* = 6.6 Hz, 3H, Val-CH₃)

¹³C NMR (75 MHz, CDCl₃, HMQC, rotamers present) δ 173.6 (Val - CO), 172.6 (γ -Lac - CO), 169.8 (Ala - CO), 155.4 (Boc - CO), 138.9 (C₆H₅), 138.3 (C₆H₅), 129.4 (C₆H₅), 128.7 (C₆H₅), 128.6 (C₆H₅), 128.4 (C₆H₅), 127.9 (C₆H₅), 127.3 (C₆H₅), 80.3 (Boc - C(CH₃)₃), 68.8 (Pro α -C), 59.5 (CH(C₆H₅)₂), 56.2 (Val α -C), 50.6 (Ala α -C), 48.9 (Pro δ -

C), 40.9 (NCH₂), 36.1 (Pro γ -C), 31.9 (Pro β -C), 29.6 (NCH₂CH₂), 28.7 (Boc - C(CH₃)₃), 24.3 (Val β -C), 19.7 (Val-CH₃), 18.5 (Ala-CH₃), 18.2 (Val-CH₃)
 ESI HRMS m/z calcd for C₃₃H₄₅N₄O₅ (MH)⁺, 599.3209; found, 599.3205.

Boc- α -Me-D-Pro-L-Val- (R)-7-benzyl-6-oxo-1,7-diazaspiro[4.4]nonane (5.22)



Boc -L-Val- (R)-7-benzyl-6-oxo-1,7-diazaspiro[4.4]nonan-1-yl (**5.18**) (0.09 g, 0.2 mmol) was dissolved in 10 mL of 4N HCl in dioxane and the solution was stirred under nitrogen for 4-24 hours while it was monitored by TLC. Upon completion, the reaction was concentrated under reduced pressure. The residue was dissolved in CH₂Cl₂ and evaporated three times to azeotropically remove any last traces of dioxane. The white compound was then allowed to dry under vacuum for 24 – 48 hours. The white solid was then used in the subsequent coupling reaction without further purification.

Boc- α -Me-D-Proline (**5.17**) (43.5 mg, 0.19 mmol) and L-Val- (R)-7-benzyl-6-oxo-1,7-diazaspiro[4.4]nonane•HCl (0.2 mmol) were dissolved in DMF which had been dried over 5Å molecular sieves. While this solution was stirred, HOBt (28.8 mg, 0.2 mmol) was added and the solution was cooled to -78° C. EDC • HCl (40.6 mg, 0.2 mmol) and NMM (46.2 μ L, 0.4 mmol) were added consecutively to the cooled solution, which then was allowed to warm slowly to room temperature where upon it was stirred for 3 days. On the third day the reaction mixture was concentrated *in vacuo* to give an orange residue

to which a small portion of xylenes was added to remove the remaining traces of DMF. The orange residue was then partitioned between H₂O (50 mL) and EtOAc (50 mL). The organic layer was washed consecutively with 0.5 M HCl (50 mL), 1M NaHCO₃ (50 mL) and brine (50 mL), dried with MgSO₄ and concentrated under reduced pressure to yield 0.1 grams of crude product. The crude Boc- α -Me-D-Pro-L-Val- (*R*)-7-benzyl-6-oxo-1,7-diazaspiro[4.4]nonan-1-yl (**5.22**) was purified by silica gel chromatography (3 x 5cm) eluting with ethyl acetate in hexanes (3:1) to yield 85 mg. (82.5 %) of pure **5.22** as a clear colorless oil.

TLC R_f = 0.24 (EtOAc / Hexanes, 3:1)

[α]_D 4.24 (*c* 0.9, CH₂Cl₂)

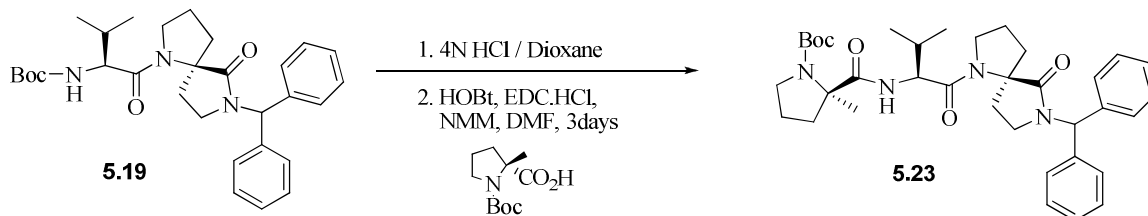
¹H NMR (300 MHz, CDCl₃, COSY): δ 7.17-7.27 (m, 5H, C₆H₅), 6.60 (br d, 1H, Val-NH), 4.67(br s, 1H, CH₂C₆H₅), 4.45 (t, *J* = 8.7 Hz, 15.6 Hz, 1H, Val α -CH₃), 4.18 (br s, 1H, CH₂C₆H₅), 3.88-3.93 (m, 1H, L-Pro δ -CH₂), 3.53 - 3.64 (m, 3H, D-Pro δ -CH₂, L-Pro δ -CH₂), 3.25 (t, *J* = 9.6 Hz, 17.1 Hz, 1H, CONCH₂), 3.02 (dd, *J* = 8.4 Hz, 17.7 Hz, 1H, CONCH₂), 2.45 (dd, *J* = 9.3 Hz, 20.7 Hz, 1H, CONCH₂CH₂), 1.65 - 2.19 (m, 10H, CONCH₂CH₂, Val β -CH₂, D-Pro β -CH₂, L-Pro β -CH₂, D-Pro γ -CH₂, L-Pro γ -CH₂), 1.53 (s, 3H, D-Pro CH₃), 1.38 (s, 9H, Boc-(CH₃)₃), 1.02 (d, *J* = 6.3 Hz, 3H, Val CH₃), 0.91 (d, *J* = 6.6 Hz, 3H, Val CH₃).

¹³C NMR (75 MHz., CDCl₃, HMQC, rotamers present) δ 174.4 and 174.9 (D-Pro CO), 173.4 (L-Pro CO), 170.0 (Val CO), 153.8 (Boc - CO), 136.6 (C₆H₅), 128.7 (C₆H₅), 128.2 (C₆H₅), 127.5 (C₆H₅), 80.0 and 80.6 (Boc - C(CH₃)₃), 68.5 (L-Pro δ -C), 66.4 and 66.7 (D-Pro δ -C), 56.4 (Val α -C), 48.6 (Pro δ -C), 47.6 (CH₂C₆H₅), 43.3 (CONCH₂), 40.3 and 42.1 (D-Pro β -C), 36.4 (L-Pro β -C), 31.4 (Pro γ -C), 29.8 and 30.0 (CONCH₂CH₂), 28.7 (Boc

C(CH₃)₃), 24.4 (Pro γ -C), 23.0 (D-Pro CH₃), 22.0 and 22.5 (Val β -CH), 19.8 (Val CH₃), 18.0 and 18.3 (Val CH₃).

ESI HRMS m/z calcd for C₂₇H₄₀N₄O₅ (MH)⁺, 541.3390 ; found, 541.3375.

Boc- α -Me-D-Pro-L-Val-(R)-7-benzhydryl-6-oxo-1,7-diazaspiro[4.4]nonane (5.23)



Boc -L-Val-(R)-7-benzhydryl-6-oxo-1,7-diazaspiro[4.4]nonan-1-yl **5.19** (0.24 g, 0.5 mmol) was dissolved in 10 mL of 4N HCl in dioxane and the solution was stirred under nitrogen for 4-24 hours while it was monitored by TLC. Upon completion, the reaction was concentrated under reduced pressure. The residue was dissolved in CH₂Cl₂ and evaporated three times to azeotropically remove any last traces of dioxane. The white compound was then allowed to dry under vacuum for 24 - 48 hours. The white solid was then used in the subsequent coupling reaction without further purification.

Boc- α -Me-D-Pro-OH (100 mg, 0.45 mmol) and L-Val-(R)-7-benzhydryl-6-oxo-1,7-diazaspiro[4.4]nonane•HCl (0.45 mmol) were dissolved in DMF which had been dried over 5Å molecular sieves. While this solution was stirred, HOBt (61 mg, 0.5 mmol) was added and the solution was cooled to -78 °C. EDC • HCl (87 mg, 0.5 mmol) and NMM (100 μ L, 0.9 mmol) were added consecutively to the cooled solution, which then was allowed to warm slowly to room temperature whereupon it was stirred for 3 days. On the third day, the reaction mixture was concentrated *in vacuo* to give an orange

residue to which a small portion of xylenes was added to remove the remaining traces of DMF. The orange residue was then partitioned between H₂O (50 mL) and EtOAc (50 mL). The organic layer was washed consecutively with 0.5 M HCl (50 mL), 1M NaHCO₃ (50 mL) and brine (50 mL), dried with MgSO₄ and concentrated under reduced pressure to yield 0.1 grams of crude product. The crude Boc- α -Me-D-Pro-L-Val-(*R*)-7-benzhydryl-6-oxo-1,7-diazaspiro[4.4]nonan-1-yl (**5.23**) was purified by silica gel chromatography (3 x 5cm) and eluted with ethyl acetate in hexanes (3:1), to yield 200 mg (72%) of pure **5.23** as a clear colorless oil.

TLC R_f = 0.18 (EtOAc / Hexanes, 1:1)

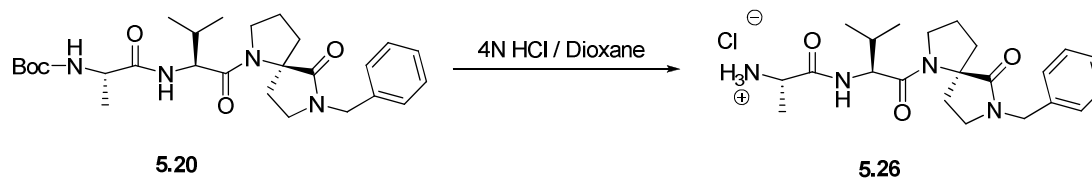
[α]_D -6.1 (*c* 0.9, CH₂Cl₂)

¹H NMR (300 MHz, CDCl₃, COSY) δ 7.19-7.33 (m, 10H, C₆H₅), 6.92 (br s, 0.5H, Val-NH), 6.65 (br s, 0.5H, Val-NH), 6.57 (s, 1H, CH(C₆H₅)₂), 4.48 (t, *J* = 7.8 Hz, 1H, Val α -CH), 3.96 (br s, 1H, Pro δ -CH₂), 3.53-3.66 (br m, 2H, Pro δ -CH₂), 3.28 (t, *J* = 9.6 Hz, NCH₂CH₂), 2.90 (q, *J* = 7.2 Hz, 9.9 Hz, 1H, NCH₂CH₂), 2.61 (q, *J* = 7.8 Hz, 9.6 Hz, 1H, NCH₂CH₂), 1.60-2.28 (m, 10H, NCH₂CH₂, Pro β -CH₂, Pro γ -CH₂, D-Pro β -CH₂, D-Pro γ -CH₂, Val β -CH), 1.60 (s, 3H, D-Pro C(CH₃)), 1.44 (s, 9H, Boc-C(CH₃)₃), 1.07 (d, *J* = 6 Hz, 3H, Val-CH₃), 0.95 (d, *J* = 6 Hz, 3H, Val-CH₃)

¹³C NMR (75 MHz, CDCl₃, HMQC, *rotamers present*) δ 174.9 (γ -Lac CO), 173.5 (Pro CO), 170.0 (Val CO), 154.2 (Boc CO), 138.9 (C₆H₅), 138.4 (C₆H₅), 129.4 (C₆H₅), 128.7 (C₆H₅), 128.5 (C₆H₅), 128.5 (C₆H₅), 127.9 (C₆H₅), 127.3 (C₆H₅), 80.2 and 80.8 (Boc - C(CH₃)₃), 68.8 (Pro α -C), 66.5 and 66.9 (D-Pro α -C), 59.5 (CH(C₆H₅)₂), 56.7 (Val α -C), 48.7 (Pro δ -C), 42.2 (D-Pro δ -C), 40.4 and 40.9 (NCH₂CH₂), 37.9 (Pro β -C), 36.0 (D-Pro

β -C), 31.6 (NCH₂CH₂), 29.6 (Pro γ -C), 28.7 and 28.8 (Boc C(CH₃)₃), 24.4 and 24.7 (D-Pro γ -C), 23.1 and 23.4 (D-Pro C(CH₃)₃), 21.4 (Val β -C), 19.8 (Val CH₃), 18.3 (Val CH₃)
ESI HRMS m/z calcd for C₃₆H₄₈N₄O₅ + Na⁺, 639.3522; found, 639.3554.

L-Ala-L-Val-(R)-7-benzyl-6-oxo-1,7-diazaspiro[4.4]nonane•HCl (5.26)



Boc-L-Ala-L-Val-(R)-7-benzyl-6-oxo-1,7-diazaspiro[4.4]nonane (**5.20**, 30mg, 0.06 mmol) was dissolved in 4N HCl in dioxane and stirred for 24 hours. The resultant crude hydrochloride salt was purified by silica gel chromatography (1 x 5cm) eluting with methanol in chloroform (1:5), to yield 85 mg (82.5 %) of pure **5.26** as white solid. TLC R_f = 0.30 (Propanol / NH₄Cl, 4:1)

[α]_D – 66.8 (*c* 0.26, MeOH)

¹H NMR (300 MHz, CDCl₃, COSY) δ 7.22 (s, 5H, C₆H₅), 4.40 (s, 2H, CH₂C₆H₅), 4.30 - 4.34 (m, 1H, Val α -CH), 3.92 - 3.97 (m, 2H, Ala α -CH, Pro δ -CH₂), 3.56 - 3.57 (br d, *J* = 5.1 Hz, 1H, Pro δ -CH₂), 3.12 - 3.26 (m, 2H, CONCH₂), 2.32 - 2.35 (m, 1H, CONCH₂CH₂). 1.84 - 2.03 (m, 6H, CONCH₂CH₂, Val β -CH₂, Pro β -CH₂, Pro γ -CH₂), 1.38 (d, *J* = 6.6 Hz, 3H, Ala - CH₃), 1.0 (d, *J* = 6.9 Hz, 3H, Val - CH₃), 0.93 (d, *J* = 6.3 Hz, 3H, Val-CH₃)

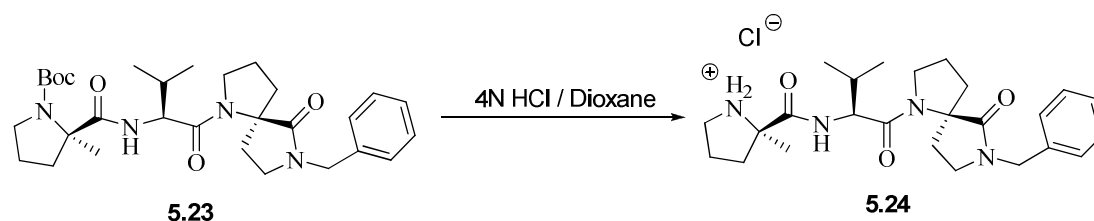
¹³C NMR (75 MHz, CDCl₃, HMQC, rotamers present) δ 176.8 (CONHCH₂C₆H₅), 172.5 (Ala CO), 172.1 (Val CO), 138.5 (C₆H₅), 130.9 (C₆H₅), 130.1 (C₆H₅), 129.8 (C₆H₅), 71.5 (Pro α - C), 59.9 and 60.0 (Ala α - C, Val α - C), 49.3 (Pro δ - C), 45.8 (CH₂C₆H₅),

41.4(NCH₂CH₂), 38.3(Pro β - C), 32.8 (NCH₂CH₂), 31.6 (Pro γ - C), 26.4 (Val β - C),
21.0 (Val - CH₃), 20.2 (Val - CH₃), 19.1 (Ala - CH₃)

ESI HRMS *m/z* calcd for C₂₇H₄₀N₄O₅ (MH)⁺, 423.2372; found, 423.2374.

HPLC: t_R (2% H₂O in 98% CH₃CN) 7.48 minutes; t_R (2% MeOH in 98% CH₃CN) 8.57
minutes. Sample was dissolved in CHCl₃ and MeOH

α-Me-D-Pro-L-Val- (R)-7-benzyl-6-oxo-1,7-diazaspiro[4.4]nonane•HCl (5.24)



Boc-αMe-D-Pro-L-Val- (R)-7-benzyl-6-oxo-1,7-diazaspiro[4.4]nonan-1-yl (**5.23**)
(30mg, 0.06mmol) was dissolved in 4N HCl in Dioxane and stirred for 24 hours. The
resultant crude hydrochloride salt was purified by silica gel chromatography (1 x 5cm)
eluting with methanol in chloroform (1:5) to yield 24.5 mg (93 %) of pure **5.24** as a light
yellow solid.

TLC R_f = 0.33 (Propanol / NH₄Cl, 4:1)

[α]_D – 51.4 (*c* 0.9, MeOH)

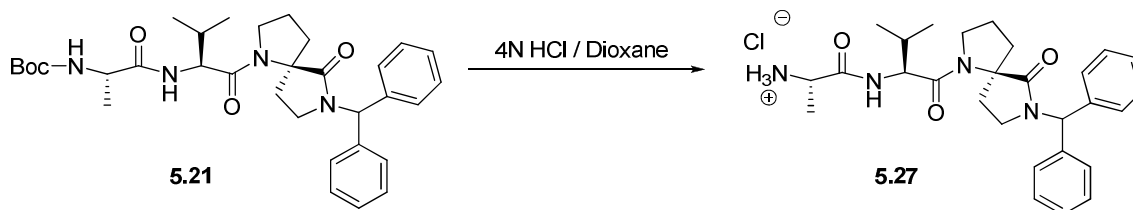
¹H NMR (300 MHz, CDCl₃, COSY) δ 7.62-7.76 (m, 5H, C₆H₅), 5.72-5.74 (m, 0.5H, D-
Pro-NH₂), 4.60 (d, *J* = 7.2 Hz, 2H, CH₂C₆H₅), 4.24-4.33 (m, 1H, Val α-CH), 4.00-4.07
(m, 1H, Val-NH), 3.46-3.72 (m, 3H, D-Pro δ-CH₂, Pro δ-CH₂, NCH₂CH₂), 3.09-3.29 (m,
3H, D-Pro δ -CH₂, Pro δ-CH₂, NCH₂CH₂), 2.17-2.38 (m, 2H, NCH₂CH₂), 1.80-2.11 (m,
9H, D-Pro γ-CH₂, D-Pro β-CH₂, Pro β-CH₂, Pro γ-CH₂, Val β-CH), 1.59 (D-Pro CH₃),
1.00 (d, *J* = 6.9 Hz, 3H, Val-CH₃), 0.91-0.94 (m, 3H, Val-CH₃)

^{13}C NMR (75 MHz, CDCl_3 , HMQC) δ 173.6 (D-Pro-CO), 171.5 (Val-CO), 170.0 (γ -Lac CO), 137.2 (C_6H_5), 129.2 (C_6H_5), 128.3 (C_6H_5), 127.9 (C_6H_5), 70.2 (D-Pro CCH_3), 69.3 (Pro α -C), 58.1 (Val α -C), 49.3 (D-Pro δ -C), 47.7 (Pro δ -C), 45.9 ($\text{CH}_2\text{C}_6\text{H}_5$), 43.8 (NCH_2CH_2), 37.4 (Pro β - CH_2), 36.7 (D-Pro β - CH_2), 31.6 (NCH_2CH_2), 30.0 (D-Pro γ - CH_2), 24.8 (Pro γ - CH_2), 23.9 (D-Pro CH_3), 22.3 (Val β -CH), 19.8 (Val- CH_3), 18.7 (Val- CH_3)

ESI HRMS m/z calcd for $\text{C}_{27}\text{H}_{40}\text{N}_4\text{O}_5$ (MH) $^+$, 441.2866; found, 441.2867.

HPLC: t_R (2% H_2O in 98% CH_3CN) 10.7 minutes; t_R (2% MeOH in 98% CH_3CN) 9.21 minutes. Sample was dissolved in CHCl_3 and MeOH

L-Ala-L-Val- (*R*)-7-benzhydryl-6-oxo-1,7-diazaspiro[4.4]nonane•HCl (5.27)



Boc-L-Ala-L-Val- (*R*)-7-benzhydryl-6-oxo-1,7-diazaspiro[4.4]nonan-1-yl (**5.21**)

(30 mg, 0.8 mmol) was dissolved in 4N HCl in doxane and stirred for 24 hours. The resultant crude hydrochloride salt was purified by silica gel chromatography (1 x 5cm)eluting with methanol in chloroform (1:5), to yield 85 mg (82.5 %) of pure **5.27** as white solid.

TLC R_f = 0.45 (Propanol / NH_4Cl , 4:1)

$[\alpha]_D - 53.6$ (c 0.5, MeOH)

^1H NMR (300 MHz, CDCl_3 , COSY) δ 8.50 (br s, 2H, Ala NH), 7.52 (br s, 1H, Val NH), 7.09 - 7.31 (m, 10H, C_6H_5), 6.50 (s, 1H, $\text{CH}(\text{C}_6\text{H}_5)_2$), 4.32-4.42 (m, 1H, Ala α -CH), 4.03

(br s, 1H, Val α -CH), 3.57-3.69 (m, 3H, Pro δ -CH₂, NCH₂CH₂), 3.28 (br s, 1H, NCH₂CH₂), 2.82 (br s, 1H, NCH₂CH₂), 2.61 (br s, 1H, NCH₂CH₂), 1.36-2.10 (m, 5H, Pro γ -CH₂, Pro β -CH₂, Val β -CH), 1.18 (s, 3H, Ala CH₃), 1.01 (s, 3H, Val CH₃), 0.94 (s, 3H, Val CH₃)

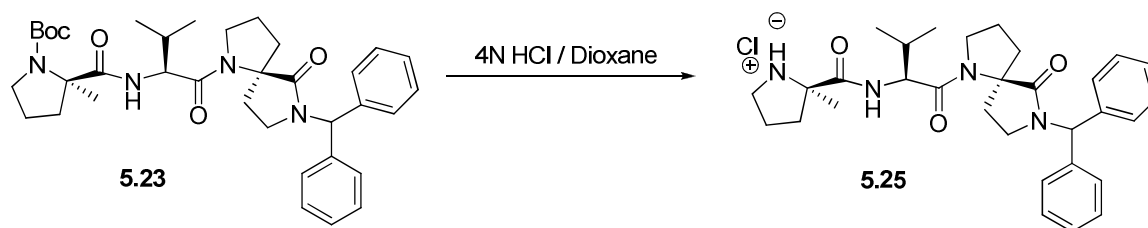
¹³C NMR (75 MHz, CDCl₃, HMQC, rotamers present) δ 173.6 (γ -Lac CO), 169.9 (Ala CO), 169.5 (Val CO), 138.9 (C₆H₅), 138.4 (C₆H₅), 129.3 (C₆H₅), 128.8 (C₆H₅), 128.3 (C₆H₅), 128.0 (C₆H₅), 127.6 (C₆H₅), 69.2 (Pro α -CH), 59.8 (CH(C₆H₅)₂), 57.8 (Val α -CH), 50.2 (Ala α -CH), 49.3 (Pro δ -C), 41.1 (NCH₂CH₂), 35.7 (Pro β -C), 29.7 (NCH₂CH₂), 24.4 (Val β -CH), 19.7 (Val CH₃), 19.0 (Ala CH₃), 18.0 (Val CH₃)

ESI HRMS m/z calcd for C₂₈H₃₆N₄O₃ (MNa)⁺, 499.2685; found, 499.2694.

HPLC: t_R (2% H₂O in 98% CH₃CN) 7.89 minutes; t_R (2% MeOH in 98% CH₃CN)

7.23minutes. Sample dissolved in CHCl₃ and MeOH

α -Me-D-Pro-L-Val-(R)-7-benzhydryl-6-oxo-1,7-diazaspiro[4.4]nonane•HCl (5.25)



Boc- α -Me-D-Pro-L-Val-(R)-7-benzhydryl-6-oxo-1,7-diazaspiro[4.4]nonan-1-yl

5.23 (30 mg) was dissolved in 4N HCl in dioxane and stirred for 24 hours. The resultant crude hydrochloride salt was purified by silica gel chromatography (1 x 5 cm) eluting with methanol in chloroform (1:5) to yield 85 mg (82.5 %) of pure **5.25** as a white solid.

TLC R_f = 0.64 (Propanol / NH₄OH, 4:1)

$[\alpha]_D - 45.4$ (c 0.01, MeOH)

^1H NMR (300 MHz, CDCl_3 , COSY) δ 7.13-7.23 (m, 10H, C_6H_5), 6.52 (s, 1H, $\text{CH}(\text{C}_6\text{H}_5)_2$), 4.35 (dd, $J = 3.9$ Hz, 1H, Val $\alpha\text{-CH}$), 3.56-3.69 (m, 1H, D-Pro $\delta\text{-CH}_2$), 3.24-3.30 (t, $J = 9.9$ Hz, 17.7 Hz, 1H, Pro $\delta\text{-CH}_2$), 2.80-3.13 (m, 3H, Pro $\delta\text{-CH}_2$, NCH_2CH_2), 2.52 - 2.62 (m, 1H, NCH_2CH_2), 1.41-2.46 (m, 10H, Val $\beta\text{-CH}_2$, Pro $\beta\text{-CH}_2$, Pro $\gamma\text{-CH}_2$, D-Pro $\beta\text{-CH}_2$, D-Pro $\gamma\text{-CH}_2$, NCH_2CH_2), 1.39 (D-Pro CH_3), 1.00 (d, $J = 6.9$ Hz, 3H, Val CH_3), 0.88 (d, $J = 6.9$ Hz, 3H, Val CH_3)

^{13}C NMR (75 MHz, CDCl_3 , HMQC) δ 173.4 (D-Pro CO), 170.4 (Val $\alpha\text{-C}$), 169.6 ($\gamma\text{-Lac}$ CO), 141.7 (C_6H_5), 139.0 (C_6H_5), 138.4 (C_6H_5), 135.1 (C_6H_5), 129.4 (C_6H_5), 128.7 (C_6H_5), 128.5 (C_6H_5), 128.5 (C_6H_5), 127.9 (C_6H_5), 127.3 (C_6H_5), 66.8 (D-Pro $\alpha\text{-C}$), 67.3 (Pro $\alpha\text{-C}$), 59.5 ($\text{CH}_2(\text{C}_6\text{H}_5)_2$), 56.6 (Val $\alpha\text{-C}$), 48.8 (Pro $\delta\text{-C}$), 47.1 (Pro $\delta\text{-C}$), 40.9 (NCH_2CH_2), 37.9 (Pro $\beta\text{-C}$), 36.0 (D-Pro $\beta\text{-C}$), 31.3 (D-Pro $\gamma\text{-C}$), 29.5 (NCH_2CH_2), 26.4 (Pro $\gamma\text{-C}$), 24.3 (D-Pro CH_3), 21.4 (Val $\beta\text{-C}$), 19.7 (Val CH_3), 18.5 (Val CH_3)

ESI HRMS m/z calcd for $\text{C}_{31}\text{H}_{41}\text{N}_4\text{O}_3 + \text{Na}^+$, 539.2998; found, 539.3019.

HPLC: t_R (2% H_2O in 98% CH_3CN) 7.23 minutes; t_R (2% MeOH in 98% CH_3CN) 8.40 minutes. Sample was dissolved in CHCl_3 and MeOH

5.6. References

1. Genin, M.J.; Gleason, W.B.; Johnson, R.L. Design, synthesis, and X-ray crystallographic analysis of two novel spriolactam systems as β – turn mimics. *J. Org. Chem.* **1993**, *58*, 860 – 866.
2. Genin, M. J.; Ojala, W. H.; Gleason, W. B.; Johnson, R.L. Synthesis and crystal structure of a peptidomimetic containing the (*R*)-4.4-sprio lactam type-II β – turn mimic. *J. Org. Chem.* **1993**, *58*, 2334 – 2337.
3. Pang, Y. P.; Perola, E.; Xu, K.; Prenderast, F. G. EUDOC: A computer program for identification of drug interaction sites in macromolecules and drug leads from chemical databases. *J. Comp. Chem.* **2001**, *22*, 1750 – 1771.
4. Chai, J. Structural and biochemical basis of apoptotic activation by Smac/DIABLO. *Nature* **2000**, *406*, 855 – 862.
5. Wu, G.; Chai, J.; Suber, T. L.; Wu, J. W.; Du, C.; Wang, X.; Shi, Y. Structural basis of IAP recognition by Smac / DIABLO. *Nature* **2000**, *408*, 1008 – 1012.
6. Nikolovska-Coleska, Z.; Wang, R.; Fang, X.; Pan, H.; Tomita, Y.; Li, P.; Roller, P. P.; Krajewski, K.; Saito, N. G.; Stuckey, J. A.; Wang, S. Development and optimization of a binding assay for the XIAP- BIR3 domain assay fluorescence polarization. *Anal. Biochem.* **2004**, *332*, 261-273.
7. Ward, P.; Ewan, G.B.; Jordan, C.C.; Ireland, S.J.; Magan, R. M.; Brown, J. R. Potent and highly selective neurokinin antagonists. *J. Med. Chem.* **1990**, *33*, 1848 – 1851.

8. Hinds, M. G.; Welsh, J. H.; Brennand, D. M.; Fisher, J.; Glennie, M. J.; Richards, N.G.J.; Turner, D. L.; Robinson, J. A. Synthesis, conformational properties, and antibody recognition of peptides containing β -turn mimetics based on α -alkylproline derivatives. *J. Med. Chem.* **1991**, *34*, 1777 – 1789.
9. Hinds, M. G.; Richards, N. G. J.; Robinson, J. A. Design and synthesis of a novel peptide β – turn mimetic. *Chem. Commun.* **1988**, *22*, 1447 – 1449.
10. Long, R. D.; Moeller, K. D. Conformationally constrained peptide mimetics: the use of a small lactam ring as an HIV-1 antigen **constraint**. *J. Am. Chem. Soc.* **1997**, *119*, 12394 – 12395
11. Seebach, D.; Does, M.; Naef, R.; Schwizer, B. Alkylation of amino acids without loss of the optical activity: preparation of *R* – substituted proline derivatives. A case of self-reproduction of chirality. *J. Am. Chem. Soc.* **1983**, *105*, 5390 – 5398.
12. Shatzmiller, S.; Dolitzky, B.; Bahar, E. Preparation and use of chloromethyl (-)-menthyl ether in the synthesis of optically pure α -branched α -amino nitriles. *Liebigs Ann. Chem.* **1991**, *4*, 375–379.
13. Seebach, D.; Dziadulewicz, E.; Behrendt, L.; Cantoreggi, S.; Fitzi, R. Synthesis of Nonproteinogenic (R)- or (S)-Amino Acids Analogues of Phenylalanine, Isotopically Labelled and Cyclic Amino Acids from tert-Butyl 2-(tert-Butyl)-3-methyl-4-oxo-1-imidazolidinecarboxylate (Boc-BMI). *Liebigs Ann. Chem.* **1989**, *12*, 1215–1232.

14. Khalil, E. M.; Subasinghe, N. L.; Johnson, R. L.; An efficient and high yield method for the N-tert-butoxycarbonyl protection of sterically hindered amino acids. *Tetrahedron Lett.* **1996**, *37*, 3441–3444.
15. Wu, G.; Chai, J.; Suber, T. L.; Wu, J.; Du, C.; Wang, X.; Shi, Y. Structural Basis of IAP Recognition by Smac / DIABLO. *Nature* **2000**, *408*, 1008–1012.
16. Sun, C. NMR structure and mutagenesis of the inhibitor of apoptosis protein XIAP. *Nature* **1999**, *401*, 818 – 822.
17. Shi, Y. Survivin structure: crystal unclear. *Nature Struct. Biol.* **2000**, *7*, 620 – 623.
18. Verdecia, M.A. Structure of the human anti-apoptotic protein surviving reveals a dimeric arrangement. *Nature Struct. Biol.* **2000**, *7*, 602 – 608.
19. Chantalat, L. Crystal structure of human surviving reveals a bow tie shaped dimer with two unusual alpha helical extensions. *Mol. Cell* **2000**, *6*, 183 – 189.
20. Genin, M. J.; Johnson, R.L.; Design, Synthesis, and Conformational Analysis of a Novel Spiro-Bicyclic System as a Type II β -Turn Peptidomimetic, *J. Amer. Chem. Soc.* **1992**, *114*, 8778 – 8783

Bibliography

1. Kaufmann, S. H.; Vaux, D. L. Alterations in the apoptotic machinery and their potential role in anticancer drug resistance. *Oncogene* **2003**, *22*, 7414 – 7430.
2. Greenless, R. T.; Hill-Harmon, M. B.; Murray, T.; Thun, M. Cancer Statistics, 2001. *CA-A Cancer J. Clin.* **2001**, *51*, 15 – 36.
3. Theodoropoulos, P. A.; Polioudake, H.; Kostake, O.; Derdas, S. P.; Georogoulis, V.; Dargemont, C.; Georgatos, S. D. Taxol affects nuclear lamina and pore complex organization and inhibits import of keryophilic proteins into the cell nucleus. *Cancer Res.* **1999**, *59*, 4625 – 4633.
4. Blajewski, A. L.; Kaufmann, S. H. A multistep model for paclitaxel-induced apoptosis in human breast cancer cell lines. *Exp. Cell. Res.* **2001**, *270*, 277 – 288.
5. Hashimoto, H.; Chatterjee, S.; Berger, N. A. Mutagenic activity of topoisomerase I inhibitors. *Clin. Cancer Res.* **1995**, *1*, 369 – 376.
6. Ryan, A. J.; Squires, S.; Strutt, H. L.; Johnson, R. T. Camptothecin cytotoxicity in mammalian cells is associated with the induction of persistent double strand breaks in replicating DNA. *Nucleic Acid Res.* **1991**, *19*, 3295 – 3300.
7. Vaux, D. L.; Cory, S.; Adams, J. M. Bcl-2 Gene promotes haemopoietic cell survival and cooperates with c-myc to immortalize pre-B cells. *Nature* **1998**, *355*, 400 – 442.

8. Kaufmann, S. H.; Gores, G. J. Apoptosis in cancer cause and cure. *Bioessays* **2000**, *22*, 1007 – 1017.
9. Liu, X.; Zou H.; Slaughter, C.; Wang, X. DFF, a heterodimeric protein that functions downstream of caspase-3 to trigger DNA fragmentation during apoptosis. *Cell* **1997**, *89*, 175 – 184.
10. Enari, M.; Sakahira, H.; Yokohama, H.; Okawa, K.; Iwamatsu, A.; Nagata, S. A caspase-activated DNase that degrades DNA during apoptosis, and its inhibitor ICAD. *Nature* **1998**, *391*, 43 – 50.
11. Porter, A. G.; Ng, P.; Janicke, R. U. Death substrates come alive. *Bioessays* **1997**, *19*, 501 – 507.
12. Earnshaw, W. C.; Martins, L. M.; Kaufmann, S. H. Mammalian caspases: structure, activation, substrates and functions during apoptosis. *Ann. Rev. Biochem.* **1999**, *68*, 383 – 424.
13. Nicholson, D. W. Caspase structure, preteolytic substrates, and function during apoptotic cell death. *Cell Death Diff.* **1999**, *6*, 1028 – 1042.
14. Slee, E. A.; Adrain, C.; Martin, S. J. Serial killers: ordering caspase activation events in apoptosis. *Cell Death Diff.* **1999**, *6*, 1067-1074.
15. Kottke, T. J.; Blajeski, A. L.; Meng, X.; Svingen, P. A.; Ruchaud, S.; Mesner Jr, P. W.; Boerner, S. A.; Samejima, K.; Henriquez, N. V.; Chilcote, T. J.; Lord, J.; Salmon,

- M.; Earnshaw, W. C.; Kaufmann, S. H. Lack of correlation between caspase activation and caspase activity assays in paclitaxel-treated MCF-7 breast cancer cells. *J. Biol. Chem.* **2002**, *277*, 804 – 815.
- 16.** Slee, E. A.; Harte, M. T.; Kluck, R. M.; Wolf, B. B.; Casiano, C. A.; Newmeyer, D. D.; Wang H-G.; Reed, J. C.; Nicholson, D. W.; Alnemri, E. S.; Green D. R.; Martin, S. J. Ordering the cytochrome c-initiated cascade: hierarchical activation of caspases-2, -3, -6, -7, -8, and -10 in a caspase-9-dependent manner. *J. Cell. Biol.* **1999**, *144*, 281 – 292.
- 17.** Hengartner, M. O. The biochemistry of apoptosis *Nature* **2000**, *407*, 770 – 776.
- 18.** Muzio, M.; Stockwell, B. R.; Stennicke, H. R.; Salvesen, G. S.; Dixit, V. M. An induced proximity model for caspase-8 activation. *J. Biol. Chem.* **1998**, *273*, 2926 – 2930.
- 19.** Yang, X.; Chang, H. Y.; Baltimore, D. Essential role of CED-4 oligomerization in CED-3 activation and apoptosis. *Science* **1998**, *281*, 1355 – 1357.
- 20.** Salvesen, G. S.; Dixit, V. M. Caspase activation: the induced proximity model. *Proc. Natl. Acad. Sci. USA*, **1999**, *96*, 10964 – 10967.
- 21.** Rodriguez, J.; Lazebrink, Y. Caspase-9 and APAF-1 form an active holoenzyme. *Genes Dev.* **1999**, *13*, 3179 – 3184.

22. Zou, H.; Henzel, W. J.; Lie, X.; Lutschg, A.; Wang, X. Apaf-1, a human protein homologous to *C. elegans* CED-4, participates in cytochrome c-dependent activation of caspase-3. *Cell* **1997**, *90*, 405 – 413.
23. Li, P. Cytochrome c and dATPF-dependent formation of Apaf-1/caspase-9 complex initiates an apoptotic protease cascade. *Cell* **1997**, *91*, 479 – 489.
24. Stennicke, H. R. Caspase-9 can be activated without proteolytic processing. *J. Biol. Chem.* **1999**, *274*, 8359 – 8362.
25. Beere, H. M. Heat shock protein 70 inhibits apoptosis by preventing recruitment of procaspase-9 to the Apaf- apoptosome. *Nature Cell Biol.* **2000**, *2*, 469 – 475.
26. Cain, K.; Brown, D. G.; Langlais, C.; Cohen, G. M. Caspase activation involves the formation of the aposome, a large (approximately 700 kDa) caspase-activation complex. *J. Biol. Chem.* **1999**, *274*, 22686 – 22692.
27. Schulze-Osthoff, K.; Ferrari, D.; Los, M.; Wesselborg, S.; Peter, M. E. Apoptosis signaling by death receptors. *Eur. J. Biochem.* **1998**, *254*, 439 – 459.
28. Peter, M. E.; Krammer, P. H. Mechanisms of CD95 (APO-1/Fas)-mediated apoptosis. *Curr. Opin. Immunol.* **1998**, *10*, 545-551.
29. Ashkenazi, A.; Dixit, V. M. Apoptosis control by death and decoy receptors. *Curr. Opin. Cell Biol.* **1999**, *11*, 255 – 260.

- 30.** Irmeler, M. Inhibition of death receptor signals by cellular FLIP. *Nature* **1997**, 388, 190 – 195.
- 31.** Thome, M.; Schneider, P.; Hofmann, K.; Fickenscher, H.; Meinel, E.; Neipel, F.; Mattmann, C.; Burns, K.; Bodmer, J. L.; Schroter, M.; Scaffidi, C.; Krammer, P. H.; Peter, M. E.; Tschopp J. Viral FLICE-inhibitory proteins (FLIPs) prevent apoptosis induced by death receptors. *Nature* **1997**, 386, 517 – 521.
- 32.** Medema, J. P.; de Jong, J.; van Hall, T.; Melief, C. J.; Offringa, R. Immune escape of tumors *in vivo* by expression of cellular FLICE-inhibitory protein. *J. Exp. Med.* **1999**, 190, 1033 – 1038.
- 33.** Adams, J. M.; Cory, S. The Bcl-2 protein family: arbiters of cell survival. *Science* **1998**, 281, 1322 – 1326.
- 34.** Huang, D. C. S.; Strasser, A. BH3-only proteins-essential initiators of apoptotic cell death. *Cell* **2000**, 103, 839 – 842.
- 35.** Budihardjo, I.; Oliver, H.; Lutter, M.; Luo, X.; Wang, X. Biochemical pathways of caspase activation during apoptosis. *Ann. Rev. Cell Dev. Biol.* **1999**, 15, 269 – 290.
- 36.** Rodriguez, J.; Lazebnik, Y. Caspase-9 and APAF-1 form an active holoenzyme. *Genes Dev.* **1999**, 13, 3179 – 3184.
- 37.** Liu, X.; Zou, H.; Slaughter, C.; Wang, X. DFF, a heterodimeric protein that functions downstream of caspase-3 to trigger DNA fragmentation during apoptosis. *Cell* **1997**, 89, 175 – 184.

38. Enari, M. A caspase-activated DNase that degrades DNA during apoptosis, and its inhibitor ICAD. *Nature* **1998**, *391*, 43-50.
39. Sakahira, H.; Enari, M.; Nagata, S. Cleavage of CAD inhibitor in CAD activation and DNA degradation during apoptosis. *Nature* **1998**, *391*, 96 – 99.
40. Ashkenazi, A.; Dixit, V. M. Apoptosis control by death and decoy receptors. *Curr. Opin. Cell. Biol.* **1999**, *11*, 255 – 260.
41. Reed, J. C.; Bcl-2 family proteins. *Oncogene* **1998**, *17*, 3225 – 3236.
42. Gross, A.; McDonnell, J. M.; Korsmeyer, S. J. BCL-2 family members and the mitochondria in apoptosis. *Genes Dev.* **1999**, *13*, 1899 – 1911.
43. Crook, N. E.; Clem, R. J.; Miller, L. K. An apoptosis-inhibiting baculovirus gene with a zinc finger-like motif. *J. Virol.* **1993**, *67*, 2168 – 2174.
44. Huang, H. K.; Joazeiro, C. A. P.; Bonfoco, E.; Kamada, S.; Leverson, J. D.; Hunter, T. The inhibitor of apoptosis, cIAP2, functions as a ubiquitin-protein ligase and promotes *in vitro* monoubiquitination of caspases 3 and 7. *J. Biol. Chem.* **2000**, *275*, 26661 – 26664.
45. Suzuki, Y., Nakabayashi, Y.; Takahashi, R. Ubiquitin-protein ligase activity of X-linked inhibitor of apoptosis protein promotes proteasomal degradation of caspase-3 and enhances its anti-apoptotic effect in Fas-induced cell death. *Proc. Natl. Acad. Sci. USA* **2001**, *98*, 8662 – 8667.

46. Yang, Y.; Fang, S.; Jensen, J. P.; Weissman, A. M.; Ashwell, J. D. Ubiquitin protein ligase activity of IAPs and their degradation in proteasomes in response to apoptotic stimuli. *Science* **2000**, *288*, 874 – 877.
47. Srinvasula, S. M.; Hegde, R.; Saleh, A.; Datta, P.; Shiozaki, E.; Chai, J.; Lee, R. A.; Robbins, P. D.; Fernandes-Alnemri, T.; Shi, Y.; Alnemrie, E. S. A conserved XIAP-interaction motif in caspase-9 and Smac/DIABLO regulates caspase activity and apoptosis. *Nature* **2001**, *410*, 112 – 116.
48. Wu, G.; Chai, J.; Suber, T. L.; Wu, J. W.; Du, C.; Wang, X.; Shi, Y. *Nature* **2000**, *408*, 1008 – 1012.
49. Lie, Z.; Sun, c.; Olejniczak, E. T.; Meadows, R.; Betz, S. F.; Oost, T.; Herrmann, J.; Wu, J. C.; Fesik, S. W. Structural basis for binding of Smac/DIABLO to the XIAP BIR3 domain. *Nature* **2000**, *408*, 1004 – 1008.
50. Sun, H.; Nikolovska-Coleska, Z.; Chen, J.; Yang, C.; Tomita, Y.; Pan, H.; Yoskioka, Y.; Krajewski, K.; Roller, P. P.; Wang, S. Structure – based design, synthesis and biochemical testing of novel and potent Smac peptido-mimetics. *Biorg. Med. Chem. Lett.* **2005**, *15*, 793 – 797.
51. Wu, G.; Chai, J.; Suber, T. L.; Wu, J.; Du, C.; Wang, X.; Shi, Y. Structural basis of IAP recognition by Smac / DIABLO. *Nature* **2000**, *408*, 1008-1012.

52. Salvesen, G. S.; Duckett, C. S. IAP proteins: blocking the road to death's door. *Nat. Rev. Mol. Cell Bio.* **2002**, *3*, 401 – 410.
53. Srinivasula, S. M. *sickle* a novel *Drosophila* death gene in the *reaper-hid-grim* region, encodes an IAP-inhibitory protein. *Curr. Biol.* **2002**, *12*, 125 – 130.
54. Christich, A. The damage-responsive *Drosophila* gene *sickle* encodes a novel IAP binding protein similar to but distinct from *reaper*, *grim*, and *hid*. *Curr. Biol.* **2000**, *12*, 137 – 140.
55. Wright, C. W.; Clem, R. J. Sequence requirements for hid binding and apoptosis regulation in the anti-apoptotic baculovirus protein Op-IAP: hid binds Op-IAP in a manner similar to Smac binding of XIAP. *J. Biol. Chem.* **2001**, *277*, 2454 – 2462.
56. Glover, C. J.; Hite, K.; Delosh, R.; Scudiero, D. A.; Fivash, M. J.; Smith, L. R.; Fisher, R. J.; Wu, J. W.; Shi, Y.; Kipp, R. A.; McLendon, G. L.; Sausville, E. A.; Shoemaker, R. H. A high throughput screen for identification of molecular mimics of Smac/Diablo utilizing a fluorescence polarization assay. *Anal. Biochem.* **2003**, *320*, 157 – 169.
57. Wu, T. Y.; Wagner, K. W.; Bursulaya, B.; Schultz, P. G.; Deveraux, Q. L. Development and characterization of nonpeptidic small molecule inhibitors of the XIAP/caspase-3 interaction. *Chem. Bio.* **2003**, *10*, 759 – 767.
58. Schimmer, A.D.; Welsh, K.; Pinilla, C.; Wang, Z.; Krajewska, M.; Bonneau, M. J.; Pedersen, I. M.; Kitada, S.; Scott, F. L.; Bailly-Maitre, B.; Glinsky, G.; Scudiero, D.;

Sausville, E.; Salvesen, G.; Nefzi, A.; Ostresh, J. M.; Houghten, R. A.; Reed, J. C.

Small-molecule antagonists of apoptosis suppressor XIAP exhibit broad antitumor activity. *Cancer Cell*, **2004**, *5*, 25 – 35.

59. Oost, T. K.; Sun, C.; Armstrong, R. C.; Al-Assaad, A. S.; Betz, S. F.; Deckwerth, T. L.; Ding, H.; Elmore, S. W.; Meadows, R. P.; Olejniczak, E. T.; Oleksijew, A.; Oltersdorf, T.; Rosenberg, S. H.; Shoemaker, A. R.; Tomaselli, K. J.; Zou, H.; Fesik, S. W. Discovery of potent antagonists of the antiapoptotic protein XIAP for the treatment of cancer. *J. Med. Chem.* **2004**, *47*, 4417 – 4426.

60. Banerjee, D.; Genasense (Genta Inc). *Curr. Opin. Inves. Drugs.* **2001**, *2*, 574-580.

61. Tolcher, A. W. Regulators of apoptosis as anticancer targets. *Hematology/Oncology Clinics of N. Amer.* **2002**, *16*, 1255 – 1267.

62. Zobel, K.; Wang, L.; Varfolomeev, E.; Franklin, M. C.; Elliott, L. O.; Wallweber, J. J. A.; Okawa, D. C.; Flygare, J.A.; Vucic, D.; Fairbrother, W. J.; Deshayes, K. Design, synthesis, and biological activity of a potent Smac mimetic that sensitizes cancer cells to apoptosis by antagonizing IAPs. *ACS Chem. Biol* **2006**, *1*, 525 – 533.

63. Li, L.; Thomas, R. M.; Suzuki, H.; Debrabander, J. K.; Wang, X.; Harran, P. G. A small molecule Smac mimic potentiates TRAIL- and TNFalpha-mediated cell death. *Science* **2004**, *305*, 1471 – 1474.

64. Park, C.; Sun, C.; Olejniczak, E. T.; Wilson, A. E.; Meadows, R. P.; Betz, S. F.; Elmore, S. W.; Fesik, S. W. Non-peptidic small molecule inhibitors of XIAP. *Bioorg. Med. Chem. Lett.* **2005**, *15*, 771 – 775.

- 65.** Yang, L.; Mashima, T.; Sato, S.; Mochizuki, M.; Sakamoto, H.; Yamori, T.; Oh-Hara, T.; Tsuru, T. Predominant suppression of apoptosome by inhibitor of apoptosis protein in non-small lung cancer H460 cells: therapeutic effect of a novel polyarginine-conjugated Smac peptide. *Cancer Res.* **2003**, *63*, 831 – 837.
- 66.** Meng, X.; Lee, S.; Kaufmann, S. H. Apoptosis in the treatment of cancer: a promise kept? *Cur. Op. Cell Biol.* **2006**, *18*, 668 – 676.
- 67.** Pang, Y. P.; Perola, E.; Xu, K.; and Prenderast, F. G. EUDOC: A computer program for identification of drug interaction sites in macromolecules and drug leads from chemical databases. *J. Comp. Chem.* **2001**, *22*, 1750 – 1771.
- 68.** Wu, G.; Chai, J.; Suber, T. L.; Wu, J. W.; Du, C.; Wang, X.; Shi, Y. Structural basis of IAP recognition by Smac / DIABLO. *Nature* **2000**, *408*, 1008-1012.
- 69.** Liu, Z.; Sun, C.; Olejniczak, E. T.; Meadows, R. P.; Betz, S. F.; Oost, T.; Herrmann, J.; Wu, J. C.; Fesik, S. W. Structural basis for binding of Smac/DIABLO to the XIAP BIR3 domain. *Nature* **2000**, *408*, 1004 – 1008.
- 70.** Seebach, D.; Does, M.; Naef, R.; Schwizer, B. Alkylation of amino acids without loss of the optical activity: Preparation of *R* – substituted proline derivatives. A case of self-reproduction of chirality. *J. Am. Chem. Soc.* **1983**, *105*, 5390 – 5398.

- 71.** Khalil, E. M.; Subasinghe, N. L.; Johnson, R. L. An efficient and high yield method for the N-tert-butoxycarbonyl protection of sterically hindered amino acids. *Tetrahedron Lett.* **1996**, *37*, 3441-3444.
- 72.** Huang, H.; Iwasawa, N.; and Mukaiyama, T.A. A Convenient Method for the Construction of Beta-Lactam Compounds from Beta-Amino Acids. *Chem. Lett.* **1984**, 1465-1466.
- 73.** Perrin, D. D.; Armarego, L.F. Purification of Laboratory Chemicals, 3rd Edition. Pergamon Press. pgs. 157-158.
- 74.** Richmond, M.L.; Seto, C.T. Modular ligands derived from amino acids for the enantioselective addition of organozinc reagents to aldehydes. *J. Org. Chem.* **2003**, *68*, 7505-7508.
- 75.** Friener, R. A.; Bank, J. L.; Murphy, R. B.; Halgren, T. A.; Kiere, J. J.; Mainz, D. T.; Repasky, M. P.; Knoll, E. H.; Shelly, M.; Perry, J. K.; Shaw, D. E.; Francis, P.; Shenkin, P. S. Glide: a new approach for rapid, accurate docking and scoring. 1. Method and assessment of docking accuracy. *J. Med. Chem.* **2004**, *47*, 1739 – 1749.
- 76.** Nikolovska-Coleska, Z.; Wang, R.; Fang, X.; Pan, H.; Tomita, Y.; Li, P.; Roller, P. P.; Krajewski, K.; Saito, N. G.; Stuckey, J. A.; Wang, S. Development and

- optimization of a binding assay for the XIAP- BIR3 domain assay fluorescence polarization. *Anal. Biochem.* **2004**, *332*, 261- 273.
- 77.** Sun, H.; Nikolovska-Coleska, Z.; Chen, J.; Yang, C.; Tomita, Y.; Pan, H.; Yoskioka, Y.; Krajewski, K.; Roller, P. P.; Wang, S. Structure – based design, synthesis and biochemical testing of novel and potent Smac peptido-mimetics. *Bioorg. Med. Chem. Lett.* **2005**, *15*, 793 – 797.
- 78.** Shatzmiller, S.; Dolitzky, B.; Bahar, E. Preparation and use of chloromethyl (-)-menthyl ether in the synthesis of optically pure α -branched α -amino nitriles. *Liebigs Ann. Chem.* **1991**, *4*, 375-379.
- 79.** Seebach, D.; Dziadulewicz, E.; Behrendt, L.; Cantoreggi, S.; Fitzi, R. Synthesis of Nonproteinogenic (*R*)- or (*S*)-Amino Acids Analogues of Phenylalanine, Isotopically Labelled and Cyclic Amino Acids from tert-Butyl 2-(tert-Butyl)-3-methyl-4-oxo-1-imidazolidinecarboxylate (Boc-BMI). *Liebigs Ann. Chem.* **1989**, *12*, 1215-1232.
- 80.** Long, J.; Yuan, Yi.; Shi, Y. Asymmetric Simmons-Smith cyclopropanation of unfunctionalized olefins. *J. Am. Chem. Soc.* **2003**, *125*, 13632-13633.
- 81.** Kipp, R. A.; Case, M. A.; Wist, A. D.; Cresson, C. M.; Carrel, M.; Gringer, E.; Wiita, A.; Albiniaak, P. A.; Chai, J. J.; Shi, Y. G.; Semmelhack, M. F.; McLendon, G. L. *Biochemistry* **2002**, *41*, 7344 – 7349.

- 82.** Wist, A. D.; Gu, L.; Riedl, S. J.; Shi, Y.; McLendon, G. L. Structure-activity based study of the Smac-binding pocket within the BIR3 domain of XIAP. *Bioorg. Med. Chem.* **2007**, *15*, 2935 – 2943.
- 83.** Pang, Y. P.; Perola, E.; Xu, K.; Prenderast, F. G. EUDOC: A computer program for identification of drug interaction sites in macromolecules and drug leads from chemical databases. *J. Comp. Chem.* **2001**, *22*, 1750 – 1771.
- 84.** Freidinger, R. M.; Schwenk, D.; Veber, D. F. Protected lactam bridged dipeptides for use as conformational constraints in peptides. *J. Org. Chem.* **1982**, *67*, 104 – 109.
- 85.** Zydowsky, T. M.; Dellaria, Jr. J. F.; Nellans, H. N. Efficient and versatile synthesis of dipeptide isosteres containing γ - or δ -lactams. *J. Org. Chem.* **1988**, *53*, 5607 – 5616.
- 86.** Genin, M.J.; Gleason, W.B.; Johnson, R.L. Design, synthesis, and X-ray crystallographic analysis of two novel spriolactam systems as β -turn mimics. *J. Org. Chem.* **1993**, *58*, 860 – 866.
- 87.** Genin, M. J.; Ojala, W. H.; Gleason, W. B.; Johnson, R.L. Synthesis and crystal structure of a peptidomimetic containing the (*R*)-4.4-sprio lactam type-II β – turn mimic. *J. Org. Chem.* **1993**, *58*, 2334 – 2337.
- 88.** Palomo, C.; Aizpurua, J. M.; Benito, A; Miranda, J. I.; Fratila, R. M.; Matute, C.; Domercq, M.; Gago, F.; Martin-Santamaria, S.; Linden, A. α -Alkyl- α -amino- β -

- lactam peptides: design, synthesis and conformational features. *Angew. Chem., Int. Ed.* **1999**, *38*, 3056 – 3058.
- 89.** Kapadia, S. R.; Spero, D. M.; Eriksson, M. An improved synthesis of chiral α -(4-Bromobenzyl)alanine Ethyl Ester and its application to the synthesis of LFA-1 antagonist BIRT-377. *J. Org. Chem.* **2001**, *66*, 1903 – 1905.
- 90.** *Initial modeling studies were prepared by Dr. Pang's group utilizing the EUDOC modeling program*
- Pang, Y.P.; Perola, E.; Xu, K.; Prenderast, F. G. EUDOC: A computer program for identification of drug interaction sites in macromolecules and drug leads from chemical databases. *J. Comp. Chem.* **2001**, *22*, 1750 – 1771.
- 91.** Nikolovska-Coleska, Z.; Wang, R.; Fang, X.; Pan, H.; Tomita, Y.; Li, P.; Roller, P. P.; Krajewski, K.; Saito, N. G.; Stuckey, J. A.; Wang, S. Development and optimization of a binding assay for the XIAP – BIR3 domain assay fluorescence polarization. *Anal. Biochem.* **2004**, *332*, 261 – 273.
- 92.** Sun, H.; Nikolovska-Coleska, Z.; Chen, J.; Yang, C.; Tomita, Y.; Pan, H.; Yoskioka, Y.; Krajewski, K.; Roller, P. P.; Wang, S. Structure – based design, synthesis and biochemical testing of novel and potent Smac peptido-mimetics. *Biorganic Med. Chem. Lett.* **2005**, *15*, 793 – 797.
- 93.** Genin, M. J.; Ojala, W. H.; Gleason, W. B.; Johnson, R.L. Synthesis and crystal structure of a peptidomimetic containing the (*R*)-4.4-sprio lactam type-II β – turn mimic. *J. Org. Chem.* **1993**, *58*, 2334 – 2337.

- 94.** Somu, R. V.; Johnson, R. L. Synthesis of pipercolic acid based spiro bicyclic lactam scaffolds as β – turn mimics. *J. Org. Chem.* **2005**, *70*, 5954 – 5963.
- 95.** Subashinge, N. L.; Bontems, R. J.; McIntee, E.; Mishra, R. K.; Johnson, R. L. Bicyclic thiazolidine lactam peptidomimetics of the dopamine receptor modulating peptide Pro-Leu-Gly-NH₂. *J. Med. Chem.* **1993**, *36*, 2356 – 2361.
- 96.** Khalil, E. M.; Pradhan, A.; Ojala, W. J.; Gleason, W. B.; Mishra, R. K.; Johnson, R. L.; Nair, V.; Design, synthesis and dopamine receptor modulating activity of spiro bicyclic peptidomimetics of L-prolyl-L-leucyl-glycinamine. *J. Med. Chem.* **1999**, *42*, 628 – 637.
- 97.** Seebach, D.; Does, M.; Naef, R.; Schwizer, B. Alkylation of amino acids without loss of the optical activity: preparation of *R* – substituted proline derivatives. A case of self-reproduction of chirality. *J. Am. Chem. Soc.* **1983**, *105*, 5390 – 5398.
- 98.** Coppola, G. N. Schuster, H. F. Asymmetric synthesis: construction of chiral molecules using amino acids; Wiley: New York, 1987.
- 99.** Duthaler, R. O. Recent developments in the stereoselective synthesis of α -amino acids. *Tetrahedron* **1994**, *50*, 1539-1650.

- 100.** O'Donnell, M. J.; Bennett, W. D.; Wu, S. The stereoselective synthesis of alpha-amino acids by phase-transfer catalysis. *J. Am. Chem. Soc.* **1989**, *111*, 2353-2355.
- 101.** Myers, A. G.; Gleason, J. L.; Yoon, T. Practical method for the synthesis of D- or L- alpha-amino acids by the alkylation of (+)- or (-)-pseudoephedrine glycinamide. *J. Am. Chem. Soc.* **1995**, *117*, 8488.
- 102.** Lee, B. H.; Miller, M. J.; Constituents of microbial iron chelators. The synthesis of optically active derivatives of δ -N-hydroxy-L-ornithine. *Tetrahedron Lett.* **1984**, *25*, 927 – 930.
- 103.** Karady, S.; Amato, J. S.; Weinstock, I. M. Enantioselective alkylation of acyclic amino acids. *Tetrahedron Lett.* **1984**, *25*, 4337 – 4340.
- 104.** Myers, A. G.; Gleason, J. L.; Yoon, T.; Kung, D. W. Highly practical methodology for the synthesis of D- and L- α -amino acids, N-protected α -amino acids, and N-methyl- α -amino acids. *J. Amer. Chem. Soc.* **1997**, *119*, 656- 673.
- 105.** Myers, A. G.; Schnider, P.; Kwon, S.; Kung, D. W. Greatly simplified procedures for the synthesis of α -amino acids by the direct alkylation of pseudoephedrine glycinamide hydrate. *J. Org. Chem.* **1999**, *64*, 3322 – 3327.
- 106.** Overman, L. E.; Smool, J.; Overman, J. D. The reduction of aryl disulfides with triphenyl phosphine. *Synthesis*, **1974**, 59 – 60.

- 107.** Han, C.; Lee, J. P.; Lobkovsky, E.; Porco, J. A. Catalytic ester – amide exchange using group (IV) metal alkoxide – activator complexes. *J. Am. Chem. Soc.* **2005**, *127*, 10039 – 10044.
- 108.** Chai, J. Structural and biochemical basis of apoptotic activation by Smac/DIABLO. *Nature*, **2000**, *406*, 855 – 862.
- 109.** Wu, G.; Chai, J.; Suber, T. L.; Wu, J.; Du, C.; Wang, X.; Shi, Y. Structural Basis of IAP Recognition by Smac / DIABLO. *Nature* **2000**, *408*, 1008-1012.
- 110.** Sun, C. NMR structure and mutagenesis of the inhibitor of apoptosis protein XIAP. *Nature*, **1999**, *401*, 818 – 822.
- 111.** Shi, Y. Survivin structure: crystal unclear. *Nature Struct. Biol.* **2000**, *7*, 620 – 623.
- 112.** Verdecia, M.A. Structure of the human anti-apoptotic protein surviving reveals a dimeric arrangement. *Nature Struct. Biol.* **2000**, *7*, 602 – 608.
- 113.** Chantalat, L. Crystal structure of human surviving reveals a bow tie shaped dimer with two unusual alpha helical extensions. *Mol. Cell* **2000**, *6*, 183 – 189.
- 114.** Genin, M.J.; Gleason, W.B.; Johnson, R.L. Design, synthesis, and X-ray crystallographic analysis of two novel spriolactam systems as β – turn mimics. *J. Org. Chem.* **1993**, *58*, 860 – 866.

- 115.** Genin, M. J.; Ojala, W. H.; Gleason, W. B.; Johnson, R.L. Synthesis and crystal structure of a peptidomimetic containing the (*R*)-4.4-sprio lactam type-II β – turn mimic. *J. Org. Chem.* **1993**, *58*, 2334 – 2337.
- 116.** Pang, Y. P.; Perola, E.; Xu, K.; Prenderast, F. G. EUDOC: A computer program for identification of drug interaction sites in macromolecules and drug leads from chemical databases. *J. Comp. Chem.* **2001**, *22*, 1750 – 1771.
- 117.** Chai, J. Structural and biochemical basis of apoptotic activation by Smac/DIABLO. *Nature* **2000**, *406*, 855 – 862.
- 118.** Wu, G.; Chai, J.; Suber, T. L.; Wu, J. W.; Du, C.; Wang, X.; Shi, Y. Structural basis of IAP recognition by Smac / DIABLO. *Nature* **2000**, *408*, 1008 – 1012.
- 119.** Nikolovska-Coleska, Z.; Wang, R.; Fang, X.; Pan, H.; Tomita, Y.; Li, P.; Roller, P. P.; Krajewski, K.; Saito, N. G.; Stuckey, J. A.; Wang, S. Development and optimization of a binding assay for the XIAP- BIR3 domain assay fluorescence polarization. *Anal. Biochem.* **2004**, *332*, 261-273.
- 120.** Ward, P.; Ewan, G.B.; Jordan, C.C.; Ireland, S.J.; Magan, R. M.; Brown, J. R. Potent and highly selective neurokinin antagonists. *J. Med. Chem.* **1990**, *33*, 1848 – 1851.
- 121.** Hinds, M. G.; Welsh, J. H.; Brennand, D. M.; Fisher, J.; Glennie, M. J.; Richards, N.G.J.; Turner, D. L.; Robinson, J. A. Synthesis, conformational properties, and

- antibody recognition of peptides containing β -turn mimetics based on α -alkylproline derivatives. *J. Med. Chem.* **1991**, *34*, 1777 – 1789.
- 122.** Hinds, M. G.; Richards, N. G. J.; Robinson, J. A. Design and synthesis of a novel peptide β – turn mimetic. *Chem. Commun.* **1988**, *22*, 1447 – 1449.
- 123.** Long, R. D.; Moeller, K. D. Conformationally constrained peptide mimetics: the use of a small lactam ring as an HIV-1 antigen **constraint**. *J. Am. Chem. Soc.* **1997**, *119*, 12394 – 12395
- 124.** Seebach, D.; Does, M.; Naef, R.; Schwizer, B. Alkylation of amino acids without loss of the optical activity: preparation of *R* – substituted proline derivatives. A case of self-reproduction of chirality. *J. Am. Chem. Soc.* **1983**, *105*, 5390 – 5398.
- 125.** Shatzmiller, S.; Dolitzky, B.; Bahar, E. Preparation and use of chloromethyl (-)-menthyl ether in the synthesis of optically pure α -branched α -amino nitriles. *Liebigs Ann. Chem.* **1991**, *4*, 375–379.
- 126.** Seebach, D.; Dziadulewicz, E.; Behrendt, L.; Cantoreggi, S.; Fitzi, R. Synthesis of Nonproteinogenic (*R*)- or (*S*)-Amino Acids Analogues of Phenylalanine, Isotopically Labelled and Cyclic Amino Acids from tert-Butyl 2-(tert-Butyl)-3-methyl-4-oxo-1-imidazolidinecarboxylate (Boc-BMI). *Liebigs Ann. Chem.* **1989**, *12*, 1215–1232.
- 127.** Khalil, E. M.; Subasinghe, N. L.; Johnson, R. L.; An efficient and high yield method for the N-tert-butoxycarbonyl protection of sterically hindered amino acids. *Tetrahedron Lett.* **1996**, *37*, 3441–3444.

- 128.** Wu, G.; Chai, J.; Suber, T. L.; Wu, J.; Du, C.; Wang, X.; Shi, Y. Structural Basis of IAP Recognition by Smac / DIABLO. *Nature* **2000**, *408*, 1008–1012.
- 129.** Sun, C. NMR structure and mutagenesis of the inhibitor of apoptosis protein XIAP. *Nature* **1999**, *401*, 818 – 822.
- 130.** Shi, Y. Survivin structure: crystal unclear. *Nature Struct. Biol.* **2000**, *7*, 620 – 623.
- 131.** Verdecia, M.A. Structure of the human anti-apoptotic protein surviving reveals a dimeric arrangement. *Nature Struct. Biol.* **2000**, *7*, 602 – 608.
- 132.** Chantalat, L. Crystal structure of human surviving reveals a bow tie shaped dimer with two unusual alpha helical extensions. *Mol. Cell* **2000**, *6*, 183 – 189.
- 133.** Genin, M. J.; Johnson, R.L.; Design, Synthesis, and Conformational Analysis of a Novel Spiro-Bicyclic System as a Type II β -Turn Peptidomimetic, *J. Amer. Chem. Soc.* 1992, *114*, 8778 – 8783